ICFM 2023

International Conference "Functional Materials" ICFM - 2023

BOOK OF ABSTRACTS

October 2 - 6, 2023

Crimea, Foros

ЭМТИОН

М-Гранат

International Conference
"Functional Materials"

ICFM-2023

BOOK OF ABSTRACTS

October 2 – 6, 2023
Russia, Crimea, Foros

International Conference “Functional Materials” ICFM-2023

Program Committee

V. Berzhansky (co-chairman),
V. Belotelov (co-chairman),
S. Nikitov (co-chairman)
V. Achanta
N. Bebenin
N. Bebenin
I. Bychkov
E. Ekomasov
Y. Fetisov
A. Fraerman
S. Hamedi
X. Han
A. Kalashnikova
G. Kurlyandskaya
I. Lyubutin
N. Mushnikov
S. Ovchinnikov
N. Perov
R. Pisarev
A. Pyatakov
K. Rozanov
A. Sadovnikov
V. Shavrov
A. Sigov
V. Shur
V. Ustinov
V.Varyukhin
A. Zvezdin

Local Committee

S. Polulyakh (chairman)
S. Alieva
E. Barshak
N. Lugovskoy
T. Mikhailova
V. Popov
S. Tomilin
M. Yavorsky

Address of the Organizing Committee

ICFM’2023
V. I. Vernadsky Crimean Federal University,Vernadsky Ave.,
Simferopol, 295007 Russia
Phone:89787665730
E-mail: icfm@cfuv.ru
https://icfm-crimea.ru/

Table of content

Plenary reports

A1-L/1

The van der Waals magnets: new functional materials for magnetic electronics

Pyatakov A.P.[1,2]

[1]*M.V. Lomonosov Moscow State University, 119991, Moscow, Russia*
[2] *MIREA - Russian Technological University, 119454, Moscow, Russia*
alexander.pyatakov@yandex.ru

Recently the graphene-like two dimensional (2D) magnets [1], and multiferroics [2] were discovered that are also called van der Waals (vdW) ferromagnets since the interlayer van der Waals forces enable them to be exfoliated from the bulk crystal and stacked in multilayers. Due to their flexible 2D geometry [3,4] and possibility of electric gating without screening effects [2] these materials provide a rich playground for cross-coupling effects between magnetic, ferroelectric and mechanical subsystems of crystals.

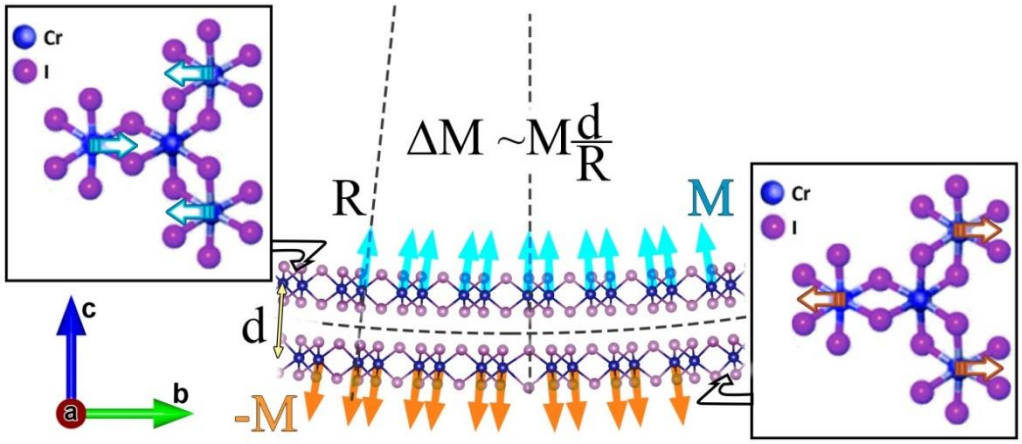

Figure 1. The strain-induced magnetization ΔM in CrI_3 bilayer (***M*** is one-layer magnetization, ***R*** is curvature radius, ***d*** is the interlayer distance The compressed top layer with enhanced magnetic exchange and the stretched bottom layer with reduced exchange are shown in the insets: this difference in the exchange induced by flexural deformation leads to the decompensated magnetization ΔM.

In particular, the coupling between mechanical and ferroelectric subsystems in 2D materials manifests itself in flexoelectric effect (strain gradient-induced electric polarization) and flexomagnetic phenomena (the appearance of decompensated magnetization in antiferromagnetically coupled bilayers, fig.1).

These effects are of practical importance for various branches of magnetic electronics such as spintronics, straintronics and neuromorphic electronics.

The work is supported by Russian Ministry of Science and Education (Project No. 075-15-2022-1131).

References

[1] B. Huang, G. Clark, E. Navarro-Moratalla et al, *Nature* 546, 270 (2017).

[2] Sh. Liang et al, *Nature Electronics* 6, 199–205 (2023)

[3] A. Edström, D. Amoroso, S. Picozzi et al, *Phys. Rev. Lett.* 128, 177202 (2022).

[4] L. Qiao, J. Sladek, V. Sladek, A.S. Kaminskiy, A.P. Pyatakov, W. Ren, *arXiv:*2307.05084 (2023)

A1-L/2

Introduction to metamaterials with selected examples

Lapine M.

ITMO University, St. Petersburg, 191002, Russia

A1-L/3

From Microelectronics to Spintronics and Magnonics

Han X.F.

Beijing National Laboratory for Condensed Matter Physics, Institute of Physics, University of Chinese Academy of Sciences, Chinese Academy of Sciences, Beijing 100190, China
Center of Materials Science and Optoelectronics Engineering, University of Chinese Academy of Sciences, Beijing 100049, China

A2-1L/1

Magnetic nanoclusters

Zvezdin A.K.

Prokhorov General Physics Institute RAS, Moscow 119991, Russia

B1-L/1

Metamaterials for sensing

Achanta V.G.

CSIR-National Physical Laboratory, Dr.K.S.Krishnan Marg, New Delhi, 110012, India
Academy of Scientific & Innovative Research, Ghaziabad, Uttar Pradesh, 201002, India

C1-L/1

Ultrafast magnetism of antiferromagnets

Kimel A.

Radboud University Nijmegen, Institute for Molecules and Materials, Nijmegen, The Netherlands

CO1-3O/1

Magnetoplasmonic nanostructures for detection of Ru atoms *(Invited)*

Hamidi S.M.

Magneto-Plasmonic Lab, Laser and Plasma Research Institute, Shahid Beheshti University, Tehran, Iran

B1-L/2

Topological magnetic memory with multiply-connected planar magnetic nanoelements

Metlov K.L.[1,2]

[1]*Galkin Donetsk Institute for Physics and Engineering, R Luxemburg str. 72, 283048, Donetsk, Russia*
[2] *Marchuk Institute of Numerical Mathematics RAS, Gubkin str. 8, 119333 , Moscow, Russia*
metlov@donfti.ru

Topological effects are currently actively studied in the framework of condensed matter physics. In magnetism they are especially abundant when dealing with magnetic topological solitons (skyrmions). A racetrack memory concept [1] is one of the key guiding designs in a developing field of skyrmionics [2].

While the topology of the magnetization configuration in skyrmions-based racetrack memory is non-trivial, the racetrack itself is a simply-connected object. In this talk, based on an approximate analytical approach to the planar micromagnetics [3], a multiply-connected generalization [4] of the racetrack magnetic memory will be presented. It can effectively store a graph of interconnected symbols with each degree of connectivity adding an additional symbol and anti-symbol to the dictionary. The corresponding configurations (examples are shown in Figure below) are developed analytically up to a homotopy and the energy barriers, protecting their stability, are discussed.

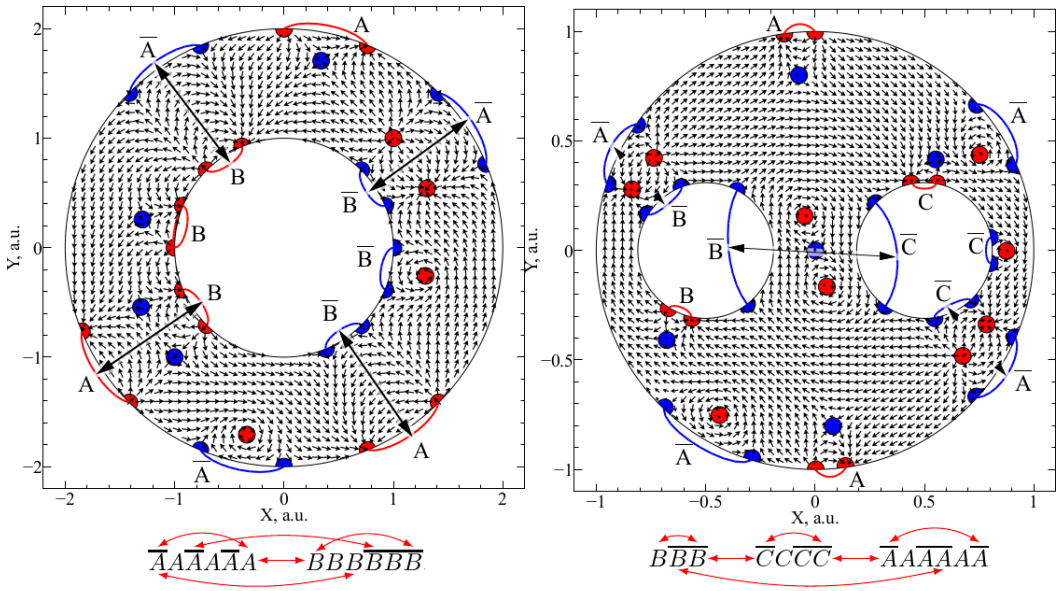

Figure 1. Magnetic configurations of doubly- and triply-connected planar nanorings, storing the indicated graphs of symbols. The dots mark the centres of magnetic vortices and antivortices.

The support of the Russian Science Foundation under the project # 21-11-00325 is gratefully acknowledged.

References

[1] S. S. P. Parkin, M. Hayashi, and L. Thomas, Science 320, 190 (2008).

[2] A. Fert, V. Cros, and J. Sampaio, Nat. Nanotechnol 8, 152 (2013).

[3] K. L. Metlov, Phys. Rev. Lett. 105, 107201 (2010).

[4] K. L. Metlov, JETP Lett. (2023), DOI: 10.1134/S0021364023601823

C1-L/2

Topological properties of Tamm plasmon polariton in one-dimensional photonic crystal covered by metasurface *(invited)*

Timofeev I.V.[1]

[1] *Kirensky Institute of Physics, FRC KSC SB RAS, Krasnoyarsk 660036, Russia*
tiv@iph.krasn.ru

Topological ideas from condensed matter physics were effectively adopted in photonics [1] to pave the way for novel miniature photonic devices, such as highly curved reflection-free waveguides, delay lines, spin-polarized switches, and unidirectional signal transmission devices. On the one hand, the immediate causes of the boom lie in the development of nanotechnology. On the other hand, mastering the subwavelength scale allows us to rethink the ways of generating light and controlling this subtlest form of matter. Historically, the first generation of optical devices is based on the control of light through the geometric shape of the surface (classical mirrors, lenses, prisms). The second generation is based on the difference in the refractive index (reflection coatings, flat lenses). The third generation is based on birefringence control (liquid crystal displays). The fourth generation of photonic devices is supported by such concepts as photonic crystals and metamaterials, including birefringent ones, for example, diffractive phase wave plates and metasurfaces. They use the ability of the medium to change the orientation of the optical axis on the wave and subwave scales.

In chiral photonic structures [2], where the mirror symmetry is broken due to structural chirality, it becomes essential to take into account the geometric (topological) phase, which was used long before by Vladimirsky, Rytov, Pancharatnam, Berry and others in describing the features of the band structure, polarization on the Poincare sphere and a singular phase near zero amplitude at the center of the optical vortex. Thus, topology finds applications in high-resolution imaging, in fiber optic communications, and in the creation of new protocols for processing quantum information. In the technologically important near infrared and visible frequency ranges, topological states were obtained using an array of helical waveguides and an array of ring resonators. A wide range of other platforms are being actively explored, including polariton circuits and prism resonator arrays [3].

Tamm plasmon polariton is an electromagnetic wave excited at a common boundary of two reflecting photonic structures that combine a high quality factor and strong field localization [4]. Its defining feature is Bragg reflection at arbitrary angles of incidence not limited by the angle of total internal reflection. Compared to multidimensional periodic structures, one-dimensional Bragg multilayer films are easy to manufacture. For such structures, the topological nature of the surface states is described by the Zack phase. Besides, Tamm state can be easily hybridized with other types of resonances [5].

Metasurface is a sheet of metamaterial with a subwavelength thickness. Losses in it, as a rule, are less than in bulk metamaterial, and manufacturing is simpler. The metasurface deposited on a photonic crystal provides new degrees of freedom for controlling the Tamm plasmon polariton properties. Non-trivial topology ensures the stability of the spectral properties of the Tamm plasmon polariton with a change in the parameters of electrically controlled photonic devices, in particular, for smart transport and telecommunications. In an autonomous control system for smart transport,

an important component is sensors that replace the human driver vision. Here, the responsibility for making a decision is high, and in order to compete with a human driver, an ordinary video camera is often not enough, radars and parking sensors are added. Another sensor designed to replace the driver's eyes is lidar, a photonics device, which is a laser radar for accurate recognition of objects at close distances. Mechanically controlling the orientation of the source or deflecting mirror is not always optimal. Therefore, instead of deflecting the laser beam from the initial direction specified during generation, it is desirable to change the parameters of the laser itself so that the beam is generated in a new direction. Mirrorless beam rotation of a microlaser based on a Tamm plasmon polariton can provide a significant gain in speed, accuracy, reliability, and ease of manufacture. Such beam rotation can be attempted using multilayer mirrors and metasurfaces based on highly refractive materials: silicon, tellurium, and germanium, as well as controllable transparent materials, such as conducting oxides, polymers, and liquid crystals. In addition, in the presence of layers of anisotropic materials, a nontrivial topology appears due to polarization, which provides two independent relaxation channels, as in the case of chiral Tamm plasmon polaritons [6].

This research was funded by the Russian Science Foundation (project no. 22-42-08003)

References

[1] T. Ozawa et al. // Rev.Mod. Phys. 91, № 1. P. 15006 (2019).
[2] S.Y. Vetrov, I.V. Timofeev and V.F. Shabanov // Physics-Uspekhi, 63, 33 (2020).
[3] D.P. Fedchenko, P.N. Kim and I.V. Timofeev // Symmetry, 14, 2673 (2022).
[4] M.A. Kaliteevski et al. // Phys.Rev.B. 76, P.165415.b (2007).
[5] T.V. Mikhailova et al. Optical Materials Express, 12(2), 685-696 (2022).
[6] M.-Y. Lin, W.-H. Xu, R. G. Bikbaev et al. // Materials (Basel). 14, 2788 (2021).

C1-L/3

Ultrafast magnetism and domain walls

Logunov M.V.[1,2]

[1]*Kotel'nikov Institute of Radio Engineering and Electronics of RAS, 125009, Moscow, Russia*
[2]*Moscow Institute of Physics and Technology, 141701, Dolgoprudny, Moscow Region, Russia*
logunov@cplire.ru

The study of ultrafast processes in magnetism began with the detection of Ni-film demagnetization in less than 1 ps as a result of femtosecond laser-pulse effect [1,2]. Other actively investigated processes induced by laser pulses are coherent magnetization oscillations in ferromagnets and antiferromagnets in the frequency range from several of GHz to 22 THz [3,4].

Present report provides a brief review of the domain-wall movement study in magnetic films and platelets under the action of laser pulses. This field of ultrafast magnetism is also starting to develop rapidly. The possibilities of optical and X-ray research techniques for these purposes, the proposed mechanisms of domain-wall movement and the results of the study of domains, domain walls and other spin textures [5-14] are discussed.

The work was supported by the Government of the Russian Federation for state support of scientific research conducted under guidance of leading scientists (Project No. 075-15-2022-1098) and the Russian Science Foundation (Project No. 19-19-00607-P).

References

[1] E. Beaurepaire, J.-C. Merle, A. Daunois, J.-Y. Bigot, Phys. Rev. Lett. 76, 4250 (1996).
[2] P. Scheid, Q. Remy, S. Lebègue et al., J. Magn. Magn. Mater. 560, 169596 (2022).
[3] A. Kirilyuk, A.V. Kimel, T. Rasing, Rev. Mod. Phys. 82, 2731 (2010).
[4] A.V. Kimel, M. Li, Nature Rev. Mater. 4, 189 (2019).
[5] G.M. Genkin, I.D. Tokman, Sov. Phys. JETP 55, 887 (1982).
[6] B. Pfau, S. Schaffert, L. Muller et al., Nat. Commun. 3, 1100 (2012).
[7] G.M. Genkin, Yu.N. Nozdrin, A.V. Okomel'kov, I.D. Tokman, Phys. Rev. B 86, 024405 (2012).
[8] M.V. Gerasimov, M.V. Logunov, A.V. Spirin et al., Phys.Rev. B 94, 014434 (2016).
[9] M.V. Gerasimov, S.V. Ilin, M.V. Logunov et al., Instr. Exper. Tech. 60, 716 (2017).
[10] Y. Quessab, R. Medapalli, M.S. El Hadri et al., Phys. Rev. B 97, 054419 (2018).
[11] K.H. Prabhakara, T.B. Shapaeva, M.D. Davydova et al., J. Phys.: Condens. Matter 33, 075802 (2021).
[12] C. Léveillé, E. Burgos-Parra, Y. Sassi et al., Nature Commun. 13, 1412 (2022).
[13] D. Zusin, E. Iacocca, L. Le Guyader et al., Phys. Rev. B 106, 144422 (2022).
[14] A. Dolgikh, D. Afanasiev, V.V. Yurlov et al., Phys. Rev. B 107, 094424 (2023).

Section
Fundamental Physics of Functional Materials

BO1-1O/1

From Theory to Reality: Recent Advances in 2D Diamond Research (*invited*)

Sorokin P.B.

National University of Science and Technology MISIS, 119049, Moscow, Russian Federation
pbsorokin@misis.ru

With the developments in the field of 2D materials, nowadays of growing interest is synthesis and investigation of 2D diamond or diamane [1]. Diamane possesses a range of notable properties, comparable to established nanostructures such as graphene, h-BN, and MoS_2. These properties make diamane suitable for various applications, including ultrahard coatings, quantum computing, superconductivity, biologically active substrates, biosensors etc [2].

Synthesizing diamane remains a complex process. I will discuss approaches for producing ultrathin diamond films from few-layer graphene by employing hydrogenation or fluorination to initiate phase transformation without high pressure. This "chemically induced phase transition" [3] is a nanoscale phenomenon, with surface conditions directly impacting thermodynamics and transition pressure.

Additionally, I will address the various factors influencing diamond formation, such as the number of graphene layers, stacking, adatom type and arrangement, and external parameters [4]. Fine-tuning these factors in experimental settings is crucial for achieving desired outcomes. I will also examine how the adsorption of different functional groups can result in films with varied structures and properties [5]. Lastly, I will review recent experimental data demonstrating the successful synthesis of 2D diamond through chemically induced phase transition and other approaches.

P.B.S. gratefully acknowledges the financial support of Russian Science Foundation (Project identifier 21-12-00399).

References

[1] Chernozatonskii L.A., Sorokin P.B., Kvashnin A.G., Kvashnin D.G., JETP Lett. 90, 134 (2009).
[2] Sorokin P.B., Yakobson B.I., Nano Letters 21, 5475 (2021)
[3] Kvashnin A.G., Chernozatonskii L.A., Yakobson B.I., Sorokin P.B., Nano Lett. 14, 676 (2014).
[4] Erohin S.V., Ruan Q., Sorokin P.B., Yakobson B.I., Small 16, 2004782 (2020).
[5] Varlamova L.A., Erohin S.V., Larionov K.V., Sorokin P.B. J. Phys. Chem. Lett. 13, 11383 (2022).

BO1-1O/2

Structure and state stability of magnetic vortex-like inhomogeneities in modulated ultrathin magnetic films

Vakhitov R.M.[1], Solonetsky R.V.[1], Akhmetova A.A.[1], Filippov M.A.[1]

[1]*Ufa University of Science and Technology, 450076, Ufa, Russia*
mikhail.filippov.99@mail.ru

Magnetic skyrmions, first discovered in chiral magnets back in 2009 [1], still attract the attention of researchers. They are topologically protected vortex–like structures and are stabilized in non-centrosymmetric magnets due to the presence of the Dzyaloshinskii–Moriya interaction (DMI) in them, which is called bulk DMI. In addition, magnetic skyrmions can also be observed in multilayer ultrathin films, in which interfacial DMI is responsible for their stability. They have a number of unique properties (nanoscale dimensions, high speeds, the ability to manipulate them with a low-density electric current, etc.) This allows them to be used in high-density, low-power and multifunctional computing and storage devices of a new generation, as well as in artificial neural networks [2].

However, there are methods for obtaining stable single skyrmions even in the absence of DMI in the materials. One of these possible options is considered in [3]. It consists in the use of uniaxial ferromagnetic films with spatially modulated material parameters. In this case, the magnetic skyrmion is stabilized on a columnar defect of the "potential pit" type in the center of this film. In [4], theoretical analysis and micromagnetic modeling of vortex-like structures that occur in such magnetic films were carried out. Studies have shown that they come in different types (four in total), two of which are non-topological solitons, and two are magnetic skyrmions. They differ in the orientation of the core and the direction of magnetization at the periphery (outside the defect). However, they also have common topological features; in their structure, three sections of rotation of magnetic moments can be distinguished: core, intermediate and boundary sections. Stable states of Bloch-type skyrmions were obtained using micromagnetic modeling on films with a defect [4].

The purpose of this work is to find stable states of vortex-like inhomogeneities of Neel type using the OOMMF open access software package [5] with an additional module [6]. A disk of finite dimensions with a columnar defect in the center is considered. It is assumed that the material parameters on the disk and on the defect are identical except for the anisotropy constant Ku: $Ku_2<0$ – on the defect, $Ku_1>0$ – in the rest of the disk. The presence of an interfacial DMI (isotropic) in the entire disk space is also taken into account.

According to the simulation results, it turned out that skyrmions in the absence of any external fields are stable at the following material parameters: disk diameter 600 nm, disk thickness 5 nm, defect diameter 60 nm, $Ku_1=3\times10^4$ J/m^3 (outside the defect), $Ku_2=-0.5\times10^4$ J/m^3 (on the defect), $Ms=2.0\times10^5$ A/m, $A=2.5\times10^{-11}$ J/m, $D=0.85\times10^{-3}$ J/m. With these parameters, a magnetic skyrmion was numerically found (Figure 1). With a further increase in the DMI constant to the value $D = 1\times10^{-3}$ J/m, a 2π-skyrmion (skyrmionium) is formed on the defect in the center of the disk (Figure 2), in which the magnetization reversal occurs by 360°. With the subsequent increase of DMI to the value $D= 1.4 \times 10^{-3}$ J/m, the transition of 2π-skyrmion to 3π-skyrmion occurs. In it, the magnetization reversal already occurs at 540°.

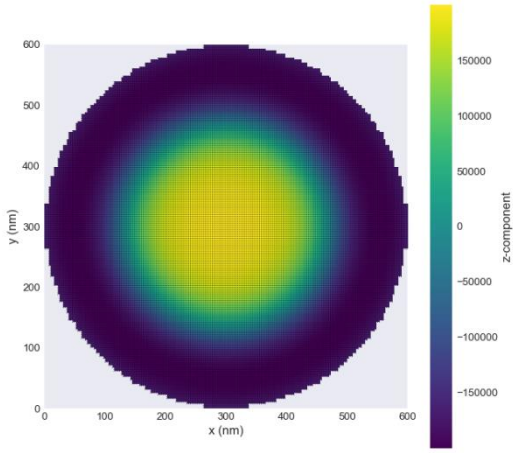

Fig. 1. Stable state of the magnetic skyrmion

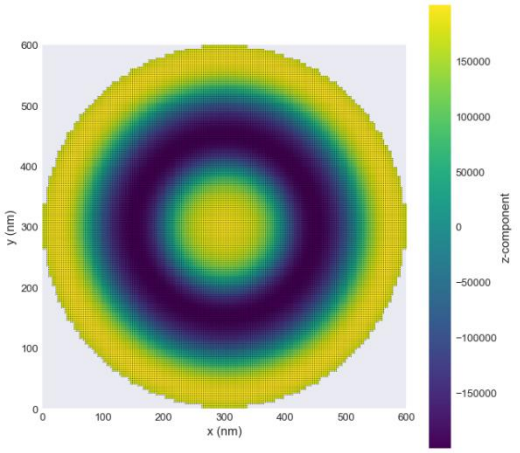

Fig. 2. Stable state of the magnetic skyrmionium

References

[1] K. Everschor-Sitte, J. Masell, R.M. Reeve, M. Kläui, JAP 124, 240901 (2019).
[2] M. Kläui, K. Everschor-Sitte, O. Lee, R. Msiska et al, Appl. Phys. Lett. 122, 260501 (2023).
[3] M.V. Sapozhnikov, JMMM 396, 338-344 (2015).
[4] R.M. Vakhitov, R.V. Solonetsky, A.A. Akhmetova, M.A. Filippov, Symmetry 14(3), 612 (2022).
[5] M.J. Donahue, D.G. Porter, OOMMF User’s Guide, version 2.0a2 (2019).
[6] D.A. Tatarskiy, JMMM 509, 166899 (2022).

BO1-1O/3

Structure and properties of skyrmion-like inhomogeneities in ferromagnetic films with a columnar defect

Vakhitov R.M. [1], Ilyasova G.F. [1], Solonetsky R.V.[1]

[1] *Ufa University of Science and Technology, 450076, Ufa, Russia*
galiya.siraeva2014@yandex.ru

Currently, there is a steady interest in research related to magnetic skyrmions: their possible types, properties, magnetic materials in which they are stabilized, etc. Such attention to them is explained not only by the prospects for their application in spintronic devices, but also by their unusual properties, which are demonstrated in various works [1]. For the first time, magnetic skyrmions were discovered in chiral magnets, in which, due to the presence of the Dzyaloshinskii-Moriya interaction, they form stable states [2]. In most subsequent studies, magnetic skyrmions were understood as vortex-like inhomogeneities in which the unit magnetization vector ***m*** rotates by 180° when the radial variable r changes from 0 to ∞ (π-skyrmions). At the same time, studies appeared in which the possibility of the existence of $k\pi$-skyrmions ($k \in 1, 2, 3...$) was predicted [3].

Due to the fact that certain problems with the stability of magnetic skyrmions appeared in chiral magnets [4], there was a demand for alternative methods for their stabilization in other materials in which there is no Dzyaloshinskii-Moriya interaction. One of the possible ways to implement this approach was proposed in [4, 5], where it was shown that such magnets can be ferromagnetic films with spatially modulated material parameters. Later it was established (both experimentally [4] and theoretically [5]) that magnetic skyrmions can exist in such materials in a wide range of temperature and magnetic fields.

In this paper, we study the stable states of magnetic $k\pi$-skyrmions formed on columnar defects of the "potential well" type in uniaxial ferromagnetic films [5]. Such studies in non-chiral magnets have not yet been carried out, except for [6], where the effect of a magnetic field on $k\pi$-skyrmions ($k \in 2,3,4$) that appear in Fe_3Sn_2 magnetic nanodisks was studied. As a defect model, we consider the structural inhomogeneity of a magnet, in which the material parameters $P = \{A, K_u, M_s\}$ change abruptly in the region of the defect:

$$P = \begin{cases} P_1, r > R_0 \\ P_2, r \le R_0, \end{cases} \quad (1)$$

where $P_i = \{A_i, K_{ui}, M_{si}\}$ are the material parameters outside the columnar defect (i = 1) and in the region of the defect (i = 2), A is the exchange parameter, K_u is the uniaxial anisotropy constant, and M_s is the saturation magnetization.

Numerical analysis of the Euler–Lagrange integro-differential equation, which describes the distribution of magnetization in the region of a defect, taking into account the energy of magnetic inhomogeneities [5], makes it possible to find the distribution of magnetization ***m*** in the region of a columnar defect and its characteristics: the characteristic sizes of $k\pi$-skyrmions and their energy. It should be noted that all parameters having the dimension of length are reduced to the value $\Delta_0 = \sqrt{A_1/K_{u1}}$, where Δ_0 is the characteristic size of the domain wall in uniaxial ferromagnets. Based on the calculations of the structure and stability of $k\pi$-skyrmions, it follows that they can exist as stable formations in magnetically uniaxial films on columnar defects of the potential well type.

The topology and dimensions of these inhomogeneities essentially depend on the characteristics of the defect (A_2, K_{u2}, M_{s2}, R_0) and, above all, on its radius R_0 and the depth of the potential well K_{u2}. Studies show that the π-skyrmion is more energetically favorable, and $3\pi,5\pi$-skyrmions exist as metastable states. In addition, diagrams of stable states of $k\pi$-skyrmions were constructed (Fig. 1.), where the lower threshold of stability of π-skyrmions with respect to the size of the defect starts from small R_0 ($R_0 \geq 1$), 3π-skyrmions - from large R_0 ($R_0 \geq 14$), and 5π-skyrmions - from even larger R_0 ($R_0 \geq 25$).

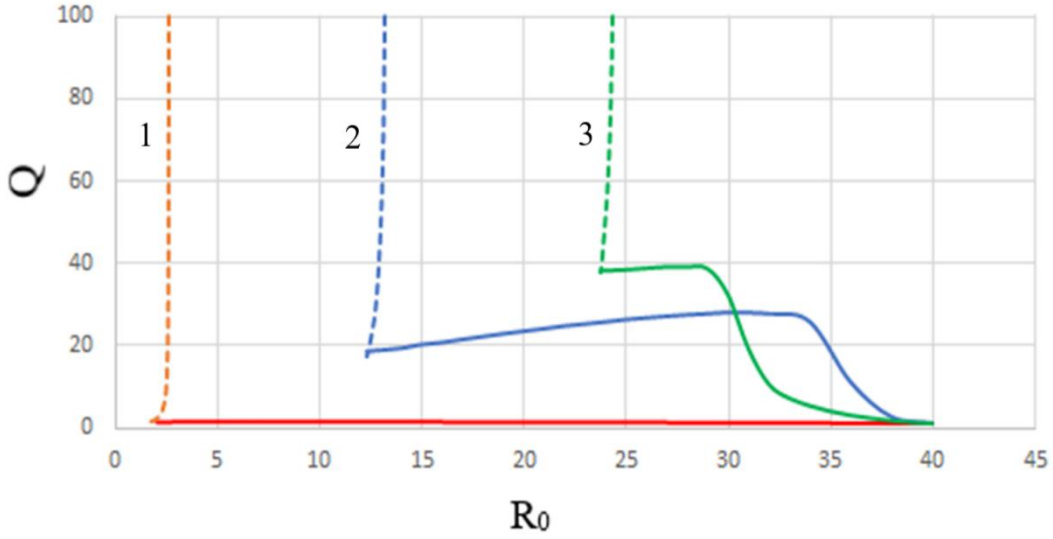

Fig. 1. Stability region diagram for 1-π-skyrmion (red line), 2-3π-skyrmion (blue line), 3-5π-skyrmion (green line) for the following values of material parameters $K_{u2} = -2K_{u1}$, $A_2 = A_1$, $M_{s2} = M_{S1}$.

References

[1] K. Everschor-Sitte, J. Masell, R.M. Reeve, et al, J. Appl. Phys. 124, 240901 (2018);
[2] S.Muhlbauer, B.Binz,F.Jonetz, A.Neubauer, Georgii, Science, 323, 915 (2009).
[3] Julian Hagemeister, Ansgar Siemens, Levente Rózsa, Elena Y. Vedmedenko, and Roland Wiesendanger Phys. Rev. B 97, 174436 (2018)
[4] M. V. Sapozhnikov, S. N. Vdovichev, O. L. Ermolaeva, N. S. Gusev, A. A. Fraerman, S. A. Gusev, Y. V. Petrov, Appl. Phys. Lett., 109, 042406 606 (2016).
[5] R. M. Vakhitov, R.V. Solonetsky, A. A. Akhmetova, J. Appl. Phys., 128, 000000 (2020)
[6] Jialiang Jiang, Yaodong Wu, Lingyao Kong, Yihao Wang, Junbo Li, Yimin Xiong, Jin Tang Acta Materialia, 215 (2021) 117084

BO1-1O/4

Discrete thermokinetic computational model of laser-induced phase transitions in phase-change materials

A.A. Nevzorov, V.A. Mikhalevsky, N.N. Eliseev, A.V. Kiselev, A.A. Burtsev, V.V. Ionin, D.N. Khmelenin, and A.A. Lotin

ILIT RAS — Branch of FSRC "Crystallography and Photonics" RAS, 1, Svyatoozerskaya Str., 140700, Shatura, Moscow Region, Russia
terrapevt@mail.ru

Phase change materials (PCM) are a unique class of solid materials with a high contrast of electrical and optical properties of the amorphous and crystalline phases [1]. Recently GST_{225} emerged as an important candidate for the electronic nonvolatile memory devices [2]. By utilizing the difference in optical properties between different phases, researchers have developed GST-based reconfigurable light modulators, optical limiters, optical switches, and polarizing reflectors [3].

In order to develop and optimize PCM-based devices, one should have a reliable model describing the effect of optical pulsed impact on the phase state and dynamics of the device properties. The formalism based on the Johnson–Mel–Avrami–Kolmogorov (JMAK) theory is violated in real PCM-based devices [4]. Gillespie cellular automata-based models and two-temperature approaches taking into account the interaction of electrons with lattice atoms at ultrashort pulses are often based on indirect data and are difficult to prove experimentally [5]. We present a model based on the thermokinetic approach with corrective parameters to be selected according to the experimental results. Phase transformations shall be analyzed based on the transmission electron microscopy and Raman spectra of GST_{225} thin film samples irradiated with nano- and femtosecond laser pulses with different energy fluences [6].

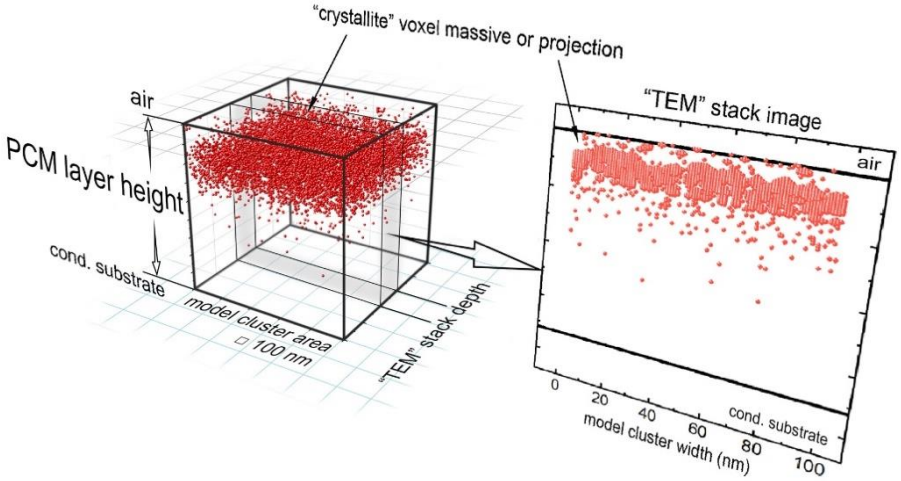

Fig. 1 - 3D model of a film computational cluster area and virtual "TEM image" obtained from "TEM" layer stack

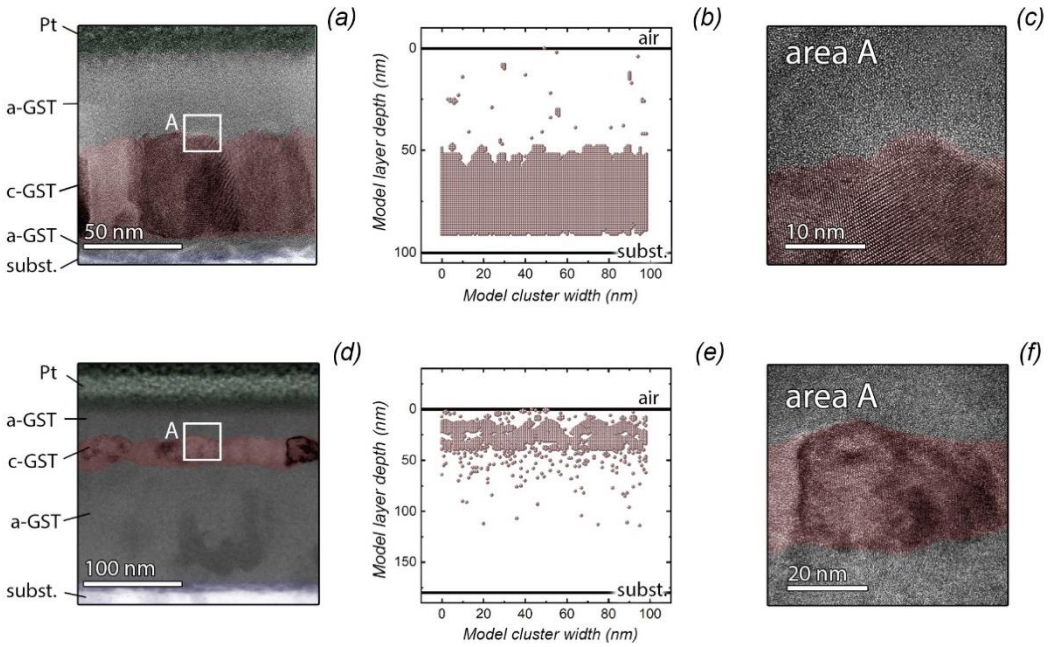

Fig. 2 - TEM image and the result of structure modeling after exposure to two laser pulses. a - TEM image after exposure to nanopulses, b - virtual "TEM image" for nanopulses, c - enlarged scale of TEM for nanopulses, d - TEM image after exposure to femtopulses, e - virtual "TEM image" for femtopulses, f - enlarged scale of the crystalline layer.

The developed model plausibly describes the processes of phase transformations in PCM films induced by laser pulses. The analysis of the phase transformation dynamics obtained during the model operation can be used to substantiate the main physical processes occurring in PCM thin films after impact of laser pulses. The use of this model can help to optimize the duration, shape, and spatial distribution of laser pulses for controlling the state of thin-film PCM-based devices [7].

References

[1] M. Wuttig, N. Yamada. Nat. Mater. 6, 824–832 (2007).

[2] W. Zhang, R. Mazzarello, M. Wuttig and E. Ma. Nature Reviews Materials, 4, 150–168 (2019).

[3] P. Guo, A. M. Sarangan and I. Agha. Applied Sciences, 9, 3, 530 (2019).

[4] P. Ashwin, B. S. V. Patnaik, and C. D. Wright. J. Appl. Phys. 104, 8, 084901 (2008).

[5] Q. Yang, et al. Mater. Sci. Eng. B, 193, 189–197 (2015).

[6] A. A. Nevzorov, V. A. Mikhalevsky, N. N. Eliseev, et. al. Appl. Phys. Lett. 122, 191106 (2023)

[7] J. Wang, L. Wang, J. Liu. IEEE Access., 8, 121211-121245 (2020).

BO1-1O/5

Coupled spin-orbit dynamics of an anisotropic ferromagnet

Butrim V.I., Osmanov R.S.

V.I. Vernadsky Crimean Federal University, Simferopol, Russian Federation
butrimv@mail.ru

In this paper, the dynamics of the angular momentum of a simple anisotropic single-element ferromagnet is considered with sequential consideration of both spin and orbital degrees of freedom, taking into account the incomplete "freezing" of the orbital moment. Special attention is paid to the effects of competition between spin magnetic anisotropy and the crystal field.

We will consider for FM, in which magnetic ions have an orbital moment l equal to one and some arbitrary spin value S. The quantum microscopic Hamiltonian includes the energy of the spin orbital interaction with a positive constant, the energy of the crystal field with constants and, the energy of uniaxial magnetic anisotropy with a constant, is the constant of the exchange interaction of spins.

$$\hat{H} = \sum_{\mathbf{n}} \left[\lambda \hat{\mathbf{S}}_{\mathbf{n}} \hat{\mathbf{l}}_{\mathbf{n}} - J \sum_{\mathbf{a}} \hat{\mathbf{S}}_{\mathbf{n}} \hat{\mathbf{S}}_{\mathbf{n+a}} - C \hat{l}^2_{\mathbf{n},z} + B \hat{l}^2_{\mathbf{n},y} - K \hat{S}^2_{\mathbf{n},z} \right] \quad (1)$$

Here and are the operators of the spin and orbital moments in the node.

The procedure of transition from the quantum description to the classical one is carried out by averaging over generalized coherent states [1,2]. In this case, the average value of the Hamiltonian (1) represents the energy of the system. Minimizing this energy allows us to establish that one of three phases is realized in the ground state: the collinear phase of CF1 with a quantization axis along the axis, the collinear phase of CF2 with a quantization axis along , for which or the angular phase (UV). The length of the orbital moment in collinear phases.

$$l_0 = |< \hat{\mathbf{l}} >| = \frac{2\lambda S l}{\sqrt{4\lambda^2 S^2 + (B + C\sin^2\alpha_0)^2}} \quad (2)$$

Here for the CF1 and CF2 phases, respectively. The conditions of phase stability are found and a phase diagram of states is constructed. Phase transitions between the angular phase and collinear phases are second-order OP.

The spectrum of magnetic oscillations contains three branches of different types. One branch of the longitudinal oscillations of the orbital moment length and two transverse modes corresponding to the associated oscillations of the spin and orbital moment components. For collinear phases , the longitudinal mode is dispersionless with frequency . The laws of dispersion of coupled spin orbital oscillations are studied in detail

References

[1] V.I.Butrim, Low Temp. Phys. 40, 508 (2014).

[2] T. Satoh, R. Iida, T. Higuchi, Y. Fujii, A. Koreeda, H. Ueda, T. Shimura, K. Kuroda, V. I. Butrim & B. A. Ivanov, Nat. Comm. 8, 638 (2017).

BO1-1O/6

Anomalous current-voltage characteristics of SFIFS Josephson junctions with weak ferromagnetic interlayers

A.V. Guravova [1] , T.Karabassov [1] , E. A. Kazakova [2] , A. S. Vasenko [1]

[1] *National Research University Higher School of Economics, 101000 Moscow, Russia*
[2] *Sechenov First Moscow State Medical University, 119991 Moscow, Russia*
avasenko@hse.ru

We present a quantitative study of the current-voltage characteristics (CVC) of SFIFS Josephson junctions (S denotes bulk superconductor, F - metallic ferromagnet, I - insulating barrier) with weak ferromagnetic interlayers in the diffusive limit. The problem is solved in the framework of the nonlinear Usadel equations. We consider the case of a strong tunnel barrier such that the left SF and the right FS bilayers are decoupled. We calculate the density of states (DOS) in SF bilayers using a self-consistent numerical method. Then we obtain the CVC of corresponding SFIFS junctions, and discuss their properties for different set of parameters including the thicknesses of ferromagnetic layers, the exchange field, and the magnetic scattering time [1]. We observe the anomalous nonmonotonic CVC behavior in case of weak ferromagnetic interlayers, which we ascribe by DOS energy dependencies in case of small exchange fields in F layers [1].

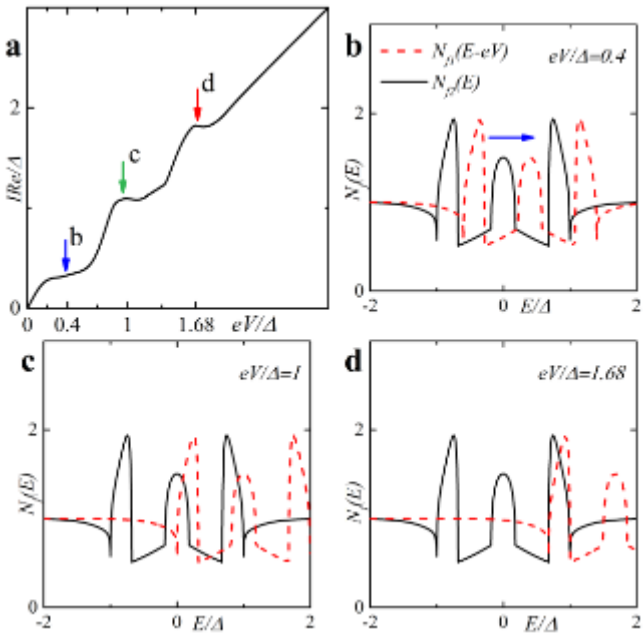

Fig. 1: *The explanation of the characteristic behavior of the quasiparticle current in a SFIFS junction (a). Plots (b)-(d) show the DOS N(E) in the left SF (solid black line) and the right FS (dashed red line) bilayers at particular value of bias voltage eV revealing the origin of the current features in plot (a). See details in [1].*

References

1. T. Karabassov, A. V. Guravova, A. Yu. Kuzin, E. A. Kazakova, S. Kawabata, B. G. Lvov and A. S. Vasenko, Beilstein Archives (2019), doi:10.3762/bxiv.2019.140.v1

BO1-1O/7

Phase states and excitation spectra of a non-Heisenberg ferrimagnet

Matyunina [1]Ya.Yu., Yarygina [1]E.A., Kosmachev [1]O.A., Fridman [1]Yu.A.

[1]*V.I. Vernadsky Crimean Federal University, 295007, Simferopol, Russian Federation*
yuriifridman@gmail.com

It is well known that the effects of exchange amplification of dynamic parameters, similar to those known for antiferromagnets, occur for ferrimagnets located in the vicinity of the sublattice compensation point, which makes it possible to use ferrimagnets in various devices of microelectronics and spintronics.

The dynamic and static properties of a non-Heisenberg (isotropic and anisotropic) ferrimagnet with sublattices S=1 and $\sigma = 1/2$. The Hamiltonian of the model under study has the form:

$$H = -\frac{1}{2}\sum_{n,n'}\left[J^{(2)}\left(n-n'\right)(\mathbf{S}_n\mathbf{S}_{n'}) + K\left(n-n'\right)(\mathbf{S}_n\mathbf{S}_{n'})^2 \right] - \frac{1}{2}\sum_{m,m'} J^{(1)}\left(m-m'\right)(\boldsymbol{\sigma}_m\boldsymbol{\sigma}_{m'}) -$$
$$-\frac{1}{2}\sum_{n,m} A\left(n-m\right)\left(\boldsymbol{\sigma}_m\mathbf{S}_n\right) + \frac{\beta}{2}\sum_n \left(S_n^x\right)^2 \qquad (1)$$

where $J^{(1)}>0$ is the exchange interaction constant for a sublattice with spin σ=1/2; $J^{(2)}>0$, K>0 – constants of bilinear and biquadratic exchange interactions for S=1; A<0 – intersublattice interaction constant, $\beta > 0$ – single-ion anisotropy constant of the "easy plane" type (ZOY basal plane).

It is shown that in the isotropic case ($\beta = 0$) or in the case of low anisotropy ($\beta << J, K$), two phase states can be realized in the system: at $J > K$, a ferrimagnetic phase (FiM) with a maximum value $\langle S^z \rangle = 1$ (the second sublattice $\langle \sigma^z \rangle = 1/2$ is the "magnetizing field") is realized, and at $J < K$, a quadrupole-ferrimagnetic phase is realized (QFiM), in which $\langle S^z \rangle < 1$. The phase transition FiM-QFiM in the isotropic case is a second-order transition, and if even a small single-ion anisotropy is taken into account, the "easy plane" changes the type of phase transition to a first-order phase transition.

In addition, in QFiM, under certain material parameters, the effect of sublattice spin compensation is realized.

The phase diagram of a non-Heisenberg ferrimagnet is constructed in both isotropic and anisotropic magnets. Phase transition lines and sublattice spin compensation lines are determined.

The work was supported by the Russian Science Foundation (grant no. 23-22-00054)

References

[1].B.A. Ivanov, Low Temp. Phys. 45, 935 (2019)
[2].A. V. Krivtsova, Ya. Yu. Matyunina, and Yu. A. Fridman JETP 131, 302 (2020)

BO2-1O/1

Determination of the isotropic gap for iron borate film taking into account the higher-order magnetoelastic invariants

Prilepsky D.Yu., Mogilenec Yu.A., Seleznyova K.A., Yagupov S.V., Strugatsky M.B.

[1]*Physics and Technology Institute, Crimean Federal University, Simferopol, Russia*
prilepskii.ivan@yandex.ru

Our AFMR studies [1] of a recently synthesized thin magnetic film of iron borate, $FeBO_3$ on an isostructural diamagnetic gallium borate, $GaBO_3$ substrate (Fig. 1) [2] have shown that the isotropic energy gap, H_Δ^2, of a low-frequency AFMR mode, $n = g\left[H\left(H + H_D\right) + H_\Delta^2\right]^{\frac{1}{2}}$, is significantly larger for the film in comparison with those for a $FeBO_3$ single crystal. Such an increase, apparently, is due to significant deformations u that occur in the iron borate film due to a mismatch between the crystal lattice parameters of the film and the substrate. However, the isotropic gap does not explicitly depend on the deformations: $H_\Delta^2 : B^2/C$, B and C being magnetoelastic and elastic constants, respectively. The elastic constants are almost independent on the deformations, see *e.g.* [3].

The experimental results can be interpreted under the assumption that the magnetoelastic constants B linearly depend on the deformations [1]. It means the existence in the thermodynamic potential of new magnetoelastic invariants that are quadratic in the components of the deformation tensor $\boldsymbol{u}$ and the antiferromagnetic vector $\boldsymbol{l}$: $l_i l_j u_{kl} u_{mn}$. Such invariants should be used along with the well-known invariants that are linear in deformations: $l_i l_j u_{kl}$. In the present work we have obtained an expression for a low-frequency AFMR mode using abovementioned extended thermodynamic potential. As a result, we have estimated the deformations caused by the mismatch between the crystal lattice parameters of the film and the substrate that lead to experimentally determined values of the magnetoelastic gap in iron borate.

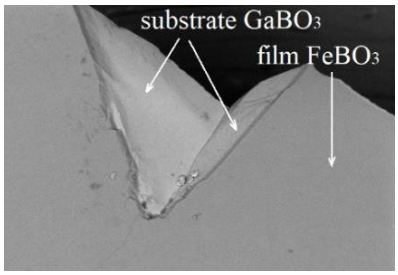

Fig. 1. $FeBO_3$ film on $GaBO_3$ substrate.

A support by the RSCF and the Ministry of Education, Science and Youth of the Republic of Crimea, in the framework of scientific project Grant no. 22-22-20112 is acknowledged.

References

[1] K. Seleznyova, Yu. Mogilenec, D. Prilepsky *et al*., J. Appl. Phys. 128(12), 1055 (2022).
[2] S. Yagupov, M. Strugatsky, K. Seleznyova *et al*., J. Magn. Magn. Mater. 417**,** 338 (2016).
[3] D. P. Dandekar, Phys. Rev. 172, 873 (1968).

BO2-1O/2

Electronic structure and exchange interactions in $Mn_{2-x}Zn_xSb$

Golovchan A.V.[1],Nirkov N.Yu.[1], Andreychenko E.P.[1], Mitsiuk V.I.[2], Mashirov A.V.[3]

[1]*Galkin Donetsk Institute for Physics and Engineering, 283048, Donetsk, DPR, Russia*
[2] *Scientific and Practical Materials Research Centre, National Academy of Sciences of Belarus, Minsk, 220072 Belarus*
[3] *Kotelnikov Institute of Radio Engineering and Electronics, Russian Academy of Sciences, Moscow, 125009 Russia*
golovchan1@yandex.ru

The recent active study of magnetic materials based on manganese pnictides has been stimulated by the wide variety of magnetic phase transformations found in them and, as a consequence, by the large value of the inverse magnetocaloric effect. The latter makes it possible to significantly simplify the design of magnetic refrigerators and reduce heat losses on structural elements. A promising system for magnetic cooling in the cryogenic temperature range is the $Mn_{2-x}Zn_xSb$ system, in which an order–order transition is observed in the region of 100 K. In the presented work, an *ab initio* calculation of the electronic structure and an estimation of the parameters of interatomic exchange interactions[1] were performed using the fully-relativistic SPRKKR package(Fig.1).

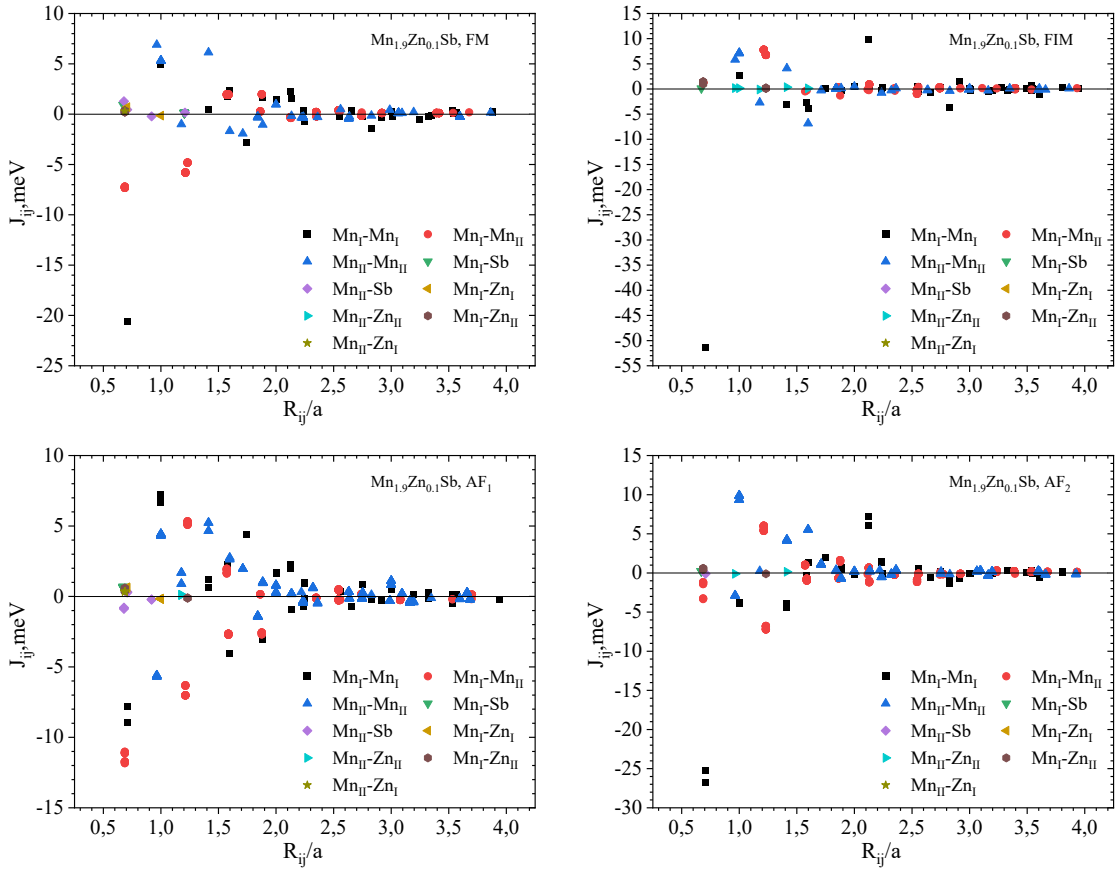

Fig.1. The isotropic exchange coupling parameters J_{ij} for $Mn_{1.9}Zn_{0.1}Sb$.

References

[1] A.I. Liechtenstein et al., JMMM. 67, 65 (1987).

BO2-1O/3

Detection of Packing Defects by X-ray Diffraction with Synchrotron Radiation Using

Akimova O.V.

Faculty of Physics, Lomonosov Moscow State University, Moscow, Russia
akimova@physics.msu.ru

The development of high-tech technologies requires the expansion of opportunities to influence the structurally sensitive properties of materials [1]. For palladium-based metal alloys, this complex problem isn't finally solved at present. Its solution requires the study of subsystems of defects formed by atoms of different grades in the crystal lattice of palladium [2]. In this work the problem of establishing the possible presence of one of the most widespread defects of the crystal lattice - packing defects (PD) - in palladium-lead alloys based on the results of X-ray diffraction is set. The problem posed in this work is relevant: PD can influence the processes of plastic deformation of the material, hardening and fracture [3].

In our papers on palladium membrane alloys with indium, ruthenium and lead, we are reported onto nanodispersed substructure of samples and features introduced by various palladium-alloying elements. [4-6]. In this work, the study of subsystems of defects in the crystal lattice of palladium deformed by the introduction of its alloying elements is continued. The calculation of PD concentration is carried out based on the values of the effective size of the coherent scattering regions (CSR) determined in [4-6] by the Williamson–Hall method [7]. The calculation of the content of the PD is carried out according to Formula (1) [8].

$$\frac{1}{D_{эф}} = \frac{1}{D} + \frac{1.5\alpha + \beta}{a(u+b)h}\sum_{b}|L| \qquad (1)$$

where D is the size of CSR(hkl) if we are taking into account the influence of PD onto diffraction pattern; *a* is lattice period of palladium alloys; u is the number of components of lines {HKL}, which can't shifting in the presence of PD; bis the number of components of lines {HKL}, which can shifting in the presence of PD; |L|=3q±1(q=0,1,2…); (1.5α+β) takes into account deformation and twin packing errors in crystal lattice, which is PD.

As one can see from Table 1, the effect of palladium–alloying elements on the crystal lattice, and, therefore, on the functional properties, is not uniquely determined by the geometric dilation parameter δ_{Pd}, which is evaluated using the lattice period of palladium alloys. This problem is complex.

Table 1. Fraction of PD, effective size of CSR(100) and CSR(111), dilatation of the palladium crystal lattice.

Alloys (wt. %)	$<D_{ef100}>$, nm	$<D_{ef111}>$, nm	*a*, nm	δ_{Pd}, 10^{-2}	PD, fraction	D, nm
$Pd_{93.5}In_{6.0}Ru_{0.5}$ [4]	32	34	0.39077±0.00007	0.41	0.005	34
$Pd_{95.0}Pb_{5.0}$ [5]	24	32	0.39054±0.00008	0.36	0.029	34
$Pd_{79.4}Pb_{20.6}$ [5]	18	37	0.39525±0.00014	1.58	0.079	45

$Pd_{93.0}Ru_{7.0}$ [6]	23	37	0.38939±0.00005	0.18	0.045	24

The obtained results are undoubtedly important in the light of solving the problem of influence on the structurally sensitive properties of materials.

References

[1] J.J. Conde, M. Maroño, J.M. Sánchez-Hervás, Sep. & Purif. Rev. 46, 152 (2017).
[2] S. Queyreau, G. Monnet, B. Devincre, Acta Mater. 58, 5586 (2010)
[3] O.P. Maksimkin, Packing defects, their energy and influence on properties of irradiated metals and alloys (Almaty, 2010).
[4] O.V. Akimova, R.D. Svetogorov, Mater. Today: Proc. 38, 1416 (2021)
[5] O.V. Akimova, R.D. Svetogorov, A.V. Ovcharov, N.R. Roshan, Membranes, 12, 1132(2022)
[6] O.V. Akimova, A.V. Ovcharov, N.R. Roshan, Scientific Lomonosov conference MSU, 64, (2023)
[7] G.K. Williamson, W.H. Hall, Acta Metall. 1, 22 (1953)
[8] V.I. Iveronova, G.P. Revkevich, Theory of X-ray scattering (Moscow, MSU, 1978)

BP1-1P/1

Optical excitation and registration of spin dynamics in epitaxial film of cation-substituted iron garnet with magnetic compensation temperature

Prilepsky I. V.[1], Prisyazhnyuk A. V.[1], Polulyakh S. N.[1], Berzhansky V. N.[1], Gusev N. A.[2], Ignatyeva D. O.[2,3]. Zvezdin A. K.[2], Belotelov V. I.[1,2,3]

[1] *Vernadsky Crimean Federal University, 295007, Simferopol, Russia*
[2] *Russian Quantum Center, 121205, Moscow, Russia*
[3] *Lomonosov Moscow State University, Moscow, 119991, Russia*

Ferrimagnetic materials having the magnetic compensation temperature are attractive object to study spin dynamics in different magnetic phases. We have taken an epitaxial film of $(YBiLu)_3(FeGa)_5O_{12}$ iron garnet with a thickness of 3.5 mkm as a sample of such material. The sample has two magnetic sub-lattices formed by Fe^{3+} ions in octahedral and tetrahedral garnet positions. Octahedral contribution dominates below the compensation temperature $T_C \approx 333K$. The magnetization of tetrahedral iron overcomes the octahedral magnetization above the compensation temperature up to the Neel temperature $T_N \approx 358K$.

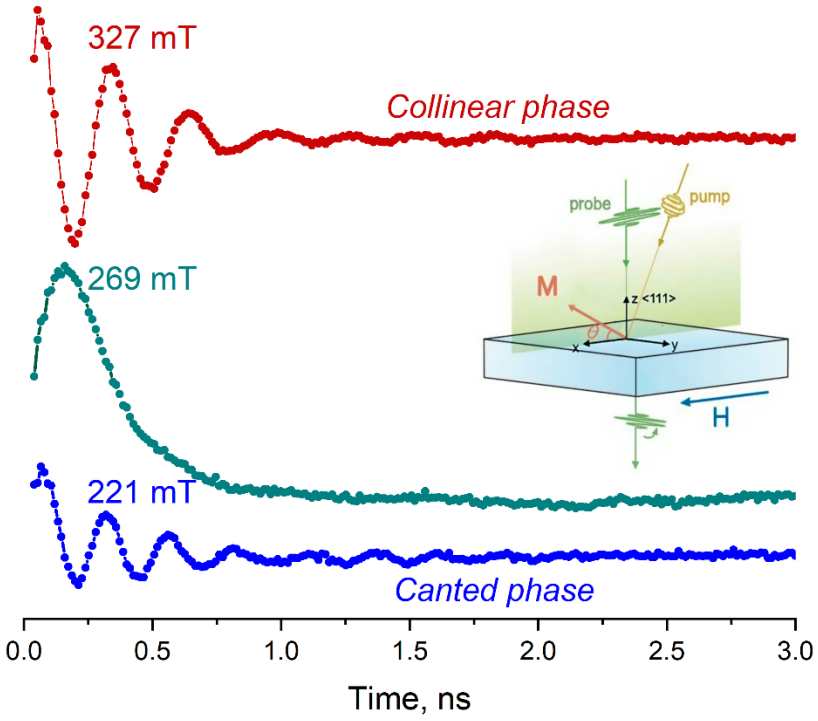

Fig. 1. Pump-probe experiment, the time dependence of Faraday rotation at the temperature $T = 298\ K$ in different magnetic fields.
Schema of the pump-probe experiment (inserted picture).

The film of cation-substituted iron garnet has (111) orientation and demonstrates «easy-axis» magnetic anisotropy. The in-plane magnetic field results the non-collinear (canted) magnetizations near the compensation temperature. The field range of the non-collinear region depends on the temperature. To perform the experiments we have applied the in-plane magnetic

fields below some critical value, where the increasing field narrows the temperature range of non-collinear magnetization.

We have used the optical (wavelength $\lambda = 787\ nm$) pump pulses of femtosecond range to excite the spin dynamics due to the optomagnetic inverse Faraday effect. The circular polarized light influences on the magnetization like an effective magnetic field that deviates magnetization from equilibria and starts magnetization precession.

The registration of magnetization has been performed with the magneto-optical Faraday effect. We have used linearly polarized probe light of the wavelength $\lambda = 516\ nm$. The probe time scale we selected to register the low-frequency branch of magnetization precession that corresponds to the quasy-ferromagnetic mode. The contribution of the high-frequency precession with fast decay corresponding to the qasy-antiferromagnetic mode is out of registration for a selected time-scale.

The results of pump-probe experiments in different magnetic fields at the temperature $T = 298\ K$ are given in the figure 1. The field 221 mT corresponds to the non-collinear phase while the collinear phase presented by a dependence for the field 327 mT. The transition between collinear and canted phases we consider as a field-stimulated phase transition of the second order. The decay of spin dynamic in the region of phase transition is presented by a dependence for the field 269 mT in the figure 1.

We have defined frequency and magnitude of spin precession approximating experimental data by the decaying sine function. The field increase results the frequency decrease of and the magnitude increase in the canted phase. On the contrary, the field grows above the phase transition field increases the frequency and decreases the magnitude of spin precession. The critical magnetization decay takes a place in the phase transition region.

To detect the regions of different magnetic phases we have used additional experiments to measure the static field influence on the Faraday rotation in the studied sample. The results of these experiments confirm the data of pump-probe measurements.

We have evolved the theory of spin dynamics for the two-sublattice ferrimagnetic materials with the magnetic compensation temperature. The theoretical results agree the experimental data.

This work was supported by the Russian Science Foundation, project № 23-62-10024.

BP1-1P/2

Light-modified cubic anisotropy in (111) epitaxial films of impure iron garnet

Polulyakh S. N.[1], Avdeenko D .V.[1], Berzhansky V. N.[1], Semuk E. Yu.[1], Popov V. V.[1], Vetoshko P. M.[2], Belotelov V. I.[3]

[1]*V. I. Vernadsky Crimean Federal University, 295007, Simferopol, Russia*
[2] *Kotelnikov Institute of Radioengineering and Electronic, 125009, Moscow, Russia*
[3] *Lomonosov Moscow State University, 119991, Moscow, Russia*
danila.avdeenko@mail.ru

To study the photo-induced magnetic anisotropy in epitaxial films of cation-substituted iron garnet we have improved a magneto-optical method proposed in work [1] for magnetic sensor. We have used (111) oriented garnet films of combined cubic and easy-plane magnetic anisotropy. The controlled magnetic field up to 100 Oe revolves in the film plane. Rotating field result the rotation of film magnetization with the same speed, but magnetization is not parallel to the filed. The out-of-plane magnetization appears due to the cubic anisotropy. The maxima values of out-of-plane magnetization take a place when magnetic field is directed along projection of trigonal <111> axis on film plane (Fig.1a).

To measure the out-of-plane magnetization we have applied magneto-optical Faraday effect with low-power probe laser. To enhance Faraday rotation we have selected films of bismuth-substituted yttrium iron garnet $(BiY)_3(FeGa)_5O_{12}$, epitaxially synthesized on the (111) substrate of gadolinium-gallium garnet.

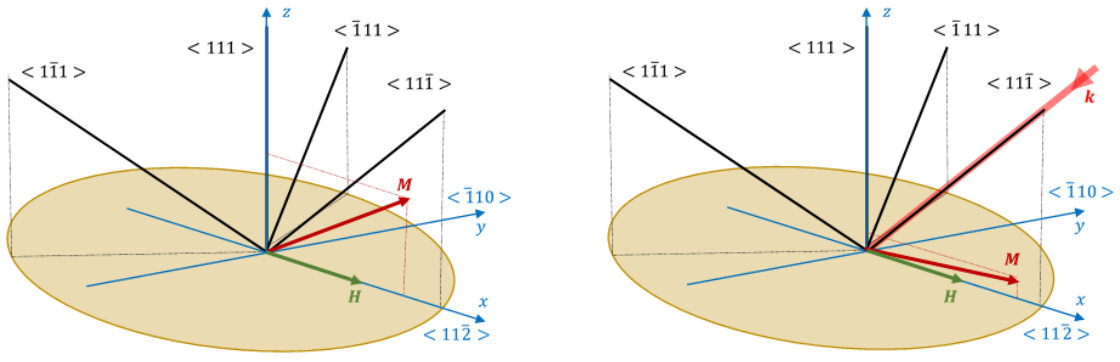

a *b*

Fig. 1. Magnetization ***M*** in (111) iron garnet film. External magnetic field ***H*** is directed along projection of trigonal axis on film plane. Optical pumping is off (a) and optical pumping of wave vector ***k*** is directed along trigonal axis (b).

To modify magnetic anisotropy we have used pumping laser (max power 50 W, light line length 780 nm). The pumping beam directed along a trigonal axis (Fig 1b) decrease out-of-plane magnetization, when magnetic field is directed along pumping beam projection on the film plane. For other two trigonal axises the pumping depress out-of-plane magnetization insignificantly.

We have found the exponential decay of the out-of-plane magnetization M_z due to optical pumping:

$$M_z(t) = M_{z0} - \Delta M_z(1 - \exp(-t/\tau)). \quad (1)$$

Here M_{z0} is out-of-plane magnetization without optical pumping, ΔM_z is optically induced decrease in magnetization, τ^{-1} – decrease rate.

Both magnetization decrease ΔM_z and decrease rate τ^{-1} rise due to the pumping power increase and do not depend on the speed of field rotation in the range from 0.01 rad/s to 1 rad/sec. The influence of pumping polarization is about 10% of main effect that agrees the results of work [2].

To explain the observed phenomena we are using an assumption about influence of Fe^{4+} ions. The tetravalent iron appears due to the charge compensation because platinum and lead impurities come into the garnet film during epitaxial synthesis. Unlike primary for iron garnet trivalent iron, tetravalent iron demonstrate strong spin-orbit interaction and contribute to magnetic anisotropy. Each tetravalent iron contribute to uniaxial anisotropy and anisotropy axis is defined by local symmetry of iron position in garnet crystal. The concentration of tetravalent iron gives the energy of uniaxial anisotropy. If the optical pumping is absent, each trigonal axis give the same contribution into the total anisotropy, which is cubic as a result.

The optical pumping stimulates $Fe^{4+} \leftrightarrow Fe^{3+}$ transitions due to the electron transfer from divalent impure center to iron ions. As a result, optical pumping decreases tetravalent iron concentration. This decrease depends on the pumping beam direction in crystal and is different for different trigonal axises. The symmetry of magnetic anisotropy becomes low then cubic and depends on the direction of optical pumping.

This work was financially supported by the Ministry of Science and Higher Education of the Russian Federation, Megagrant project N 075-15-2022-1108 and Russian Science Foundation (RSF), project N 23-62-10024.

References

[1] A. E. Rogachev, P. M. Vetoshko, N. A. Gusev et al. Appl. Phys. Lett. **109**, 162403 (2016).
[2] S. N. Polulyakh, E. Yu. Semuk, A. K. Zvezdin, et al. JETP Lett. **115**, 196 (2022).

BP1-1P/3

Possible types of discrete breathers and their stability in linear chain of magnetic nanoparticles

I.V. Bychkov [1], D.A. Kuzmin [1], E.G. Ekomasov [2], V.G. Shavrov [3]

[1]*Chelyabinsk State University, 454001, Chelyabinsk, Russia*
[2]*Ufa University of Science and Technology, 450076, Ufa, Russia*
[3] *Kotelnikov Institute of Radio-Engineering and Electronics of RAS, 125009, Moscow, Russia*
bychkov@csu.ru

The work is devoted to the study of the possibility and conditions for the existence of discrete breathers in a chain of magnetic nanoparticles coupled by a dipole-dipole interaction (see Fig. 1). Each particle is an ellipsoid with *a*, *b*, and *c* semiaxes. It is assumed that the size of the particles and the temperature regime make it possible to consider the particles as single-domain particles with a uniform distribution of magnetization. The simulation of the dynamics of magnetization in such a chain of nanoparticles was carried out within the framework of the numerical solution of the Landau-Lifshitz equation, considering the dissipative term in the Hilbert form.

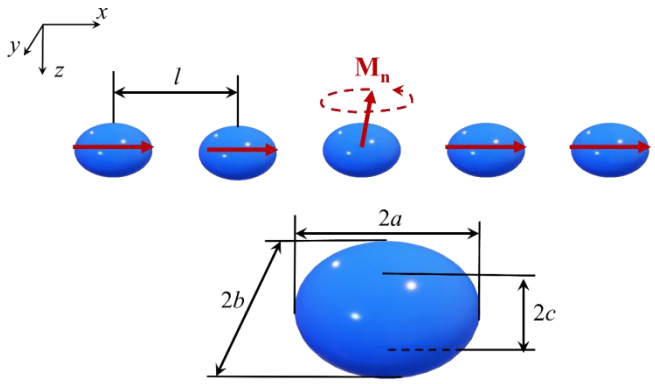

Fig. 1. The chain of ellipsoidal magnetic nanoparticles.

In this chain of magnetic nanoparticles, the existence of solitary periodic solutions (discrete breathers) was found, which are especially pronounced in chains of particles with $a = b >> c$ (i.e., close in shape to disks). In this case, magnetization oscillations occur in the x-y plane, while the *z* component of the magnetization vector remains unchanged. When dissipation is considered, the magnetization vector relaxes to the ground state with $M_z = 0$, and the discrete breather has a finite lifetime. For realistic dissipation parameters, the lifetime of a discrete breather substantially exceeds the oscillation period.

Fig. 2 shows an example of modeling a discrete breather in chains of 50 Ni nanoparticles with dimensions $a = b = 100$ nm, $c = 10$ nm and a distance between particles $l = 300$ nm. During the simulation, the initial deviation of the 25th particle was $M_z = 0.85M_0$, and the magnetizations of all other particles were directed along the x axis.

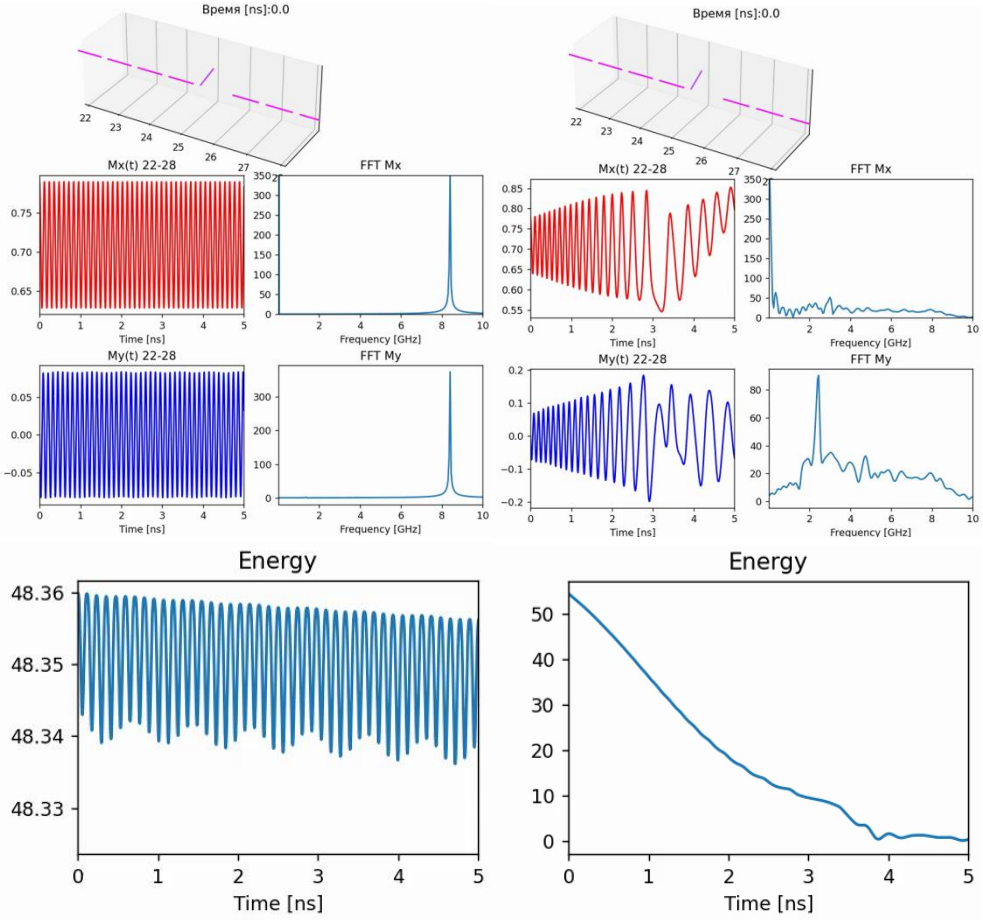

Fig. 2. Discrete breather into chains of 50 Ni nanoparticles. The time dependences of the components of the total magnetization of particles with numbers from 22 to 28, their Fourier transforms, and time evolution of the breather’s energy are presented.

Without dissipation, the magnetization components M_x and M_y oscillate, while the M_z component remains almost unchanged. From the Fourier spectrum, one can estimate frequency of the DB, which is 8 GHz; note that this frequency is determined by the initial deviation of the magnetization. When dissipation is considered, there is a gradual decrease in the frequency of discrete breathers, accompanied by an increase in the amplitude of oscillations of the M_x and M_y components. A qualitative change in the behavior of the system is observed at a time of about 3 ns. Then, oscillations of the magnetization in the *xy* plane are replaced by oscillations in the *yz* plane, i.e., standard magnon vibrations near the equilibrium state. In this case, the M_x component relaxes to the equilibrium state $M_x = 1$. In the Fourier spectrum, one can note a wide band of oscillation frequencies corresponding to a smooth decrease in the oscillation frequency of DBs and a peak at a frequency of 2.5 GHz in the spectrum of M_y, which is absent in the spectrum of M_x, which corresponds to the frequency of linear magnons in the chain. The DB energy also decreases with time.

Support by Russian Science Foundation (22-19-00355) is acknowledged.

BP1-1P/4

Effect of photomagnetic anisotropy and magnetoelastic interactions on FMR in epitaxial iron garnet films

Polulyakh S. N.[1], Kholin A. A.[1], Berzhansky V. N.[1], Semuk E. Yu.[1],
Vetoshko P. M.[2], Belotelov V. I.[3]

[1]*V. I. Vernadsky Crimean Federal University, 295007, Simferopol, Russia*
[2] *Kotelnikov Institute of Radioengineering and Electronic, 125009, Moscow, Russia*
[3] *Lomonosov Moscow State University, 119991, Moscow, Russia*
sunellsters@gmail.com

To record the spectra of ferromagnetic resonance (FMR) or the frequency sweeping at the fixed magnetic field, or the field sweeping at the fixed frequency are used. The authors of work [1] applied the frequency sweeping to record FMR spectra in epitaxial film of cation-substituted iron garnet. They found the light-induced shift of FMR frequency the sign and value of which depends on the magnetic field direction in the film plane. The other result is the fine structure of FMR spectra caused by standing modes of transverse elastic waves along the thickness of the film-substrate structure [1]. Such experiments are impossible using the field sweeping because the substrate thickness gives the dominant contribution into resonance frequencies of elastic waves and these frequencies weakly depend on the magnetic field.

We have applied the frequency sweeping to record FMR spectra of epitaxial iron garnet films in magnetic field directed along the film normal. We have used the vector network analyzer together with the specially designed FMR sensor. We have found experimentally the light-induced increase in the FRM frequency using the optical pumping along the film normal (laser: λ=780 nm, max power 50 W). The observed frequency shift we relate to the effect of photoinduced magnetic anisotropy. Similar to the report [1], we have established the dominant contribution of the polarization independent effects.

The fine structure of FMR spectra caused by elastic waves takes a place too. Unlike the report [1], we have found irregular distances between spectral lines of fine structure. The preferable condition to observe elastic resonances is the big radiofrequency power making asymmetrical FMR spectral line. The possible elastic waves excited due to the magneto-elastic interactions in the film magnetized along the normal is a subject for discussion.

The iron garnet contains trivalent iron only. Technological impurities like platinum or lead appear during epitaxial synthesis and result in divalent or tetravalent iron due to the charge compensation. The divalent iron contribute to the polarization dependent photomagnetic anisotropy while tetravalent iron responses for the polarization independent effects as we suppose.

This work was financially supported by the Ministry of Science and Higher Education of the Russian Federation, Megagrant project N 075-15-2022-1108 and Russian Science Foundation, project № 23-62-10024.

References

[1] S. N. Polulyakh, E. Yu. Semuk, A. K. Zvezdin, et al. JETP Lett. **115**, 196 (2022).

BP1-1P/5

Raman scattering of RCo_3 (R = Y, Ho, Er, Lu) intermetallic compounds

Ponomareva E.A.[1], Neznakhin D.S.[1, 2], Druzhinin A.V.[1, 2] Radzivonchik D.I.[1], Kuznetsova T.V.[1, 2]

[1]*M.N. Miheev Institute of Metal Physics UB RAS, 620137, Ekaterinburg, Russia*
[2]*Ural Federal University, 620002, Ekaterinburg, Russia*
ponomareva@imp.uran.ru

Binary intermetallic compounds RCo_3 (R = Y, Ho, Er, Lu) with trigonal $PuNi_3$-type structure (space group $R\bar{3}m$) have unique magnetic properties such as magnetocaloric effect, magnetostriction and high coercive force, which makes it possible to use them as functional materials [1-2]. The Co magnetic moment depends on the rare-earth element sublattice, and the magnetic state of the compound, in turn, depends on the Co-Co and Co-R exchange interactions. The RCo_3 compounds are ferromagnets for R = Y, Lu, and ferrimagnets for R = Ho, Er [3-4]. The presence of sufficiently high Curie temperatures (≈ 300 – 400 K) makes it possible to analyze the change in the electronic structure at temperatures near the magnetic phase transition using the Raman spectroscopy method.

Raman spectroscopy is an indispensable method for determining changes in a single crystal symmetry under the influence of temperature, pressure or ionizing radiation. Temperature dependent Raman spectra of RCo_3 (R = Y, Ho, Er, Lu) were obtained and changes in the intensities and energies of vibrational modes of rare-earth ions were determined.

The research was supported by RSF project №23-72-00067.

References

[1] J.J.M. Franse and R.J. Radwa´ nski, Handbook of Magnetic Materials (North-Holland, Amsterdam, 1993).
[2] V.N. Fokin, V.B. Son, E.E. Fokina, and B.P. Tarasov, Russ. J. Appl. Chem. 93, 1831 (2020).
[3] Q. He, and Y. Guo, IEEE Trans. Magn. 51, 2101304 (2015).
[4] D.S. Neznakhin, D.I. Radzivonchik, D.I. Gorbunov, A.V. Andreev, J. Šebek, A.V. Lukoyanov, and M.I. Bartashevich, Phys. Rev. B 101, 224432 (2020).

BP1-1P/6

Segregation tendency of Ni-Co-Mn-Z (Z = Ga, In, Sn, Sb) Heusler alloys

Erager K.R., Sokolovskiy V.V., Buchelnikov V.D.

Chelyabinsk State University, Chelyabinsk, Russia
eragerk@rambler.ru

This work presents the results of a study of the properties of $Ni_{2-x}Co_xMn_{1+y}Z_{1-y}$ alloys (x = 0, 0.25, 0.5, and y = 0, 0.25, 0.5 and 0.75) where *Z* = Ga, In, Sn, Sb. The calculations were performed with the help of VASP software package [1], in the GGA-PBE approximation [2]. Two cases of magnetic moment ordering were considered: ferromagnetic - FM and ferrimagnetic - FIM, as well as the arrangement of magnetic moment as «staggered ($tetr_s$)» and «layered ($tetr_l$)». The stability of the compounds was evaluated using the formula:

$$E_{dec} = E_{tot} - \sum_i E_i E_{dec} = E_{tot} - \sum_i E_i,$$

where E_{tot} is the total energy of the alloy, and E_i are the energies of the triple, binary compounds and isolated elements, which were calculated using the above-mentioned potentials, taking into account data from the Materials project electronic resource.

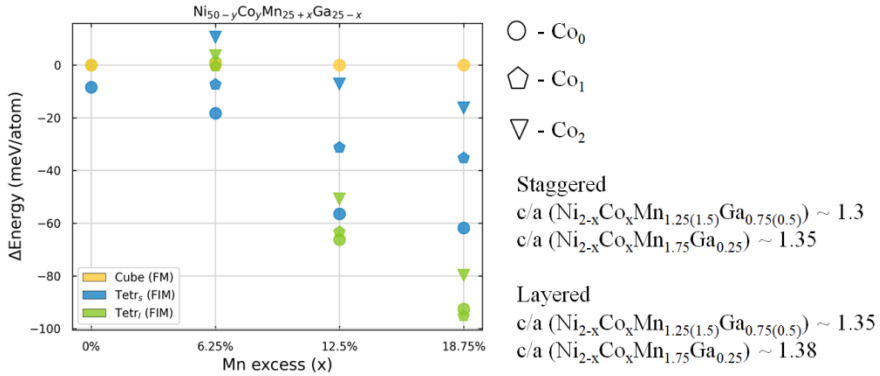

Fig. 1. The total energy of martensitic phases plotted relative to the austenite phase of the $Ni_{2-x}Co_xMn_{1+y}Ga_{1-y}$ alloys.

It is known that increasing the Co concentration in Ni-Co-Mn-Z alloys (Z = Ga, In, Sn, Sb) stabilizes the FM austenitic phase relative to the FIM staggered martensitic phase and results in disappearance the phase transition. However, for tetragonal FIM layered compositions, the opposite dependence is observed as the total energy of the layered martensite increases with increasing Co. In this connection, the main conclusion is that non-stoichiometric Ni-Co-Mn-Z Heusler alloys with a Mn excess of ~12.5% tend to the ground state with FIM layered ordering.

This work was supported by the Ministry of Science and Higher Education of the Russian Federation within the framework of the Russian State Assignment under contract No. 075-01493-23-00. K.R. Erager gratefully acknowledges the Young Scientists Support Fund of the Chelyabinsk State University.

References

[1] G. Kresse, J. Furthmüller. *Phys. Rev. B.*, **54** (1996) 11169.
[2] J. P. Perdew, K. Burke, M. Ernzerhof. *Phys. Rev. Lett.*, **77** (1996) 3865.

BP1-1P/8

Magneto-optical studies of diamagnetically diluted iron borate single crystals

Yagupov S.V., Seleznev K., Strugatsky M.B.

[1]*Physics and Technology Institute, Crimean Federal University, Simferopol, Russia*
yagupov@cfuv.ru

Due to the rare combination of magnetic, elastic, optical and resonance properties, iron borate single crystal, $FeBO_3$, is a unique model object for studies in the field of solid state physics and magnetism. In recent years, the possibilities of high-tech applications of this material have been outlined. Iron borate can be used as an ideal monochromator for synchrotron radiation that is based on nuclear transitions of the Fe^{57} isotope. A modern synchrotron equipped with such a monochromator becomes, in particular, a powerful high-performance facility for Mössbauer studies.

The possibilities of using iron borate in fundamental science and applications are significantly expanded with using diamagnetically diluted $Fe_{1-x}Ga_xBO_3$ crystals. In such materials a part of paramagnetic iron ions is isomorphously substituted by diamagnetic gallium ions. The various mechanisms responsible for the properties of the crystal can change in a different way depending on the degree of diamagnetic dilution. Therefore, it becomes possible studying different mechanisms separately not only in theory, but also in experiment. For the optimal operation of abovementioned monochromators, it is important to decrease the Néel temperature and bring it closer to the room temperature that can be achieved with diamagnetic dilution. Previously, we synthesized a series of $Fe_{1-x}Ga_xBO_3$ crystals in a wide range of substitutions (Fig. 1) [1].

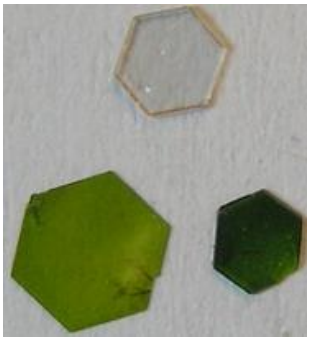

Fig. 1. $Fe_{1-x}Ga_xBO_3$ single crystals.

In the present work, we have carried out magnetometry studies of a series of $Fe_{1-x}Ga_xBO_3$ single crystals with $0 \le x \le 0.14$ that possess magnetic ordering is preserved at room temperature. For this purpose we have designed a highly-sensitive magneto-optical magnetometer that allows studying crystals with weak magnetization. As a result, we have obtained the magnetization curves for single crystals with different x, determined the Faraday rotation angles and the concentration dependence of the Verdet constant for the first time.

A support by the RSCF and the Ministry of Education, Science and Youth of the Republic of Crimea, in the framework of scientific project Grant no. 22-22-20112 is acknowledged.

References

[1] S. Yagupov, M. Strugatsky, K. Seleznyova et al., Appl. Phys. A 121, 179 (2015).

BP1-1P/9

Magnetoelastic invariants of higher orders for a trigonal easy-plane antiferromagnet

Prilepsky D.Yu., Seleznyova K.A., Strugatsky M.B.

[1]*Physics and Technology Institute, Crimean Federal University, Simferopol, Russia*
prilepskii.ivan@yandex.ru

Due to the peculiarities of the crystal and magnetic structure, magnetoelastic effects in trigonal easy-plane antiferromagnets manifest itself quite significantly. The most remarkable representative of such materials is iron borate, $FeBO_3$, single crystal – a transparent antiferromagnet with weak ferromagnetism.

D. Afanasiev *et al*. have observed coherent magnetization oscillations in iron borate single crystal induced by longitudinal acoustic wave; the latter one has been excited by femtosecond laser pulses [1]. The coupling of the magnetic and elastic subsystems has been described under the assumption that the constants *d* and *e*, which appear in the expressions for the magnetic hexagonal anisotropy energy $(½_i)d\,[(l_x+il_y)^3 - (l_x-il_y)^3]l_z$ and $(½)e[(l_x+il_y)^6 + (l_x-il_y)^6]$, depend linearly on the dynamic deformations caused by the acoustic wave. Such assumption is equivalent to constructing new magnetoelastic invariants of the forms $(½_i)G_4[(l_x+il_y)^3 - (l_x-il_y)^3]l_z u_{zz}$ and $(½)G_6[(l_x+il_y)^6 + (l_x-il_y)^6]u_{zz}$. As can be seen, these invariants turn out to be of the fourth and sixth orders in the components of the antiferromagnetic vector $\boldsymbol{l}$ that differs significantly from the usually used second-order invariants $B_{ijkl}l_i l_j u_{kl}$.

AFMR studies of thin magnetic iron borate film on an isostructural diamagnetic gallium borate substrate have shown that the isotropic energy gap of a low-frequency AFMR mode is significantly larger for the film in comparison with those for a $FeBO_3$ single crystal [2, 3]. This result was explained under the assumption that the magnetoelastic constants of iron borate are linearly dependent on the deformations: $B_{ijkl} = B^0_{ijkl} + B^1_{ijklmn}u_{mn}$ [2]. Significant deformations in the iron borate film arise due to the discrepancy between the parameters of the crystal lattice of the film and the substrate. The linear dependence $B(u)$ means the existence in the expression for the thermodynamic potential of new magnetoelastic invariants that are quadratic in the components of the deformation tensor $\boldsymbol{u}$ and the antiferromagnetic vector

In the present work, on the basis of symmetry analysis, here we constructed a complete set of magnetoelastic invariants of the form $G_{ijklmn}l_i l_j l_k l_l u_{mn}$, which are a generalization of some of the invariants given above, and $S_{ijklmn}l_i l_j u_{kl} u_{mn}$.

A support by the RSCF and the Ministry of Education, Science and Youth of the Republic of Crimea, in the framework of scientific project Grant no. 22-22-20112 is acknowledged.

References

[1]. D. Afanasiev, I. Razdolski, K.M. Skibinsky *et al*., Phys. Rev. Lett. 112, 147403 (2014).
[2]. K. Seleznyova, Yu. Mogilenec, D. Prilepsky *et al*., J. Appl. Phys. 128(12), 1055 (2022).
[3]. S. Yagupov, M. Strugatsky, K. Seleznyova *et al*., J. Magn. Magn.
Mater. 417**,** 338 (2016).

BP1-1P/10

Faraday Effect in $FeBO_3$ Caused by the Magnetization Component Parallel to the C_3 Axis

Zubov V.E. [1], Kudakov A.D. [1], Bulatov D.A. [1], Strugatsky M.B. [2], Yagupov S.V. [2]

[1]*Faculty of Physics, Moscow University, Moscow, 119992 Russia*
[2]*Physics and Technology Institute, Crimean Federal University, Symferopol, 295007 Russia*
strugatskymb@cfuv.ru

The Faraday effect in the rhombohedral weak ferromagnet $FeBO_3$, which is due to the magnetization component parallel to the C_3 axis of the crystal, is experimentally observed for the first time. This magnetization component is almost three and a half orders of magnitude smaller than the magnetization in the basal plane. The measured effect is six orders of magnitude smaller than the Faraday effect caused by the magnetization in the basal plane.

The weak ferromagnet iron borate $FeBO_3$ has been well studied by now, but this crystal still attracts attention of researchers as a model object for studying new magnetic properties. Dzyaloshinskii showed that the appearance of a small spontaneous magnetization ($\mathbf{m}_D$) in the basal plane of rhombohedral antiferromagnets is a natural consequence of the symmetry of these crystals [1]. The magnetization $\mathbf{m}_D$ arises when the terms not higher than the second order ones are taken into account in the expansion of the thermodynamic potential of an antiferromagnet in the magnetization components of the sublattices. Spontaneous magnetization is due relativistic spin-lattice interactions of the crystal. The ratio of $\mathbf{m}_D$ to the sum of magnetizations of the sublattices of the antiferromagnet is proportional to the square of the ratio of the velocity of electrons in a crystal to the speed of light $(v/c)^2$ and usually it is 10^{-5}-10^{-2}. When the fourth-order terms of the sublattices magnetization components are taken into account in the thermodynamic potential, the theory predicts the spontaneous magnetization ($\mathbf{m}_z$) along third-order C_3 axis in the crystal perpendicular to the basal plane. The magnetization $\mathbf{m}_z$ is determined by doubly relativistic interactions and its relative magnitude is proportional $(v/c)^4$. The predicted angular dependence of around the C_3 axis is described by the expression $\mathbf{m}_z = \mathbf{m}_{z0} \cos 3\varphi$, where φ is the angle in the basal plane between the direction the line of the intersection of the basal plane with the mirror symmetry plane. The existence of the predicted magnetization component was discovered in hematite (α-Fe_2O_3) [2], iron borate ($FeBO_3$) [2] and in $CoCO_3$ [3]. The measured magnetization along the C_3 axis was several orders of magnitude smaller than the magnetization in the basal plane. In particular, in iron borate, the $\mathbf{m}_z$ value was two and half thousand times smaller than the $\mathbf{m}_D$ value [2]. The order of magnitude and angular dependence of $\mathbf{m}_z$ are in complete agreement with conclusions obtained in [1]. We note the considerable differences between $\mathbf{m}_D$ and $\mathbf{m}_z$: 1) very large differences in magnitude, 2) $\mathbf{m}_D$ lies in the basal plane of the crystal and its magnitude is independent of the orientation in this plane, 3) $\mathbf{m}_z$ is perpendicular to the basal plane, and when rotating $\mathbf{m}_D$ and spins of magnetic sublattices around C_3 axis by 360^0, the component $\mathbf{m}_z$ changes its sign six times. Thus, there are two mutually perpendicular magnetization components in the sample that are completely different in their properties.

Magneto-optical effects linear in magnetization were observed in all magnets with a spontaneous magnetic moment: ferromagnets, amorphous ferromagnets, ferrimagnets, and weak ferromagnets. Therefore, it is natural to assume the possibility of linear magneto-optical effects in

rhombohedral antiferromagnets due to the magnetization component $\mathbf{m}_z$, in particular, the magneto-optical Faraday effect.

Iron borate single crystals are transparent in the visible region of the spectrum. Therefore, among magneto-optical effects linear in magnetization (Faraday effect, Kerr effects, etc.) the Faraday effect is the most suitable for solving the problem, since its value usually exceeds the value of other indicated effects by several orders of magnitude. The studied samples were thin green plates parallel to the basal plane of the crystal with transverse dimensions ~3mm. The thicknesses of the samples were 5 and 8 μm. Among the available samples, the thinnest ones chosen because they have high optical homogeneity and perfect facets. The measurements were carried out in the transparency region of iron borate. An arc xenon lamp served as a light source. Light from the source passes through the polarizer, then the sample and then through the analyzer, the polarization plane of which is rotated to the polarization plane of the polarizer by an angle of 45^0. As a result, the rotation of the polarization plane of the light passing through the sample is converted after the analyzer into a change in the light intensity. The sample was placed in a rotating magnetic field whose rotation plane coincided with basal plane of the $FeBO_3$ crystal. The rotating magnetic field was produced by two pairs of identical Helmholtz coils perpendicular to each other. The phase of the current in the pairs of coils differed by 90^0. The frequency of the rotating magnetic field was f=265 Hz, and its magnitude was 10 Oe, which is an order of magnitude higher than the saturation field in the basal plane of the samples. Light was directed along the C_3 axis. The Faraday effect was measured at the triple frequency 3f. The signal from the photomultiplier tube was fed to a selective measuring amplifier tuned to the frequency 3f and then to the phase detector tuned to the same frequency.

The Faraday effect due to component $\mathbf{m}_z$, with a period of 120^0 at the rotation of the sample around the C_3 axis was found in both samples 5 and 8 μm thick. The experimental points are approximated by a sinusoid. The amplitude of the sinusoid for the first and second sample was $\alpha_0=(2.3\pm0.5)\cdot10^{-3}$ deg/cm, для второго – $\alpha_0=(1.9\pm0.5)\cdot10^{-3}$ deg/cm, respectively. The maximum effect is observed at angles of φ=0°, 120°, 240°, 360°, which is in agreement with the results of [1]. The Faraday rotation, which is due to the component $\mathbf{m}_D$, is 2300 deg/cm in the region of maximum transparency of iron borate at wavelength of λ=525 nm [4]. Thus, the values of the Faraday effect due to magnetization components $\mathbf{m}_D$ and $\mathbf{m}_z$ differ by six orders of magnitude.

References

[1]. I.E.Dzyaloshinskii, Sov. Phys. JETP **5**,1259 (1957).
[2]. P.J. Flanders, J. Appl. Phys. **43**, 2430 (1972).
[3]. A.N. Bazhan, N. M. Kreines, JETP Lett **15**, 377 (1972).
[4]. R. Wolfe, A.J., Kurtzig, and R. C. le Craw, J. Appl. Phys. **41**, 1218 (1970).

BP1-1P/11

Investigation of structural transitions of troilite from ordinary chondrite Calama 009

Dyundik S.S., Maksimova E.M., Nauhatsky I.A.

V.I. Vernadsky Crimean Federal University, Simferopol, Russian Federation
sweta15@mail.ru

Troilite, FeS, is main accessory minerals in different types of meteorites, but it's also found on Earth. Nowadays, this mineral draws much attention of scientists with its unique properties and the possibility of use in spintronics [1].

It is known that, at room temperature, troilite, FeS, has the symmetry space group $P\bar{6}2c$ with unit cell of a = $\sqrt{3}$A and c = 2C, where A and C refer to an NiAs-type structure. When heated to t ~ 140 °C, troilite transforms into a orthorhombic structure of the MnP-type (Pnma, a=C, b=A, c=$\sqrt{3}$A) and transforms into a hexagonal structure of the NiAs ($P6_3/mmc$, a=A, c=C) at t ~ 340°C [2].

Structural studies were carried out for troilite separated magnetically from a fragment of the Calama 009. The temperature dependence of relative change of parameters unit cell (A and C) of troilite was studied by the method of high-temperature X-ray diffractometry, Fig.1.

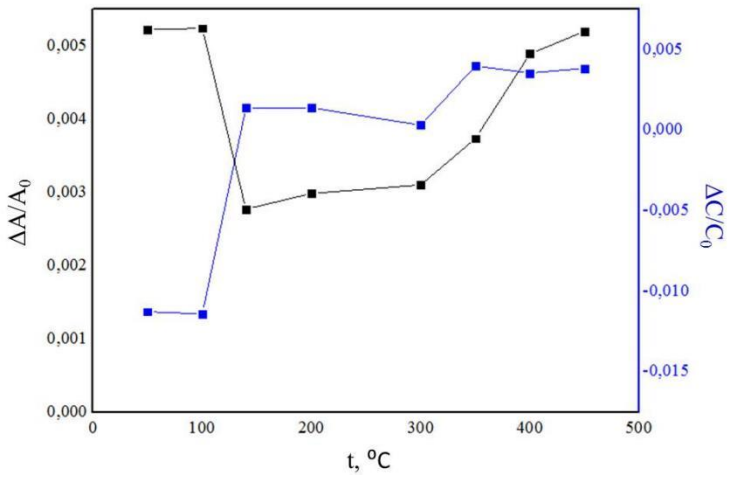

Fig. 1. Dependence of parameters of unit cell (A and C) of troilite on temperature

The graph shows the presence of two reference points around 100 ^{0}C and 300 ^{0}C, where the course of the temperature dependence changes. The values of structural transition temperatures for troilite from the studied meteorite may differ from similar temperatures of troilite from other meteorites and synthesized samples, which may be due to its different degree of non-stoichiometry. Using this method [2], we determined the degree of non-stoichiometry x for the troilite from Calama 009. The degree of non-stoichiometry is x = 0.008.

References

[1] F. Ricci, E. Bousquet, Phys. Rev. Let. 116. 227601 (2016).
[2] O. Kruse, Am. Mineral. A. 75, 755–763 (1990).

BP1-1P/12

Singular points of an isotropic non-Heisenberg magnet

Matyunina Ya. Yu, Kosmachev O. A., Fridman Yu. A.

V.I. Vernadsky Crimean Federal University, 295007, Simferopol, Russian Federation
lkosma@list.ru

The question of the invariance of the equations of motion with respect to certain group transformations is directly related to the commutation properties of the Hamiltonian of the system and operators of the transformation group [1]. Knowledge of the symmetry properties of the Hamiltonian makes it possible to move from solving a complex quantum mechanical problem to studying a relatively simple model problem.

In this work, we study the invariance of an isotropic magnet with spin S=1 and S=3/2 under transformations of the SU (2S+1) group. The Hamiltonian of a magnet with spin S=1 has the form:

$$H = -\frac{1}{2}\sum_{n\neq n'}\left(J\left(n-n'\right)\left(\vec{S}_n\vec{S}_{n'}\right) + K\left(n-n'\right)\left(\vec{S}_n\vec{S}_{n'}\right)^2\right), \qquad (1)$$

where J and K are the Heisenberg and biquadratic exchange constants, respectively.

The work shows that the Hamiltonian (1) is transformation invariant relative to the transformation group SU(2).

It also shows that the point $J = K$ is an SU(3) point for the system under consideration.

The condition J=K determines the phase transition line "ferromagnetic-nematic phase" [2].

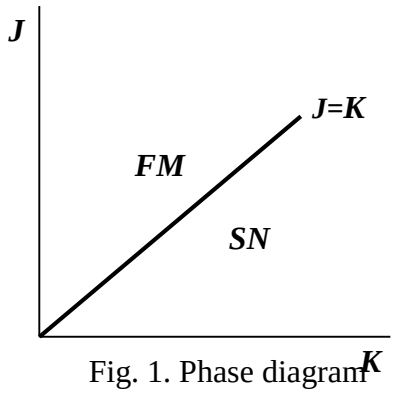

Fig. 1. Phase diagram magnet with S=1 at J, K>0

As a result of studying a magnet with a magnetic ion spin S = 3/2, taking into account all possible spin invariants

$$H = -\frac{1}{2}\sum_{n\neq n'}\left[J\left(n-n'\right)\left(\vec{S}_n\vec{S}_{n'}\right) + K\left(n-n'\right)\left(\vec{S}_n\vec{S}_{n'}\right)^2 + L\left(n-n'\right)\left(\vec{S}_n\vec{S}_{n'}\right)^3\right] \qquad (2)$$

it was possible to show that the Hamiltonian (2) is invariant under the transformation relative to the transformation group SU(2).

In addition, the joint application of the two conditions $J = K/2 - 103L/16$ and $K = 11L/4$ makes it possible to determine the SU(4) point for the Hamiltonian (2) of a non-Heisenberg magnet with S=3/2.

The work was supported by the Russian Science Foundation (grant no. 23-22-00054)

References

[1] A. Messia, Quantum Mechanics (New York, 1962).
[2] Yu.A. Fridman, O.A. Kosmachev, Ph.N. Klevets, JMMM 325, 125 (2013).

BP1-1P/13

Schiff-based cobalt(II) complexes as single-molecule magnets: structural features and relaxation dynamics

Baluda Yu.I.[1], Gusev A.N.[1], Kryukova M.A.[2], Kiskin M.A.[3], Yefimov N.N.[3], Nemec I.[4]

[1]*Crimean Federal V.I. Vernadsky University, 295007, Simferopol, Russia*
[2]*Saint-Petersburg State University, 198504, Saint-Petersburg, Russia*
[3]*Kurnakov Institute of General and Inorganic Chemistry of RAS, 119991, Moscow, Russia*
[4]*Central Europe Institute of Technology, 60177, Brno, Czech Republic*
yury.baluda@yandex.ru

Single-molecule magnets (SMM) are the compounds demonstrating slow magnetic relaxation in scale of individual molecule. In comparison to traditional ferromagnetics, where retention of magnetization may be observed only in scale of magnetic domain, SMMs are potentially much more favorable candidates for new generation data storage devices of ultrahigh capacity; also, magnetic bistabilty is a key feature for quantum computing and spintronics. The most important parameters of SMM are the values of blocking temperature T_b and spin reversal barrier U_{eff}, depending predominately on zero-field splitting (ZFS) parameter D, which is a measure of magnetic anisotropy. First of all, the successful improvement of relaxation dynamics requires controlling the anisotropy of paramagnetic ions environment [1], as well as supramolecular structure and interactions between the ions. In present work we describe an investigation of structural features and magnetic properties of two series of cobalt(II) complexes with Schiff bases derived from 4-acylpyrazol-5-ones, representing a novel class of β-diketone analogues.

Schiff base ligands HL^1-HL^6 were synthesized by condensation of 4-formyl-3-methyl-1-phenylpyrazol-5-one with aniline or 2-substituted anilines (-F, -Cl, -Br, -I, -Me) in ethanol media. By the same procedure were obtained ligands HL^7-HL^{12} based on 4-benzoyl-3-methyl-1-phenylpyrazol-5-one as carbonyl component. Coordination compounds **1-12** were obtained by reaction between $Co(AcO)_2$ and HL^1-HL^{12} respectively, in acetonitrile solutions in presence of 2 eq. of triethylamine (Scheme 1). All the complexes have a simple composition of $[CoL_2]$.

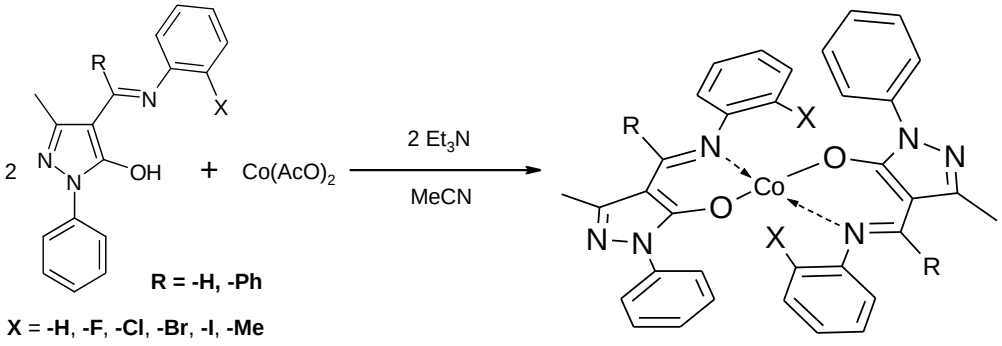

Scheme 1. Synthesis route.

According to X-ray study results (Fig. 1), Co(II) ions possess a distorted tetrahedral environment. The degree of distortion may be well controlled by modification of the azomethine ligand; it was evaluated by modified Addison parameter τ_4 [2].

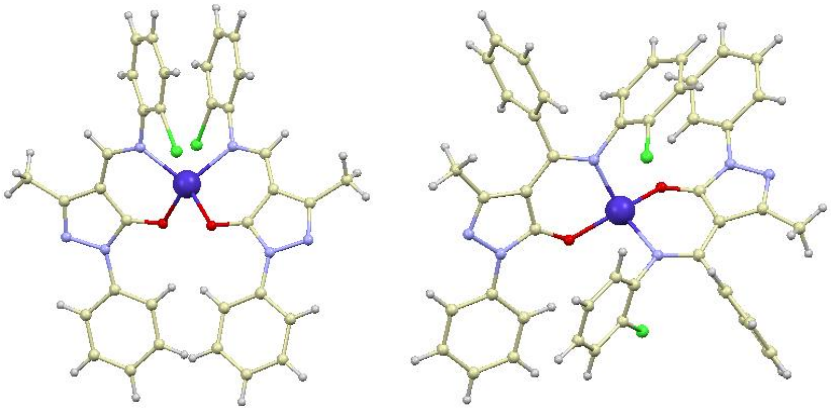

Fig. 1. Molecular structure of **3** (R = H, X = Cl) and **9** (R = Ph, X = Cl).

AC susceptibility measurements (ν = 0,1-10 kHz, T = 2-6 K) indicated slow magnetic relaxation of complexes **1** (R = H, X = H) and **9** in zero field; the others need the application of weak DC field (H = 500-2500 Oe). From the dependences χ"(ν) were extracted the sets of relaxation times τ, and were built lnτ(1/T) plots (Fig. 2). Approximation was performed by Arrhenius equation for Orbach (thermal activated) relaxation mechanism or by more complicated models taking into account Raman, direct and QT mechanisms.

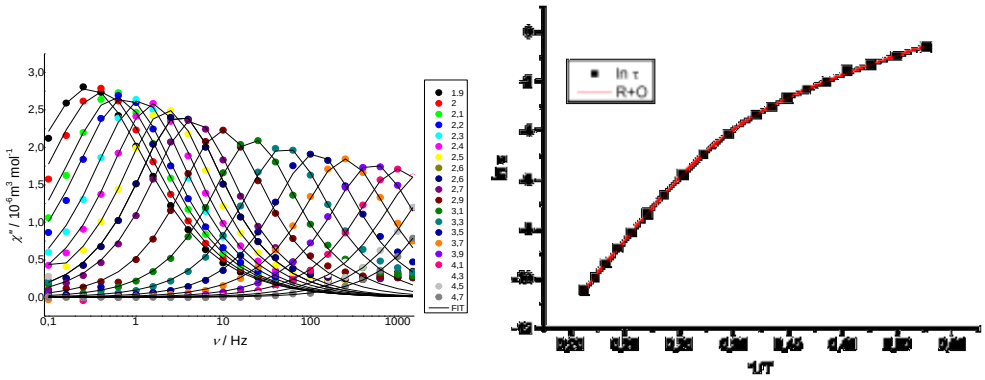

Fig. 2. χ"(ν) dependences and the best fit of lnτ(1/T) function for **3**.

U_{eff} values obtained from the best fits are summarized in table 1 (excluding **3**, **8** and **12**). All the studied compounds exhibit clear SMM or field-induced SMM behavior. According to theoretical calculations, the predicted ZFS patterns are in good agreement with progressive transition from T_d to C_{2V} symmetry, promoted by substituents. In some cases the U_{eff} values agree well with ones following from ZFS patterns, confirming the predominance of thermal activated relaxation; the discrepancy between U predicted and U_{eff} could be attributed to relaxation with significant contribution of alternative pathways. Table 1.

	1	**2**	**4**	**5**	**6**	**7**	**9**	**10**	**11**
U_{eff}, K	49(0)	41	75	35	66	79	30 (0)	50	46
(H_{dc}, Oe)	55(500)	(500)	(2500)	(500)	(500)	(500)		(1000)	(1500)

References

[1] L. Ungur, L. F. Chibotaru, Inorg. Chem., 55, 10043 (2016)
[2] L. Yang, D. R. Powell, R. P. Houser, Dalton Trans., 9, 955 (2007)

BP1-1P/14

Logic gates Based on Carbon Nanotubes

Dzedolik I.V., Tomilin S.V.

Institute of Physics and Technology, V.I. Vernadsky Crimean Federal University, Vernadsky avenue, 4, Simferopol, Russia
igor.dzedolik@cfuv.ru

In this work, the propagation of plasmonic signals in carbon nanotubes is investigated and schemes of plasmonic logic gates based on nanotubes are proposed. It is possible to create a completely plasmonic logic gate "NOT" because of following of the plasmonic signals along the various branches of nanotubes representing Mach-Zehnder-type interferometers. The plasmonic logic gate "OR" is implemented on the basis of Y-splitter made of nanotubes.

Using well known technologies [1], the plasmon structures shown in Fig. 1 can be created from carbon nanotubes with a diameter of 1–2 nm and a length of up to 5 μm. The design of the logic gate "NOT" (Fig. 1a) includes two nanoplasmonic interferometers of the Mach-Zehnder- type. The principle of operation of the logic gate "NOT" is based on the destructive interference with the simultaneous input of two pulse signals into ports *A* and *B* of the logic gate, such as a clock pulse and a signal pulse corresponding to a logical unit. The principle of operation of the logic gate "OR" (Fig.1b) is based on the unhindered passage of pulse signals received at port *A* or port *B* of the Y-splitter.

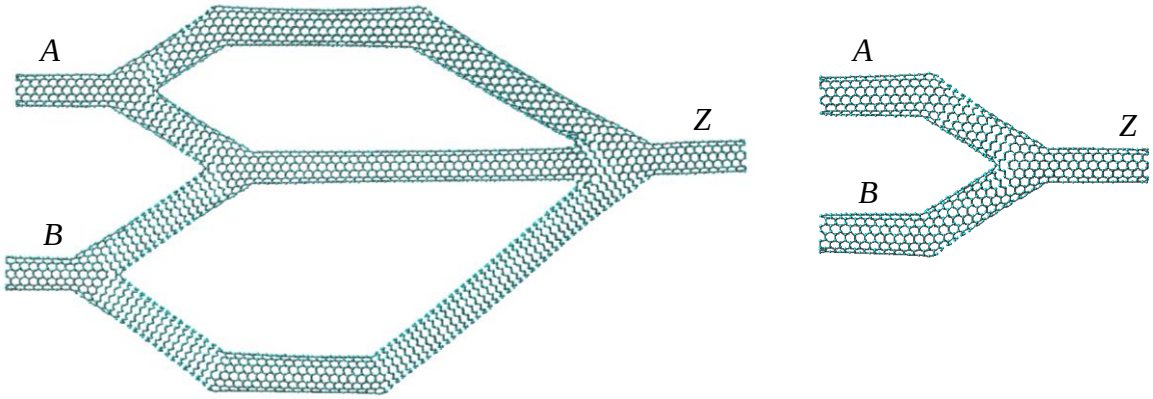

a b

Fig. 1. Plasmonic logic gates based on carbon nanotubes: a – "NOT", b – "OR" (*A* and *B* are input ports; *Z* is output port).

The proposed logic gates "NOT" and "OR" based on carbon nanotubes constitute a complete functional basis for binary logic and can be used in plasmonic circuitry in the optical frequency range, that allows significantly reduce the size of devices operating at optical frequencies.

The research was financially supported by the Russian Science Foundation, grant No. 19-72-20154, https://rscf.ru/project/19-72-20154/

References

[1] Lozovik Yu.E., Popov A.M. Formation and growth of carbon nanostructures: fullerenes, nanoparticles, nanotubes and cones // Uspekhi Phys. Nauk. – 1997. – V. 167, N. 7. – P. 751–774.

BP1-1P/15

Thermal expansion of epitaxial structures based on garnet

Maximov G.S., Strugatsky M.B., Maximova E.M.

V.I. Vernadsky Crimean Federal University, Simferopol, Russian Federation
maximo.a@mail.ru

The practical application of epitaxial films with ferrite-garnet structure requires high mperfection of their crystal structure: a small value of the difference between the parameters of elementary cells of the film and the substrate, similar values of thermal expansion coefficients, and a low quantity of deformations occurring during phase transitions.

In this work, ferrite-garnet epitaxial films grown by liquid-phase epitaxy on nonmagnetic garnet substrates of crystallographic orientation (111) were studied by X-ray diffractometry (Table 1).

Table 1. Film and substrate composition, film thickness (h).

Sample	Film composition	Substrate composition	h, μm
№ 1	$(Bi,Lu,Gd,Ca)_3(Fe,V)_5O_{12}$	$(GdCa)_3(GaMgZr)_5O_{12}$	0,8
№ 2	$(Y,La,Be)_3(Fe,In,Sc,Ge,Co)_5O_{12}$	$Y_3Sc_2Ga_3O_{12}$	3,75

Structural studies of the samples were realized on a diffractometer Shimadzu XRD 7000 Maxima using a low-temperature camera Anton Paar TTK-450 at temperatures from 20° C to 450° C. The measurements were carried out in Cu Kα- radiation using graphite monochromator and Si as an external standard, in angular range 2θ from 50 to 53°. The angle step was 0,02 °.

Diffractograms of samples at some temperatures are presented in Fig.1.

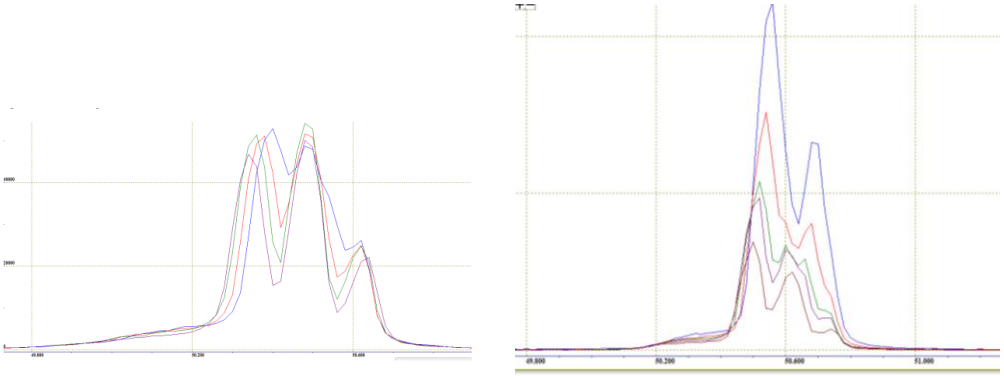

a) b)

Fig. 1. a) diffractograms of sample № 1 at temperatures 100°C (blue), 200°C (red), 300°C (green), 400°C (violet);
b) diffractograms of sample № 2 at temperatures 20°C (blue), 100°C (red), 200°C (green), 300°C (violet), 440°C (brown).

Three lines (1, 2, 3) are clearly visible in the diffractograms of sample № 1 at each temperature. The lines were described as follows: 1 - $(444)_{\alpha 1}$ for film; 2 - $(444)_{\alpha 2}$ for film + $(444)_{\alpha 1}$ for substrate; 3 - $(444)_{\alpha 2}$ for substrate. The diffractograms of sample № 2 at each temperature clearly show two or three lines. The line with the smallest angle 2θ was interpreted as $(444)_{\alpha 1}$ for

film; the swell on this first line on the part of high angle (for temperatures from 20 to 100° C) or a second line (starting from 200° C) was interpreted as $(444)_{\alpha 1}$ for substrate.

The error in determining the cell parameter during thermostatization of samples is determined by the error in determining the position of the diffraction line and was 0.001 Å. The position of the lines was determined using the program XRL-edit [1]. We previously subtracted the background and performed doublet separation α1/α2 using the Reschinger method.

According to the formulas (1-3), the parameters of the elementary cells of the film and substrate a, the value of their mismatch Δa and the coefficients of thermal expansion α were calculated for different temperatures:

$$a = \frac{\lambda}{2\sin\theta}\sqrt{h^2 + k^2 + l^2} \quad (1)$$

where λ is the wavelength of X-ray radiation; θ is the Bragg angle; h, k, l are the interference indices.

$$\Delta a = a_{substrate} - a_{film} \quad (2)$$

$$\alpha = \frac{1}{a_0}\frac{a - a_0}{t - t_0} \quad (3)$$

The values of dislocation densities in the film and substrate were also determined:

$$\rho_{\text{дисл}} = \frac{\beta^2\, ctg^2\,\theta}{B^2}\frac{1}{l\, f(\mu, hkl)} \quad (4)$$

where β – diffraction peak width; B - Burgers vector, $B = a/\sqrt{2}$; $l = \ln\left[\sqrt{\pi\alpha}\,\ln(\sqrt{\pi\alpha}\,C)\right]$. For the volume − centered lattice: $\alpha = 0{,}08; C = 5 - 6;$ $f(\mu, hkl)$ – function that takes into account orientational and elastic characteristics of dislocations, $f(\mu, hkl) = \frac{4}{9}(1 - 2\Gamma)$. Where $\Gamma = (h^2k^2 + h^2l^2 + l^2k^2)/(h^2 + k^2 + l^2)$.

According to the temperature dependences of the structural parameters, it was found that there are special temperature regions in which the thermal expansion coefficients of the film and the substrate differ from each other approximately in 2, while in other regions they are practically equal to each other. At the same sites, the greatest variation of the mismatch parameter and the temperature of maxima and minima of the ratio of the dislocation density in the film to the dislocation density in the substrate are observed. We associate the thermal expansion anomalies at these regions with the presence of compensation and Curie temperatures in them.

References

[1] XRL - editor of primary treatment of diffractometric data. Version 2.96. 2005. Freeware http://xray.physics.usu.ru/.

BP1-1P/16

Magnetic states of iron borate at high quasi-hydrostatic pressure

M.B. Strugatsky, K. Seleznyova, S.V. Yagupov, K. Seleznev

Physics and Technology Institute, Crimean Federal University, Simferopol, Russia
seleznyova@cfuv.ru

P. Glazkov *et al*. have observed changes in the orientation of the magnetic moments of iron ions in $FeBO_3$ with respect to the trigonal axis under conditions of high quasi-hydrostatic pressure up to 4 GPa [1]. Neutron diffraction experiments were carried out using polycrystalline samples of iron borate that were placed in a high pressure chamber with sapphire anvils. Inasmuch as no additional transmission medium has been used, such a technique should lead to a violation of the hydrostatic conditions and the appearance of the anisotropy of the pressure.

Previously [2], we have studied magnetic orientational transitions in the field and pressure in $FeBO_3$. In this case, the axial pressure applied in the basal plane was relatively low. In the present work, we have studied the possible magnetic states of iron borate subjected to high quasi-hydrostatic pressure. As the simplest model of such pressure, we have considered a superposition of the hydrostatic p_h and uniaxial pressure $p \sim p_h$.

The developed theory confirms the experimental results (Fig. 1). Indeed, in view of the randomness of the orientation and the shape of crystallites in a polycrystalline sample [1], it can be assumed that some of the crystallites were subjected to pressure with a uniaxial component in basal plane. In this case, as we have shown, the orientation of the magnetic moments relative to the trigonal axis should change [1].

A support by the RSCF and the Ministry of Education, Science and Youth of the Republic of Crimea, in the framework of scientific project Grant no. 22-22-20112 is acknowledged.

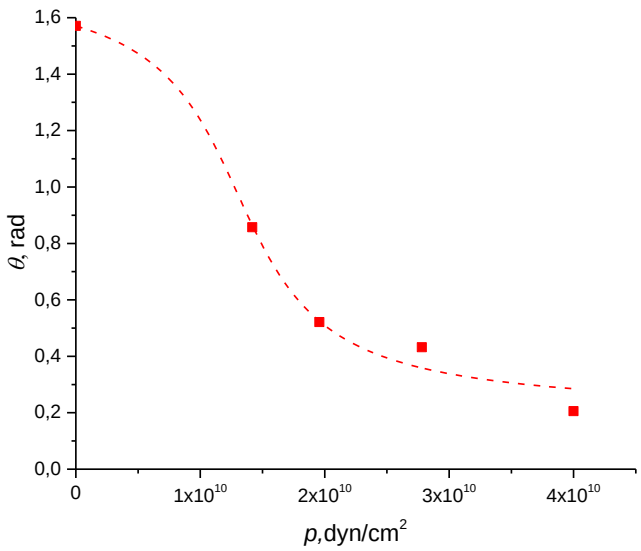

Fig. 1. Experimental [1], dots, and theoretical, curve, pressure dependence of the angle of the magnetic moments relative to the trigonal axis.

References

[1].V. P. Glazkov, S. E. Kichanov, D. P. Kozlenko, B. N. Savenko, V. A. Somenkov, JETP Letters 76, 215 (2002).

[2]. M.B. Strugatsky, S.VYagupov, Functional Materials 9(1), 72 (2002).

Magnetic state of cobalt in layered chalcogenides $Co_7(Se,Te)_8$ and $Fe_4Co_3Se_8$

Piskunov Yu.V.[1], Ogloblichev V.V.[1], Sadykov A.F.[1], Akramov D.F.[2], Smol'nikov A.G.[1], Gerashchenko A.P.[1], Selezneva N.V.[2], Baranov N.V.[1,2]

[1] *Mikheev Institute of Metal Physics, Ural Branch, Russian Academy of Sciences, Ekaterinburg, 620108 Russia*

[2]*Ural Federal University, Ekaterinburg, 620002 Russia*

piskunov@imp.uran.ru

The layered chalcogenides studied in this work belongs to the cation-deficient layered compounds M_7X_8, where M are transition metal atoms, and X are divalent of Group VI anions S, Se, Te. These compounds are characterized by vacancies in metal layers, as well as the formation of various superstructures as a result of the ordering of vacancies and M atoms in the layers [1]. Depending on the type of 3d metal M, both the structural and magnetic properties of the above chalcogenides can change.

Recently the chalcogenides containing cobalt have been considered as promising catalysts, particularly for the water electrolysis [2]. The study of the reasons for the charge and spin instability of cobalt ions in these compounds seems to be extremely important for a deeper understanding of the mechanisms of these compounds' catalytic activity.

In this work the structural and magnetic properties of the Co_7Se_8, Co_7Te_8 and $Fe_4Co_3Se_8$ compounds have been studied using X-ray diffraction, measurements of the magnetic susceptibility, and nuclear magnetic resonance spectroscopy on ^{59}Co nuclei. The isotropic magnetic shift (Fig. 1) and electric field gradient tensors at the location of ^{59}Co nuclei have been determined from NMR spectra of these nuclei. The analysis of these spectra has revealed a significant local charge and magnetic inhomogeneity of studied chalcogenides. The hyperfine fields in Co ions has been estimated from the temperature dependences of the shift and susceptibility in Co_7Te_8 and $Fe_4Co_3Se_8$ (insets in Fig. 1).

It has been found that the ordering of vacancies and Co atoms in cation layers is absent in the Co_7Te_8 compound, and its crystal structure is more planar and is characterized by a significantly smaller ratio c/a (c and a are the lattice parameters) compared to Co_7Se_8. This difference is apparently due to a larger polarizability of Te ions and to a higher degree of covalence of Co–Te bonds compared to Co–Se bonds. It was shown that both Co_7Se_8 and Co_7Te_8 compounds remain a Pauli paramagnets down to the lowest temperatures. Since an increase in the interatomic distances from Co_7Se_8 to Co_7Te_8 occurs predominantly in the plane, it does not lead to a stronger localization of electrons or to the appearance of magnetic moments on Co atoms, as could be expected. The Co_7Te_8 compound is even closer to classical Pauli paramagnets than Co_7Se_8. It has been shown that a nonmonotonic temperature-induced change in the magnetic susceptibility and the spin–lattice relaxation rate in the Co_7Se_8 compound can be due to strong electron–electron correlations.

It was found that the temperature dependence of the magnetic susceptibility in $Fe_4Co_3Se_8$ does not show any anomalies in the magnetically ordered region (at $T < 196$ K) that would indicate a spin-reorientation transition. We suggest that in $Fe_4Co_3Se_8$ the magnetic moments of Fe are oriented perpendicular to the plane of the layers in the entire temperature range below 196 K. From the T-dependence of the susceptibility in the paramagnetic state of $Fe_4Co_3Se_8$ the sample-averaged value of the effective magnetic moment $\mu_{eff} = 4.5\ \mu_B$ was

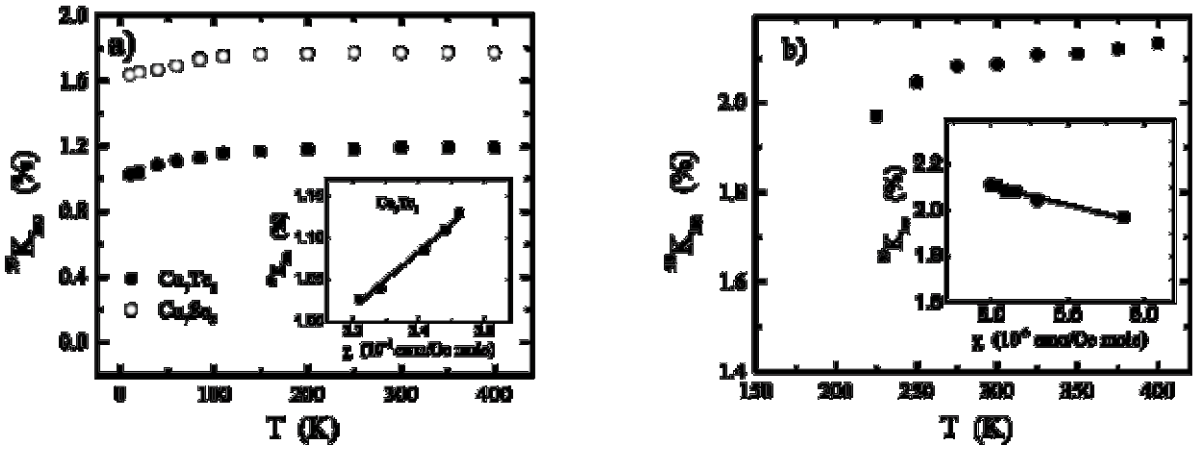

Fig. 1. Temperature dependences of the ^{59}Co magnetic shift K_{iso} in in powder Co_7Se_8, Co_7Te_8 – (a), and $Fe_4Co_3Se_8$ – (b) compounds. The insets show the dependences in Co_7Te_8 and $Fe_4Co_3Se_8$ of $K_{iso}(\chi)$ with the temperature as a parameter, approximated by a straight line. The slopes of straight lines correspond to the values of hyperfine fields at cobalt nuclei H_{hf} (Co_7Te_8) = 188 kOe/μ_B and H_{hf} ($Fe_4Co_3Se_8$) = -9 kOe/μ_B.

determined, which, in terms of Fe atoms only, is μ_{eff} = 5.90(5) μ_B. The last value is very close to μ_{eff} = 5.80 μ_B, obtained in [1] for the initial composition of Fe_7Se_8.

We found out that cobalt ions in $Fe_4Co_3Se_8$ as well as in completely substituted Co_7Se_8 do not have their own magnetic moments. However, due to the overlap of the 3d shells of cobalt and iron ions, part of the magnetic moments of Fe can be transferred to the Co ion, leading to the appearance of an induced effective magnetic moment on cobalt $\mu_{eff}^{Co} = 0.36(4)\mu_B$. In the magnetically ordered state of $Fe_4Co_3Se_8$, the magnetic moment μ_{eff}^{Co} is significantly reduced to the value $\mu_{eff}^{Co} = 0.07(1)\mu_B$ due to mutual compensation of contributions to the induced moment from iron ions located inside the plane and in two neighboring ones. A Korringa-like behavior of the spin-lattice relaxation of the ^{59}Co nuclear moments in $Fe_4Co_3Se_8$ and the absence of a contribution to spin lattice relaxation from localized magnetic moments of cobalt ions also indirectly evidences about littleness of μ_{eff}^{Co}. Thus, this study has shown that cobalt ions having no own magnetic moments in $Fe_{7-x}Co_xSe_8$ chalcogenides act mainly as a diluent of the magnetic subsystem of iron.

This work was supported by the Russian Science Foundation (project no. 22-12-00220).

References

[1] M. Sato, T. Kamimura, T. Iwata, J. Appl. Phys. 57, 3244 (1985).

[2] J. Wang, W. Cui, Q. Liu, Z. Xing, A.M. Asiri, and X. Sun, Adv. Mater. 28, 215 (2016).

High strain rate deformation of metals with giant magnetostriction

Varyukhin V.N.[1], Malashenko V.V. [1, 3], Malashenko T.I.[2]

[1]*O.O. Galkin Donetsk Institute for Physics and Engineering, Donetsk, Russia*
[2] *Donetsk National Technical University, Donetsk, Russia*
[3] *Donetsk State University, Donetsk, Russia*
malashenko@donfti.ru

High strain rate deformation is quite different from quasi-static one [1-3]. Under high-energy impacts, dislocations make over-barrier movement. In this case, the dissipation mechanism consists in the transition of the energy of external influences into the energy of dislocation vibrations in the sliding plane. The efficiency of such a mechanism is largely determined by the conditions for the occurrence of dislocation vibrations, primarily by the presence of a gap in the spectrum of dislocation vibrations. The gap in the spectrum arises because the dislocation oscillates in the potential well moving along with the dislocation. Such a well can arise both as a result of the collective interaction of point defects with each moving dislocation, and as a result of the collective interaction of the moving dislocations of the assembly with each dislocation.

In crystals with giant magnetostriction, the main contribution to the gap formation is made by the magnetoelastic interaction [4]. Such materials are currently attracting more and more attention of researchers. Giant magnetostriction at low temperatures is demonstrated by Tb, Dy, Ho, Er and iron garnets of these metals (for example, $Tb_3Fe_5O_{12}$). Their magnetostriction is two or three orders of magnitude higher than the magnetostriction in alloys and ferrites of the Fe group. At room temperatures, such values of magnetostriction can be obtained using ferrimagnetic compounds $DyFe_2$, $TbFe_2$, $HoFe_2$, $DyFe_3$. Materials with giant magnetostriction are widely used in microsystems engineering. They are used to manufacture pressure indicators, sensors, sonars, anti-vibration systems. The dependence of the yield strength on the magnetic characteristics of the material is obtained

$$\tau = K\frac{n\dot{\varepsilon}}{\lambda^2 M_0^3}$$

Here $\dot{\varepsilon}$ is the plastic strain rate, M_0 – saturation magnetization, λ – magnetoelastic coupling constant, n – volume concentration of impurities.

The increase of the magnetostriction constant results an increase of the contribution of the magnetoelastic interaction to the magnitude of the spectral gap. In this case, the contribution of impurity atoms to the yield stress decreases with increasing magnetostriction constant. The results obtained are applicable to intermetallic compounds of rare-earth elements with iron-group metals having giant magnetostriction.

References

[1] S. Kodambaka, V. Khare, W. Swich, K. Ohmori, I. Petrov, J. E. Greene. Nature 429, 49 (2004).
[2] D. Batani. EPL. 114, 6500 (2016).
[3] V.V. Malashenko. Physica B: Phys. Cond. Mat. 404, No 2, 3890 (2009).
[4] V.V. Malashenko. Phys. Sol. State. 64(10), 2300 (2022).

Section
Ferro and Antiferromagnetic Spintronics and Magnonics

AO1-2O/1

Dynamics and transformation of magnetic vortices in a spin-transfer nanooscillator

Ekomasov E.G.1, Zvezdin K.A.2, Antonov G.I.1, Filippova V.V.1

[1] *Ufa University of Scince and Technology (former Bashkir state university), Ufa, Russia*
[2] *General Physics Institute A.M. Prokhorov RAS, Moscow, Russia.*
EkomasovEG@gmail.com

The structure and dynamics of magnetization in a spin-transfer vortex nanooscillator (STNO), which is a three-layer magnetic nanopillar with a spin valve, with the passage of a spin-polarized current and the presence of an external magnetic field is investigated [1]. Using micromagnetic modeling in a small-diameter nanopillar, we studied the dynamic change in the structure of vortices, the formation of the vortex state of the C-structure and edge vortices, the trajectory of motion and the time required to achieve various dynamic modes [2]. The time needed for the vortices to reach various dynamic modes was found. The possibility of dynamic generation of radial edge vortices without the presence of a Dzyaloshinsky field or an external inhomogeneous magnetic field is shown. We demonstrate that a vortex in a thick magnetic layer can be a generator of spin waves in a thin magnetic layer with an adjustable oscillation frequency. The effect of the thickness of a non-magnetic layer on the coupled dynamics of two magnetic vortices in a spin moment nanogenerator was studied [3]. A thick permalloy magnetic layer has a thickness of 15 nm, an average non-magnetic layer has a thickness of 12.5 nm in the first case and 15 nm in the second, and a thin permalloy magnetic layer has a thickness of 4 nm. The numerical calculation of the dynamics of magnetostatically coupled vortices was carried out using the SpinPM software package for micromagnetic modeling. The features of the dynamics of vortex motion at different thickness of a non-magnetic layer are studied. It is shown that in all cases of thickness of a non-magnetic layer, three modes of vortex dynamics are observed: time-damped oscillations of magnetic vortices, the mode of stationary coupled oscillations of magnetic vortices and the mode when the vortices "leave" the edge of the disk. It is established that an increase in the thickness of the non-magnetic layer leads to a decrease in the values of the first, second and third critical currents.

For large-diameter STNO, the effect of a current with large spin polarization on the associated dynamics of vortices in nanoscillators with a spin transfer with a diameter of 400 nm was studied. The effect of the appearance of new regions of stationary modes of coupled oscillations of P- and AP-vortices is found. A diagram of the dependences of the frequency of stationary coupled oscillations of magnetic vortices on the spin of the polarized current is constructed. The discovered effect can be used to increase the operating frequencies of nanoscillators with rotation transfer of large diameters.

References

[1] K.A. Zvezdin, E.G. Ekomasov, Phys. Metals Metallogr., 123, (2022), 201.
[2] S.V. Stepanov, V.N. Nazarov, K.A. Zvezdin, E.G. Ekomasov, JMMM, 562 (2022) 169758
[3] V. V. Mukhamadeeva, S. V. Stepanov, K. A. Zvezdin, E. G. Ekomasov, Letters on Materials 12 (4) (2022) 327-331.

AO1-2O/2

Spin-orbit coupling mediated size effects in magnetoresistance of Ta nanolayers *(invited)*

Ustinov V.V. [1,2], Naumova L.I. [1,2], Zavornitsyn R.S. [1,2], Yasyulevich I.A. [1], Maksimova I.K. [1], Krinitsina T.P. [1], Pavlova A.Y. [1], Proglyado V.V. [1], Milyaev M.A. [1,2]

[1] *M.N. Mikheev Institute of Metal Physics UB RAS, 620108, Ekaterinburg, Russia*
[2] *Ural Federal University, 620026, Ekaterinburg, Russia*
naumova@imp.uran.ru

The principle of operation of spintronic devices is based on the transfer of the spin of an electron, not charge. Spin Hall effect is one possible mechanism for spin current generation. Electric current generates a transverse spin current in metals with strong spin-orbital interaction. This results in spin accumulation at the sample boundaries. It was reported [1, 2] that the external magnetic field leads to the destruction of spin polarization and the appearance of longitudinal magnetoresistance due to the Hanle effect. In the present work, a theoretical and experimental study of the dimensional effects induced by spin-orbital interaction in tantalum nanolayers is carried out.

Tantalum films were obtained by magnetron sputtering and patterned into Hall bars by photolithography. Transmission electron microscopy and X-ray diffraction studies have shown that a pseudo-amorphous phase of β -Ta has formed in tantalum films. Negative temperature coefficient of resistance, which is characteristic of highly disordered systems, was observed for β-tantalum films. Field dependences of magnetoresistance were measured at different fixed angles (α) between current and magnetic field in the range from 20 to -20 kOe applied in the film plane. The magnetoresistance was evaluated as $(\rho_H - \rho_0)/\rho_0$, where ρ_H is the resistivity in the field H and ρ_0 is the resistivity at H = 0. Maximum magnetoresistance was evaluated for H = 20 kOe. Experimental points on the angular dependence of $((\rho_H - \rho_0)/\rho_0)_{max}$ are close to the line of approximating function $(\Delta\rho/\rho_0)_{max}(\alpha) \sim \cos^2(\alpha)$ (Fig.1).

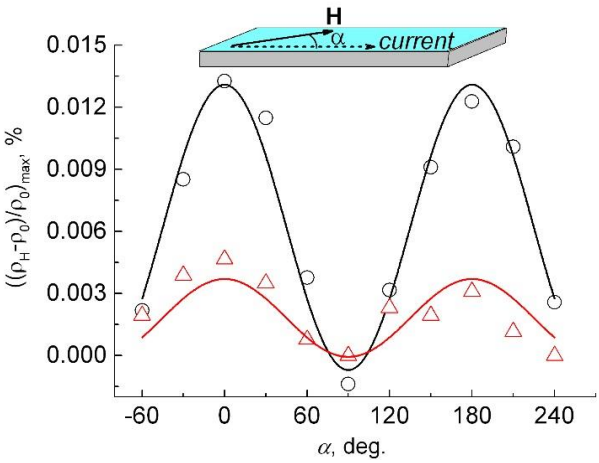

Fig. 1. Angular dependence of magnetoresistance of β -Ta films with thicknesses of 5 nm (○) and 8 nm () at T = 103K.

A theory was built to analyze the experimental data. Fig. 2 shows experimental and theoretical field dependencies of longitudinal magnetoresistance of tantalum films.

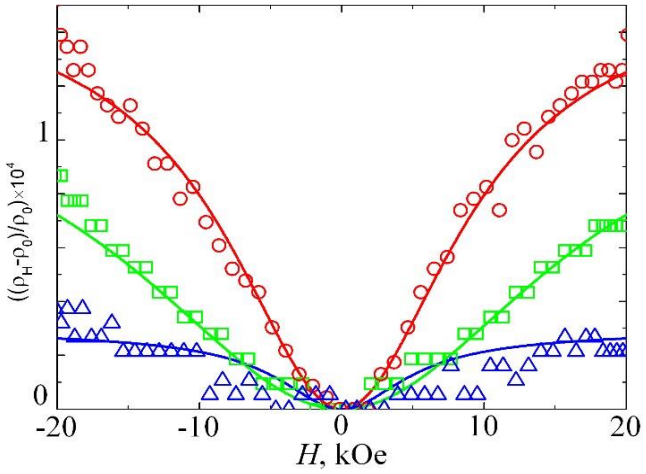

Fig. 2. Longitudinal magnetoresistance on the external magnetic field dependencies for β-Ta films with 3 nm (□), 5 nm (○) and 8 nm (Δ) thicknesses. Symbols are experimental data. Solid curves are theoretical dependencies.

Within the framework of the theory, the length of spin diffusion, the time of spin relaxation, and the Hall angle in the nano-layers of β -Ta were quantified.

The theory of electrical resistance arising from the presence of spin-orbital interaction in thin films of normal metals is built. It has been shown that the an external magnetic field leads to a decrease in the depth at which there is a non-equilibrium spin density in a thin film. As the result, the amount of electron flow near the surfaces of a thin film approaches the amount of electron flow in an unlimited normal metal. It is shown that the film conductivity decreases in the presence of spin-flip scattering of electrons on the surfaces of a thin film.

This study was supported by the Russian Science Foundation (project no. 22-22-00220)

References

[1] M. I. Dyakonov, Phys. Rev. Lett.99, 126601 (2007).

[2] Saül Vélez et al, Phys. Rev. Lett.116, 016603 (2016).

AO2-2O/1

Direct observation of magnon BEC in YIG film at room temperature *(invited)*

Bunkov Yu. M.[1], Belotelov V. I. [1, 2], Knyazev G. A. [1, 2], Kuzmichev A. N. [1], Petrov P. E. [1, 2]
Savochkin I. V. [1], Vetoshko P. M. [1, 3]

[1]1 Russian Quantum Center, Skolkovo, Moscow, Russia
[2] Moscow State University, Moscow, Russia
[3]KFU, Simferopol, Russia
y.bunkov@rqc.ru

Bose-Einstein condensation occurs at an appropriate density of bosonic particles, depending on their mass and temperature. We were able to experimentally observe the transition from the spin wave regime to the magnon Bose-Einstein condensed state (mBEC) with an increase in the magnon density due to microwave pumping. We used an optical setup based on the Faraday rotation effect to record the spatial distribution of the magnon density and phase.

We used the sample of 6 μm YIG film in the form of an ellipse with axes 4.5 by 1.5 mm. A strip line 0.2 mm wide excited magnons near one of the ends of the sample. The external magnetic field was directed out of plan of the film. We have investigated the propagation of magnons outside the region of excitation. At a low amplitude of resonant microwave excitation, we observed the formation of spin waves, the parameters of which are in good agreement with calculations based on the Landau-Lifshitz-Gilbert (LLG) equations for the experimental conditions.

At a critical density of excited magnons, its properties changed dramatically. Instead of a pattern of spin waves, a coherent precession was observed even far from the region of excitation. This pattern clearly corresponds to Bose condensation of magnons [1]. We performed a spatial Fourier analysis of the signal outside the excitation region as a function of the excitation energy and found a sharp transition from a wide spectrum in the spin wave mode to a narrow line in the BEC mode. The critical magnon density for the transition corresponds to a 3° deviation of the magnetization, which is in good agreement with the prediction [2].

The Bose condensation of magnons studied by us is formed from magnons with k = 0. It has the same basic properties as the magnon BEC in antiferromagnetic superfluid 3He discovered in 1984 [3-5]. In both cases, it has direct analogies with the atomic Bose condensate. Another type of magnon BEC occurs in in plane magnetized YIG film [6]. In this case, it is formed by traveling magnons with nonzero momentum k. As a result, this type of magnon BEC can be considered in analogy with photon BEC in media.

This work was supported by the Russian Science Foundation (project no. 22-12-00322)

References:

[1] P. E. Petrov, et al., *Optics Express* **31**, (2023) 8335-8341.
[2] Yu. M. Bunkov and V. L. Safonov, *J. Magn. Magn. Mat.* **452**, (2018), 30–34.
[3] A.S.Borovik-Romanov, et al., *JETP Letters*,**40**, (1984) 1033- 1037.
[4] Yu. M. Bunkov, *J. Low Temp. Phys.*, **138**, (2005) 753-758.
[5] Yu.M. Bunkov and G.E. Volovik, *Phys. Rev. Lett.* **98**, (2007) 265302.
[6] A. A. Serga, et al., *Nat. Commun*. **5** (2014) 3452–3458

AO2-2O/2

Spin-wave diagnostics of ultrathin YIG films

Tikhonov V.V., Gubanov V.A., Sadovnikov A.V.

Saratov State University, Saratov, Russian Federation
tvlad4@yandex.ru

A method of non-destructive control of the layered structure of ultrathin (submicron) ferrite films comparable to the thickness of the transition layer at the film-substrate interface has been proposed. The technique was based on the measurement of spin-wave resonance (SWR) frequencies and mathematical processing of the measurement results [1].

The experiments used a 200nm thick YIG film grown by liquid phase epitaxy. The SWR excitation was carried out with a microstrip transducer shorted at the end. A resonant absorption peak was observed in the spectrum of the reflected signal, as shown in Figure 1. The frequency of the peak was smoothly tuned by the magnetic field.

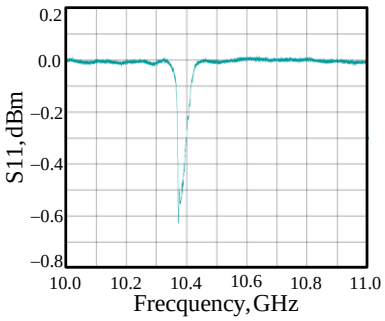

Fig.1.

The inhomogeneity of the magnetisation in the transition layer was described by an exponential distribution function $M(z)=M_0\left[1-\exp(-\sigma z)\right]$, where σ - the phenomenological parameter of the distribution. Methodology for calculating the parameter σ was based on the joint solution of the Landau-Lifshitz equation taking into account inhomogeneous exchange and a system of Maxwell equations. Solutions were sought in the form of plane monochromatic waves propagating in the direction of the applied field. As a result, the dispersion equation was obtained $\left(k^2-k_{S0}{}^2\right)\left(k^2-k_{E0}{}^2\right)=k_{E0}^2\omega_M/\eta$, which had a simple analytical solution

$$k_{S,E}=\sqrt{\left(k_{S0}{}^2+k_{E0}{}^2\right)/2\pm\sqrt{\left(k_{S0}{}^2+k_{E0}{}^2\right)^2/4+k_{E0}^2\omega_M/\eta}}\,, \qquad (1)$$

where $k_{S0}=\sqrt{(\omega-\omega_H)/\eta}$, $k_{E0}=\sqrt{\varepsilon}k_0$, $\omega=2\pi f$, $\omega_M=4\pi\gamma M(z)$, $\omega_H=\gamma H_0-\omega_M$, $\gamma=1{,}76\times10^7$ Oe^{-1}s^{-1} – gyromagnetic ratio, $\eta=7.64\times10^{-2}$ cm^{2}s^{-1} - heterogeneous exchange constant. In equation (1), the sign (+) under the radical corresponded to the dispersion of quasi-spin waves $k_S=F_S(f,H_0,\sigma,z)$, but a sign (–) – dispersions of quasielectromagnetic waves $k_E=F_E(f,H_0,\sigma,z)$.

Parameter σ was calculated numerically from the excitation condition of the first mode of SWR $F_S(f_n,H_{0n},\sigma,d)-\pi/d=0$, where d - is the thickness of the YIG film. The result was a parameter value of which was used in further calculations.

Fig.2.a shows the coordinate dependencies of the magnetisation $M(z)$ and internal field $H_i(z)$. The area of the experimental sample of the YIG film is highlighted in colour. Fig.2.b shows the 3d plots of the partial laws of electromagnetic dispersion $k_{E0}(f,z)$ and exchange spin

waves $k_{S0}(f,z)$. On the line of intersecting 3d graphics $k_{E0}(f,z)=k_{S0}(f,z)$ the condition of phase synchronism (hybridisation) of coupled waves was fulfilled. In the vicinity of synchronism points, dispersion branching occurred. Fig.2.c shows coordinate dependences of hybrid quasi-spin wave $k_S(z)$, which illustrate the transformation processes of electromagnetic and exchange spin waves.

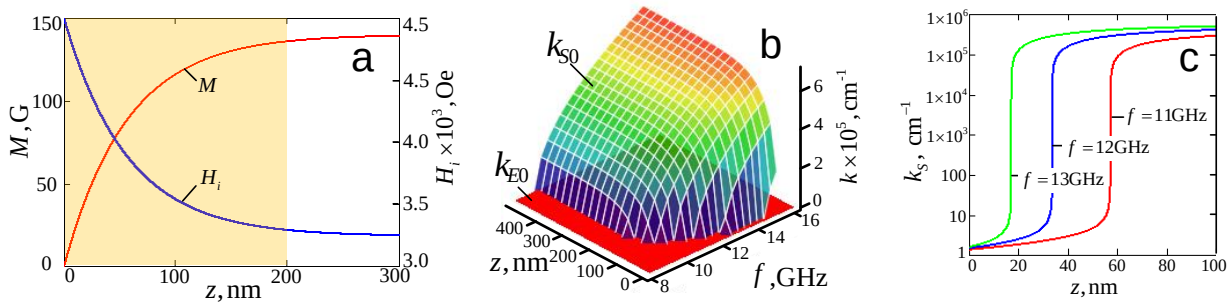

Fig.2.

The nucleation processes of the ESWs are illustrated in the 3d diagram in Fig. 3.a. It can be seen that the ESW excitation occurs at some distance from the film-substrate boundary. This was confirmed by calculations of electromagnetic intensity I_E and spin oscillations at SWR frequencies (see Figure 3.b).

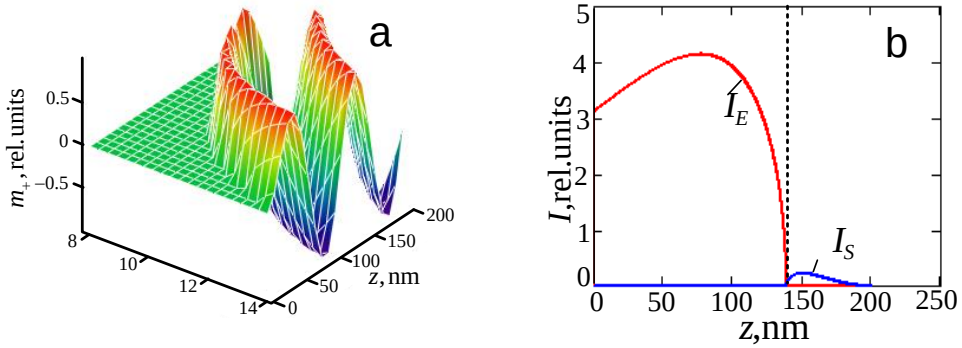

Fig.3.

The electromagnetic oscillations were localised near the inner boundary of the film and the spin oscillations were localised near the outer boundary of the YIG film. At the same time, the region of energy accumulation of spin oscillations turned out to be narrower, which explained the weak excitation of SWR. Obviously, if the film thickness were reduced to a certain critical thickness, the excitation of SWR would become impossible at all.

The proposed spin-wave technique can be used for nondestructive inspection of all types of ferrite dielectric film structures and can be useful in the development of new epitaxial growth technologies.

This work was supported by a grant from the Russian Science Foundation (No 23-79-30027).

References

[1] V.V. Tikhonov, V.A. Gubanov, S.A. Nikitov, et al, JMMM, 562, 169763 (2022).

AO2-2O/3

Bound states in the radiation spectrum of Leaky Surface Magnon Polarons

O. S. Sukhorukova[1], A. S. Tarasenko[1], S. V. Tarasenko[1], and V. G. Shavrov[2]

[1] *Donetsk Institute of Physics and Technology,Donetsk, 83114 Russia*
[2] *Kotel'nikov Institute of Radio Engineering and Electronics, Russian Academy of Sciences, 125009, Moscow, Russia*
al.meshcheryakov@gmail.com

According to [1], the formation of an interference bound state in the continuous emission spectrum of two resonant states is possible if, without taking into account the radiative interaction between them, their energies are degenerate and the emission of both states occurs in the same radiation channel and has the character of destructive interference. Such bound states in a continuum (BIC) have zero radiation width and do not interact with any state of the continuous spectrum, but, in the vicinity of the BIC, in the nondissipative model, the Q-factor of the corresponding radiative state can be made arbitrarily large [1] ("super-resonant" states, according to the terminology of [2]). This is of not only scientific, but also practical interest, stimulating a constant, ever-increasing flow of scientific publications in this direction. At the same time, in recent years, attention has also sharply increased to the prospects for creating a new class of energy-efficient spintronic devices, which use as a unit of information the electron spin torque instead of the electron spin. However, the creation of realistic models of the corresponding magnetic heterostructures requires correct consideration of the dynamics of magnon polarons (hybrid states resulting from the coherent magnetoelastic (ME) coupling between spin and elastic waves) [3]. Nevertheless, the possibility of the formation of these "interference" BIC in the spectrum of leaky surface magnon polarons has not yet been discussed, despite the fact that the conditions for the formation of surface BIC in the electromagnetic emission spectrum of open semi-bounded optoelectronic structures were considered in [4].

The aim of this communication is to elucidate, in the dissipationless approximation, the conditions under which, for a magnetic sandwich structure, the formation of interference BIC in the spectrum of leaky surface magnon polarons is possible and to analyze the features of the realization of nonspecular effects accompanying in this case the reflection of a bulk quasi-plane or a quasi-mono-chromatic external elastic wave incident on the surface of a layered magnetic heterostructure.

For the first time, it has been shown that the hybridization of magnetoelastic and inhomogeneous exchange interactions can lead to the formation of interference-type bound states in the emission spectrum of leaky surface magnon polarons. In the vicinity of such "dark" states, their radiation width can be arbitrarily small ("super-resonance"), as a result of which, for an external quasi-plane elastic wave incident on the magnetic layer, the longitudinal Schoch effect increases indefinitely (in the nondissipative approximation) and the effects of zero scattering of the incident wave field and splitting of the
reflected waveform are suppressed.

References

1. H. Friedrich and D. Wintgen, Phys. Rev. A 32, 3231 (1985).
2. M. V. Rybin and M. F. Limonov, Phys. Usp. 62, 823 (2019).
3. Y. Li, C. Zhao, W. Zhang, et al., APL Mater. 9, 060902 (2021).
4. M. I. Molina, A. E. Miroshnichenko, and Y. S. Kivshar, Phys. Rev. Lett. 108, 070401 (2012).

AP1-2P/1

Non-reciprocal propagation and coupling of spin waves in an asymmetric magnonic structure

Grachev A.A.[1], Odintsov S.A.[1], Beginin E.N.[1], Sadovnikov A.V.[1]

[1]*Laboratory "Metamaterials", Saratov State University, Saratov 410012, Russia*
stig133@gmail.com

The use of elementary quanta of magnetic excitations, such as magnons or spin waves, as carriers of information signals, has recently garnered increasing interest. This is primarily due to their ability to transfer the magnetic moment (spin) of an electron without transferring electric charge, thus avoiding the heat generation inherent in semiconductor technologies [1,2]. The properties of spin waves are determined by dipole and exchange interactions in magnetic media and can be significantly altered through the structuring of magnetic films. Spin waves find applications in various fields, including generation [3], transmission [4], and processing [5] of information signals at the micro- and nanoscale.

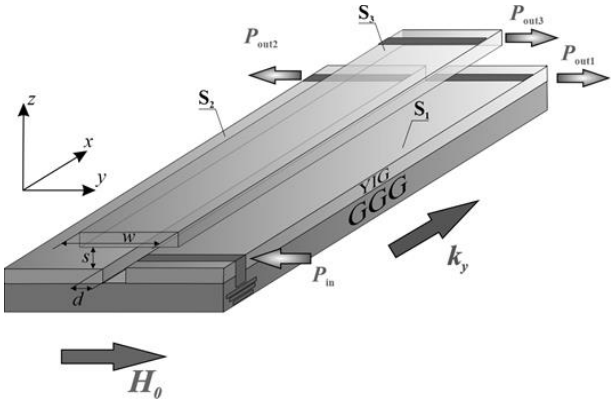

Fig. 1. Schematic representation of an asymmetric magnonic structure.

The study revealed a three-dimensional magnonic structure (see Fig. 1) based on lateral stripes with an overlying magnetic stripe. This research demonstrates that in three-dimensional magnonic structures, the coupling length of spin waves decreases, allowing for increased density of functional elements in the design of three-dimensional magnonic networks. Furthermore, the non-reciprocal distribution of dynamic magnetic fields and dispersion characteristics of waves propagating in opposite directions within the structure can be utilized to achieve three-dimensional spatial separation of spin-wave beams at different carrier frequencies. These findings present new possibilities for three-dimensional spatial multiplexing and demultiplexing in the field of magnonics.

This work was supported by a grant from the Russian Science Foundation (Project No. 23-79-30027).

References

[1] A. Barman et al. Journal of Physics: Condensed Matter, 33, 41, (2021) 413001.
[2] A.A. Grachev, A.V. Sadovnikov, S.A. Nikitov, Nanomaterials, 12, 9, (2022) 1520.
[3] A.A. Grachev et al. Phys. Rev. Applied 19, 054089 (2023).

AP1-2P/2

Control of the spectrum of spin waves in a rounded structure with the introduction of local laser heating

Gubanov V.A.[1],Kruglyak V.V.[2], Sadovnikov A.V.[1]

[1]*Laboratory "Magnetic Metamaterials", Saratov State University, Saratov, Russian Federation*
[2]*University of Exeter, Exeter, EX4 4QL, UK.*
vladmeen@gmail.com

Recently, there has been great interest in creating a new complementary base for the implementation of multidimensional information signal processing and storage devices based on the principles of magnonics [1,2]. Ferromagnetic Iron-Ittrium Garnet films are a good candidate for the realization of this concept due to their low attenuation.

Of particular interest are structures in which the type of propagating spin wave - from magnetostatic surface spin wave (MSSW) to backward volume magnetostatic spin wave (BVMSW) and vice versa, depending on the direction of the applied external magnetic field [3,4]- is transformed by breaking the translational symmetry.

Important in creating information signal processing devices is the ability to control the signal. One of possible variants is local laser heating.

The investigated structure is a waveguide with translational symmetry breaking in the form of a horseshoe (U-shape). The waveguide is formed from a 10 μm thick Iron-Ittrium-Garnet film on a 500 μm thick Gadolinium-Gallium-Garnet substrate obtained by liquid-phase epitaxy, using the MiniMarker-2 precision laser cutting method. The spin wave was excited by a 30 μm wide microstrip antenna P_1. The captured spin wave was picked up at the output microstrip antenna P_2.

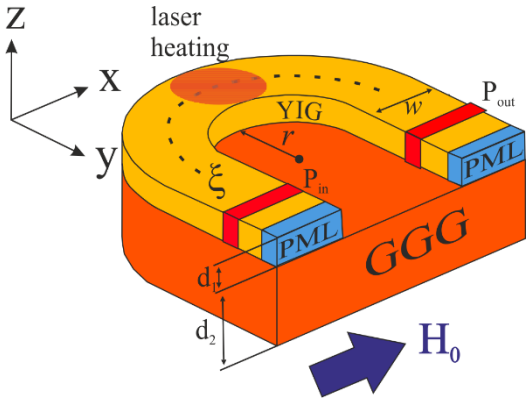

Fig. 1. Schematically view of the structure with translational symmetry breaking.

In this system, an external magnetic field H_0 was applied along the *x*-axis to effectively excite the MSSW, and an external magnetic field H_0 was applied along the *y*-axis to effectively excite the BVMSW. Local laser heating was created using a laser source with a wavelength of 830 nm, which was subsequently applied to the curved area. The heating was quantified with an infrared camera.

The transfer characteristics S_{21} for the structure in question were derived in the case of BVMSW and MSSW excitation under the application of local laser heating and without heating. The following were considered modes of decreasing and increasing the power transmitted to the output microstrip antenna spin-wave signal. Using the experimental method of Brillouin light spectroscopy, maps of the spin wave intensity squared distribution were obtained, and the mode of mode transformation of the spin wave after passing the rounding region when local laser heating is applied are presented.

The work was supported by Russian Science Foundation (Project 23-79-30027).

References

[1] Q. Wang, P. Pirro, R. Verba et al., Sci. Adv., 4(1), e1701517 (2018).
[2] A.V. Chumak, V.I. Vasyuchka, A.A. Serga & B. Hillebrands, Nat. Phys., 11(6), 453 (2015).
[3] A.V. Sadovnikov, C.S. Davies, V.V. Kruglyak et. al., Phys. Rev. B., 96(6), 060401 (2017).
[4] T. Brächer, P. Pirro, J. Westermann et. al., Appl. Phys. Lett., 102(13), 132411 (2013).

AP1-2P/3

Nonreciprocal caustic spin waves in partially metallized T-shape waveguide

Martyshkin A.A.[1], Lock E.H.[2], Ogrin F.[3],Sadovnikov A.V.[1]

[1]*Saratov State University, Laboratory "Magnetic Metamaterials", 410012, Saratov, Russia*
[2]*Institute of Radioengineering and Electronics, Moscow, Russia*
[3]*Department of Physics and Astronomy, University of Exeter, Physics Building, Stocker Road, Exeter EX4 4QL, UK*
tvlad4@yandex.ru

In connection with the development of the technological process of fabrication thin magnetic films, the study of spin waves (SW) during their propagation in regular and irregular magnon structures is of great interest [1]. Magnonics is a branch of condensed matter physics that aims to study the characteristics and methods of controlling spin-wave transport in various wave-bearing systems. Currently, devices based on the principles of magnon logic, which demonstrate reconfigurable propagation of SW in two-dimensional magnetic structures, are of great interest [2]. Signals can be encoded in the amplitude and/or phase of the SW as a unit of information using the physical wave effects in the form of a transfer of the amplitude of the angular momentum of the spins forming SW. In recent years, a large amount of research has been devoted to the development of SW technologies, and many goals have already been accomplished in the form of SW logic gates. The study of control mechanisms for non-reciprocal propagation of magnetostatic spin waves in monocrystalline magnetic films is an interesting area of research as it opens up new design possibilities in creating logically reconfigurable devices [3].

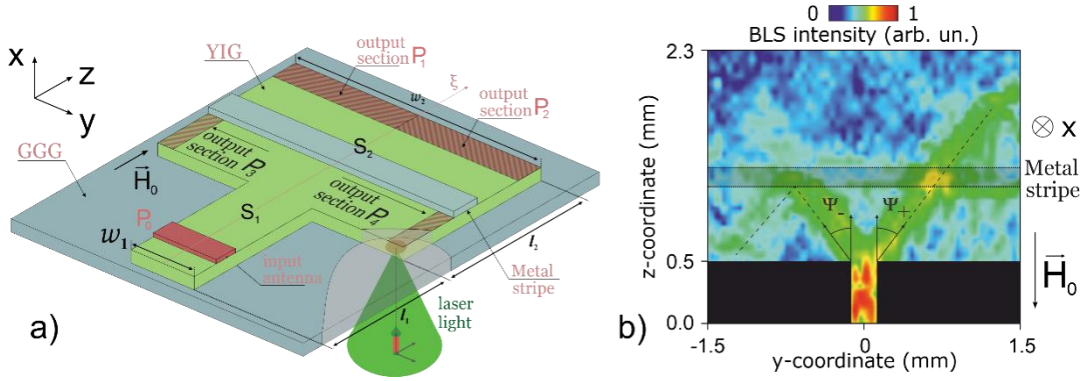

Fig. 1. Schematic structure (a), BLS intensity map (b).

The building block of reconfigurable magnon circuits can be a splitter based on the coupling of a spatially constrained waveguide element and an unconstrained magnetic film in which directional focusing of spin waves is possible. One of the requirements for focusing is the presence of anisotropy, which provides different group and phase velocity directions [4].

In this work, caustic SW beams propagating nonreciprocally in a T-shaped magnetic structure with a partially metallized surface are investigated using numerical and experimental methods. Using the Mandelstam-Brillouin microwave spectroscopy and micromagnetic simulation, the possibility of controlling the spatial selection of SW frequency in a T-shaped magnetic structure with a partially metallized surface is demonstrated.

The proposed implementation of a spin-wave signal demultiplexer based on a T-shaped magnetic film of an yttrium iron garnet signal is schematically shown in Fig. 1(a). For the experiment, a waveguide structure was made of yttrium iron garnet [Y3Fe5O12, (111)] with a saturation magnetization of $4\pi Ms = 1750$ G, epitaxially grown on a gallium-gadolinium garnet substrate [Gd3Ga5O12, (111)]. A system of local laser ablation was used to form a T-shaped waveguide structure. A metallized layer is deposited on the surface of the waveguide in the transverse direction. Using a microstrip antenna with a width of 30 μm, located at the beginning of the waveguide structure, a spin-wave front propagating in the direction of the metallized layer was excited. To obtain maps of the spatial distribution of dynamic magnetization by Brillouin spectroscopy, an experiment was carried out in a quasi-backscattering configuration, while the intensity of the reflected optical signal was proportional to the square of dynamic magnetization.

Stationary spatial magnetisation distributions for different external magnetic field directions on Fig. 1(b) shows the spatial distribution of spin-wave signal intensity. We observe that the magnetic field direction along the Oy axis permits the observation of the effect of the nonreciprocal propagation of the quasi-caustic beams of the diffracted spin-wave signal. The presented device design allows changing the direction of propagation of the spin-wave signal due to non-uniform distribution of the internal magnetic field generated by the metallised layer.

In this paper, we investigate the non-reciprocal propagation of super-directional quasi-caustic beams of SWs in a waveguide structure with a partially metallized surface. The experimental method of Brillouin spectroscopy and numerical micromagnetic methods reveal the mechanisms for controlling the SW signal in a T-shaped structure during tangential magnetization of a film of yttrium ferrite garnet. Partial surface metallization as a control element for the propagation of SW caustics is demonstrated. A method is demonstrated for controlling the power of the detected signal at different outputs by changing the direction of the external magnetic field and increase or decrease frequency value the excited signal. The proposed structure can be used as a functional element of signal branching in planar topologies of magnon networks and signal processing devices based on them.

This work was supported by Russian Science Foundation (№ 23-79-30027)

References

[1] F. Heussner, A. A. Serga, T. Brächer et. al. Appl. Phys. Lett., 111, 122401 (2017).

[2] A Barman, G. Gubbiotti et. al. J Phys Condens Matter., 33, 413001 (2021).

[3] A.V. Sadovnikov, E.N. Beginin, S.E. Sheshukova, D.V. Romanenko, Y.P. Sharaevsky, and S.A. Nikitov, Appl. Phys. Lett. 107, 202405 (2015).

AP1-2P/4

Strain-magneto-optical phenomena in ferrite-spinel crystals

Telegin A.V., Surzhikov E.A., Sukhorukov Yu.P., Naumov S.V.
M.N. Mikheev Institute of Metal Physics UB of RAS, 620137, Ekaterinburg, Russia
telegin@imp.uran.ru

Recently a new strain-magneto-optical (SMO) effect in the IR spectral range was discovered in ferrite-spinels with giant magnetostriction [1-3]. Being discovered SMO determined the emergence and development of a new scientific direction via the combination of the physics of magnetic phenomena and straintronics.

Here we will present the results of study of the optical and MO properties in $MnFe_2O_4$ single crystals compared to $CoFe_2O_4$ crystals. These ferrimagnetic spinel are characterized by high transparency in the IR spectral region, high the Curie temperature, magnetization and strong magnetostriction.

High-quality single crystals of spinel were synthesized by the zone floating method with radiation heating. By using EDAX and XRD methods it has been confirmed that the samples are single-phase and their chemical composition corresponds to the formula unit. All optical measurements were carried out at room temperature by using the IR prism monochromator in magnetic fields of up to 3 kOe directed in-plane to the sample surface and along various crystallographic axes of the samples.

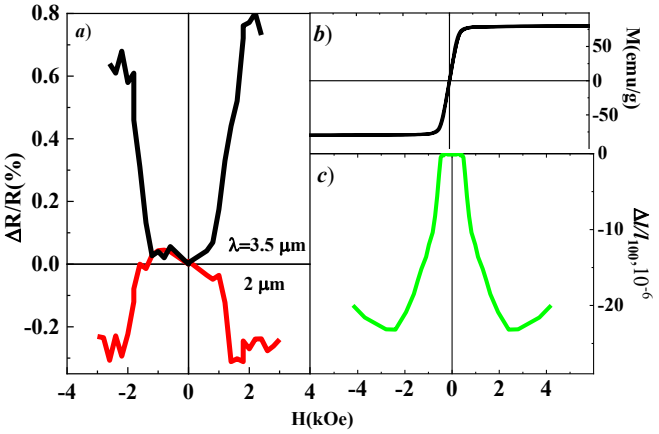

Fig.1 Field dependences of *a*) magnetoreflection *R/R* at different wavelengths and H||[100] at *T*=295 K, *b*) magnetization *M* and *c*) magnetostriction $\Delta l/l_{100}$ for the $MnFe_2O_4$ single

The study of $MnFe_2O_4$ crystals revealed the existence of a high magnetoreflection effect within a wide IR wavelength range, which was most pronounced near the absorption edge and impurity-type bands similar to those observed for $CoFe_2O_4$ crystals. The magnetoreflection in $MnFe_2O_4$ changes its sign as a function of the magnetic field and reaches 1 % at a magnetic field of 3 kOe at wavelength λ=2.5 μm (Fig.1). According to [1-3] it is suggested the magnetoreflection effect in $MnFe_2O_4$ is related to the absorption edge shift and to magnetoelastic strains. The magnetorefractive and magnetoabsorption effects in $MnFe_2O_4$ spinel was also estimated using the Kramers-Kronig analysis of the reflectivity data. The geometry of the experiment made it possible to estimate the anisotropy of the magnetoreflection effect in spinel which has 180^0 symmetry. The highest magnitude of the effect was obtained in case of the magnetic field directed along [001] direction of the crystal.

Finally, the obtained results could help in understanding the SMO phenomena in ferrites and developing novel MO devices based on magnetostrictive magnetics.

The work is carried out within the framework of the state task of the Ministry of Science and Higher Education of Russia ("Spin" No. 122021000036-3).

References

[1] Yu. Sukhorukov, N. Loshkareva, A. Telegin et al. Optics and Spectroscopy, 116, 878 (2014).
[2] Yu. Sukhorukov, A. Telegin, N. Bebenin et al. Magnetochemistry, 8, 135 (2022).
[3] Yu. Sukhorukov, A. Telegin, N. Bebenin et al. Phys. of Met. and Metallogr., 119, 1167 (2018).

AP1-2P/5

Nonreciprocal modes of selection of spin waves in the low-frequency and high-frequency ranges in multilayer magnonic crystals

Odintsov S.A.[1], Ptashenko A.S.[1], Lock E.H.[2], Beginin E.N. [1], Sadovnikov A.V. [1]

[1]*Saratov State University, 410012, Saratov, Russia*
[2] *Fryazino Branch of Institute of Radioengineering and Electronics, 141190, Fryazino, Russia*
odinoff@gmail.com

For a number of decades, multilayer films based on ferromagnetic materials that support the propagation of spin-wave signals have attracted a large number of researchers due to the constant development of both technologies for creating magnetic layers on non-magnetic substrates and the development of ideas for using magnetization waves to solve information signal processing problems. [1]. Magnetic thin-film structures are made in the form of single magnetic films, double magnetic films and multilayer magnetic films consisting of ferromagnetic (FM), antiferromagnetic (AFM) and non-magnetic (NM) films of various thicknesses and arrangement of layers, as well as in the form of magnonic crystals [2]. In turn, based on ferrimagnetic films with periodic modulation of geometric or material parameters (MC), it is also possible to use them to control the spectrum of magnetic waves. Magnonics opens up a promising alternative to the concept of non-CMOS signal processing devices in which information is carried by spin waves (SW) instead of electrons. Ferrimagnetic thin films of yttrium iron garnet (YIG) have a much lower dynamic attenuation of spin waves compared to metal magnetic waveguides.

.

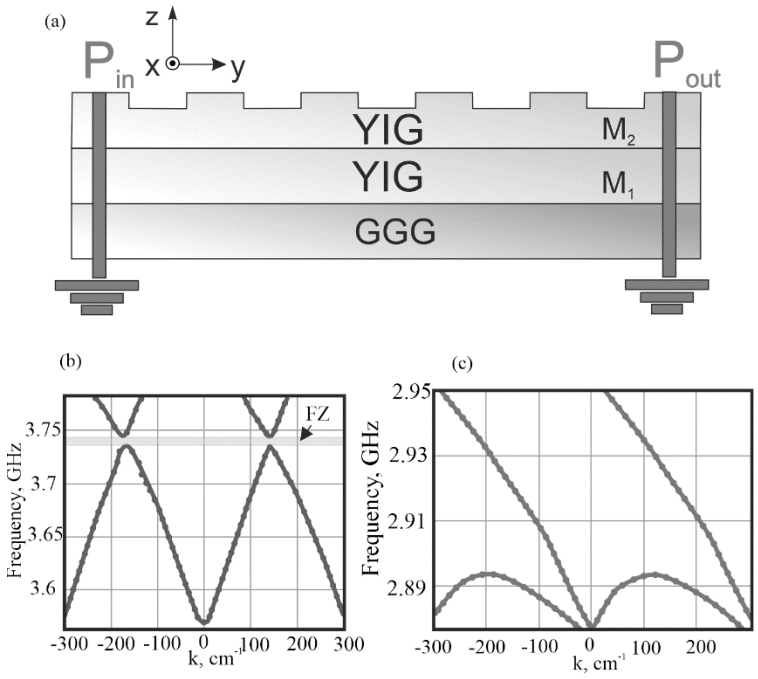

Fig. 1. Scheme of the structure under consideration(a), dispersion characteristics of spin waves in a two-layer waveguide with different magnetizations in the layers: (b) HF region, (c) LF region;

It is known that the amplitude of the precession of the magnetization of surface modes should be asymmetric with respect to the direction of propagation is called the nonreciprocity of

spin waves. This behavior is well known and has been experimentally measured in micro- and nanoscale magnetic films using Mandelstam-Brillouin spectroscopy [3]. The use of YIG dielectric films offers more advantages compared to metal films due to significantly lower spin losses in YIG. The spectrum of MSWs propagating in the MC consists of alternating transmission and non-transmission zones [1]. Blocking zones, also called band gaps, are formed at frequencies where the wave numbers satisfy the Bragg resonance condition [4].

On the other hand, in the context of data processing, the nonreciprocity of spin waves, which can manifest itself in the phase, amplitude, or frequency dependence of the direction of SW propagation, is a powerful tool for possible applications in communications. and logical devices [1].

In the present work, we consider structures consisting of two-layer YIG waveguides with different saturation magnetizations in layers in different layers, and the upper layer is a magnonic crystal (MC). Such structures can be used as basic elements to create various devices such as filters, couplers, dividers, multiplexers, etc. On fig. 1 shows a schematic representation of the structure under study. The waveguide width is w = 200 μm, and the thickness t = 15.8 μm. The length of the waveguides was 6 mm. Film layer on a GGG YIG substrate 7 μm thick with saturation magnetization $4\pi M1 = 1738$ G, and on it is a YIG layer 9 μm thick with saturation magnetization $4\pi M2 = 904$ G. A periodic structure is created on the surface of the upper layer. The system under study was placed in a uniform static magnetic field H = 1200 Oe, oriented along the x axis of each waveguide to effectively excite a guided magnetostatic surface wave (MSSW). During the study, the field changed direction to the opposite, to excite the MSSW, which propagated in the opposite direction, thus it was possible to observe the effect of SW nonreciprocity in the structure under study. The spectrum of MSWs propagating in the MC consists of alternating transmission and non-transmission zones [1]. Blocking zones, also called band gaps, are formed at frequencies where the wave numbers satisfy the Bragg resonance condition [4]

Micromagnetic simulation of the structure under study was carried out by the finite difference method. The finite element method was used to numerically simulate and study the dynamics of SW propagation in a two-layer system with an MC limited in the transverse direction from yttrium iron garnet. Forbidden zones in such a system were identified, and it was also shown how the geometric parameters of waveguides affect the dynamics of spin waves in and the impassable zones during wave propagation in different directions

This work was supported by the grant from Russian Science Foundation (No 23-29-00610)

References

[1] Nikitov, S A et al., Physics-Uspekhi, 63 (10), 945(2020)

[2] S. Tacchi, P. Gruszecki, M. Madami, *et al.*, Sci Rep 5 (2015) 10367

[3] Odintsov S.A., Lock E.H., Beginin E.N., Sadovnikov A.V. Russian Technological Journal. 10(4), 55-64(2022).

[4] Odintsov, S.A., Sadovnikov, A.V., Grachev, A.A. et al., Jetp Lett. 104, 563–567 (2016).

AP1-2P/6

Effects of the spatial distribution of the spin-wave signal power in a system of orthogonal YIG waveguides

Masliy R.V. [1], Khutieva A.B. [1], Sadovnikov A.V. [1]

[1]*Saratov State University, 410012, Saratov, Russia*

At present, methods for constructing information signal processing systems based on the effects of the transfer of magnetic moments or electron spins without charge transfer are being actively studied [1]. In such devices based on magnon principles, the information signal encoded in the phase or amplitude of spin waves (SW), and logical operations are implemented based on the principles of spin-wave interference [2]. Planar ferrite waveguide microstructures of finite width based on yttrium iron garnet (YIG) films can be used as the basic elements of "magnon networks" to create various signal processing devices: delay lines, filters, interferometers, switches, multiplexers [3-4].

In this work, we study the influence of the dipole coupling of magnon microwave guides for the implementation of vertical and lateral transport of magnons. To study the dynamics of SW propagation in a system of YIG waveguides, the method of coupled waves was used [5–6]. With the help of micromagnetic modeling, the modes of SW propagation in arrays of microwave guides formed by an array of YIG strips were studied [7]. The mechanisms leading to the formation of various "patterns" formed by a spin-wave signal during its propagation in longitudinally irregular thin-film magnon microwaveguides are investigated.

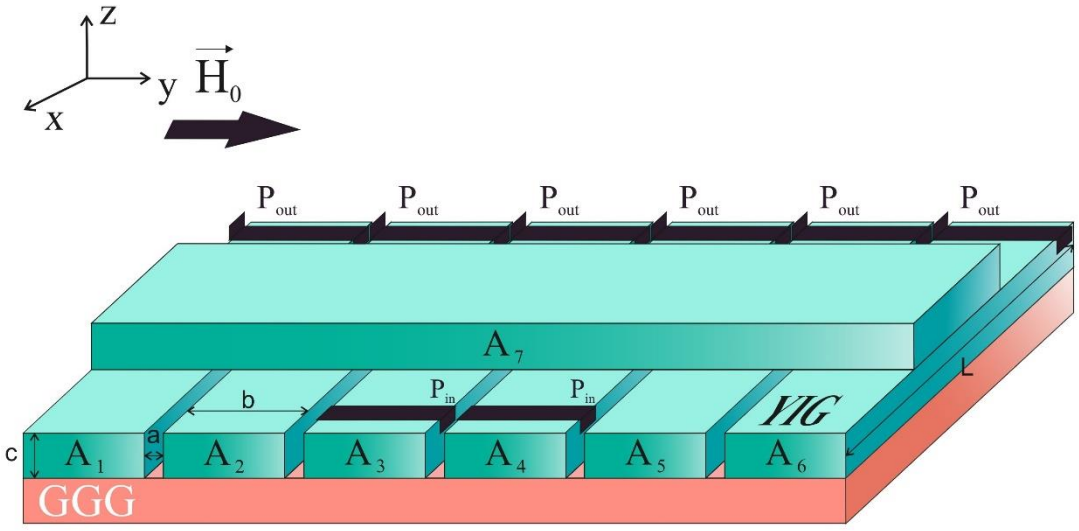

Fig. 1. Schematic representation of a microwave guide array, *a* – horizontal gap, *b* – width, *c* – thickness, *L* – length of the microwave guides, P_{in} and P_{out} – antennas for excitation and reception of SW, respectively.

Micromagnetic modeling [8] was carried out for a system of laterally and vertically coupled ferrite microwave guides (Fig. 1) made of an yttrium iron garnet film, located on a gallium

gadolinium garnet (GGG) substrate. Microwaveguides are made in the form of elongated strips, length L = 4 mm, width b = 300 μm and thickness c = 10 μm, forming a grating of a horizontal layer, which contains six waveguides located with gaps in the horizontal plane, and one waveguide located perpendicular to them. The saturation magnetization of yttrium iron garnet films is **M** = 139 Gs, and the value of the external magnetic field is $\mathbf{H_0}$ = 1200 Oe directed along the y-axis, which ensures effective excitation of surface spin waves (SWs). The radiative damping of weak modes differs from the damping of strong modes by two orders of magnitude, which makes it possible to reduce the amount of pumping required to enter the lasing regime. The pump value can be reduced, practically, to the level of compensation for dissipative losses. The decay frequency of weak modes is about 0.0005 THz, while the decay frequency of strong modes is about 0.08 THz. The amplification mode requires compensation not only for dissipative losses, but also for radiation losses. Thus, a decrease in radiative damping substantially lowers the lasing threshold.

The work was supported by the Russian Science Foundation (project №20-79-10191).

References

[1] A. Barman, G. Gubbiotti, S. Ladak, J. Phys.: Condens. Matter. V. 33, 41, 413001 (2021).
[2] D. D. Stancil, A. Prabhakar, Springer (2009).
[3] Q. Wang, P. Pirro, R. Verba, S. Adv. 4, e1701517 (2018).
[4] K. Vogt, H. Schultheiss, S. Jain, Appl. Phys. Lett. 101, 042410 (2012).
[5] A. B. Khutieva, B. R. Akimova, E. N. Beginin, A. V. Sadovnikov, Phys. Sol. St. V. 9, 1279 (2022).
[6] A. B. Khutieva, E. N. Beginin, S. E. Sheshukova, A. V. Sadovnikov, Phys. Sol. St. V. 14, 2344 (2022).
[7] A. B. Khutieva, B. R. Akimova, E. N. Beginin, A. V. Sadovnikov, Bull. Rus. Acad. Sc. Phys. V. 87, 679-700 (2023)
[8] A. Vansteenkiste, J. Leliaert, M. Dvornik, AIP Adv. 4, 107133 (2014).

AP1-2P/7

Investigation of filtration regimes in the composite structure of ferromagnetic waveguides with variated width

Garanin F.E., Gubanov V.A., Khutieva A.B., Sadovnikov A.V.

[1]*Saratov State University, 410012, Saratov, Russia*

At the moment, the study of the propagation of magnetostatic waves in ferromagnetic structures is of great interest [1-4] due to the fact that they can be used for processing and storing information signals. The possibility of creating different elements of interconnections in which the properties of spin waves can be changed using various methods – changing the power and frequency of the input signal, applying external interactions (creating elastic deformations [5], changing the properties of the structure by laser heating [6]), etc. It is possible to create irregular

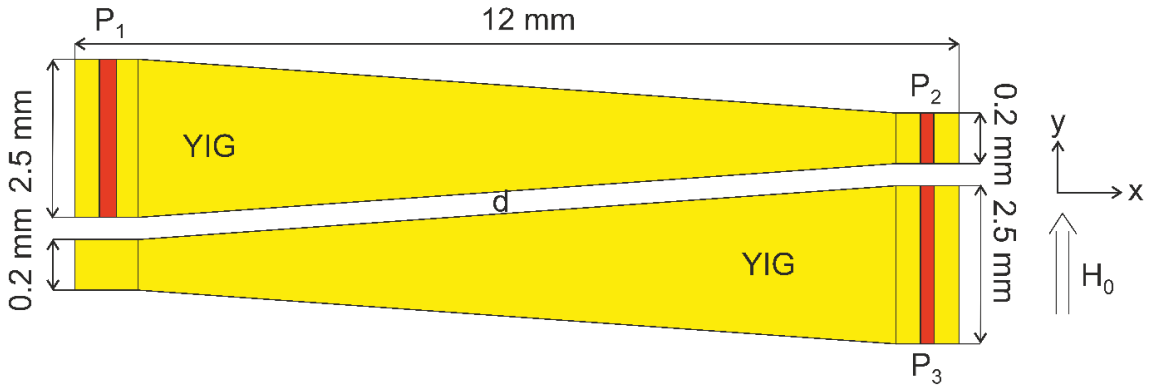

structures, for example waveguides with varying widths.

Fig. 1. A system of two waveguides located parallel to the gap d with varying width.

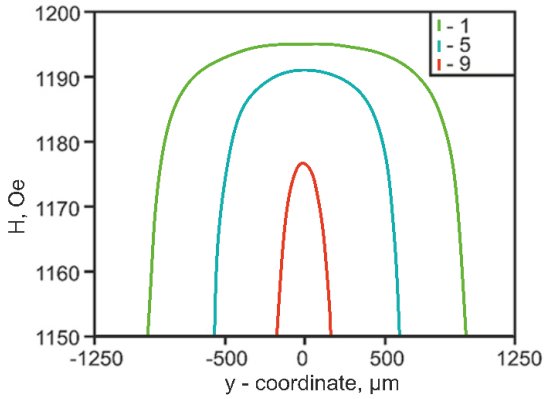

Fig. 2. Distribution of the internal magnetic field in a microwave with decreasing width in slices x = 1, 5, 9 mm.

Figure 1 schematically shows a system of magnetic microwave guides connected through the side wall, the total length of which is 12 mm. There is a 10 mm long segment with a variable width from 2.5 mm to 200 microns for each microwave. Also in the structure on the left and right there are areas with a length of 1 mm, on which the input port P1 and output ports P2 and P3 are located.

These regions were introduced for efficient excitation and reception of the spin wave in the system. The distance between the microwave diodes was d = 20 microns, which came from experimentally obtained samples. Experimental samples were obtained using the laser ablation method at the MiniMarker2 installation. The structure was placed in a homogeneous external magnetic field H0 = 1200 E, which was directed along the y axis, at hich surface magnetostatic waves (PMSW) were excited.

This system was studied using experimental methods of microwave spectroscopy and the method of Mandelstam-Brillouin spectroscopy (MBS), as well as the method of micromagnetic modeling in the program MuMax3. The distributions of the internal magnetic field in these microwave diodes were obtained separately and its heterogeneous nature was shown. The case of a coupled system is considered and the transformation of internal magnetic fields in specific sections along the x-axis is investigated.

In micromagnetic modeling, a structure with a varying gap between waveguide structures d = 40 microns and 80 microns was also considered. It has been shown that as d increases, the coupling between the waveguides decreases.

When modeling the structure at the ends of the waveguide, regions with an increased attenuation parameter at the boundaries of the structure were used to reduce the influence of the reflected signal. The excitation of the PMSV occurred by applying a microwave signal to a microstrip antenna with a width of 30 microns, located in a wide area above the microwave. The spectra of the spinwave signal transmission in the structure of coupled magnon microwave diodes with different widths at the output ports P2 and P3 were obtained. The modes of redistribution of the PMSV power are obtained depending on the frequency of excitation of the signal at the input port P1. The first mode was obtained at a frequency of f = 5.21 GHz, at which the PMSV propagates to port P2. The second mode was obtained at a frequency f = 5.16 GHz, at which the PMSV propagates to the output port P3. For characteristic frequencies associated with non-transmission frequencies for a separate output port, maps of the intensity distribution of the PMSV were obtained by MBS and micromagnetic modeling methods, demonstrating the modes of power redistribution between microwave diodes.

This structure can be used as a directional coupler of a microwave signal on magnetostatic waves.

This work was supported by the Russian Science Foundation (grant № 23-79-30027).

References

[1] V.V. Kruglyak, S.O. Demokritov, and D. Grundler // J. Phys. D: Appl. Phys. 2010. V. 43. No 26. P. 264001.

[2] Sander, D., Valenzuela, S. O., Makarov, D., et. al. // J. Phys. D: Appl. Phys. 2017. V. 50. No 36. P. 363001.

[3] V.A. Gubanov, A.A. Martyshkin, S.E. Sheshukova, and Sadovnikov A.V.// ЖТФ 2019. Т. 89. В. 11. С. 1726.

[4] A.V. Sadovnikov, A.A. Grachev, V.A. Gubanov, S.A. Odincov, A.A. Martyshkin, S.E. Sheshukova, Yu.P. Sharaevskii, and S.A. Nikitov // Appl. Phys. Lett. 2018. V. 112. P.142402.

[5] A.A. Grachev et al. // AIP Advances 2021. V. 11. P. 035316.

[6] V.A. Gubanov et al. // Phys. Rev. B 2023. V. 107. P. 024427.

AP1-2P/8

Comparative analysis of properties of magnetooptical magnon junctions on the base TmBiIG and YBiIG

Lyashko S.D.[1], Semuk E.Yu.[1], Nauhatsky I.A.[1], Osmanov S.V.[1], Mikhailova T.V.[1], Berzhansky V.N.[1], Belotelov V.I.[1,2], Han X.F.[4]

[1] V.I. Vernadsky Crimean Federal University, 295007, Simferopol, Russia
[2] Lomonosov Moscow State University, 119991, Moscow, Russia
[3] Beijing National Laboratory for Condensed Matter Physics, Institute of Physics
[4]Chinese Academy of Sciences, Beijing 100190, China

Yttrium iron garnet $Y_3Fe_5O_{12}$ (YIG) films have a minimal spin wave attenuation parameter and are promising materials for spintronics and magnonics. Recently, they have been used to create devices such as magnon valves and magnon junctions (MJ) [1]. YIG films have high magnetization and, due to shape anisotropy exhibit an "easy plane" (EP) anisotropy. Therefore, as a second layer for magnon junctions, a search is underway for materials with strong uniaxial anisotropy. It is believed that such a material may be $Tm_3Fe_5O_{12}$(TmIG), which has strong magnetostriction and can contribute to uniaxial anisotropy due to deformation effects. Moreover, when part of the thulium is replaced by diamagnetic Bi ions, which have a large ionic radius and are included in dodecahedral positions, uniaxial growth anisotropy can also form. It is also very important that Bi-substituted garnets have significant magneto-optical effects.

The goal of the work was to study two series of MJ structures based on bismuth-substituted YBiIG garnet ferrites. The YBiIG(10)/NiO(6)/YIG(10) and TmBiIG/NiO/YIG structures were obtained by the magnetron method on two types of substrates with significantly different crystal lattice parameters GGG ($Gd_3Ga_5O_{12}$) and SGGG ($Gd_{2.6}Ca_{0.4}Ga_{4.1}Mg_{0.25}Zr_{0.65}O_{12}$). Additionally, separate 10 nm monolayers of YBiIG and TmBiIG, which represented the lower part of such magnon junctions, were studied.

The morphological characterization and crystal structure analysis are performed by atomic force microscopy (AFM, NT-MDT, Russia) and (high-resolution) x-ray diffraction (Rigaku SmartLab). Optical transmittance and magneto-optic Faraday effect were measured by ORMS FR/KR2 (Holmarc, India). The FMR property is measured using a EPR spectrometer SPINSCAN X (Belarus) at room temperature.

The effective anisotropy field Ha and, accordingly, the uniaxial anisotropy constant Ku in films and structures were determined by the FMR method. FMR measurements were carried out with the magnetic field oriented out of plane H(0) and in plane H(90) to the film . In this case, a single line with a width from 30 to 200 Oe was observed in almost all MJ structures. Table 1 shows the main results.

All MJ-structures except SGGG/TmBiIG/NiO/YiG have easy plain type anisotropy. The value EP anisotropy field Ha compared to monolayers in GGG/YBiIG/NiO/YIG MJ structure increased almost 2 times, while in SGGG/YBiIG/NiO/YIG it changed slightly.

Table 1.

		h, nm	RMS, nm	H_u^*, Oe	Ku 10^3 erg/cm^3	Hres$^{\perp}$ Oe	$\Delta H^{\perp}$ Oe	Hres$_{||}$ Oe	$\Delta H_{||}$ Oe	θ_{Fs}, 10^6 deg/cm
1	GGG/YBiIG	10	-	-1769	-1,32	5130	210	2590	180	-9.37
2	SGGG/YBiIG	10	-	-1225	36,6	4571	60	2789	31	-2.99
3	GGG/YBiIG/NiO/YIG	10\6\10	1.0	-3340	-110,7	6720	140	2100	44	-13.12
4	SGGG/YBiIG/NiO/YIG	10\6\10	1.2	-1130	43,1	4510	50	2860	30	-2.41
5	GGG/TmBiIG	10	-	-2580	-65,7	6450	190	2790	100	-3.27
6	SGGG/TmBiIG	10	-	-170	68,5	4000	100	3750	85	-5.56
7	GGG/TmBiIG/NiO/YIG	10\6\10	0.621	-2144	-41,4	5845	200	2780	100	-1.56
8	SGGG/TmBiIG/NiO/YIG	10\6\10	2.548	429	101,9	3290	170	3940	70	<0,1

When forming MJ structures based on thulium ferrite, the deformation contribution to the uniaxial anisotropy field Hu with respect to the monolayer was Hud=440 Oe in the GGG/TmBiIG/NiO/YIG structure, and Hud=600 Oe in the SGGG/TmBiIG/NiO/YIG structure. Thus, perpendicular uniaxial anisotropy was realized in the only one MJ structure SGGG/TmBiIG/NiO/YIG with an anisotropy field Hu= 429 Oe.

The SGGG/TmBiIG/NiO/YIG structure has the maximum surface roughness value RMS = 2.5 nm. The minimum roughness value of RMS = 0.5 nm has the GGG/YBiIG/NiO/YIG structure. The monolayer SGGG/BiYIG has a roughness of about 0.36 nm

Films and structures based on YBiIG had the maximum values Faraday effect, while the in the MJ structures Faraday effect was lower than on monolayers, it turned out to be especially low in a structure with perpendicular anisotropy.

This work was financially supported by the Ministry of Science and Higher Education of the Russian Federation, Megagrant project N 075-15-2022-1108 and Russian Science Foundation, project № 23-62-10024.

References

[1] Xiu-Feng Han et all, From microelectronics to spintronics and magnonics
Chin. Phys. B, 2022, 31 (11): 117504.

Interfacial Dzyaloshinskii-Moriya interaction in HM/FM multilayers and alloys

Telegin A.V.[1], Bessonov V.D.[1], Teplov V.S.[1], Makarova M.S.[1], Samardak A.S.[2], Park J.[3]

[1] *M.N. Mikheev Institute of Metal Physics UB of RAS, 620137, Ekaterinburg, Russia*
[2]*Far Eastern Federal University, 690922, Vladivostok, Russia*
[3]*Korea University, Seoul, Republic of Korea*
telegin@imp.uran.ru

The interfacial DMI is of particular importance in the context of systems consisting of an ultrathin ferromagnetic (FM) film with PMA, in contact with a heavy metal (HM) layer. In such a system the interfacial DMI arises due to the broken inversion symmetry at the interface and the large SOC of the HM atoms. HM/FM multilayers are particularly interesting from the application point of view due to the fast domain-wall motion driven by an electric current in the presence of the DMI. Speaking about the interfacial DMI it is of the high importance to be able to measure the magnitude and sign of D constant in order to be able to optimize the effect. One of the most commonly used experimental technique is a Brillion light scattering (BLS), where D is extracted by measuring the nonreciprocity of propagating spin waves in in-plane magnetized films.

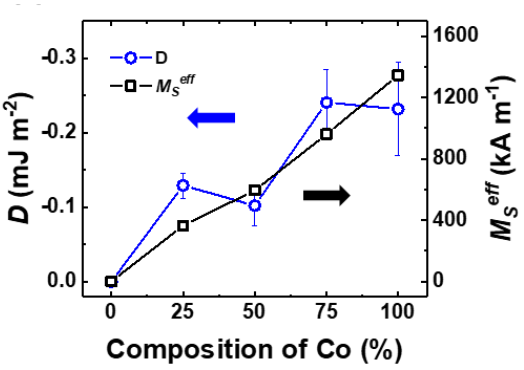

Fig.1. The saturation magnetization M_s and D constant vs. concentration of Co for $Pt_{100-x}Co_x$ alloys.

Here we aim to provide the results of study of DMI in ferro- and ferrimagnetic thin-film nanostructures with compositional gradient layers by BLS technique. It was shown that the DMI has a complex behavior attributed mainly to the strong variation of interfacial contributions in Pt-Co alloys with various compositions due to the composition gradient-induced bulk magnetic asymmetry and the face-centered cubic (fcc) (111) crystal structure. Actually, single Pt-Co alloys showed a significant (~57.8%) of the D value while for the gradual Pt-Co alloy enhancement reached 61.4% increase relative to layered Pt/Co sample. It should be note there was a weak temperature variation of D obtained while cooling samples from 450 K to 80 K.

Finally, the controllable spatial composition will allow manipulating the distribution of DMI vectors in three dimensions, that is essential for designing future spin-orbitronics devices, especially skyrmion-based.

Support of the Russian Science Foundation № 21-72-20160 (https://rscf.ru/en/project/21-72-20160) is acknowledged.

References

[1] J.Park, T. Kim, G.W. Kim, V. Bessonov et al. Acta Materialia, 241, 118383 (2022).

Bolometric prospects of laser-induced porous graphene

Telegin A.[1], Sukhorukov Yu.[1], Mikheev K.[2], Zonov R.[2], Naumova L.[1], Mikheev G.[2]

[1]*M.N. Mikheev Institute of Metal Physics UB of RAS, 620137, Ekaterinburg, Russia*
[2]*Udmurt Federal Research Center, UB of RAS, 42606, Izhevsk, Russia*
telegin@imp.uran.ru

The idea of creating a broadband detector of electromagnetic radiation based on graphene is based on its unique physicochemical properties, for example, near to zero band gap. However, conventional single layer graphene has low light absorption and low optical efficiency. To address this issue, researchers have developed a method for synthesizing porous graphene, or LIG, through thermal decomposition (pyrolysis) of a polyimide film [1]. The resulting porous 3D structure significantly increases light absorption and enables the detection of ultrafast photo-induced effects in LIG [2].

This study focuses on the bolometric characteristics of the synthesized LIG. The results show that the thermal resistance coefficient of LIG is β ~0.05%·K^{-1} at room temperature, increasing to ~0.15%·K^{-1} at lower temperatures. The maximum LIG detector sensitivity at 532 nm is ~0.08% W^{-1} at frequencies up to 10 kHz, which is an order of magnitude lower than the literature data for multilayer graphene. The spectral dependencies of the detector sensitivity are described by the Wien law, with the exception of features associated with the generation of photoelectrons in porous graphene and light losses in the optical scheme of the setup. The frequency dependence of the detector sensitivity is determined by the contribution of at least two photo-processes [3]. The first process is thermal and is associated with the heating of LIG due to light absorption, while the second process weakly depends on the frequency of the emitter and is associated with the photo-induced change in the mobility and concentration of charge carriers due to trapping at defects.

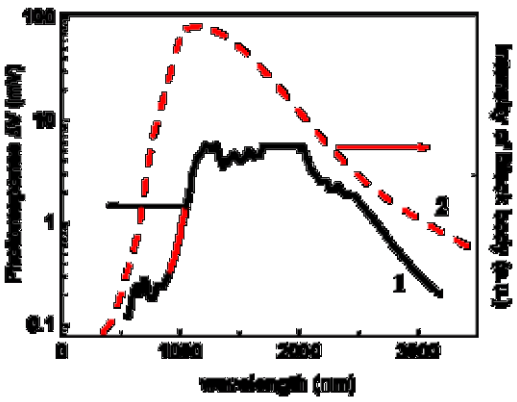

Fig. 1. Sensitivity spectrum of the LIG at f = 10 Hz (1) and the spectrum of blackbody emission (2) at T=300 K.

Due to its relatively wide spectral and frequency ranges and simple synthesis technology, LIG is a promising material for the development of bolometric-type detectors. Further research is needed to improve the sensitivity of LIG and to explore its potential applications in various fields.

Supported by the Ministry of Education and Science of the Russian Federation (SPIN) № 122021000036-3.

References

[1] Y. Ruquan, Dustin K. James, James M. Tour. Adv. Mater., 31, 1803621 (2019).
[2] K.G. Mikheev et al. Technical Physics Letters, 46, 458 (2020).
[3] Yu.P. Sukhorukov et al. Optical materials, 133, 112957 (2022).

Ultrafast carrier dynamics in classical ferromagnetic spinel

Telegin A.V.

[1]*M.N. Mikheev Institute of Metal Physics UB of RAS, 620137, Ekaterinburg, Russia*

The further development of spintronics requires new materials with ultrafast magnetooptical (MO) phenomena and spin transport at terahertz (THz) and even higher frequencies. Yet being underestimated magnetic semiconductors can be one of the promising materials. For example, chromium chalcogenide spinels show relatively high charge carrier mobility, high spin polarization, anisotropic magnetoresistance and giant MO effects, and numerous applied applications [1]. Here we will present some data regarding the ultrafast MO response and high-frequency carriers transport for $Hg_{1-x}Cd_xCr_2Se_4$ ($0 \le x \le 1$) thin films and bulk crystals in the IR/THz spectral range.

The $Hg_{1-x}Cd_xCr_2Se_4$ single crystals demonstrate giant IR magnetoabsorption and magnetoreflection effects [1]. The sign and magnitude of the effects are controlled by the external magnetic field and depend on the peculiarities of electronic structure of spinel, the type of conductivity, level of doping [2], etc. The impurity transitions play a decisive role and leads to a distinct anomaly in the magnetoabsorption. The dynamic of these transitions is studied by an optical pump-probe method. The estimated signal risen front and the decay time are about 1 ps and 3-6 ps, respectively, depending on the temperature of spinel.

The femtosecond laser pulses are able to trigger oscillations of the Faraday rotation in the ferromagnetic $CdCr_2Se_4$ films below the Curie point. Tuning the photon energy of the pump pulses we revealed two different mechanisms, pump polarization dependent and the polarity of the applied magnetic field dependent one, which induce precession in this material [3].

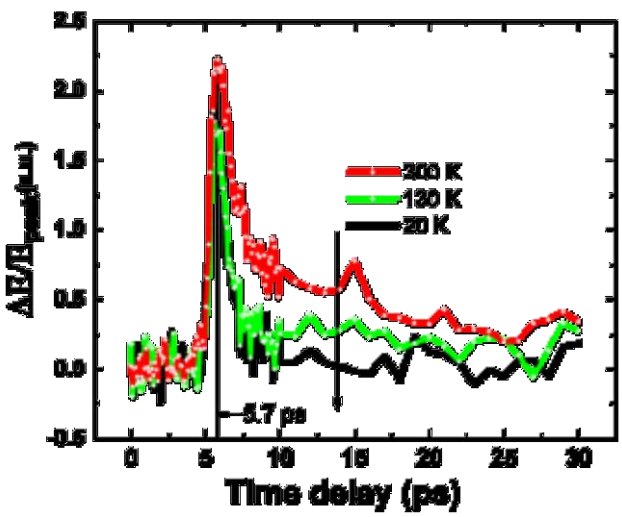

Fig.1. The temporal profile of the THz dynamic response in spinel film at different temperatures.

The ultrafast dynamic in spinel crystals and films is saved in case of a THz pump-probe scheme (Fig.1). The effects of magnetic linear birefringence and dichroism are observed in spinel crystals in the frequency range 0.5-2.5 THz at temperatures below the magnetic ordering by a THz pump-probe method. The maximal rotation of the light polarization plane associated with a high-frequency response to the DC anisotropic magnetoresistance in spinel reaches about 4.3 rad/cm at H=1 kOe [4]. Therefore, chromium spinels can be considered for studying various ultrafast IR and THz phenomena.

Supported by the program "Spin" No. AAAA-A18-118020290104-2.

References:

[1] Yu.P. Sukhorukov et al., JETP 121, 437–445 (2015).
[2] M.I. Auslender and N.G. Bebenin, Sol. State Comm. 69, 761 (1989).
[3] S. Barsaume et al., J. of Phys. Cond. Matt. 29, 325502 (2017).
[4] A. Pogrebna et al., Physical Review B 98, 214427 (2018).
[5] T.J. Huisman et al., Appl. Phys. Lett. 106, 132411 (2015).

Section
Plasmonics and Nanophotonics

CO1-3O/2

Topological properties of Tamm plasmon polariton in one-dimensional photonic crystal covered by metasurface

Fedchenko D.P.[1], Zuev A.S.[1], Timofeev I.V.[1]

[1]*Kirensky Institute of Physics, Federal Research Center KSC SB RAS, Krasnoyarsk 660036, Russia*

DFedchenko@sfu-kras.ru

Among the important problems in topological photonics, one can note the study of topological insulators [1], Tamm edge states [2], lasing in topological states [3], and so on.

We implement a 1D lattice to construct a topological and edge state. For this reason, we consider Su-Schrieffer-Heeger (SSH) model [4] with a defect in the middle part of the lattice. As shown in the figure 1(**A**), a typical lattice under consideration is formed by identical micropillars coupled with different hopping strength t and t' (t > t'). This is achieved, for example, by placing micropillars in a zigzag pattern [3].

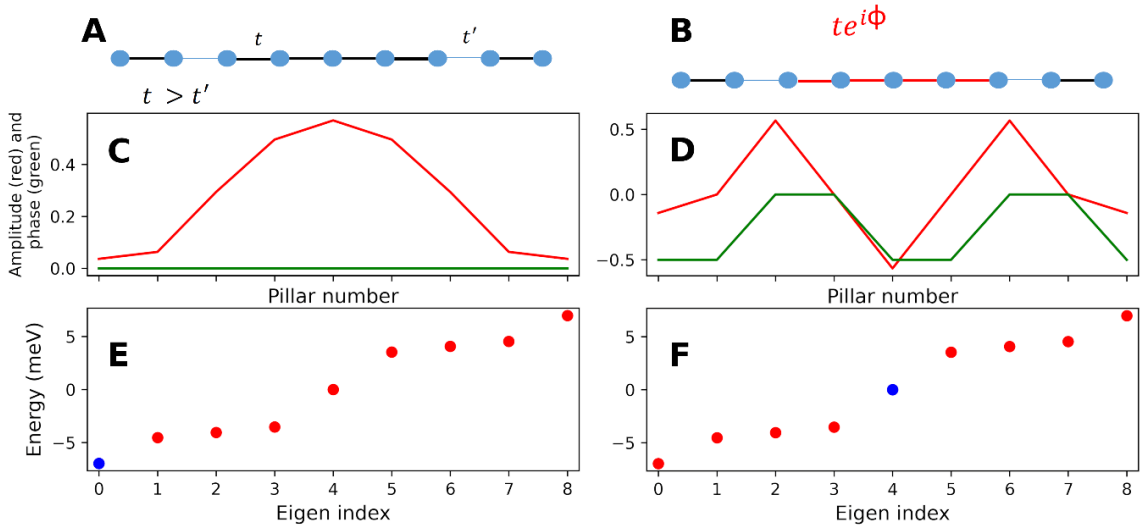

Figure 1. (A) Schematic representation of the dimerization in the SSH model with a defect in the middle of the lattice. Here λ = t/t′ is equal to four. (E), (F) Band structure associated with defect lattice. Blue dot shows the eigen index of the radiation mode. (C), (D) The red plot shows the amplitude of the radiation, the green plot shows the phase of the radiation. (B) Defect lattice twisted by an angle ϕ.

Pillars, which are located at the edges of the lattice, are strongly couple. The periodic alternation of the coupling parameters t and t' is broken by adding several strong couplings at the middle part. For symmetry, we consider chains with an odd number of pillars. Due to the linearity of the Eigen Problem, the Hamiltonian for such a lattice can be represent as a two-diagonal matrix H. The complex exponents in the Hamiltonian correspond to twisted coupling coefficients. The critical importance is to find an experimental implementation behind the mathematical construction of complex coupling coefficients [5].

$$H = \begin{pmatrix} 0 & 4 & 0 & 0 & 0 & 0 & 0 & 0 & 0 \\ 4 & 0 & 1 & 0 & 0 & 0 & 0 & 0 & 0 \\ 0 & 1 & 0 & 4e^{i\phi} & 0 & 0 & 0 & 0 & 0 \\ 0 & 0 & 4e^{-i\phi} & 0 & 4e^{i\phi} & 0 & 0 & 0 & 0 \\ 0 & 0 & 0 & 4e^{-i\phi} & 0 & 4e^{i\phi} & 0 & 0 & 0 \\ 0 & 0 & 0 & 0 & 4e^{-i\phi} & 0 & 4e^{i\phi} & 0 & 0 \\ 0 & 0 & 0 & 0 & 0 & 4e^{-i\phi} & 0 & 1 & 0 \\ 0 & 0 & 0 & 0 & 0 & 0 & 1 & 0 & 4 \\ 0 & 0 & 0 & 0 & 0 & 0 & 0 & 4 & 0 \end{pmatrix}$$

The matrix H is self-adjoint (equivalently, the Hermitian matrix), which guarantees that its spectrum is real. The band structure of the lattice shown in figure 1(**E** and **F**). Defect modes in contrast to Tamm modes are not radiating on the edges of the lattice, see figure 1(**C** and **D**), that is, their amplitudes are almost equal to zero. The largest radiation amplitudes are concentrated in the middle of the lattice, on a defect in a periodic structure.

It is also possible to observe Tamm states in periodic lattices, with the violated property that for any coupling constant its nearest neighbors have different values (this is a property of the SSH model).

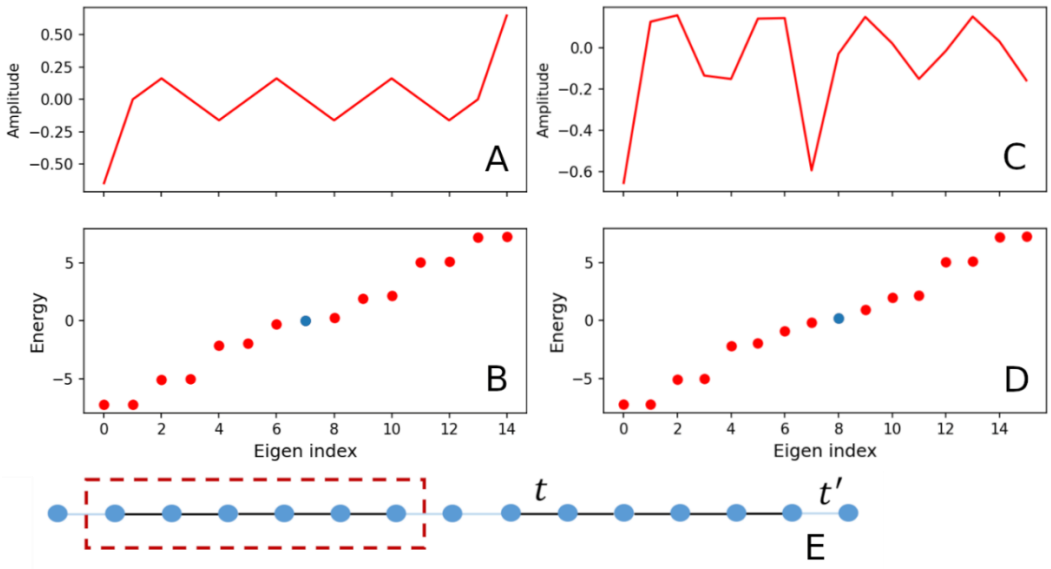

Figure 2. (A and B) Radiation amplitudes and band structure in the case when the number of coupling constants in the unit cell is a divisor of the number of coupling constants in the periodic structure. (C and D) Radiation amplitudes and band structure in the case when the number of coupling constants in the unit cell is not a divisor of the number of coupling constants in the periodic structure. (E) Periodic structure.

This research was funded by the Russian Science Foundation (project no. 22-42-08003).

References

[1] F. Gao, et al., Nature communications 7.1: 11619 (2016).
[2] P. St-Jean, et al., Nature Photonics, 11(10), 651-656 (2017).
[3] A. Dikopoltsev, et al., Science 373, 1514-1517 (2021).

[4] Z. He, et al., ACS Photonics 9.7: 2322-2326 (2022).
[5] D.N. Vavulin and A.A. Sukhorukov, Physical Review A 96.1: 013812 (2017).
CO2-3O/1

One-Dimensional Multiperiodic Photonic Structures *(invited)*

Lyubchanskii I. L.

Galkin Donetsk Institute for Physics and Engineering,
72 R. Luxemburg str., 283048 Donetsk, Russia
and Faculty of Physics and Technology, Donetsk State University,
24 Universitetskaya str., 283001, Donetsk, Russia
ilyubchanskii@gmail.com

In this talk the results of theoretical and numerical analysis of multiperiodic one-dimensional (1D) photonic structures composed of three and four different materials will be presented.

The conventional 1D ternary photonic crystal (PC) is the structure composed of three constituents A, B, and C with refractive indexes n_A, n_B and n_C, and thicknesses d_A, d_B, and d_C, respectively: $(ABC)^N$ and period $D = d_A + d_B + d_C$. On the base of this structure we can create the 1D PC $[(AB)^KC]^N$ with two periods, namely, internal period $D_{in} = d_A + d_B$, and external period $D_{ext} = K(d_A+d_B) + d_C$, respectively [1]. Similarly, from four-component 1D PC with the structure $(ABCD)^N$ we can construct two- and three-periodic PCs $[(ABC)^KD]^N$ and $[(AB)^K(CD)^L]^N$, respectively [2]. The quasi-periodic 1D PC with complex unit cells are also investigated [3].

The transmittivity spectra of these complex 1D photonic structures are analysed [1- 3].

References

[1] N. N. Dadoenkova, Yu. S. Dadoenkova, I. S. Panyaev, D. G. Sannikov, and I. L. Lyubchanskii, One-dimensional dielectric bi-periodic photonic structures based on ternary photonic crystals. Journal of Applied Physics. 123 (4), 043101 (2018).
[2] I. S. Panyaev, L. R. Yafarova, D. G. Sannikov, N. N. Dadoenkova, Y. S. Dadoenko-va, and I. L. Lyubchanskii, One-dimensional multiperiodic photonic structures: a new route in photonics (four-component media). Journal of Applied Physics. 126 (10), 103102 (2019).
[3] A. Biswal, R. Kumar, H. Behera, I. L. Lyubchanskii, Quasi-periodic one-dimensional photonic crystal as a perspective structures for nanophotonics: Analysis of transmittivity spectra. Materials Science and Engineering: B. 284, 115915 (2022).

CO2-3O/2

Thin Film Phase-Change Materials for Photonic Applications

A.A. Lotin, A.A. Burtsev, A.V. Kiselev, V.V. Ionin, A.A. Nevzorov, V.A. Mikhalevsky, N.N. Eliseev

ILIT RAS — Branch of FSRC "Crystallography and Photonics" RAS, 1, Svyatoozerskaya Str., 140700, Shatura, Moscow Region, Russia
lotin_82@mail.ru

Non-volatile all-photonic memory and neuro-inspired computing are promising technologies for increasing data storage and processing [1]. Photonic memory devices combine the high operation speed and non-volatility. Neuro-inspired computing unifies processing with storage in a single cell. Among materials for optical data storage and electric non-volatile memory devices, chalcogenide alloys based on germanium telluride (GeTe, $Ge_2Sb_2Te_5$) are the most mature and widely used in photonic and optoelectronic devices [2]. For applied application, the high contrast of the optical and electrical properties of PCMs between their amorphous and crystalline states is of great interest. This contrast is primarily due to a significant difference in the structural order, the concentration of charge carriers, and the mechanisms of chemical bonding [3, 4]. The presenting results include stable multilevel reversible phase transitions in thin films chalcogenide (GeTe, $Ge_2Sb_2Te_5$). Thin films were deposited by vacuum thermal sputtering. Phase transitions in thin films were induced by femto- and nanosecond pulsed laser radiation with different fluence [5, 6]. Structural information was characterized in situ optical parameters measurement, electron microscopy and X-ray diffractometry. Multi-bit devices provide a pathway towards eliminating the von Neumann bottleneck and discover a new application in all-photonic and hybrid optoelectronic data storage and computing [7-9].

References

[1] W. Zhang, R. Mazzarello, M. Wuttig and E. Ma. Nature Reviews Materials, 4, 150–168 (2019).
[2] P. Guo, A. M. Sarangan and I. Agha. Applied Sciences, 9, 3, 530 (2019).
[3] M. Wuttig, H. Bhaskaran, T. Taubner. Nature Photonics, 11, 8, 465-476 (2017).
[4] A. A. Burtsev, et al. Materials Science in Semiconductor Processing, 150, 106907 (2022).
[5] N. N. Eliseev, et al. Results in Physics, 19, 10346 (2020).
[6] A. A. Nevzorov, et al. Optical materials, 141, 113925 (2023).
[7] C. A. Ríos, et al. Nature Photonics, 9, 725 (2015).
[8] N. Youngblood, C. A. Ríos, W. H. P. Pernice & H. Bhaskaran. Nature Photonics, 1-12 (2023).
[9] G. N. Panin. Chaos, Solitons & Fractals, 142, 110523 (2021).

CO2-3O/3

Phase-change material based active cells in polymer-based waveguide photonic devices

V.V. Ionin, A.V. Kiselev, A.A. Burtsev, V.A. Mikhalevsky, N.N. Eliseev,
V.I. Sokolov and A.A. Lotin

ILIT RAS - Branch of FSRC «Crystallography and Photonics» RAS, 140700, Svyatoozerskaya st. 1, Shatura, Russia
ioninvv@gmail.com

Despite the successes achieved in the experimental implementation of prototypes of optical synapses, the creation of such devices based on solid-state optical waveguides carries a number of technological difficulties which leads to the complexity and high cost of industrial implementation [1]. Polymer-based integral photonics also offers a number of advantages over silicon. The electrical, thermal and mechanical properties of polymers can be largely tailored to the specific requirements in each case. In integral optics polymers are widely used, e.g. to improve electro-optical and optical nonlinear effects. A serious disadvantage is the low resistance to high temperatures which are often used in conventional micro- and nanomanufacturing processes. On the other hand, if high temperatures can be avoided, polymers usually provide a cheaper manufacturing platform [2]. Replacing standard silicon technology or A_{III}-B_V technology with polymers can provide additional benefits such as manufacturing flexibility, reliability, low energy consumption and the possibility of mass production accompanied by a reduction in production costs. For example, SU-8 is transparent in the visible and near-IR regions of the spectrum and is widely used to create polymer planar optical waveguides [3].

We present a developed optical synapse based on the interface between a polymer waveguide and an optically controlled GST_{225} thin film. The proposed concept of creating optical synapses is the simplest of all known planar technologies for creating waveguide optical synapses and allows the implementation of computational elements and architectures based on them with a high degree of heterogeneous integration.

Figure 1 shows experimental oscillograms of the output signal of the studied synapse-like structure after impact of 532 nm laser pulses. Fig. 1a shows the result of impact of a single pulse with an energy flux of 33 mJ/cm^2. A decrease in the intensity of the output signal by more than 40% is observed, which is associated with a change in the optical characteristics of the active PCM layer due to a laser-induced change in its phase state [4]. It is also shown that the intensity of the transmitted signal can be restored close to the initial level under pulsed laser irradiation with 35 mJ/cm^2. The phase transition is above threshold phenomena, and by controlling of pulse energy it is possible to achieve a fixed level with specified ratio between amorphous and crystalline phases in the film material. Each level corresponds to a change of the transmission modulation. Figure 1b illustrates the modulation of the output signal when the active PCM cover layer is periodically exposed to pulsed radiation with an energy flux of 19 mJ/cm^2. The inset in Fig. 1b shows an oscillogram of the change in the transmissivity of a thin GST film, the thickness of which is similar to the thickness of the capping layer on the polymer waveguide in experiment above. In the amorphous state the GST_{225} active region provides a higher transmission in the waveguide, respectively, the transmission decreases with crystallization of the material. As it follows from fig. 1b, complete crystallization of the GST_{225} cell can be achieved in a few pulses. In this case, the

transmittance drops in steps as more material becomes crystalline. The restoration of the initial signal level in the synapse can be achieved by impaction of the energy sufficient to achieve the GST_{225} melting point and subsequent rapid glass transition (Fig. 1c).

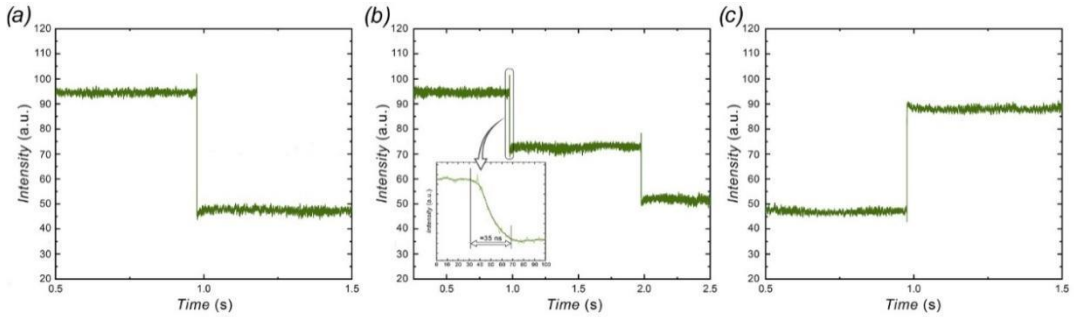

Fig. 1. Experimental waveforms of the probe radiation modulation in optical synapse based on GST-capped polymer waveguide at different values of laser energy flux on optical active GST-interface: *(a)* – 33 mJ/cm^2, *(b)* – 19 mJ/cm^2, *(c)* – 35 mJ/cm^2

It is shown that it is possible in principle to obtain a signal modulated by external optical radiation in the telecommunication C-wavelength range of 1530-1565 nm in a synapse-like structure which is a planar polymer waveguide with an active layer capping made of a phase-changing material. The simulation results of the signal transmission in such a structure show a noticeable attenuation of the transmitted radiation due to the wave flow from the polymer waveguide to the GST_{225} layer. In the amorphous state of the film radiation propagates along a waveguide with a GST_{225} capping area, and in the crystalline state, the wave is absorbed. The results demonstrated in this work have shown the operability of the prototype of a controlled synapse created on optical elements and open up the prospect of creating optical computing and storage devices based on this principle of a next generation.

References

[1] S.-T. and Y. Han Zhou. Photo-Electroactive Non-Volatile Memories for Data Storage and Neuromorphic Computing (Woodhead Publishing, Kidlington, UK, 2020).
[2] J.C. Ramirez, J.N. Schianti, M.G. Almeida et al. Opt. Mater. Express. 7, 7, 2651 (2017).
[3] V.I. Sokolov, G.V. Mishakov, V.Y. Panchenko et al. Opt. Mem. Neural Netw. (Inf. Opt.). 16, 2, 67 (2007).
[4] V.V. Ionin, A.V. Kiselev, A.A. Burtsev et al. Appl. Phys. Lett. 119, 081105 (2021).

CO2-3O/4

Controlling optical properties of GST thin films by ultrashort laser pulses series impact

A.V. Kiselev, A.A. Burtsev, V.V. Ionin, A.A. Nevzorov, V.A. Mikhalevsky, N.N. Eliseev and A.A. Lotin

ILIT RAS — Branch of FSRC "Crystallography and Photonics" RAS, 1, Svyatoozerskaya Str., 140700, Shatura, Moscow Region, Russia
kiselev.ilit.ras@gmail.com

Phase change materials (PCM) are a unique class of solid materials with a high contrast of electrical and optical properties of the amorphous and crystalline phases. They are widely used in data storage, while in recent decades such materials as $Ag_4In_3Sb_{67}Te_{26}$ (AIST) and $Ge_2Sb_2Te_5$ (GST) have also become a part of optical data recording and the focus of researchers as promising materials for development and creation of next-generation non-volatile memory modules [1]. A reversible transition between amorphous and crystalline states can be induced in various ways: by thermal heating, by the electric current pulses, or optical pulses. GST alloys have a higher rate of crystallization and amorphization, which is due to the fact that the transitions occur between the amorphous and metastable low-temperature cubic phase. This provides high switching cycling, reliability and easy applicability [2]. The use of ultrashort laser pulses opens up a lot of new possibilities in the study of ultrafast phase transitions and determining fundamental constants [3].

In order to understand the nature of changing optical properties, it is necessary to separate the set of physical processes that determine the dynamics shown in Fig. 1. After exposure to a femtosecond laser pulse, photoinduced carriers relax, and the near-surface layers of the film are strongly heated, which is caused, in particular, by the interaction of these carriers with material molecules [4]. Temperature relaxation leads to a change in the optical properties of the material. In addition, the crystallization process also affects the dynamics of optical properties. It is the latter process that interests us in the context of studying the material for use in photonic devices. The decay of photoinduced carriers occurs on a subnanosecond scale, therefore, the main contribution to the obtained dynamics is made by the processes of thermal relaxation of optical properties and the process of high-temperature crystallization. Since it is practically impossible to accurately measure the temperature at such a rate and it is very difficult to determine the thermooptical properties during pulsed heating, it is extremely difficult to separate these processes. One way to study the dynamics of optical properties caused exclusively by the crystallization process is to create a model, for the verification of which it is necessary to use the obtained experimental data.

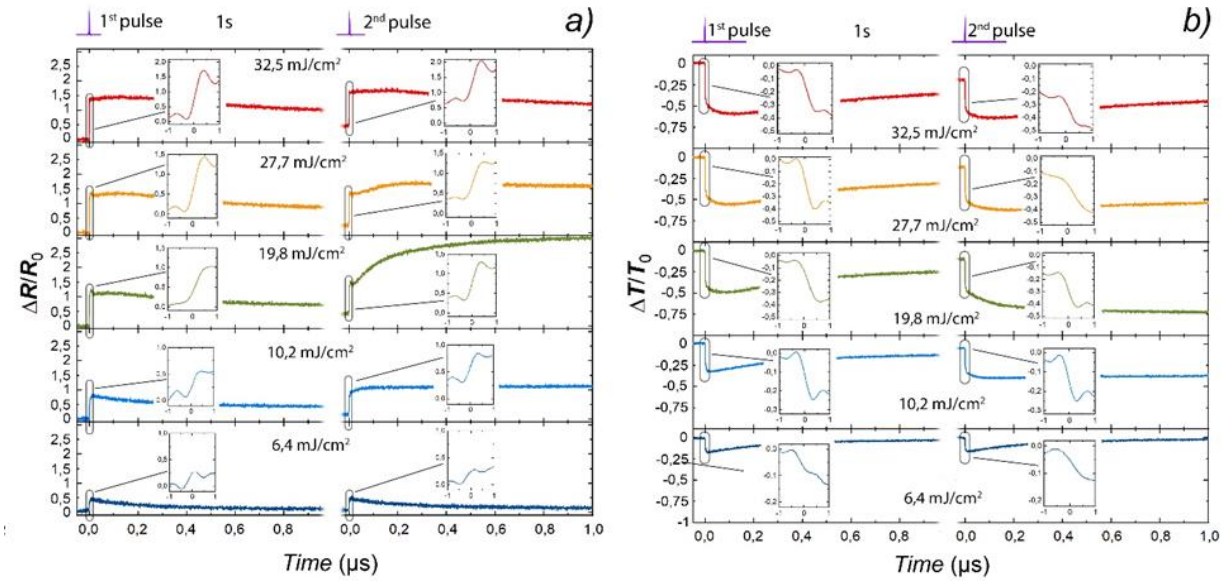

Fig. 1. The optical reflection and transmission coefficients of a thin GST film contrast changing dynamics during crystallization induced by two-pulse impact of femtosecond laser radiation with different energy fluences.

In the energy fluence range from 12 to 20 mJ/cm^2, the dependence of the excitation energy density on the fraction of the crystalline phase (as well as for electrical resistances and optical parameters) is monotonic in both single- and double-pulse modes. Judging by the structures obtained by the experimentally verified model after the first and second femtosecond pulses, the randomness of the formed crystal structure decreases with the number of pulses. In this case, the contrast of film optical properties regarding the completely amorphous state and regarding different exposure energies is quite significant. This suggests that the use of multipulse modes can allow achieving efficient reproducibility in the preparation of PCM thin film states and, in addition, provide a large number of error-free reading states. The study shows that this method of coding using identical influencing impulses, when used in optical synapses built on PCM, naturally increases the reproducibility and controllability of setting the synapse weight [5].

References

[1] M. Wuttig, H. Bhaskaran, T. Taubner. Nature Photonics, 11, 8, 465-476 (2017).
[2] A. A. Burtsev, et al. Materials Science in Semiconductor Processing, 150, 106907 (2022).
[3] S. K. Sundaram, E. Mazur. Nat. Mater., 1, 217-224 (2002).
[4] A. A. Nevzorov, et al. Optical Materials, 141, 113925 (2023).
[5] W. Zhang, R. Mazzarello, M. Wuttig and E. Ma. Nature Reviews Materials, 4, 150–168 (2019).

CO2-3O/5

Modulation of surface plasmon-polaritons on hyperbolic magnetoplasmonic metasurfaces

D.A. Kuzmin [1], M.O. Usik [1], I.V. Bychkov [1], V.G. Shavrov [2]

[1] *Chelyabinsk State University, 454001, Chelyabinsk, Russia*
[2] *Kotelnikov Institute of Radio-Engineering and Electronics of RAS, 125009, Moscow, Russia*
kuzminda89@gmail.com

Since the active magneto-plasmonics in hybrid metal-ferromagnet structures was proposed, a lot of plasmonically enhanced magneto-optical effects have been demonstrated. Incorporating magneto-active materials in plasmonic structures leads to various magnetoplasmonic effects. One of the effects is the change in the SPP wavenumber, which depends on the magnetization direction, i.e. $k_{sp}(\pm M) = k^0_{sp} + \Delta k_{sp}(\pm M)$, being the strongest for the transversal magnetization configuration with respect to the SPP *k*-vector. It was previously shown in hybrid metal-ferromagnet multilayer structures that a small modulation $|\Delta k_{sp}(M)|/k_0 \sim 10^{-4}$, accumulated over the long propagation distance, may result in noticeable values of the magneto-plasmonic signal modulation depth $2|\Delta k_{sp}(M)|d \sim 0.02$ for the SPPs propagation distance $d = 22$ μm.

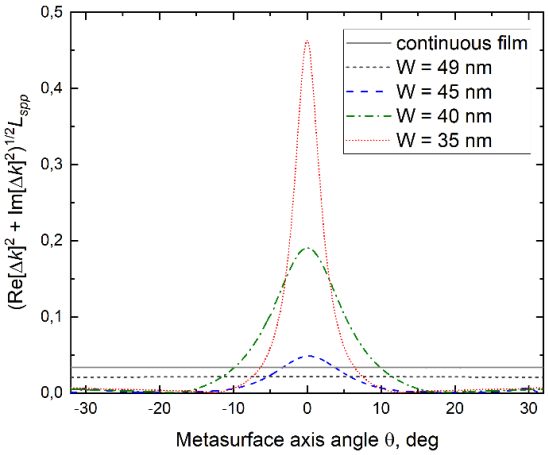

Fig. 1. Evolution of the figure of merit $(\mathrm{Re}[\Delta k]^2+\mathrm{Im}[\Delta k]^2)^{1/2}\times L_{spp}$ under variation of the SPPs propagation direction with respect to gold stripes orientation shows that maximal modulation may be observed for the SPPs propagating along the stripes. θ is an angle between gold stripes and SPPs k-vector.

We consider the simplest realization of a hyperbolic plasmonic metasurface (HPM) consisting of densely packed metallic (gold) stripes separated from each other by an air gap. Such a metasurface is deposited on a magnetic dielectric substrate (BIG).

The HPM allow to increase the magnetic SPP modulation. It can reach giant values outperforming uniform plasmonic thin films and hybrid metal-ferromagnet multilayers. The modulation of plasmonic optical properties using the magnetization control in ferromagnetic dielectric substrate suggests a straightforward application of this system as optical switches. Considering experiments with femtosecond light pulses, we believe that the switching speed of our device could eventually reach the terahertz regime in future and allow to realize all-optical magneto-plasmonic switches.

Support by Russian Science Foundation (22-19-00355) is acknowledged.

CP1-3P/1

Magneto-Plasmonic Effects in Nanocomposites

Tomilin S.V., Berzhansky V.N., Tomilina O.A.

Institute of Physics and Technology, V.I. Vernadsky Crimean Federal University, Vernadsky avenue, 4, Simferopol, Russia
tomilin_znu@mail.ru

Let's consider an electrodynamic model that makes it possible to describe the mechanism of the Faraday effect enhancement in magnetoplasmonic composite systems with a high degree of authenticity. Magnetoplasmonic composite consist of plasmonic nanoparticles in a magneto-optical matrix of bismuth-substituted ferrite garnet. This model is a theoretical calculation of the effective permittivity tensor taking into account the Maxwell-Garnett effective medium model for a composite medium.

The non-diagonal terms of the composite's effective permittivity tensor make it possible to estimate the gyration index for the magnetoplasmonic system:

$$g_{eff} = \frac{1}{i}\left[ig + \frac{3f_m}{\det B}\left(-2ig(\varepsilon_m + 2\varepsilon)(\varepsilon\varepsilon_m - \varepsilon^2 - g^2) + ig(\varepsilon_m - 2\varepsilon)(\varepsilon_m + 2\varepsilon)^2\right)\right] \quad (3)$$

where g – gyration index of an iron-garnet, ε – permittivity of a garnet, $\varepsilon_m = \varepsilon'_m + i\varepsilon''_m$ – complex permittivity of plasmonic nanoparticles, f_m – volume fraction of the plasmonic component, det B – matrix determinant.

$$B = \varepsilon_m + 2\varepsilon = \begin{pmatrix} \varepsilon_m + 2\varepsilon & -i2g & 0 \\ i2g & \varepsilon_m + 2\varepsilon & 0 \\ 0 & 0 & \varepsilon_m + 2\varepsilon \end{pmatrix} \quad (4)$$

Considering that the Faraday rotation angle is proportional to the gyration index, it is possible to calculate the Faraday effect enhancement coefficient in a magnetoplasmonic composite with respect to a pure magneto-optical medium in the form:

$$\eta = \frac{g_{eff}}{g} = 1 + \frac{3f_m}{\det B}\left[-2ig(\varepsilon_m + 2\varepsilon)(\varepsilon\varepsilon_m - \varepsilon^2 - g^2) + ig(\varepsilon_m - 2\varepsilon)(\varepsilon_m + 2\varepsilon)^2\right] = \\ = \eta' + i\eta'' = |\eta| e^{i\varphi} \quad (5)$$

On Fig. 1 shows the curves of the spectral dependence for the module |η| and the argument φ of the Faraday effect enhancement for different values of the fraction of the metallic component f_m (indicated in the legend). It can be seen that the modulus of the Faraday effect enhancement coefficient |η| (Fig. 1a) in the region of plasmon resonance (λ = 655 nm) has a local spectral maximum. The value of |η| at the maximum increases with an increase in the fraction of the metallic component f_m (with a decrease in the fraction of the dielectric component).

It should also be noted that in the region of short wavelengths relative to the LPR, the modulus of the Faraday effect enhancement |η| becomes less than 1, which indicates to attenuation of the Faraday effect.

The physical meaning of the argument φ of the complex enhancement coefficient is the angle of ellipticity. It can be seen from Fig. 1b that the ellipticity in the vicinity of the plasmon resonance changes sign upon passing from small to large wavelengths relative to the resonant wavelength, and in the resonance itself φ = 0 for any fraction of the metal phase.

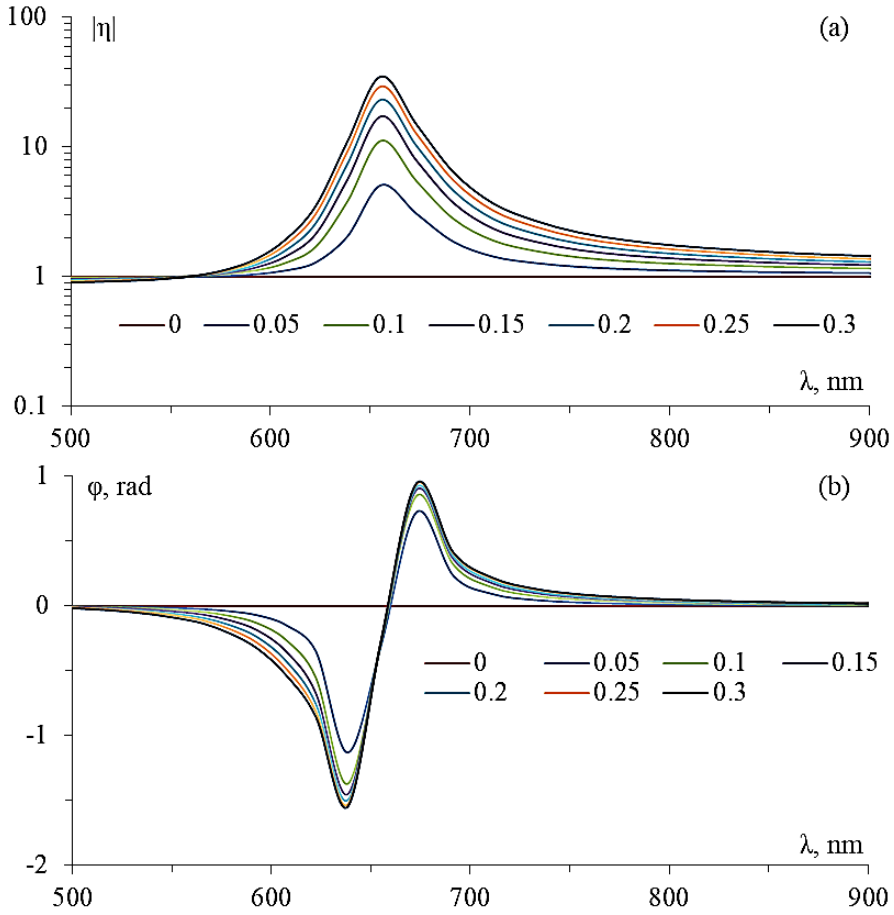

Fig. 1. Calculated spectral dependences for the modulus |η| (a) and the argument φ (b) of a complex enhancement coefficient of the Faraday effect from the plasmon component fraction f_m.

Thus, the complex gyration index in a magnetoplasmon composite, in addition to the rotation of the plane of polarization, leads to the appearance of a sign-changing ellipticity in the vicinity of the plasmon resonance. The presence of a such sign-changing ellipticity in the vicinity of the LPR in the magnetoplasmonic nanocomposite is the cause of the asymmetry effect of the Faraday rotation when the medium is magnetized along and backwards the light wave propagation vector. A such asymmetry of the magneto-optical rotation was experimentally observed and described in [1].

The research was financially supported by the Russian Science Foundation grant No. 19-72-20154, https://rscf.ru/project/19-72-20154/

References

[1] Tomilin S., Karavaynikov A., Lyashko S., at all. Asymmetric Magneto-Optical Rotation in Magnetoplasmonic Nanocomposites // J. Compos. Sci. – 2023. – V. 7. – P. 287.

CP1-3P/2

Propagation of optical vortices in loop input-output resonator

Aliyeva S.S.[1], Alexeyev C.N.[1], Yavorsky M.A.[1]

[1] *V.I. Vernadsky Crimean Federal University, Simferopol 95007, Russia*
selime_alieva@bk.ru

Currently, there is a great interest in issues related to the propagation of optical vortices in optical fibers [1,2]. This is due to the new possibilities that arise from the use of optical resonators to control the orbital angular momentum and topological charge of the optical field. One of such types of optical resonators is the input-output fiber loop resonator.

In this paper, we study the propagation of optical vortices in a fiber loop input-output resonator, which consists of a bare optical fiber loop evanescently coupled with an ideal optical fiber.

Based on theoretical analysis and numerical modeling, the dependence of the transmission coefficient on the length of the fiber interaction section was obtained (Fig. 1).

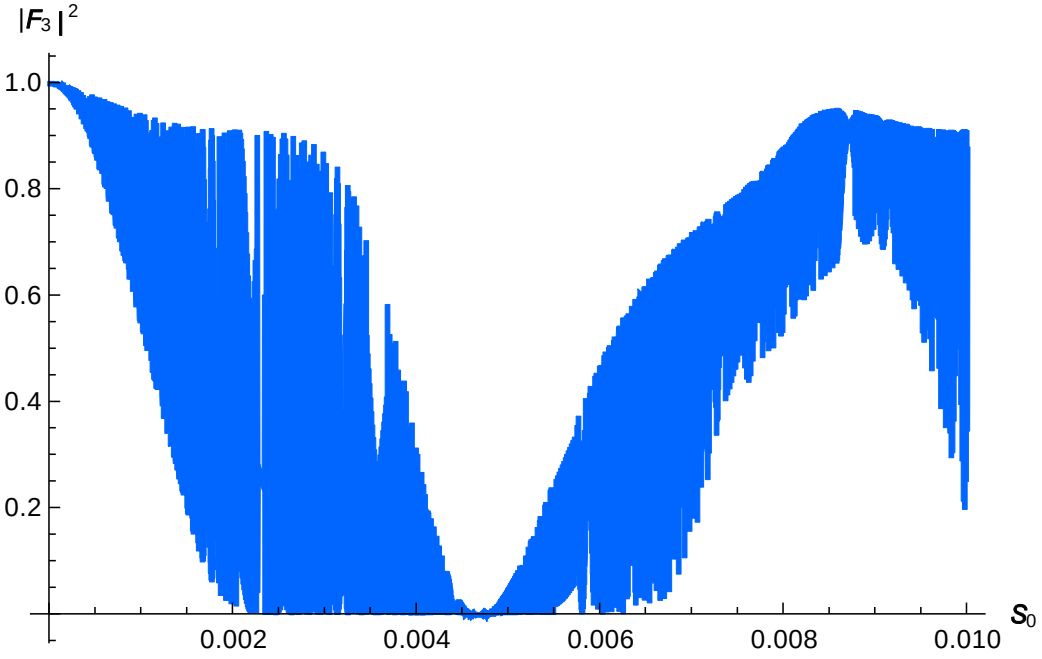

Fig.1. The dependence of the transmission coefficient $|F_3|^2$ (in units of incident beam power) of an optical vortex $|1,1\rangle$ on the length of the interaction section (in meters)

We have demonstrated that such an optical system is capable of inverting the topological charge of the incoming optical vortex at certain lengths of the coupling section. This highlights the fundamental possibility of parametrically controlling the topological charge of the outgoing optical field by varying the parameters of the resonator.

References

[1] C.N.Alexeyev, A.V. Milodan, M.C. Alexeyeva, and M. A. Yavorsky, Opt. Lett. **41**, 1526 (2016).

[2] C.N. Alexeyev, E.V. Barshak, B.P. Lapin, and M.A. Yavorsky, Opt. Lett.**44,** 4044 (2019).

CP1-3P/3

VO_2 Films for Photonics Applications

Syrov A.A., Kudryashov A.L., Titov A.V., Berzhansky V.N., Tomilin S.V.

V.I. Vernadsky Crimean Federal University, Simferopol, Russia
anatoly199824@rambler.ru

Recently, the world scientific interest in vanadium dioxide (VO_2) is due to the presence of a first-order "semiconductor–metal" phase transition in this material. This property opens up many possibilities in applied and fundamental terms. In particular, for high application in data transfer devices, electromechanical systems, generation of thermal modulations, for problems of nonlinear optics or for wavefront formation [1].

The synthesis of VO_2 film was carried out by a method of vacuum RF-frequency magnetron sputtering of initial VO_2 target on Al_2O_3 substrate at the temperature of 450°C in Ar medium. Electric conductivity was measurement by classic double-probe scheme. Fig. 1,a present the thermal hysteresis loop of electric conductivity in obtained VO_2 film with the thickness of 220 nm after deposition. The blurred phase transition with the width more than 60°C is observed in the film and the general change of electric conductivity is only 1.5 orders of magnitude. The treatment in O_2 ($P = 5.98 \cdot 10^{-3}$ Pa) medium at the temperature of 475–525°C for 120 min was carried out to transition into the stoichiometric phase and film characteristics enhancement. Fig. 1,b demonstrates the loop of thermal hysteresis of electric conductivity in VO_2 film after treatment. It is seen, that the change of film electric conductivity is the four orders of magnitude (from 0.01 to 100 mS) in the point of phase transition at the temperature of 68–69°C (the total width of phase transition is 15–18°C). The specific thermal hysteresis has been observed at the serial cycle of "heating-cooling". The width of hysteresis loop is near 6–7°C.

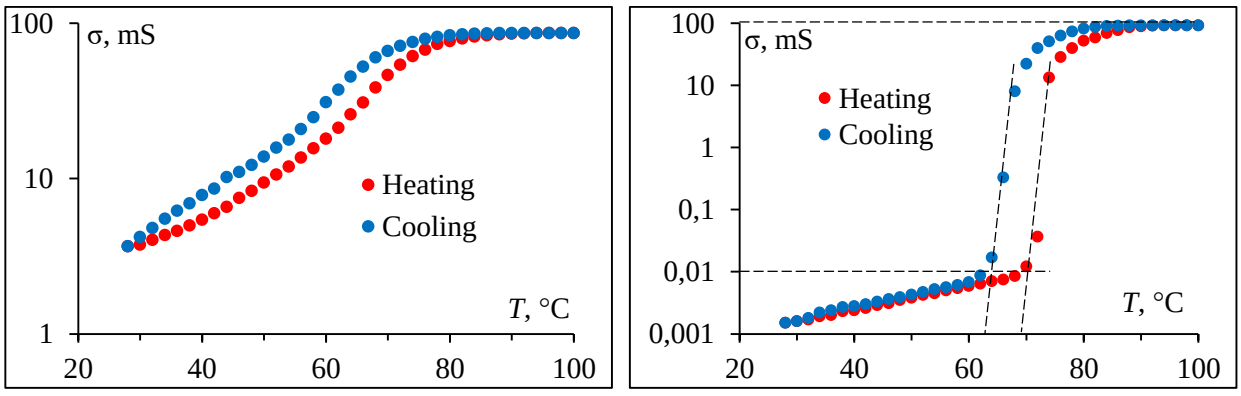

Fig. 1. Hysteresis of electric conductivity in VO_2 film with the thickness of 220 nm: a – after vacuum deposition, b – after annealing in O_2.

This work was financially supported by the grant of State Council of Crimean Republic (resolution № p653-2/23 from 30.01.2023).

References

[1] S. Cueff, J. John, Zh. Zhang, J. Parra, J. Sun, R. Orobtchouk, Sh. Ramanathan, P. Sanchis. VO_2 nanophotonics. APL Photon. 5, 110901 (2020).

CP1-3P/4

Nanostructures of Bi-substituted iron garnets: scanning near-field optical and magnetic force microscopy

Mikhailova T.V.[1,3], Ignatyeva D.O.[1,2,3], Karki D.[4], Levy M.[4], Belotelov V.I.[1,2,3]

[1]*V. I. Vernadsky Crimean Federal University, 295007, Simferopol, Russia*
[2]*Lomonosov Moscow State University, 119991, Moscow, Russia*
[3]*Russian Quantum Center, 121205, Moscow, Russia*
[4]*Michigan Technological University, Houghton, 49931-1295, USA*
tatvladismikh@cfuv.ru

The investigation of effects associated with the localization and distribution of light in two- and three-dimensional nanostructures is of interest in connection with the creation of miniature nanophotonic devices. This work examines nanostructures made of bismuth-substituted iron garnets, which are distinguished by the manifestation of magnetooptical and optomagnetic properties. The structures in the form of square arrays of nanodisks were fabricated by electron beam lithography on the basis of epitaxial film $Bi_{0.7}Gd_{0.3}Lu_{2.0}Ga_{0.8}Fe_{4.2}O_{12}$ with a thickness of 454 nm grown on gadolinium gallium garnet (001) substrate. The structures were studied using scanning near-field optical (SNOM) and magnetic force (MFM) microscopy (SPM Ntegra, NT-MDT, Russia; cantilevers SNOM_NC, MFM01 or MFM_LM). The resulting SNOM maps (Fig. 1) demonstrate the emergence of various localized and lattice modes of the structures [1].

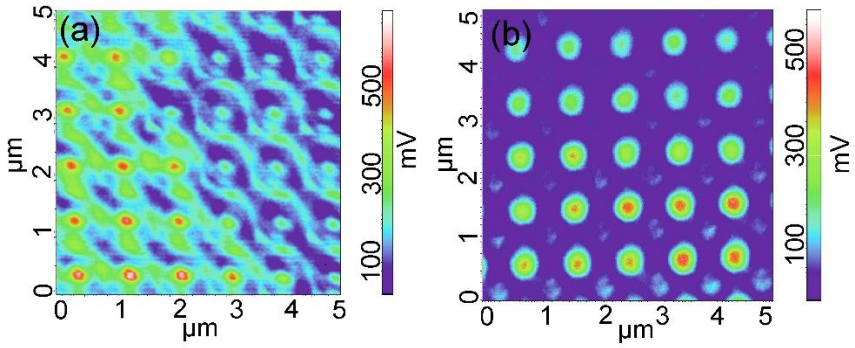

Fig. 1. SNOM images of the structure for wavelength of 633 nm (a) and 532 nm (b). Nanodisk diameter is 650 nm, structure period is 900 nm, incident beam polarization angle is 45°

MFM measurements showed that after magnetization to saturation and demagnetization in an alternating normal magnetic field, the disks remain in a uniformly magnetized state.

The research was supported by a grant from the Russian Science Foundation No. 21-72-10020.

References

[1] P.E. Zimnyakova, D.O. Ignatyeva, D. Karki, A.A. Voronov, A.N. Shaposhnikov, V.N. Berzhansky, M. Levy, V.I. Belotelov, Nanophotonics 11, 119 (2022).

CP1-3P/5

Exciton-like excitations in an imperfect one-dimensional lattice of micropores

Bezus Ju.A. [1], Rumyantsev V.V. [1], Fedorov S.A.[1]

Federal State Budgetary Scientific Institution «Galkin Donetsk Institute for Physics and Engineering»,[1]283050, Donetsk, Russia
a.bezus@donnu.ru

Consider electromagnetic excitations in a two– lattice chain of microresonators without quantum dots (hence $D^{12}_{n_\alpha,m_\beta} = D^{21}_{n_\alpha,m_\beta} = 0$) – the so-called exciton- like excitations (fig. 1).

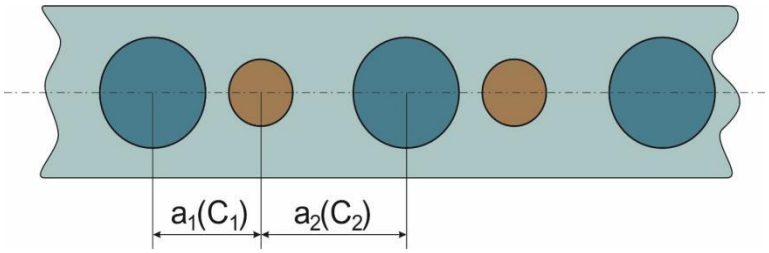

Fig. 1. A model of a two-lattice chain of microresonators without quantum dots

Hamiltonian

$$\hat{H} = \sum_{\alpha,\beta=1}^{2} \sum_{\substack{n,m,\\ \lambda,\sigma}} D^{\lambda\sigma}_{n_\alpha,m_\beta} \hat{\Phi}^{+}_{n_\alpha\lambda} \hat{\Phi}_{m_\beta\sigma} \quad , \qquad (1)$$

where are n,m – the numbers of elementary cells, are α,β – the numbers of sublattices, $D^{11}_{n_\alpha,m_\beta} = \hbar\omega^{at}_{n_\alpha}\delta_{n_\alpha,m_\beta} + V_{n_\alpha,m_\beta}$, $D^{22}_{n_\alpha,m_\beta} = \hbar\omega^{ph}_{n_\alpha}\delta_{n_\alpha,m_\beta} - A_{n_\alpha,m_\beta}$, $D^{12}_{n_\alpha,m_\beta} = D^{21}_{n_\alpha,m_\beta} = g_{n_\alpha}\delta_{n_\alpha,m_\beta}$, the actual is similar to the exciton Hamiltonian of quasi-two-dimensional semiconductor systems with strong coupling [1].

Based on such representations, it is natural to call the studied electromagnetic excitations exciton-like. It is also important to note that in this study only photonic supercrystalline excitations are considered, while no electronic transitions occur.

However, the dispersion relations of the studied electromagnetic excitations of photonic crystals in the system under consideration are very similar to Frenkel excitons in molecular crystals [1-2]. As is known, the motion of the Frenkel exciton is determined by the transfer of excitation from one atom to another, which corresponds to the concepts used in this study.

The numerical calculation of the corresponding values determining the features of the spectrum of electromagnetic excitations will be carried out within the framework of the model used for the values of the frequencies of resonant photonic modes localized in the resonators of the lattice, $\omega_1^{ph} = 2\pi \cdot 311$ THz and $\omega_2^{ph} = 2\pi \cdot 331$ THz.

And also following [3-5] we believe: $A_{12}\left[a_1(0)\right]/2\hbar = 3{,}5\cdot 10^{14}$ Hz, $A_{12}\left[a_2(0)\right]/2\hbar = 1{,}2\cdot 10^{14}$ Hz, $V_{11}/2\hbar = 1\cdot 10^{13}$ Hz, $g_1/\hbar = 5\cdot 10^{12}$ Hz, $a_1(0) = a_1^{(1)} = 1\cdot 10^{-7}$ m, $a_2(0) = a_2^{(1)} = 3\cdot 10^{-7}$ m, with $d(0) = a_1(0) + a_2(0)$.

The surfaces describing the dispersion dependence of the frequencies $\Omega_{\pm}(k, C_1, C_2)$ of the studied collective excitations in a non-ideal array of microresonators are shown in fig. 2.

At the same time k, it changes within the first Brillouin zone: $-\frac{\pi}{d(C_1,C_2)} < k < \frac{\pi}{d(C_1,C_2)}$.

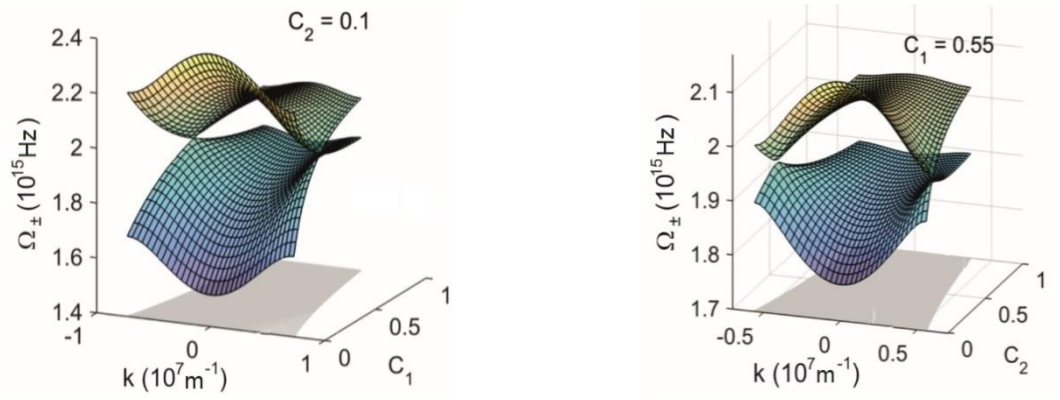

a *b*

Fig. 2. Dispersion dependence $\Omega_{\pm}(k, C_1, C_2)$ of collective excitation frequencies in microresonators: at concentrations *a* – $C_1 = 0.3$ and *b* – at $C_2 = 0.4$

The presented results make it possible to expand the possibilities of creating a new class of functional porous materials – exciton-like systems (arrays of micropores that do not contain quantum dots) [6] that allow controlling the propagation of electromagnetic excitations [6-7] in composite structures by controlled introduction of structural defects into them. Thus, it can be concluded that the possibility of creating highly integrated photonic circuits is the main task in the developing field of research – quantum nanophotonics.

References

[1] V.V. Rumyantsev, S.V. Fedorov, et al., Nature. Scientific Reports. 4, 6945 (2014).
[2] V.V. Rumyantsev, Donetsk: Nord-Press, 347 (2006).
[3] V.V. Rumyantsev, S.A. Fedorov, A.V. Kavokin, et al., Superlattices and Microstructures, 120, 642 (2018).
[4] V.V. Rumyantsev, S.V. Fedorov, et al., Physics and high pressure technology, 28(1), 87 (2018).
[5] V.V. Rumyantsev, S.V. Fedorov, et al., Problems of artificial intelligence, 7 (4), 59 (2017).
[6] V.V. Rumyantsev, S.V. Fedorov, J.A. Paladyan, et al., Physica B: Condensed Matter, 571, 296 (2019).
[7] V.V. Rumyantsev, S.V. Fedorov, J.A. Paladyan, Fundamental problems of optics – 2018, St. Petersburg: ITMO University, 321 (2018).

CP1-3P/6

Metal-dielectric structures with magnetooptical iron garnet layers

Mikhailova T.V.[1], Lyashko S.D.[1], Tomilin S.V.[1], Osmanov S.V.[1], Skorokhodov E.V.[2], Gusev S.A.[2], Karavainikov A.V.[1], Kudryashov A.L.[1], Berzhansky V.N.[1] and Shaposhnikov A.N.[1]

[1]V. I. Vernadsky Crimean Federal University, 295007, Simferopol, Russia
[2]Institute for Physics of Microstructures of the Russian Academy of Sciences (IPM RAS), 603087, Nizhny Novgorod, Russia
tatvladismikh@cfuv.ru

This work is devoted to the study of structural, optical and magneto-optical properties of metal-dielectric structures formed based on bismuth-substituted iron garnets, which have found the application as active elements of sensor systems and information storage and transmission devices [1, 2]. Double-layer "iron garnet – Au" structure synthesized on the structured surface of gadolinium gallium garnet and Tamm magnetophotonic crystals with a composite layer (SiO_2-Au) or an Au layer are considered.

For double-layer "iron garnet – Au" structure, the resonances in transmittance spectra, the amplitude and shape of which depend on the parameters of the structure, namely on the ratio of widths of the stripes and air gaps, were found. Resonances are accompanied by an increase in the angle of rotation of polarization plane of light wave. In the case of Tamm magnetophotonic crystals, it was shown that the composite (SiO_2-Au) layer enhances the localization of light inside the magneto-optical layers and increases the Faraday rotation angle of the structure [3]. The magneto-optical properties of Tamm magnetophotonic crystals with an Au layer are demonstrated at normal and oblique light wave incidence. Particular attention is paid to investigation of the influence of formation of two optical modes in the structure, the Fabry-Perot mode and Tamm plasmon polaritons, and their hybrid state [4]. It is shown that oblique incidence leads to a change in the quality factors of modes with different p- and s-polarizations. As a result, the resonant wavelengths of the modes for p- and s-polarizations at large angles of incidence will differ.

The investigation was carried out using technological and analytical equipment of the Common Research Center "Physics and Technology of Micro- and Nanostructures" of the Institute for Physics of Microstructures RAS. The research was supported by a grant from the Russian Science Foundation No. 19-72-20154, https://rscf.ru/project/19-72-20154/.

References

[1] J. Qin, S. Xia, W. Yang, H. Wang, W. Yan, Y. Yang, Z. Wei, W. Liu, Y. Luo, L. Deng, L. Bi, Nanophotonics 11, 2639 (2022).
[2] Magnetophotonics: From Theory to Applications (Springer-Verlag, Berlin, Heidelberg, 2013).
[3] T.V. Mikhailova, S.V. Osmanov, V.O. Boyko, J. Phys.: Conf. Ser. 2086, 012156 (2021).
[4] T. Mikhailova, S. Tomilin, S. Lyashko, M. Kozhaev, A. Shaposhnikov, A. Karavainikov, V. Berzhansky, V. Belotelov, Opt. Mater. Express. 12, 685 (2022).

CP1-3P/7

Plasmonic Nanoparticles for Sensing Applications

Tomilina O.A., Berzhansky V.N., Beltyukova A.G., Tomilin S.V.
Institute of Physics and Technology, V.I. Vernadsky Crimean Federal University, Vernadsky avenue, 4, Simferopol, Russia
o.tomilina.phystech@cfuv.ru

It is possible the realization of sensors and bio-sensors based on plasmonic Au nanoparticles. In this case nanoparticles coated by a layer of sensitive material (ligand) which has a specific reaction to molecules of detected matter (analyte). When the stability chemical compound of ligand and analyte is forming either the thickness or the permittivity of the sensitive layer changes. It leads to the shift of wavelength λ_{LPR} of localized plasmonic resonance (LPR) in plasmonic nanoparticles.

The investigation of λ_{LPR} resonance shift in gold nanoparticles $Au_{(NP)}$ from the influence of external dielectric shell was carried out using shell-model of electrodynamics scattering on spherical conducting clusters with quasistatic approximation. The spherical gold nanoparticles with radius of $r_{(NP)}$ = 40 nm were considered as the initial model. On the surface of nanoparticles, the ligand layer was modeled with the thickness h_{lig} and the permittivity ε_{lig}. The parameters of thickness (Fig. 1a) and permittivity (Fig. 1b) was variated for determine the range and optimal value of sensitivity.

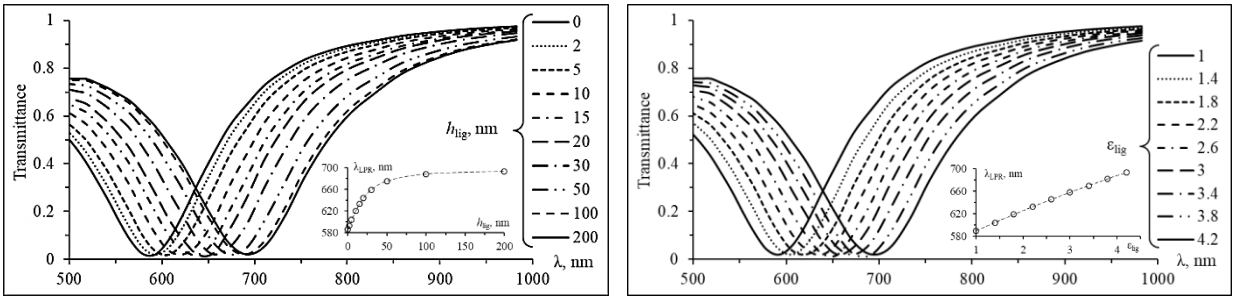

a b

Fig. 1. Modeling of LPR sensor properties: a – transmittance spectra at different value of h_{lig}, b – transmittance spectra at different value of ε_{lig} (inset – the change of λ_{LPR})

It is seen (Fig. 1a), that the significant spectral shift of LPR is observed at the small values of the ligand layer thickness. So, the deposition of a layer with the thickness of h_{lig} = 2 нм leaded to a spectral shift of $\Delta\lambda_{LPR}$ = 7 nm. When the thickness h_{lig} increases the spectral shift gradually decreases and after values of a ligand layer thickness more than 150 nm the resonance wavelength practically does not change. So, the effective penetration of near-field of resonated nanoparticles does not exceed 150 nm.

When the ε_{lig} increases (Fig. 1b) the LPR resonant wavelength monotonously shifts to the red area of the spectrum. Approximation curve is a 2nd degree polynomial. Those. in the case of a non-magnetic ligand layer around the nanoparticle (refractive index $n_{lig} = \varepsilon_{lig}^{1/2}$) the dependence between λ_{LPR} and n_{lig} is a linear.

This work was financially supported by the grant of State Council of Crimean Republic (resolution № p653-2/23 from 30.01.2023).

CP1-3P/8

Topological Faraday Effect for Optical Vortices in Magnetic Films

Yavorsky M.A.[1] , Kozhaev M.F.[2], Fedorov A.Yu.[3], Vikulin D.V.[1] , Belotelov V.I.[2]

[1]V.I. Vernadsky Crimean Federal UniversitySimferopol, 295007, Russia,
[2]Russian Quantum Center, Skolkovo, Moscow Region 143025, Russia
[3]Moscow Institute of Physics and Technology, Dolgoprudny, Moscow Region 141701, Russia

Magneto-optical effects mediate interplay between optics and magnetism and provide efficient tools for a vast range of applications including imaging of magnetic patterns and control of light at gigahertz and even terahertz rates. Up until now, the most studies of the magneto-optical effects in the films have been restricted to the usage of optical waves with the plane wave front. Such beams are able to bear only spin angular momentum, which, being associated with intrinsic polarization degrees of freedom, can take only two values $\pm\hbar$ per photon for right- and left-handed circular polarization, respectively. Only quite recently, the interaction between optical vortex beams with helical wave fronts [1] of topological charge $\ell = 0, \pm 1, \pm 2, \ldots$, which can additionally carry orbital angular momentum $\ell\hbar$ per quantum, and a magnetic system was considered [2].

Here we experimentally demonstrate the topological Faraday effect caused by the orbital angular momentum of light. It is found that the Faraday effect of the optical vortex beam passing through a transparent magnetic dielectric film differs from the Faraday effect for a plane wave. The additional contribution to the Faraday rotation depends linearly on the topological charge and radial number of the beam (see Fig. 1). These findings underline the importance of using the optical vortex beams for studies of magnetically ordered materials.

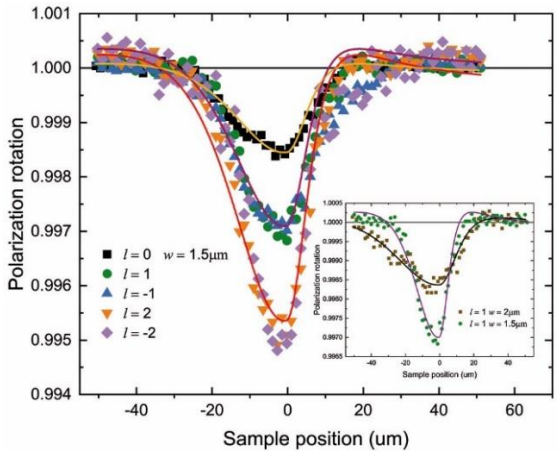

Fig 1. The normalized Faraday angle for different topological charges ℓ as a function of the position of the sample z relative to the beam waist (z=0).

This work was financially supported by Megagrant project N 075-15-2022-1108 and Russian Science Foundation (RSF), project N 23-62-10024.

References

[1] Y. Shen, X. Wang, X. Zhenwei, C. Min, X. Fu, Q. Liu, M. Gong, and X. Yuan, Light Sci. Appl. 8 (2019).

[2] A. A. Sirenko, P. Marsik, C. Bernhard, T. N. Stanislavchuk, V. Kiryukhin, and S.-W. Cheong, Phys. Rev. Lett. 122, 237401 (2019).

Section
Multiferroics and Magnetoelectric Materials

CP2-7P/1

Magnetic properties of synthetic $Co_3Ge_2O_5(OH)_4$ hydrogermanate

N. Belskaya[1*], E. Khrapova[1], A. Ivanova[1], E. Eremin[2], A. Krasilin[1]

[1]Ioffe Institute, RAS, Saint-Petersburg, Russia
[2] L.V. Kirensky Institute of Physics, SB of RAS, Krasnoyarsk, Russia
nbels@mail.ioffe.ru

Hydrogermanates with general chemical formula $Me_3Ge_2O_5(OH)_4$, (*Me* = Mg, Ni, Fe, Co, etc.) are considered to be synthetic structural analogs of phyllosilicate mineral lizardite [1]. Metal-oxygen octahedrons MeO_6 are connected by common edges to form the first sheet, which is connected by oxygen atoms to the second sublayer of germanium-oxygen tetrahedrons GeO_4. Nickel hydrogermanates have received much attention in the literature. Such compounds are well established as lithium-ion batteries and are often regarded as structurally favourable compounds for adsorption and diffusion of reagents in oxygen extraction reactions. Regarding the physical properties of other transition metal hydrogermanates, large gaps remain in the literature. This concerns the magnetic properties of such compounds. One way to change the physical magnetic properties of lizardite is to replace Mg ions with transition metal ions, such as Fe, Co, and Ni. By the time polycrystalline hydrogermanate of cobalt $Co_3Ge_2O_5(OH)_4$ was obtained, magnetic properties of this compound had not been studied. In the present work the first attempts of magnetic characterization of divalent cobalt hydrogermanate $Co_3Ge_2O_5(OH)_4$ were made.

Platy hydrogermanate $Co_3Ge_2O_5(OH)_4$ was synthesised by a hydrothermal treatment of an initial composition in aqueous medium (distilled water) at T = 200 °C and P = 2 MPa [2]. The initial composition was prepared by reverse coprecipitation. First, GeO_2 was dissolved in 2 M NaOH water solution. Then a 1 M $CoCl_2$ water solution was added dropwise to the mixture under continuous Ar flow in order to avoid oxidation of Co^{2+} to Co^{3+}. The resulting precipitate was washed of byproducts (chloride ions) and NaOH excess. The degree of washing was controlled by a qualitative reaction for chloride ions using $AgNO_3$ solution. The washed precipitate was dried and ground in an agate mortar before being placed in a PTFE-lined stainless-steel pressure vessel. The final product was a powder.

The element composition of the material was studied by energy dispersive X-ray spectroscopy on a FEI Quanta 200 scanning electron microscope. The determined Co/Ge ratio agreed well with the chemical formula. Micrographs were obtained using a JSM-7001F scanning electron microscope. The morphology of the resulting particles had the complex shape of an unfinished hexagonal plate (Fig. 1). Some particles tend to form thick platy aggregates; in that case, the agregate's thickness often overcame individual plates' width.

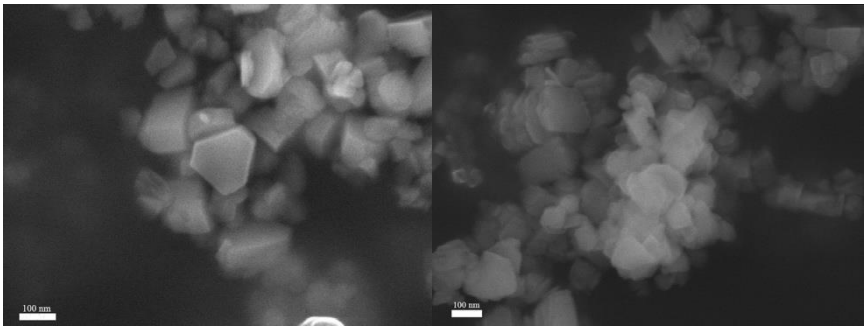

Fig. 1 – Electron micrographs of $Co_3Ge_2O_5(OH)_4$ particles

The magnetic properties of the powder sample were investigated in the 4.2-300 K temperature range and in the field range up to 90 kOe. The of magnetization experienced a sharp increase in magnetization in the low temperature region. The magnetization value was in good agreement with that expected for the ferromagnetic ordering of magnetic moments in cobalt. At low fields, the Curie point (5.9 K) was well defined on the first derivative of the magnetisation. It is worth noting the splitting of the FC FH curves, which decreased with increase in magnetic field value. Such an effect may be related to the particle size and has been reported for layered β-$Ni(OH)_2$ [3] and β-$Co(OH)_2$ [4] nanoparticles, whose layers are similar to octahedral sheets of $Co_3Ge_2O_5(OH)_4$. Treatment of the magnetic susceptibility according to the modified Curie-Weiss law with the temperature-independent term yielded paramagnetic parameter values $\chi_0 = (4.18 \pm 0.02)\cdot 10^{-3}$ emu/mol, $\theta = 6.09 \pm 0.03$ K, and $C = 10.67 \pm 0.01$ emu/mol. The latter returned an effective magnetic moment of 5.33 ± 0.06 μ_B/Co^{2+}, which agreed well with the literature values of the effective magnetic moment of divalent cobalt in the octahedral environment [5].

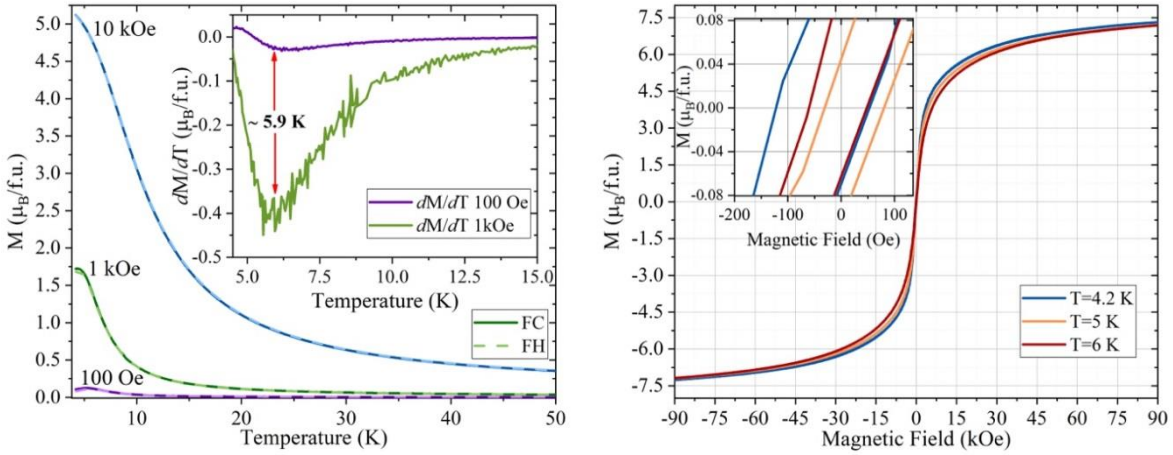

Fig. 2 – a) temperature dependences of magnetization for $Co_3Ge_2O_5(OH)_4$ powder measured in the 100 Oe, 1 kOe, and 10 kOe field. The inset shows the first derivative of magnetization. b) field dependences of magnetization measured at temperatures 4.2, 5 and 6 K. The inset shows enlarged scale of hysteresis loops

The field dependences of magnetization were measured up to 90 kOe. Quite narrow loops with a coercive field of about 50 – 100 Oe closed around 5 kOe at 4.2 K,The value of the exchange field, determined within the framework of the mean field theory, was 880 kOe. The observed hysteresis loop shift along the field axis (exchange shift) is typical for nanostructures, especially with ferromagnetic/antiferromagnetic interfaces [6]. Despite the small coercivity, $Co_3Ge_2O_5(OH)_4$ powder exhibited ferromagnetic behavior with a hysteresis loop, which is clearly visible in the magnified curves.

The study was supported by grant No. 23-22-00245 of the Russian Science Foundation, https://rscf.ru/project/23-22-00245/

References

[1] A.A. Krasilin, E.K. Khrapova, and T.P. Maslennikova, Crystals 10,654, (2020).
[2] A. A. Krasilin, E. K. Khrapova, Russ. J. Appl. Chem. 90 (1), 22–27(2017).
[3] J. D. Rall, and M. S. Seehra, J. Phys.: Condens. Matter 24 (7), 076002 (2012).
[4] P. Rabu, S. Angelov, and P. Legoll, Inorg. Chem.32 (11), 2463–2468 (1993).
[5] R. L. Carlin, Magnetochemistry, (Springer Science & Business Media, Berlin 2011).[6] J. Nogués, J. Sort, and V. Langlais, Phys. Rep. 422 (3), 65–117 (2005).

CP2-7P/2

Magnetic circular dichroism of f-f transitions in multiferroic antiferromagnet $Ho_{0.75}Nd_{0.25}Fe_3(BO_3)_4$

Malakhovskii A.V., Sokolov V.V., Sukhachev A.L. Gudim I.A.

Kirensky Institute of Physics, Federal Research Center KSC SB RAS, 660036, Krasnoyarsk, Russia

malakha@iph.krasn.ru

We studied absorption and magnetic circular dichroism (MCD) spectra of three electron transitions: $^5I_8 \rightarrow {}^5F_2$, $^5F_3$ and $^5F_5$ of Ho^{3+} ion in antiferromagnet crystal $Ho_{0.75}Nd_{0.25}Fe_3(BO_3)_4$. In Fig. 1 we present results for transition into the state $^5F_2$ (G-band), which is decomposed in the D_3 local symmetry in the following way: $A_1 + E + E$.

In paramagnets, magnetic circular dichroism (MCD) of a transition doublet→singlet in magnetic field directed along the light propagation (parallel to the C_3 axis of the crystal in our case) is given by the equation:

$$\Delta k = k_m c\, \varphi(\omega,\omega_0) + k_m \Delta\omega_0\, \partial\varphi(\omega,\omega_0)/\partial\omega_0 \,. \qquad (1)$$

The first term in (1) is the temperature dependent paramagnetic MCD (*C*-term) and the second one is the diamagnetic effect. Spectrum of the paramagnetic term, $\varphi(\omega,\omega_0)$, coincides with that of absorption. Above T_R=6.9 K the studied crystal transfers from the easy axis state to the easy plane one [1]. So, Figs. 1A and 1B present MCD in the field $H||C_3$ below and above T_R. Below the T_R (T=5 K) shape of the MCD spectrum well corresponds mainly to the diamagnetic term of MCD. Above T_R the MCD spectrum approximately repeats absorption spectrum accurate within signs. This implies that only the paramagnetic MCD remains.

Magnetic field is applied parallel to the trigonal C_3-axis. Consequently, in the easy axis state the magnetic field is directed parallel to the Ho magnetic moments, and energies of the Ho ions in two sublattices change in magnetic field on the values $\pm\mu_B g H$, and MCD acquires diamagnetic shape with some asymmetry relative to y=0 axis because of the paramagnetic component (Fig. 1A).

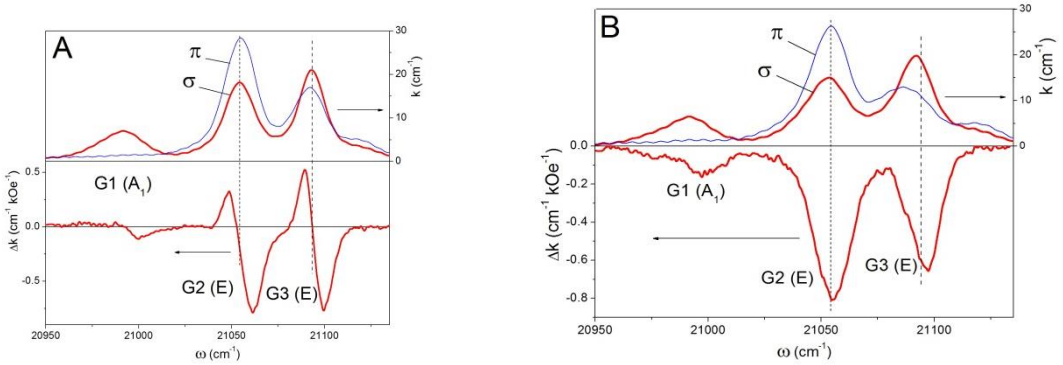

Fig. 1. Polarized absorption (k) and MCD (Δk) spectra at temperatures 5 K (A) and 8 K (B).

Above the reorientation transition the external magnetic field $H||C_3$ is perpendicular to the exchange field H_e from the Fe sublattice. The total effective field is: $H_{ef}=(H_e^2+H^2)^{1/2}$. The change of the Ho ion energy in the magnetic field $H<<H_e$ will be: $\Delta E(H)=\mu_B g(H_{eff}-H_e)\approx \mu_B g H(H/2H_e)$. According to Ref. [2], $H_e\approx$25 kOe in pure Ho ferroborate. If we suppose that in our crystal the

exchange field Fe-Ho is the same, than the splitting in the used magnetic field H=2 kOe will be 25 times decreased. The temperature dependent paramagnetic MCD will be decreased in the same degree. So, both diamagnetic and temperature dependent paramagnetic MCD become not measurable. However a strong effect with the paramagnetic type dispersion is observed (Fig. 1). Consequently, above the reorientation transition we deal with the paramagnetic B-term, or term of mixing.

In the easy axis state eigenfunctions of the Ho Hamiltonian in magnetic field $H||C_3$ coincide with those without magnetic field, when $\boldsymbol{M}_{\mathrm{Ho}},\boldsymbol{M}_{\mathrm{Fe}}||C_3$. Therefore the magnetic field does not mix the wave functions. In the easy plane state eigenfunctions of the Ho Hamiltonian in magnetic field $H||C_3$ do not coincide with those without magnetic field, when $\boldsymbol{M}_{\mathrm{Ho}},\boldsymbol{M}_{\mathrm{Fe}}\perp C_3$, i. e., in the exchange field $H_e\perp C_3$. The latter functions are mixtures of states with opposite projections M_J of Ho moments on the C_3-direction and, therefore, they have diminished magnetic moments. External magnetic field $H||C_3$ switches on the opposite process: it makes states magnetic ones. Thus, B-term appears in crystals due to mixing of states by magnetic field.

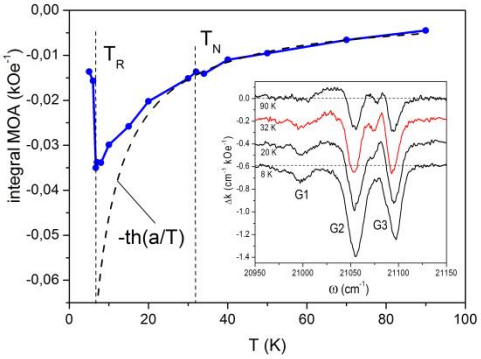

Fig. 2. MOA of ${}^5I_8 \rightarrow {}^5F_2$ transition. Inset: MCD spectrum as a function of temperature.

Fig. 2 demonstrates temperature dependence of integral magneto-optical activity (MOA) of the G-band. Additionally, the theoretical dependence of paramagnetic term c~th(a/T) from (1) is shown on the condition, that it coincides with the experimental MOA at T=70 K. The process of quenching of the temperature dependent paramagnetic MOA is well seen. Transformation of the MCD spectrum with temperature is shown in Fig. 2 inset. The diamagnetic part of MCD is gradually appearing with the temperature increase.

In magnetically ordered crystal, splitting of the ground state and difference of populations of its sublevels is mainly created by the exchange field H_e. Therefore, in the external magnetic field, directed along the exchange field in the easy axis state, we measure only change of the paramagnetic MCD due to change of the difference of the sublevels populations by the external magnetic field:

$$\Delta c(H) = H\frac{\mathrm{dc}}{\mathrm{dH}}(H = H_e) = -(\mu_B g_{\mathrm{CM}}\, H/2\, k_B T)/[\mathrm{ch}^2(\mu_B g_{\mathrm{CM}}\, H_e/2\,\mathrm{kT})].$$

This formula indeed describes the experimental behavior of MCD at $T<T_R$ (Fig. 2).

References

[1] A.V. Malakhovskii, A.L. Sukhachev, V.V. Sokolov, I.A. Gudim, V.R. Kuchesheva-Titova, Physica B 654 (2023) 414706.

[2] A.V. Malakhovskii, S.L. Gnatchenko, I.S. Kachur, V.G. Piryatinskaya, I.A. Gudim, Low Temp. Phys. 43, 610 (2017).

CP2-7P/3

Temperature tuning of orthoferrite-based spin-Hall oscillator

Meshcheryakov A.A.[1,2], Safin A.R.[1,3], Kalyabin D.V.[1,2], Nikitov S.A.[1,2], Mednikov A.M.[2]

[1]*Kotel'nikov Institute of Radio-Engineering and Electronics of RAS, 125009, Moscow, Russia*
[2] *Moscow Institute of Physics and Technology, 141701, Moscow, Russia*
[3] *Moscow Power Engineering Institute, 111250, Moscow, Russia*
anatoly199824@rambler.ru

Currently, spin-transfer nanooscillators (STNO) based on multilayer structures are being actively investigated. Previously, such structure [1] and frequency tuning by magnetostriction [2] have already been theoretically studied. In this work, the model of a STNO with the possibility of frequency tuning by temperature changing is theoretically investigated [3]. The tuning of the oscillation frequency is possible due to the properties of the active element of the oscillator - holmium orthoferrite $HoFeO_3$. In $HoFeO_3$, in temperature interval 38 K-52 K several phase transitions are taking place. The physical structure of the consideration THz-oscillator is a two-layer nanostructure, in which the antiferromagnetic (AFM) layer ($HoFeO_3$) lies on the heavy metal layer (platinum). The oscillations are excited by the DC electric current flowing through the Pt layer. To describe the oscillations of the Neel vector $\mathbf{l} = (\mathbf{M}_1 - \mathbf{M}_2)/M_s$ (where $\mathbf{M}_{1,2}$ is AFM sublattice magnetizations, M_s is the magnetic saturation of the AFM sublattice), the "sigma-model" was used, which took into account the temperature dependence of the anisotropy of $HoFeO_3$. Figure 1 shows the dependence of the oscillation frequency on the density of the input DC current for damped oscillations regime and for self-oscillations regime. This dependence demonstrates a hysteretic behavior.

We acknowledge the support from the Russian Foundation for Basic Research (Grant No. 19-29-03015, 18-57-76001, 18-29-27018).

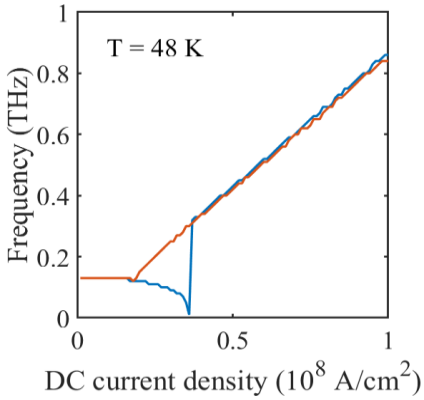

Fig. 1. Output oscillation frequency vs DC current density for the orthoferrite-based spin-Hall oscillator

References

[1] R. Khymin *et al*, Sci. Rep. 7, 43705 (2017).
[2] P.A. Popov *et al*, Phys. Rev. Applied 13, 044080 (2020).
[3] A.A. Meshcheryakov *et al*, J. Phys. D: Appl. Phys. 54, 195001 (2021).

CP2-7P/4

Double perovskite $PrBaMn_2O_{6-\delta}$: synthesis by the method of intensive plastic deformation

Naumov S.V.[1], Mostovshchikova E.V.[1], Stepanov A.E.[1], Patselova V.K.[1], Gizhevskii B.A.[1]

[1] *M.N. Mikheev Institute of Metal Physics of Ural Branch of Russian Academy of Sciences (IMP UB RAS), 620137, Ekaterinburg, Russia*
stepanov_ae@imp.uran.ru

Double layered perovskites $LnBaMn_2O_{6-\delta}$ are of interest both from the point of view of studying their fundamental properties - magnetism, conductivity, etc. and as a promising material for electrodes of solid fuel cells.

Some difficulties in obtaining ordered double perovskites cause the search for new methods for the synthesis of such materials. The most common in this case is the citrate-nitrate method of synthesis. At the same time, there are works in which the mechanochemical method of synthesis is used. So in [1], the synthesis of $PrBaMn_2O_{6-\delta}$ was used by high-energy grinding (planetary mill) of a mixture of the corresponding binary oxides. This method showed positive results, however requires a long time (up to 150 min.) for grinding the initial powders and is very energy consuming.

In our work, we consider the possibility of synthesizing double perovskites by the method of intensive plastic deformation. This method is widely used to obtain bulk nonporous nanomaterials, including the synthesis of manganites [2].

Intensive plastic deformation of the initial mixture of oxides was carried out by shear under pressure using a press with a force of 100 tons and Bridgman anvils (Fig. 1). The powder of initial oxides Pr_6O_{11}, BaO_2 and MnO was placed between anvils and compressed to 5 GPa. Shear deformation was carried out by rotating one of the anvils relative to the other at a speed of 0.3 rpm. Samples were obtained with a diameter of ~5 mm and a thickness of ~100 μm. Next, the samples were annealed in an inert atmosphere and studied using X-ray diffraction.

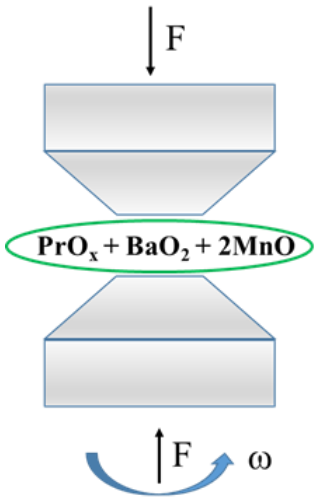

Fig.1. Schematic diagram of the use of Bridgman anvils for the synthesis of $PrBaMn_2O_{6-\delta}$ from the initial oxides.

As a result, the possibility of obtaining double layered perovskites using quasi-static deformation of the initial powders (shear under pressure) is shown. The features of this method as applied to $LnBaMn_2O_{6-\delta}$ systems and its prospects are discussed.

The work was supported by the Russian Science Foundation (Grant No. 22-22-00507).

References

[1] F.J. Garcia-Garcia, M.J. Sayagués, F.J. Gotor, Nanomaterials 11, 380 (2021)
[2] Gizhevskii B.A., Zhuravlev V.D., et.al, Doklady Chemistry. 405, 247 (2005)

CP2-7P/5

Structural, magnetic and electrical properties of $BiFe_{1-x}Mn_xO_3$ ($x \leq 0.15$) solid solutions synthesized by the sol-gel method

Tarasenko T.N.[1], Mikhaylov V.I.[1], Kravchenko Z.F.[1], Burkhovetskyi V.V.[1], Izotov A.I.[1], Legenkii Yu.A.[2], Zhyvulka A.M.[3], Yanushkevich K.I.[3], Aplesnin S.S.[4]

[1]*Galkin Donetsk Institute for Physics and Engineering, 283114, Donetsk, Russia*
[2]*Donetsk National University, 283001, Donetsk, Russia*
[3]*SSPA "Scientific-Practical Materials Research Center of NAS of Belarus", 220072, Minsk, Belarus*
[4]*Reshetnev Siberian State University of Science and Technology, 662850, Krasnoyarsk, Russia*
t.n.tarasenko@mail.ru

An actual problem for obtaining magnetoelectric materials with a large magnetoelectric effect at above room temperatures, based on $BiFeO_3$ bismuth ferrite, is the complete (or partial) suppression of the spin-modulated structure (cycloid) characteristic of $BiFeO_3$. In bulk $BiFeO_3$ samples, the presence of a spin cycloid causes the bulk magnetic moment to be zero, and thus the manifestation of the magnetoelectric effect becomes impossible [1]. The problem of obtaining single-phase multiferroics based on bismuth ferrite is that the synthesis process of $BiFeO_3$ is accompanied by low thermal stability of the perovskite phase and its partial dissociation into $Bi_{25}FeO_{39}$ and $Bi_2Fe_4O_9$.

A comprehensive study was made of samples of $BiFe_{1-x}Mn_xO_3$ solid solutions ($0.05 \leq x \leq 0.15$) synthesized using the sol–gel technique [2]. In the traditional method of solid-phase synthesis of $BiFeO_3$ from a mixture of oxides of Bi_2O_3 and Fe_2O_3 there is preferential diffusion of bismuth into the Fe_2O_3 particle, so the reaction goes through the formation of $Bi_{25}FeO_{39}$ [3]. B [3] it is shown that the production of polycrystalline multiferroic of high phase purity is associated with the use of initial substances in the form of nanodisperse powders with a narrow grain-size distribution. Using the sol-gel method, it is possible to materials in the form of nanosized powders. A xerogel is a homogeneous mixture of nanoparticles, in which the diffusion path is significantly reduced [3].

Bismuth, iron, and manganese nitrates were chosen as starting substances for obtaining $BiFe_{1-x}Mn_xO_3$ compositions. A solution of citric acid and ethylene glycol was used as a gelling agent, which was added to a solution of stoichiometric amounts of nitrates. After evaporation of excess water and subsequent removal of excess NO_2 from the concentrated solution, polymerization was carried out, resulting in ethylene glycol and metal-citrate complexes forming a polymerization matrix. By heating the product to 450°C, the organic compounds were removed. To obtain bulk samples in the form of tablets with a diameter of 8 mm and a thickness of 1.5 mm powders were milled and subjected to cold isostatic pressing (pressure in the mold ~2 kbar), followed by annealing at 850 ° C (10 min).

The crystalline structure and phase composition of the samples were determined via X-ray diffraction using a DRON-3 diffractometer with CuKα radiation. X-ray diffraction patterns of $BiFe_{1-x}Mn_xO_3$ samples ($x = 0$, 0.05 and 0.15) showed that the percentage of impurity phases decreases with increasing manganese content, while the main phase characteristic of "pure" $BiFeO_3$ (space group R3c) stabilizes [2].

Microstructural studies were performed using a JSM-6490LV scanning electron microscope (JEOL, Japan). The results from studying the morphology of the surfaces of fracture in samples of $BiFe_{1-x}Mn_xO_3$ ($x = 0$, 0.05 and 0.15) showed that with increasing manganese content

the average size of granules decreases d_{av}: 491 nm (x = 0); 234 nm (x = 0.05); 218 nm (x = 0.15). For samples containing manganese, individual grains are observed, often with well-defined faceting, whose contact surface with the main matrix is small.

We investigated magnetic and electric characteristics of $BiFe_{1-x}Mn_xO_3$ solid solutions (x=0, 0.05, and 0.15) synthesized with sol–gel technology [2]. Figs. 1a and 1b show the temperature dependences of the specific magnetization σ(T) of the compositions x = 0.05 and x = 0.15. In the concentration range $0.05 \le x \le 0.15$, the investigated compositions exhibit specific magnetization characteristic of substances with magnetic ordering. The temperatures of the magnetic order–magnetic disorder phase transformations were determined from the derivative of specific magnetization σ(T) with respect to temperature. Increasing Mn^{3+} content leads to a lower Curie temperature: T_C = 605 K for x = 0.05 and 550 K for x = 0.15.

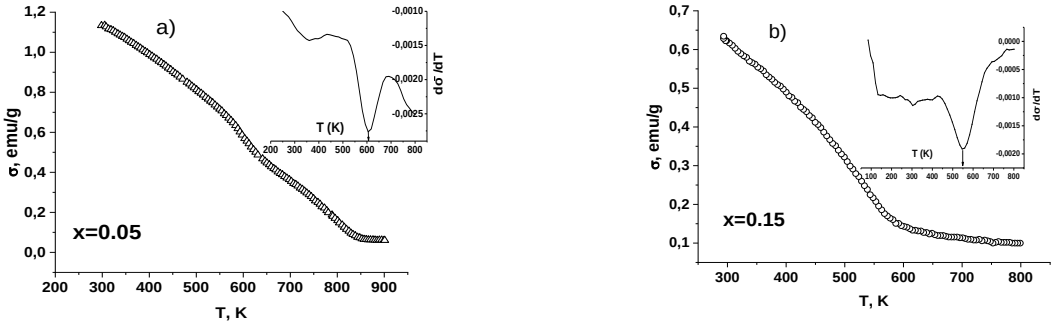

Fig. 1. Temperature dependences of specific magnetization σ(T) of $BiFe_{1-x}Mn_xO_3$ samples: (a) x = 0.05 and (b) 0.15. Temperature dependences dσ/dT(T) are shown in the insets.

While their ionic radii are identical, the Mn^{3+} ion has one 3d electron less than the Fe^{3+} ion. Four 3d electrons of magnetoactive Mn^{3+} ions disturb the electronic structure of the Fe/MnO_6 octahedra. Yahn–Teller distortions of Fe/MnO_6 oxygen octahedra arise when Fe^{3+} is substituted for Mn^{3+}. The change in specific magnetization at x = 0, 0.05, and 0.15 could be evidence of the redistribution of the volumes of ferromagnetic and antiferromagnetic phases in the compositions: the number of ferromagnetic Mn–O–Fe bonds falls correspondingly while that of antiferromagnetic bonds rises.

The studied compositions $BiFe_{1-x}Mn_xO_3$ are semiconductors at x = 0.05 and 0.15, while $BiFeO_3$ was a dielectric throughout the range of temperatures. The band-gap energy was ΔE = 1.03 eV for x = 0.05 and ΔE = 0.8 eV for x = 0.15. It was found that with the increase of concentration x there is a tendency of growth of dielectric permittivity ε at room temperature relative to dielectric permittivity of $BiFeO_3$ in 1.8 times at x = 0.05 at frequency of 1 kHz and in 7.2 times at x = 0.15. At 1 MHz the dielectric permittivity changed 1.7 times at x = 0.05 and 2.4 times at x = 0.15.

In $BiFe_{1-x}Mn_xO_3$ films ($0.0 < x < 0.15$), a photoinduced diode effect in the near-infrared and violet regions of the spectrum was detected in a wide temperature region [4].

The research was funded by the Russian Science Foundation (project No. 20-19-00745-П).

References

[1] A.P. Pyatakov and A.K. Zvezdin, Phys.—Usp., 55, 557 (2012).

[2] T.N. Tarasenko, V.I. Mikhaylov, Z.F. Kravchenko, et al., Bull. Russ. Acad. Sci.: Phys., 87, 357 (2023).

[3] A.V. Egorysheva, V.D. Volodin, O.G. Ellert, et al., Inorg. Mater., 49, 303 (2013).

[4] S.S. Aplesnin, V.V. Kretinin, et al., Semicond. Sci. Technol., 34, 095007 (2019).

Section
Nanostructured Materials and Composites

CO3-8O/1

Investigation of optical properties of III-V nanoinclusions integrated into silicon

Melnichenko I.A.[1], Komarov S. D.[1], Dragunova A.S.[1], Moiseev E.I.[1], Kryzhanovskaya N.V.[1], Makhov I.S.[1], Nadtochiy A.M.[1], Ivanov K.A.[1], Zhukov A.E.[1]

[1]HSE University, 190008, St. Petersburg, Russia
hse@hse.ru

Development of methods of integration of III-V emitting nanostructures with silicon is an essential task of photonics, the solution of which will allow to combine the technology of high-speed noise-proof optical data transmission with the developed technology of silicon integrated circuits for further application in high-performance systems of big data processing, quantum computing and artificial intelligence. However, integration is a challenging task due to the large lattice mismatch of most III-V materials with Si, significant difference in thermal expansion coefficients, and too high defect density for device applications. Currently, several competing approaches to integrate III-V semiconductors with a silicon platform are being actively investigated: the use of buffer layers [1], bonding techniques [2], selective growth methods [3], and the growth of nanostructures using catalyst drops [4].

Recently, a new epitaxial growth method based on metal-organic chemical vapor deposition (MOCVD) approach, called molten alloy driven selective area growth (MADSAG), has been introduced [5]. This method is a combination of selective area growth (SAG) and droplet growth techniques. The combination of these methods is considered promising because it eliminates the need for expensive III-V substrates, complex wafer bonding technologies, and the difficulties associated with precise positioning when combining III-V and Si components at the micro level.

In this work, we study the optical properties of such III-V heterostructures synthesized by the MADSAG method in silicon, and numerical analysis of the properties of microlasers with nanostructures in the waveguide is carried out.

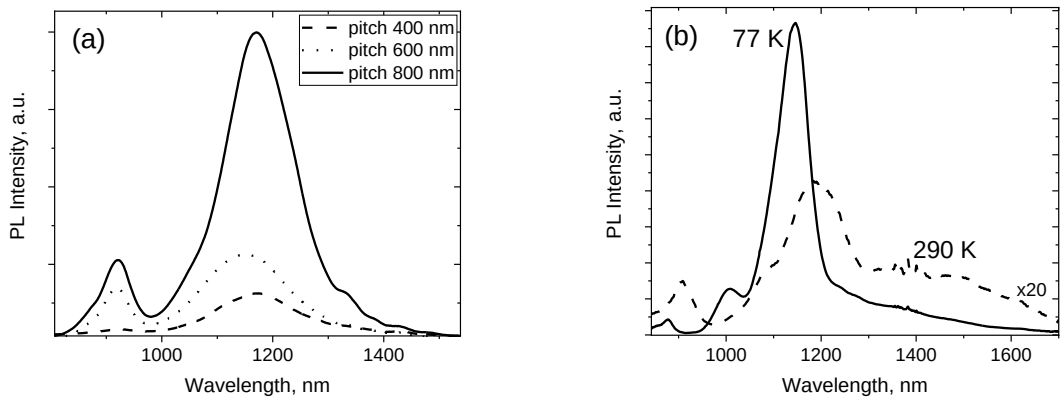

Fig.1. μPL spectra from samples with different periods of nanoinclusions (a), and μPL spectra at 77 K and 290 K (b).

The InP/InAsP/InP nanostructures were grown in preformed pits in the silicon substrate (100) using MADSAG method. A detailed description of the growth and post-growth is given in previous work [6]. The distance between the centers of the holes was 400, 600, and 800

nm. A confocal microscope was used to study the microphotoluminescence (μPL) of the resulting nanostructures. The structures were investigated in the temperature range from 77 to 290 K. Reducing the distance between the pits leads to less filling of the pits by material and a decrease in luminescence intensity. Increasing the temperature does not lead to a strong decrease in the intensity, which indicates a low level of non-radiative recombination in the epitaxial structure. Numerical simulation of waveguide modes and whispering gallery modes of microdisk resonators based on a SOI structure with emitting III-V nanostructures embedded in it has shown that the quality factor inherent for pure microdisk resonators is preserved even when III-V inserts are present. At the same time, when distributed asymmetrically with respect to the microdisk, these inserts provide directionality of the emitted radiation. The obtained results show that this novel method makes it possible to grow an ordered array of submicron In(As)P emitters in silicon with a minimum number of defects and high structural and optical quality.

This study was supported by Russian Science Foundation grant 22-22-20057, https://rscf.ru/project/22-22-20057/ and by St. Petersburg Science Foundation grant 66/2022 dated 15 April 2022.

References

[1] Y. Wan, et al. Laser & Photonics Reviews, 14, 2000037 (2020).
[2] A. Sakanas, et al. Microelectronic Engineering 214, 93-99 (2019).
[3] L. Iemmo, et al. Nanotechnology 28.49, 495705 (2017).
[4] J. Vukajlovic-Plestina,et al. Nature Communications 10(1), 869 (2019).
[5] D.V. Viazmitinov, et al., Nanoscale, 12(46), 23780-23788 (2020**).**
[6] I.A. Melnichenko, et al., Nanomaterials 12 (23), 4213 (2022).

CO3-8O/2

Structure, surface morphology, magnetic and magnetocaloric properties of RCo_2 nanostructured materials

Tereshina I.S.[1], Kaminskaya T.P.[1]

[1]*Faculty of Physics, M.V. Lomonosov Moscow State University, 119991, Moscow, Russia*
irina_tereshina@mail.ru

Solid-state magnetic cooling is modern technology based on the magnetocaloric effect (MCE) that can reduce global energy consumption and eliminate the use of environmentally unfriendly refrigerants like freon. Medicine, biology, food industry need silent, safe and compact refrigeration equipment designed for long-term storage of vaccines, biomaterials, pharmaceuticals and food products at fixed temperatures, well below room temperature (T < 300 K). This work is devoted to the study of the structure, surface morphology, magnetic and magnetocaloric properties of RCo_2 nanostructured materials with high MCE values in the temperature range of 100–290 K, suitable for solid-state magnetic cooling.

In this work, we obtained and studied the properties of multicomponent alloys of the (Tb,Dy,R)Co_2-type (R = Gd or Ho) in the poly- and nanocrystalline state. The samples were synthesized in an arc furnace in an argon atmosphere. To obtain samples in the nanocrystalline state, the method of rapid quenching from the melt was used. This method makes it possible to obtain samples in the form of thin ribbons, which will increase the surface area of the working body of the magnetic refrigerator and, consequently, significantly increase the heat transfer rate.

All obtained samples were certified using X-ray diffraction analysis. Information about the topography of the surfaces, as well as about the structural features of the surface layers of the ribbon samples, was obtained using atomic force microscopy. Sample measurements were taken on the side that was in contact with the copper wheel and opposite the free side; as well as on a break of samples.

Particular attention was paid to the study of the influence of the structural state on the magnetic and magneto-thermal characteristics. In this work, we used thermomagnetic analysis to determine the temperatures of magnetic phase transitions and a direct method for measuring the MCE, in which a thermocouple was placed between two ribbon samples.

It was found that the samples after the rapid quenching procedure contained a small amount of the amorphous phase (up to 10%). Cracks oriented in one direction were observed on the contact surface of the samples, and the surface of all the investigated ribbon samples had a grain structure. The study of the free surface of the samples showed that a predominantly smooth surface with an oriented wavy structure in local areas is observed. Single clusters were observed on the free surface of rapidly quenched samples.

The temperatures of the magnetic phase transitions of the samples in the poly- and nanocrystalline states coincided. Only a slight decrease in the magnetocaloric effect was observed in the rapidly quenched samples, which may be due to the presence of an amorphous phase.

The research was supported by project no. 22-29-00773 from the Russian Science Foundation, https://rscf.ru/project/22-29-00773/.

CO3-8O/3

Superconducting diode effect in topological hybrid structures

Vasenko A.S.[1]

[1]*HSE University, 101000 Moscow, Russia*
avasenko@hse.ru

Currently the superconducting diode effect (SDE) has become an active area of research due to its large application potential. Typically, the helical superconducting state is responsible for the SDE. Helical state is widely discussed in materials with two-dimensional (2D) superconductivity, spin-orbit coupling and induced in-plane magnetic field [1]. Here we report the presence of the SDE (helical) phase in the diffusive hybrid structures 2D superconductor/ ferromagnet (S/F) on top of the topological insulator surface (TI), see Fig. 1(a). In such a case nonuniform superconducting state is realized by means of a proximity effect [2]. This proximity induced helical state causes noticeable current nonreciprocity in the system, see Fig. 1(b-c) [2]. Employing the nonlinear quasiclassical approach we investigate the SDE quality factor for a wide range of temperatures and in-plane fields [3]. Summarizing the results of the calculations we present the phase diagram of the SDE [3]. We also provide comparison between linear and nonlinear approaches [4].

A.S.V. acknowledges support from the Mirror Laboratories Project and the Basic Research Program of the HSE University.

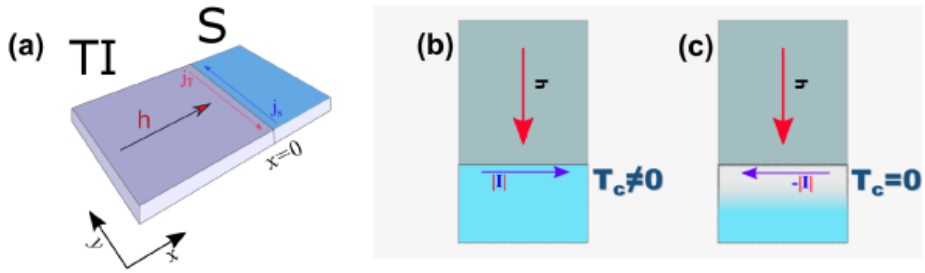

Fig. 1. (a) Schematic model of the S/F/TI hybrid structure. (b)-(c) Illustration of the SDE. Applying external supercurrent along the interface in one direction keeps the non-zero critical temperature (b), while reversing the current may completely destroy the superconducting state (c).

References

[1] F. Ando, Y. Miyasaka, T. Li, J. Ishizuka, T. Arakawa, Y. Shiota, T. Moriyama, Y. Yanase, and T. Ono, Nature 10, 584, 373 (2020).

[2] T. Karabassov, I.V. Bobkova, A.A. Golubov, and A.S. Vasenko, Phys. Rev. B 106, 224509 (2022).

[3] T. Karabassov, I. V. Bobkova, V. M. Silkin, B. G. Lvov, A. A. Golubov, and A. S. Vasenko, arXiv:2305.00549, submitted to Supercond. Sci. Technol.

[4] T. Karabassov, E.S. Amirov, I.V. Bobkova, A.A. Golubov, E.A. Kazakova, and A.S. Vasenko, Condens. Matter 8(2), 36 (2023).

CO3-8O/4

Magnetoelectric gyrator on the based three-layer magnetostrictive-piezoelectric symmetrical structures: theory and experiment

D.A. Filippov[1], E.V. Udaltsova[1], В.М. Лалетин[2], Н.Н. Поддубная[2], Jitao Zhang [3]

[1]*Yaroslav the Wise Novgorod State University, 173003, Veliky Novgorod, Russia*
[2]*Institute of Technical Acoustics, NAS of Belarus, 210009, Vitebsk, Belarus*
[3]*Zhengzhou University of Light Industry, 450002, Zhengzhou, China*

The work is focused on theoretical and experimental studies of a magnetoelectric gyrator consisting of an inductor coil, inside of which there is a magnetoelectric heterostructure, which is a mechanically connected piezoelectric layer and two magnetic layers. Using a system of equations of elasto- and electrodynamics for the piezoelectric and magnetostrictive phases, expressions for the coefficient of current/voltage conversion $|K_{IV}|$ of the gyrator through the parameters of the heterostructure phases are obtained. It is shown that I/V conversion coefficient depends both on the parameters of the inductor, the magnetoelectric heterostructure, and on the load resistance. On Fig.1 shown the frequency dependency of the $|K_{IV}|$ for ME gyrator. For the calculations was used the parameters of the structure, present in Tab.1

Table 1. Parameters of the structure

Material	Piezoelectric PZT	Magnetic layer AMAG 212N
Lengthy of the plate, mm	20	18
Width of the plate, mm	5	5
Thickness of the layer, mm	0.3	0.12
Density, kg/m^3	7000	7700
Young's modulus, GPa	67	110
Permittivity ε_{33}^{p}	1750	-
Piezomodules: d_{31}^{p}, pC/N	-175	-
q_{11}^{m}, ppm/Oe	-	0.3

As can see from Fig. 1, the dependency has a resonance character. This fact connects with electromechanical resonance of the ME heterostructure [1]. The peak of the $|K_{IV}|$ is observed at the frequency $f_{res} \cong \frac{1}{2L}\sqrt{\frac{\overline{Y}}{\overline{\rho}}}$, where $\overline{Y}$ and $\overline{\rho}$ are the average values of the Young's modulus and the density of the structure, L is the length of the sample.

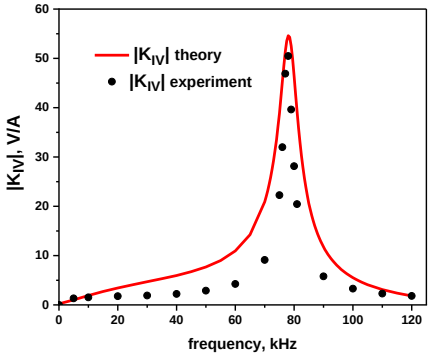

Fig.1 Frequency dependence of the I/V conversion coefficient. Solid line – theory, dots – experiment

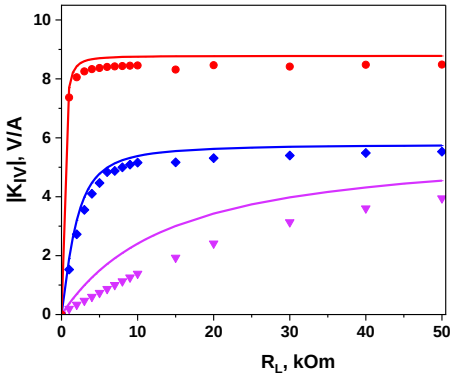

Fig. 2 Load characteristics of ME gyrator. Solid line – theory, dots – experiment. ▼ frequency $f = 1\ kHz$, ◆ – $f = 10\ kHz$, ● – $f = 50\ kHz$

The value of the I/V coefficient conversion also depends on the load resistance value R_L. On Fig.2 present the dependency $|K_{IV}|$ from the load resistance R_L at the different frequencies. As follow from Fig.2 the coefficient of the I/V conversion with increasing the frequency reaches saturation at the smaller values of the load resistance.

The load characteristics also depend on the types of the piezoelectric. On Fig.3 and Fig.4 shown the load characteristic for the ME gyrator on the based PZT, GaAs and quarts (Q) piezoelectrics at the frequencies 50 kHz.

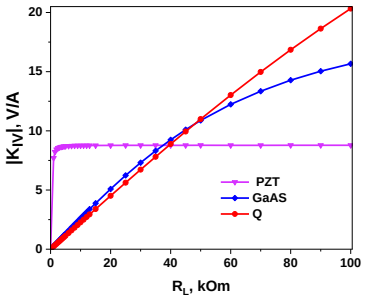

Fig.3 Load characteristics of the ME gyrator with different piezoelectric types at the frequency 50 kHz.

At low load resistances, the value $|K_{IV}|$ for a gyrator based on PZT exceeds the value for gyrators based on GaAs and Q, however, with load resistances greater than 40 kOm, gyrators using GaAs and Q as a piezoelectric show better characteristic.

This research at Novgorod State University was funded by a grant from the Russian Science Foundation project № 22-19-00763.

References

[1] Bichurin M.I., Filippov D.A., Petrov V.M., Laletsin V.M., Paddubnaya N.N., Srinivasan G., Phys. Rev. B 68, 132408 (2003).

CO3-8O/5

Synthesis, structure and properties of double perovskites $LnBaMn_2O_{6-\delta}$ (Ln= Pr, Sm, Nd)

Naumov S.V.[1], Mostovshchikova E.V.[1], Stepanov A.E.[1]

[1] *M.N. Mikheev Institute of Metal Physics of Ural Branch of Russian Academy of Sciences (IMP UB RAS), 620137, Ekaterinburg, Russia*
naumov@imp.uran.ru

Perovskite-like compounds based on manganese have been known for a long time and are widely studied. Recently, ordered double manganites, double perovskites, have attracted interest. Attention to these compounds is due to the following reasons:

- Strong connection between charge, orbital and spin degrees of freedom;
- The presence of magnetic transitions, transition metal - insulator;
- On the other hand, layered manganites such as $PrBaMn_2O_5$ and $NdBaMn_2O_5$ have shown high performance as SOFC electrodes with good redox stability and durability.

The technology for obtaining manganese-based double perovskites is somewhat more complicated than the technology for the synthesis of simple manganites with the general formula $Ln_{1-x}A_xMnO_3$ (A = Ba, Sr). In the vast majority of studies, the citrate-nitrate method is used to obtain $LnBaMn_2O_{6-\delta}$ compounds, which is not always convenient to use.

The purpose of this work is to demonstrate the possibility of solid-phase synthesis of polycrystals, grow $LnBaMn_2O_{6-\delta}$ single crystals, and study their structure and properties.

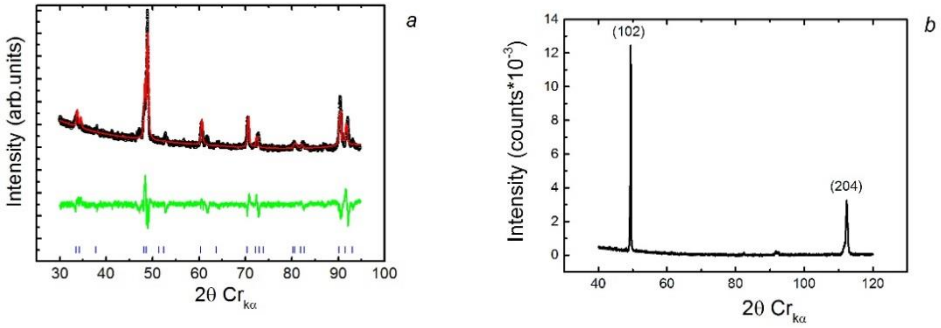

Fig. 1. X-ray diffraction pattern of the ground single crystal $Nd_{0.5}Sm_{0.5}BaMn_2O_{6-\delta}$, sg#123, a=3.974 Å, c= 7.777 Å (*a*), X-ray diffraction pattern from the surface of a single crystal (*b*). The direction [102] coincides with the direction of single crystal growth.

The work shows:

- By solid-phase synthesis under conditions of a reducing atmosphere, it is possible to synthesize single-phase polycrystalline samples of double perovskites based on manganese.
- The following compositions were obtained:

  $PrBaMn_2O_{6-\delta}$, $SmBaMn_2O_{6-\delta}$, $NdBaMn_2O_{6-\delta}$, $Nd_{0.5}Sm_{0.5}BaMn_2O_{6-\delta}$.
- Single crystals of the corresponding compositions were grown by the method of zone melting (For an example, see fig. 1).
- Studies of their structure, optical and magnetic properties were carried out.

The work was supported by the Russian Science Foundation (Grant No. 22-22-00507).

CO3-8O/6

Core-shell magnetite nanoparticles: morphology, magnetic properties, organic dyes adsorption

Ivanova O.S.[1,2], Edelman I.S.[1], Svetlitsky E.S.[1], Sokolov A.E.[1,2], Zharkov S.M.[1,2], Petrov D.A.[1], Sukhachev A.L.[1], Toropova E.S. [1], Chun-Rong Lin[3], Ying-Zhen Chen[3]

[1] Kirensky Institute of Physics, FRC KSC SB RAS, 660036, Krasnoyarsk, Russia
[2] Siberian Federal University, 660041, Krasnoyarsk, Russia
[3] National Pingtung University, 90003, Pingtung City, Taiwan
osi@iph.krasn.tu

The exponential growth of the anthropological burden has led to global problems, such as, for example, the deterioration of water quality, its pollution by various sources, which is one of the threats facing humanity. Many laboratories in the world are working to create materials for water purification as efficient as possible, inexpensive in production, and capable of withstanding many cycles including those based on magnetic NP, whose enormous advantage is the possibility of removing them from purified water using a magnetic field. Therefore, magnetic NP are the leading candidates for use in various devices for removing pollutants, in particular, dyes from aqueous solutions [1]. Adsorption of organic dyes by nanoparticles (NP) of magnetite with a core-shell structure is a subject of this talk. The time and concentration dependences of the adsorption parameters of different types of dyes are presented, and correlations between these characteristics and the type of NP's coating have been established. Adsorption mechanisms are discussed relative to anionic – eosin Y (EY) and Congo red (CR), and cationic – methylene blue (MB) and rhodomine B dyes. Core-shell nanoparticles Fe_3O_4@C, Fe_3O_4@C@Ag, Ag@Fe_3O_4, and bare Fe_3O_4 nanoparticles were synthesized by various chemical methods. In all cases, magnetic core was of magnetite crystal structure, the sizes of the nanoparticles varied in the limits 30-50 nm, the thickness of the amorphous shell was about 5 nm. Saturation magnetization values of the nanoparticles were close to that of bulk magnetite.

The mechanisms of adsorption of cationic and anionic dyes are different. For example, the values of adsorption capacity under the experimental conditions C_0 = 30 mg/L and NPs 1 mg/mL for MB were 11, 9, and 6 for Ag@Fe_3O_4, Fe_3O_4@C, and Fe_3O_4@C@Ag NPs. respectively. Although the values of the adsorption capacity vary significantly with the type of magnetite shell, the kinetic curves for the cationic dyes adsorption are described better by the pseudo-second order model for all samples, which indicates the predominance of the chemical mechanism. The model of diffusion inside NP made it possible to estimate the adsorption rates at different stages. Characteristic for all samples, the sharp rise in the $q_t=f(t^{1/2})$ curves characteristic of all samples at the first stage, due to the process of diffusion on the surface of the nanoparticle, practically completes the process of limiting diffusion inside the particle. The adsorption of anionic dyes revealed other correlations and patterns, showing the complex role of the surface and centers formed during the synthesis of particles.

The research was funded by the Russian Science Foundation (project No.23-22-10025), Government of the Krasnoyarsk Territory, Krasnoyarsk Regional Fund of Science.

References

[1] H. Xiang, Nanomaterials 11, 330 (2021).

CO3-8O/7

Effect of Inhomogeneous Magnetoelectric Interaction on Flat Magnetic Structures

Magadeev E.B.[1], Vakhitov R.M.[1]

[1]*Ufa University of Science and Technology, 450076, Ufa, Russia*
magadeeveb@gmail.com

In this paper, we study the effect of inhomogeneous magnetoelectric interaction (IMEI) on magnetic structures, which are characterized by the absence of a magnetization vector leaving the plane of a ferromagnetic film due to the presence of a strong uniaxial anisotropy of the "easy plane" type in the sample. As shown in [1–3], such flat structures have additional possibilities for the formation of topologically protected solitary inhomogeneities which are promising for creating new generation memory cells.

A uniform electric field in the case under consideration does not affect the distribution of magnetization. Therefore, it is assumed that the field is central and the sample is a punctured disk, so that the system has cylindrical symmetry. In a film with such a geometry, various magnetic structures can be formed, the topology of which is characterized by the number k of turns made by the magnetization vector when going around the puncture clockwise. Let the IMEI constants b_1 and b_2 be equal to each other to begin with. Then, when the central field is turned on, the magnetization distribution corresponding to a certain k value will also not be affected, but the ground state of the system may change. Namely, the value k corresponding to the global energy minimum will change abruptly in proportion to the voltage applied to the disk boundaries. The calculations show that the only configuration of the electric field in which the ground state of the system does not depend on the size of the sample is the field of the charged filament. Thus, the field of a charged filament is the optimal way to control the topology of the magnetic structure in an arbitrary-shaped film, including an unbounded flat film with a negligibly small hole. Further, fields of only such a configuration are considered.

If the values of the IMEI constants differ ($b_1 \neq b_2$), then the influence of the field distorts the distribution of magnetization. This also applies to homogeneous distribution ($k = 0$), in the case of which the amplitude of the angle of deviation of the magnetization vector from the initial direction is approximately $\gamma q/4$, where $\gamma = 1 - b_1/b_2$ and q is the unitless quantity proportional to the charge density of the filament. The paper also obtained exact expressions describing the spatial distribution of the magnetization vector for structures of all possible topologies.

The diagram in the Fig. 1 shows the k values corresponding to the ground state of the system, depending on the q and γ values. The blue region in the figure corresponds to $k = 0$, the red regions correspond to $k = 1$, the green and purple regions correspond to even and odd $k > 1$, and the pink and yellow regions correspond to even and odd $k < 0$. It is easy to see that for an arbitrary fixed $\gamma < 0$, the dependence of k on q turns out to be monotonically increasing. However, for large fixed $\gamma > 0$, the opposite situation is observed. At $\gamma = 2$ only two topologically nonequivalent states can be stable: $k = 0$ and $k = 1$. In this case, the states with $k = 1$, observed at opposite values of q, will in fact correspond to different magnetization distributions, since the structure will be of Bloch type at $q > 0$ and of Neel type at $q < 0$.

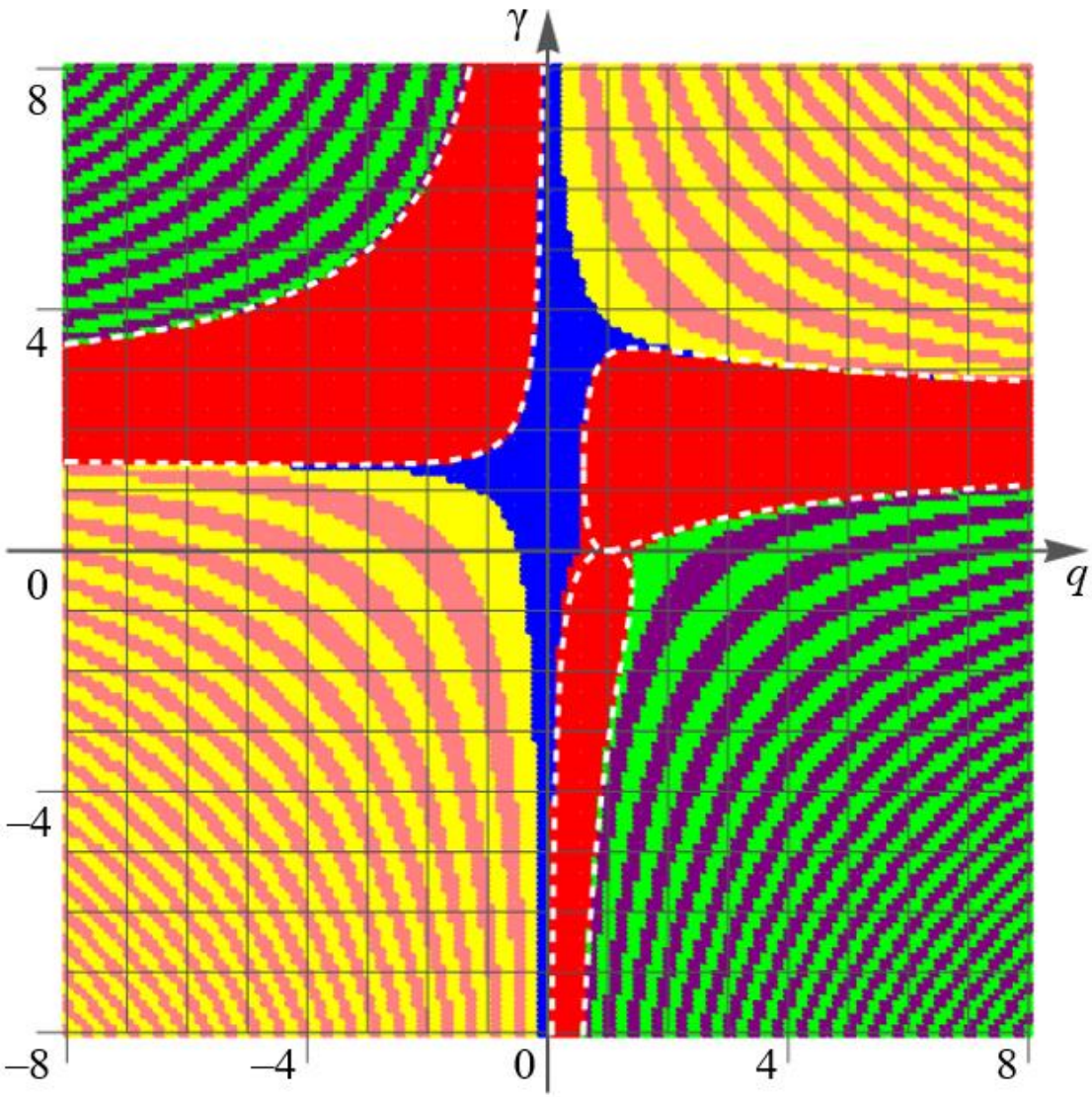

Fig. 1. Diagram of stable states of a flat magnetic structure

Thus, in the general case, a structure with an arbitrary predetermined k value can be obtained by the influence of the field of a filament having a certain charge density. The exception is a narrow area in which $\gamma \approx 2$, i.e., sum $b_1 + b_2$ takes small values. Here, under condition $|q| > 0.58$, only the structure corresponding to $k = 1$ is stabilized. Note that the boundary of the red region in the Fig. 1, in which $k = 1$ represents the ground state of the system, can be approximately described by the following expression:

$$(2 + (\gamma - 2)q)^2 < \frac{32}{\pi^2}|\gamma q|.$$

The result of using this expression is shown in the figure with a white dashed line.

References

[1] E.B. Magadeev, R.M. Vakhitov. JETP Letters. 115, 123 (2022).
[2] E.B. Magadeev, R.M. Vakhitov, R.R. Kanbekov. JETP. 162 (9), 417 (2022).
[3] E.B. Magadeev, R.M. Vakhitov, R.R. Kanbekov. J. Phys.: Condens. Matter. 35, 015802 (2023).

AP2-8P/1

Effect of unintentionally doping on internal friction and functional properties of gallium oxide single crystals

Panov D.Yu.[1], Kalganov D.A.[1], Bauman D.A.[1], Romanov A.E.[1,2]

[1]*ITMO University, 197101, Saint-Petersburg, Russia*
[2]*Ioffe Institute, 194021, Saint Petersburg, Russia*
kalganov@itmo.ru

Gallium oxide (Ga_2O_3) is a compound semiconductor with a wide band gap of about 4.9 eV for the most stable β-phase of Ga_2O_3 and high breakdown electric field of more than 8 MV/cm [1]. These properties make Ga_2O_3 a promising material for use in UV detectors, power electronics, and other applications [2]. The method of edge defined film-fed growth very promising for fabricating β-Ga_2O_3 single crystals of the controlled shape [3]. Depending on the purity of raw materials and conditions of the growth process, such as the composition of the atmosphere, material of the crucible, shaper and seed, various impurities can be incorporated in the single crystal and affect the defective structure of the material and its functional properties.

(a)  (b) 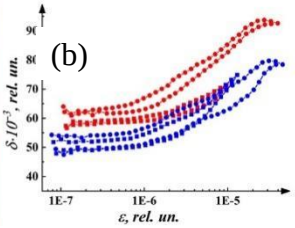

Fig. 1. Gallium oxide bulk and samples photo (a), internal friction in various samples (b) before – circle and after annealing

We studied β-Ga_2O_3 single crystals fabricated by the edge-defined film-fed growth. Samples for X-ray diffraction, electron microscopy, internal friction study and other measurements were cut with a diamond saw (Fig 1-a). To determine the internal friction, which characterizes the motion and interaction of crystal lattice defects, the resonant method with an oscillation frequency of 100 kHz was used.

In the studied samples, the internal friction at low amplitudes was mainly affected by twin structures in the $(\bar{2}01)$ plane and the interaction of dislocations with vacancies in the {101} plane system (Fig. 1-b). With an increase in the deformation amplitude to 10^{-6} and higher, the interaction of dislocations in other slip systems with impurity atoms (Si, Ir) was observed, which can be interpretated by the pinning theory.

The research was supported by the Ministry of Science and Higher Education of the Russian Federation (agreement no. 075-15-2021-1349).

References

[1] S. Stepanov, V. Nikolaev, V. Bougrov, and A. Romanov, Rev. Adv. Mater. Sci. 44, 63-86 (2016)
[2] J. Yang, K. Liu, X. Chen, et.al., Prog. Quantum. Electron. 83, 100397 (2022).
[3] D.A. Bauman, D.I. Panov, D.A. Zakgeim, et.al., Phys. Status Solidi (A) 218, 2100335 (2021).

AP2-8P/2

Magnetic and optical properties of epitaxial $(YBiCa)_3Fe_5O_{12}$ films on paramagnetic substrate in a wide temperature range

Nadezhda E. Kupchinskaya[a], Sergey N. Polulyakh[b], Alexander S. Pakhomov[c], Fedor M. Maksimov[a,c], Vladimir N. Berzhansky[b], Vladimir I. Belotelov[a,c],Alexander I. Chernov[a,c]

[a] *Center for Photonics and 2D Materials, Moscow Institute of Physics and Technology (National Research University), Moscow, Russia*
[b] *V.I. Vernadsky Crimean Federal University, 295007 Simferopol, Russia*
[c] *Russian Quantum Center, 121205 Moscow, Russia*
nadezhda-kupchin@mail.ru

In recent decades, iron garnets have been the subject of extensive fundamental research [1, 2]. As a result, a huge range of exotic and useful physical properties at room temperature, such as low magnetic attenuation [3-4] and high magneto-optical (MO) Faraday activity [5], was discovered, which opened up prospects for their technological application. Iron garnets continue to find applications in condensed matter physics, in particular, they are used in spintronics for storing and processing data using spin waves (SW). Weak damping of spin waves in the material is a key characteristic for applications, which often occurs due to the substrate, which carries its own magnetic moment, increasing with decreasing temperature. In this work we perform the epitaxial growth of $(YBiCa)_3Fe_5O_{12}$ film on non-magnetic YSGG substrate and demonstrate the improved damping properties at low temperatures. We obtain the Faraday rotation dependence on temperatures from 300 K to 6 K and the temperature dependences of the resonant field succeed by fferromagnetic resonance (FMR) and the Faraday rotation angle are similar. The increase of the Faraday rotation at around 60 K is found, which has been explained by the rearrangement of the iron garnet magnetic structure, namely, the angle of the magnetic moment relative to the axes of the of the crystal.

A $(YBiCa)_3Fe_5O_{12}$ film 2100 nm thick was investigated by ferromagnetic resonance (FMR) using a vector network analyzer. The spectra were obtained as a series of sweeps over the field with fixed frequencies. The sample was placed on a coplanar waveguide attached to the cold finger of the cryostat. The response of the system was studied by analyzing the transmitted microwave signal S21 (Fig. 1a). An external magnetic field was applied perpendicular to the sample plane.

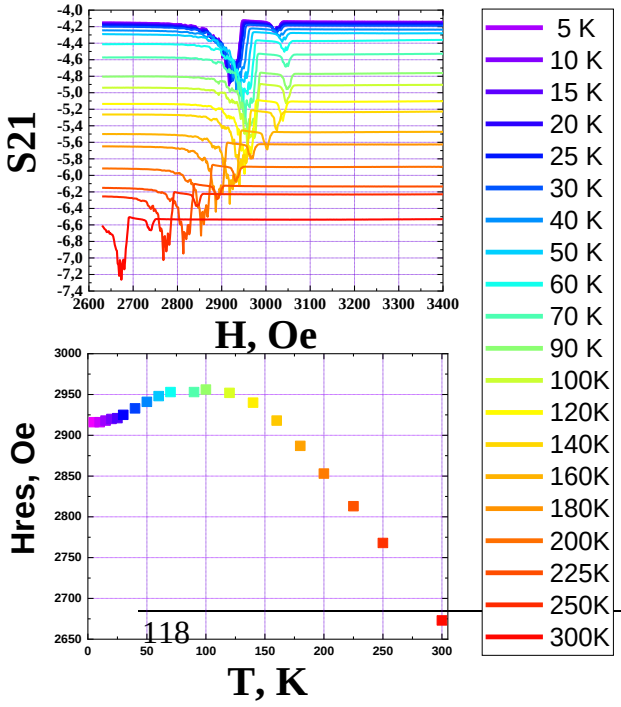

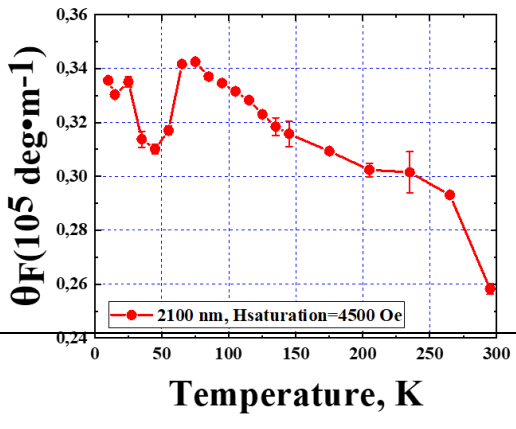

Fig.1 a) Dependence of normalized S_{21} parameter for $(YBiCa)_3Fe_5O_{12}$ on temperature for 2100 nm thick film at 4 GHz in the out-of-plane configuration. b) Dependence of the resonance peak position on temperature. c)Temperature dependence of the FMR spectrum linewidth $(YBiCa)_3Fe_5O_{12}$ 2100 nm thick

The linewidth in the FMR varies slightly in the temperature range 10–280 K, as well as the temperature dependence of the resonance field (Fig. 1b). For these temperatures, under similar conditions, the Faraday rotation of this sample was studied (Fig.1, c). In the experiment, a laser with a wavelength of 660 nm and a power of 120 mW was used, the beam passed through a polarizer and a Wollaston prism, crossed at an angle of 45°, the field switched from -4500 Oe to 4500 Oe, which is higher than the saturation field of the sample. In this case, the magneto-optical response was recorded using a balanced detector. $(YBiCa)_3Fe_5O_{12}$ showed high values of the Faraday rotation angle, which makes it a promising material for spintronic applications.

In this work we found relatively large low temperature Faraday rotation of the iron garnet $(YBiCa)_3Fe_5O_{12}$ films epitaxially grown on the Gd free YSGG substrate. Such Faraday angle values given by this material can be used in basic research and further applications. Elimination of the magnetic substrate for the epitaxial growth provides the new material that can be used in fundamental studies and further in applications. The films demonstrate only a slight increase in the FMR linewidth for lower temperatures from 22 to 36 Oe and can be used in magneto-optics since the Faraday effect is relatively large. The maximum specific Faraday rotation value reaches $\theta F = 0.34 \bullet 103$ deg/cm . Moreover, we reveal the similarities and temperature dependent behavior of the FMR and Faraday rotation. The obtained results demonstrate the potential of the magnetic films for applications at low temperatures and including ones, requiring the magneto-optical response.

References

[1] Hansen P., Krumme J.-P. Magnetic and magneto-optical properties of garnet films // Thin solid films Volume 114, Issues 1–2, 13 April 1984, Pages 69-107.
[2] Willoughby A., Capper P., Kasap S. Spintronics for Next Generation Innovative Devices // Wiley, Hoboken, NJ, 2015.
[3] Marwan D., Popova E., Hehn M.,et al. Damping of Standing Spin Waves in Bismuth-Substituted Yttrium Iron Garnet as Seen via the Time-Resolved Magneto-Optical Kerr Effect // Phys. Rev. Appl. 12, 2019
[4] Houchen Ch., Peng Li, Nanometer-Thick Yttrium Iron Garnet Films With Extremely Low Damping / Magn. Lett., Volume 5, 2014.
[5] Shaposhnikov A.N., Prokopov A.R. Magnetooptics of single and microresonator iron-garnet films at low temperatures // Opt. Mat. February, Pages 21-25, 2016.

AP2-8P/3

Influence of temperature on the structure of α-Fe2O3 thin films

Merencova K.A.[1], Korkh Yu. V.[1], Kuznetsova T.V.[1,2], Nosov A.P.[1], Dubinin S.S.[1]

[1]Mikheev Institute of Metal Physics, UB RAS, 620108, Ekaterinburg, Russia
[2]Ural Federal University named after the First President of Russia B.N. Yeltsin, 620002, Ekaterinburg, Russia
merencovak@imp.uran.ru

Hematite ($\alpha - Fe_2O_3$) is one of the best known iron oxides widely found in rocks. Studies of the magnetic properties of hematite have been conducted for over half a century. However, the objects of these studies were mainly bulk materials (mono- and polycrystals). Hematite has unique magnetic characteristics: it is antiferromagnetic below the Morin temperature, "weak" ferromagnetic in the range from Morin to the Niels temperature and paramagnetic above the Niels temperature [1].

In recent decades, multilayer and nanoheterostructures with hematite layers have been in demand in modern nanospintronics applications.

The aim of this work was to obtain $\alpha - Fe_2O_3$ thin films on single-crystal sapphire ($c - Al_2O_3$) substrates and to study the effect of temperature treatment on their structure by X-ray diffraction analysis, Raman spectroscopy and magnetic force microscopy.

Thin films of $\alpha - Fe_2O_3$ were obtained by AC magnetron sputtering of a stoichiometric solid-phase synthesis target in an atmosphere of 90%Ar + 10%O2. During the sputtering process the substrate temperature was 473 K. Sputtering occurred at a rate of 0.43 nm/min. After sputtering, the obtained films with typical dimensions of 15*11 mm were cut into samples of size ≈4.5×4.5 mm^2, each of which was heat-treated in air for 3 hours in the temperature range 673 - 1173 K.

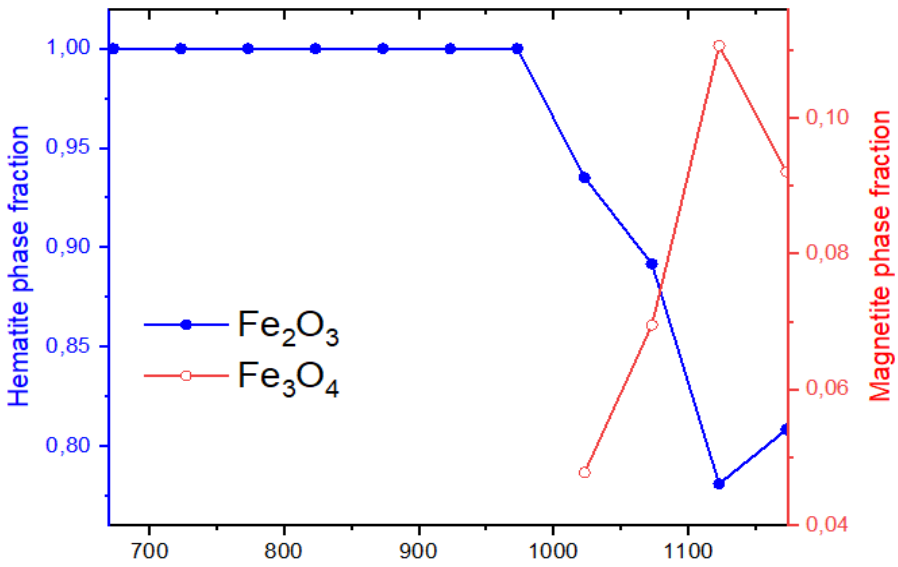

Fig. 1. Dependence of the phase composition of α-Fe_2O_3 films 100 nm thick on the heat treatment temperature

X-ray diffraction study (Fig.1) showed that up to 973 K the samples are single-phase (only $\alpha - Fe_2O_3$ phase is present), and from 1023 K an additional magnetite phase Fe_3O_4 occurs in the samples

According to the data of Raman spectroscopy (after decomposition of lines of complex composition on separate components), presented on Fig. 2, in

all samples there are spectral lines, characteristic for $\alpha - Fe_2O_3$ [2]. In the spectra of samples heat-treated at temperatures 1023, 1073, 1123, 1173 K there are lines characteristic of Fe_3O_4.[3]

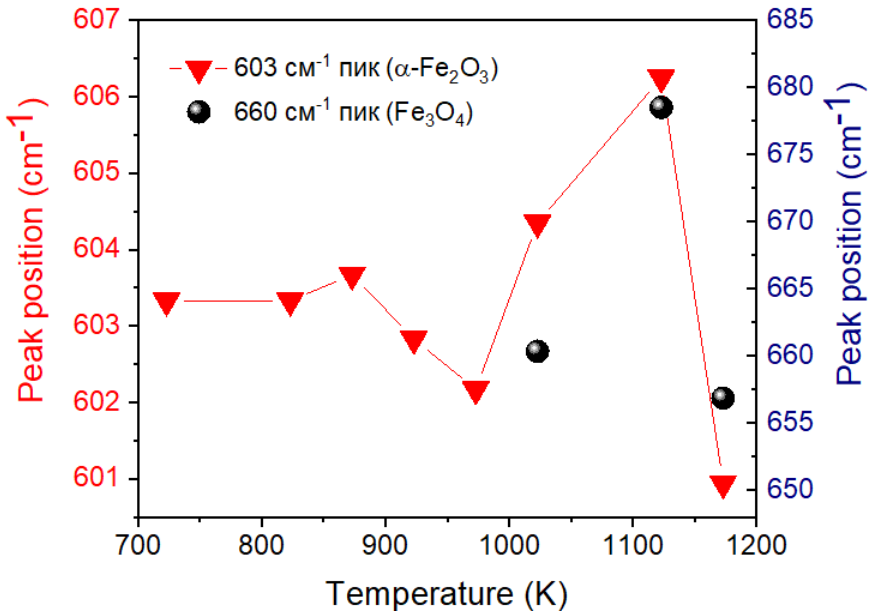

Fig. 2. Position of the maxima of the individual lines as a function of processing temperature.

Magnetic force microscopy revealed that for samples heat-treated up to 973 K, the observed signal distributions are difficult to identify as belonging to the domain structure of antiferromagnetics. Beginning at 1023 K, blurred images appear, which become clearer and more contrasting with increasing heat treatment temperature, and can be identified as corresponding to the ferromagnetic component Fe_3O_4

This work was carried out within the framework of the state assignment of the Ministry of Science and Technology of the Russian Federation (subject "Function", state registration number 122021000035-6)..

References

[1] I. Dzyaloshinsky, JETP. 32,1547 (1957).
[2] M. Giarola, G. Mariotto and D. Ajò, Raman Spectrosc. 43, 556 (2012).
[3] C. Guo, Y. Hu and H. Qian, Mater. Charact. 62, 148 (2010).

AP2-8P/4

Magneto-optical Ellipsometry of Thin Films with Optical Uniaxial Anisotropy

Maximova O.A.[1,2], Lyaschenko S.A.[1], Varnakov S.N.[1], Yakovlev I.A.[1], Shevtsov D.A.[1], Andryushchenko T.A.[1], Ovchinnikov S.G. [1,2]

[1] *Kirensky Institute of Physics, Federal Research Center KSC Siberian Branch Russian Academy of Sciences, 660036, Krasnoyarsk, Russia*
[2] *Siberian Federal University, 660041, Krasnoyarsk, Russia*
maximo.a@mail.ru

Magneto-optical ellipsometry [1] is a sensitive technique for characterizing samples that combines classical ellipsopmetry and the transverse magneto-optical Kerr effect measurements.

Here we report that the inverse problem of magneto-optical ellipsometry has been solved using the model of a single-layer medium with uniaxial optical anisotropy, taking into account the magneto-optical response without taking into account effects that are quadratic in magnetization. Mathematical expressions have been found for the reflection coefficients and transmission coefficients for the interface between the external medium and the sample and the sample-substrate interface. The refractive indices of an anisotropic structure in the plane of the sample and perpendicular to it are proposed to be obtained on the basis of multi-angle ellipsometric measurements within the framework of the same experiment. As a result, all the necessary algorithms for the analysis of optically anisotropic thick MAX films [2] and films of finite thickness by magneto-optical ellipsometry have been created. It is shown that for thick films described by the model of a semi-infinite medium, it is possible to calculate the complex magneto-optical parameter Q and the components of the permittivity tensor analytically, while for a thin-film medium it is necessary to calculate them by numerical methods.

This work was supported by the grant from the Russian Science Foundation No. 21-12-00226, http://rscf.ru/project/21-12-00226/

References

[1] O. Maximova, S. Lyaschenko, I. Tarasov, et al., Physics of the Solid State, 63, 1485–1495 (2021). DOI: 10.1134/S1063783421090274

[2] S. Lyaschenko, O. Maximova, D. Shevtsov, et al., JMMM, 528, 167803 (2021). https://doi.org/10.1016/j.jmmm.2021.167803

AP2-8P/5

Theoretical and experimental study of the two-sublattice iron garnet system with the magnetization compensation point in a two-dimensional magnetic field

Prisyazhnyuk A.V.[2], Gusev N.A.[1,2], Ignatyeva D.O.[1,2,3], Polulyakh S.N.[2], Zvezdin A.K.[1,4], Berzhansky V.N.[2], Belotelov V.I.[1,2,3]

[1] *Russian Quantum Center, 121205, Moscow, Russia*
[2] *Vernadsky Crimean Federal University, 295007, Simferopol, Russia*
[3] *Lomonosov Moscow State University, Moscow, 119991, Russia*
[4] *Prokhorov General Physics Institute of the Russian Academy of Sciences, 119991, Moscow, Russia*

Despite the fact that the studies of the temperature dependence of the magnetization of ferrimagnetic films and the corresponding temperature effects have attracted the attention of researchers since the middle of the last century [1]. At the same time, the interesting theoretical approach for such problems, named quasi-antiferromagnetic approximation, was proposed by A.K. Zvezdin [2]. The approach consists in reducing the four angular spherical coordinate variables (θ_1,φ_1 and θ_2,φ_2) of the magnetization vectors $\mathbf{M_1}$ and $\mathbf{M_2}$ of the sublattices of a two-sublattice magnetic system to the two angular spherical coordinate variables (θ and φ) of the aniferromagnetic vector **L**.

This approach makes one possible to obtain the Lagrange function of a two-sublattice system, written in terms of the angles θ and φ of the antiferromagnetic vector, to calculate the Lagrange equations and the linearized equations of small oscillations of the angles, which describe the precession of the vector **L** at different temperatures, in magnetic fields of the different magnitudes and the different spatial configurations, taking into account the antisotropy type of "easy axis" or "easy plane". The study of the energy function gives the equilibrium states of a two-sublattice system depending on the temperature, which are divided into two large groups: the **L** vector is parallel to the line along the applied magnetic field **H**, and at an angle to it. The first group of states can be called a collinear phase, and the second - a non-collinear one. The transition between them can be considered as a second-order phase transition, similar to the transition between the paramagnetic and ferrimagnetic states.

This report focuses on the describtion the statics of the antiferromagnetic vector of a two-sublattice iron garnet film in the collinear and non-collinear phases by the quasi-antiferromagnetic approximation and comparing this description with the experimental results. Based on this theory, a rare-earth ferrite-garnet phase diagram was constructed near the compensation point. The description of the behavior of a two-lattice system in a two-dimensional magnetic field is also shown, which is consistent with the experiment.

This work was supported by a grant from the Russian Science Foundation No. 19-72-20154, https://rscf.ru/project/19-72-20154/.

References

[1] S. Geschwind, and L. R. Walker. J. Appl. Phys. 30.4 (1959): S163-S170.
[2] M.D. Davydova et al. J. Phys.: Cond. Matt. 32.1 (2019): 01LT01.

AP2-8P/6

Nanocomposite thin-film structures and sensors based on them

R.B. Salikhov, A.D. Ostaltsova, T.R. Salikhov

Ufa University of Science and Technology, Ufa, Russia
salikhovrb@yandex.ru

The article is devoted to the study of nanocomposite thin films based on a polyelectrolyte complex of chitosan and chitosan succinamide (PEC). Single-walled carbon nanotubes (SWCNTs) were used as fillers. In a select few among many people, activity was detected on an ordinary area of skin. Another important advantage of natural materials is the possibility of the natural emergence of new materials and technologies for their production by selecting raw materials, their ratio in the raw mixture, called composition, and technological parameters. In the field of nanotechnology, one of the most popular scientific research is the study of polymer nanocomposites and the field of research on a wide range of topics: nanoelectronics and polymeric bionanomaterials [1–3].

Using the scanning electron microscope (SEM) TESCAN MIRA LMS and the TESCAN Essence software, images of the surface of the Indian polymer PEC and PEC-SWCNT-3 were obtained (Fig. 1a,b).

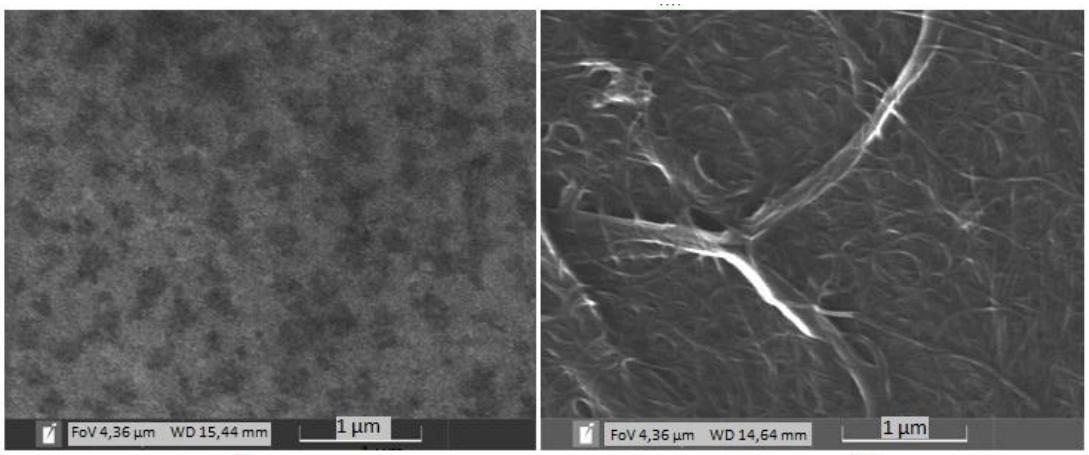

Fig. 1. SEM images of microstructures of film samples a) PEC b) PEC-SWCNT

.

In contrast to the surface of pure PEC, the surface of the nanocomposite structure of PEC with SWCNT is covered with formations in the form of filaments. It can be assumed that these filaments are complex formations formed by carbon nanotubes.

Using the methods of cyclic voltammetry and electrochemical impedance spectroscopy, it was found that nanocomposite films have a larger effective surface area and electron transfer rate compared to PEC films, which allows them to be further used in the electroanalysis of substances of various nature. It was found that the optimal content of SWCNT in PEC mg/ml. The PEC-SWCNT nanocomposite is stable for 5 days.

The research was funded with the support of a state assignment (code FZWU-2023-0002)

References

[1] A. G. Mustafin, L. R. Latypova, A. N. Andriianova, S. M. Salikhov, A. F. Sattarova, I. N. Mullagaliev, I. B. Abdrakhmanov, Macromolecules. V. 53(18), 8050-8059 (2020)

[2] A. G. Mustafin, L. R. Latypova, A. N. Andriianova, I. N. Mullagaliev, S. M. Salikhov, R. B. Salikhov, G. S. Usmanova, RSC advances. V. 11(34), 21006-21016 (2021)

[3] R. B. Salikhov, R. A. Zilberg, E. O. Bulysheva, A. D. Ostaltsova, T. R. Salikhov, Yu. B. Teres, Letters on Materials. V. 13 (2), 132-137 (2023)

AP2-8P/7

CNT-Epoxy based transistor: fabrication and application

Yumalin T.T., Salikhov R.B.

Ufa University of Science and Technology, 450076, Ufa, Russia
timur-sibay@mail.ru

Carbon nanotubes (CNTs) have found wide applications in various fields due to their unique mechanical, functional, and electronic properties. They are used in electronics, mechanical engineering, medicine, and construction thin films offer prospects for creating ultrathin and flexible electronic devices with enhanced electrical properties, energy efficiency, and versatility.

Glass coated with indium tin oxide (ITO) served as the substrate material for the fabrication process. An AlOx solution was applied onto the substrate using a centrifuge, followed by a heating step in an oven for 60 minutes, resulting in a gate dielectric layer with a thickness of 100 nm. The contact pads were generated by thermally spraying aluminum under vacuum conditions. The architecture of the resulting transistor can be observed in Figure 1.

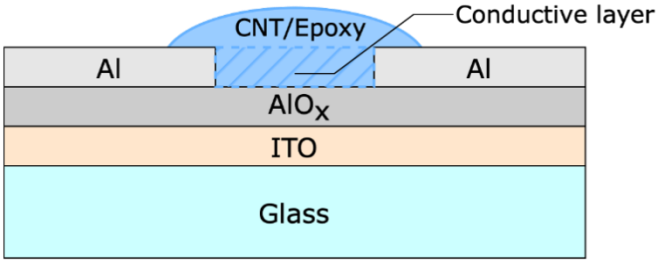

Fig. 1. Structure of a thin film transistor based on an epoxy mixture of CNTs.

The conductivity level can be adjusted by varying the concentration of the epoxy mixture. As previously mentioned, the concentration of CNTs in the mixture was approximately 0.3% by weight. Mobility calculations based on voltampere characteristics revealed a value of 28.87 $cm^2/V \cdot s$ at UDS = 12V. The utilization of such thin-film transistor-based devices can be desirable in energy-efficient solutions or IoT applications, where compact dimensions and low power consumption need to be combined with flexible properties [1-2].

This publication is based on support by the State assignment for the implementation of scientific research by laboratories (Order MN-8/1356 of 09/20/2021).

References

[1] Salikhov, T.R., Abdrakhmanov, V.K., & Yumalin, T.T. (2021). In Proceedings of the Conference "2021 International Conference on Electrotechnical Complexes and Systems (ICOECS)" (pp. 500-503)
[2] Salikhov, R.B., Abdrakhmanov, V.K., & Yumalin, T.T. (2021). In Proceedings of the Conference "2021 International Ural Conference on Electrical Power Engineering (UralCon)" (pp. 229-233).
[3] Tuktarov A. R., Salikhov R. B., Khuzin A. A., Safargalin I. N., Mullagaliev I. N., Venidiktova O. V., Valova T. M., Barachevsky V. A., Dzhemilev U. M. Mendeleev Communications. V. 29. № 2. p. 160-162. (2019).

AP2-8P/8

Inelastic Electron Scattering Cross Section Spectroscopy of SiO_2/Si(111) Structures

Parshin A.S.

Reshetnev Siberian State University of Science and Technology, 660037, Krasnoyarsk, Russia
aparshin@sibsau.ru

The SiO_2 layer of 50 nm thick was formed by thermal oxidation of Si(111) substrate in an atmosphere of dry oxygen at a temperature of 1075 ºC. The reflection electron energy loss spectra (REELS) were obtained in the integral form using a SPECS spectrometer at incident electron energies E_0 of 300 eV in the electron energy loss range from 0 to 150 eV with a step of 0.1 eV. From the experimental REELS with the software package QUASES^{TM} XS REELS [1] were calculated inelastic electron scattering cross section spectra which are products of inelastic mean free path λ and inelastic scattering cross-section $K(E_0, T)$, were T – energy loss. The energy positions of the peaks in the λK-spectra determine the probabilities of electron energy losses over the inelastic mean path per unit energy.

The small mean free path of electrons in silicon dioxide at an energy of 300 eV (1.26 nm) in comparison with the film thickness (~5 nm), which determines the depth of analysis of the surface layer, allows one to carry out a layer-by-layer analysis of atomic concentrations by the REELS with the successive removal of surface layers by etching with argon ions. The figure shows the results of measurements of the λK_{max} value versus the time of etching with Ar^+. The initial decrease in λK_{max} is associated with the removal of surface carbonaceous impurities. The value for an etching time of 5 min corresponds to the value for silicon dioxide. With further etching, λK_{max} increases monotonically, which corresponds to a gradual increase in the fraction of silicon with the depth of analysis, up to a value of approximately 0.71 eV^{-1}, corresponding to the signal from the substrate.

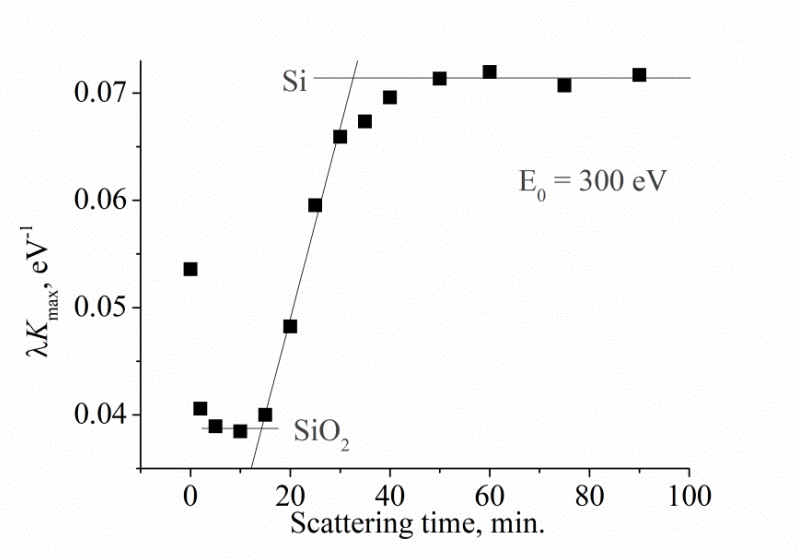

The results obtained indicate a high sensitivity of the inelastic electron scattering cross section spectroscopy to the presence of silicon oxide at the interface of the structure under study.

The work was done using the equipment Krasnoyarsk regional center of collective FRC KSC SB RAS.

References

[1] S. Tougaard, http://www.quases.com.

AP2-8P/9

Features of the fractal relief of nanosized iron films

Antonov A.S.[1], Ivanov D.V.[1], Semenova E.M.[2], Ivanova A.I.[3], Sdobnyakov N.Yu.[1]

[1]*General Physics Department, Tver State University, 170002, Tver, Russia*
[2]*Department of Condensed Matter Physics, Tver State University, 170002, Tver, Russia*
[3]*Applied Physics Department, Tver State University, 170002, Tver, Russia*
Sdobnyakov.NY@tversu.ru

Following our previous works [1, 2], we continue to study the behavior of the fractal dimension for metal nanoscale films. In [1] the patterns of formation of the fractal relief of nanosized iron films on the mica surface are considered using the atomic force microscopy. It has been established that magnetron sputtering makes it possible to obtain island films of iron, the structural element of which are truncated nanocubes – nanopyramids. The fractal dimension of the resulting agglomerates was determined at various scales: on a scale of 5 μm D_c = 2,462±0,113; on a scale of 3 μm D_c = 2,373±0,122; on a scale of 1 μm D_c = 2,298±0,139.

However, in this work, an attempt is made to determine the fractal dimension more precisely. The resulting image of the surface of island films of iron (see Fig. 1) on mica was divided by us into 9 nested big squares (size 1 μm), which in turn had 1 nested small square (size 0,33 μm). Accordingly, the calculated parameters were determined for each region separately. A non-regular distribution of fractal structures over the sample surface was established. The maximum value of the fractal dimension D_c of individual squares is 2,54, the minimum is 2,25. At the same time, on each of the 9 nested big squares, the self-similarity of structures was recorded with good accuracy, as a rule, not exceeding 0,03.

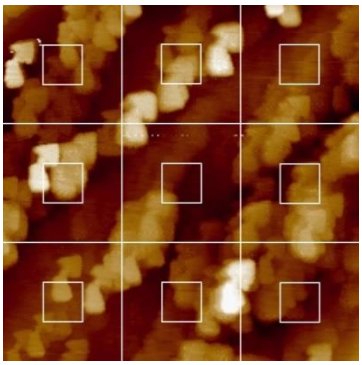

Fig. 1. Images of island films of iron on mica at a scale of 3 μm with selected areas for calculating the fractal dimension

The work was supported by the Ministry of Science and Higher Education of the Russian Federation in the framework of the State Program in the Field of the Research Activity (project no. 0817-2023-0006).

References

[1] D.V. Ivanov, A.S. Antonov, E.M. Semenova et al., Phys. Chem. Asp. Study Clust. Nanostr. Nanomat. 14, 108 (2022). (In Russian).
[2] D.V. Ivanov, A.S. Antonov, E.M. Semenova et al., J. Phys.: Conf. Ser. 1758, 012013 (2021).

AP2-8P/10

The fractal dimension behaviour of the domain patterns in ferrite-garnet films

Zigert A.D.[1], Dunaeva G.G.[2], Semenova E.M.[2], Kuz'min N.B.[1,3], Sdobnyakov N.Yu.[3]

[1]*Applied Physics Department, Tver State University, 170002, Tver, Russia*
[2]*Department of Condensed Matter Physics, Tver State University, 170002, Tver, Russia*
[3]*General Physics Department, Tver State University, 170002, Tver, Russia*
Sdobnyakov.NY@tversu.ru

Previously, in [1], the investigation of the behaviour in the fractal dimension (FD) dependence obtained on the basis of the analysis of magneto-optical images of ferrite-garnet (FG) films was carried out. In this work, we study the effect of the film composition on the field dependence of the FD. Images of the domaSdobnyakovin structure in an external changing magnetic field were obtained by optical magnetometry. For such images, the relative magnetization and FD values were determined according to the procedure [2]. The fractal analysis (FA) was carried out for three different uniaxial FG films: $(GdBiLu)_3(FeGa)_5O_{12}$ has a thickness of 25 μm (A), $(GdBiLu)_3(FeGa)_5O_{12}$ 6 μm (B) and $(GdBiLuSm)_3(FeGa)_5O_{12}$ 42 μm (C) respectively. Film A has a similar maze-like domain structure with the film studied in [1], and the results of FA as a whole completely correlate with the results of this work. Films B (see Fig. 1 left) and C have a maze-like domain structure that differs from film A. The curves of the FD dependence on the coercive field obtained for B and C films are consistent with each other, but differ from film A. In particular, film A is characterized by a dome-shaped dependence of the FD on the coercive field, while for films B and C, the branches of the graph are straight lines (see Fig. 1 right). However, the maximum FD values obtained for films B and C match the values obtained for A.

Fig. 1. Magneto-optical image of the domain structure for the FG film $(GdBiLuSm)_3(FeGa)_5O_{12}$ (left) and field dependence of the FD value (right)

The authors express their sincere gratitude to Prof. V.N. Berzhansky (V.I. Vernadsky Crimean Federal University) for samples of ferrite-garnet films. The work was supported by the Ministry of Science and Higher Education of the Russian Federation in the framework of the State Program in the Field of the Research Activity (project no. 0817-2023-0006).

References

[1] A.D. Zigert, G.G. Dunaeva, E.M. Semenova et al., J. Supercond. Nov. Magn. 35, 2187 (2022).
[2] A.D. Zigert, G.G. Dunaeva, N.Yu. Sdobnyakov, Phys. Chem. Asp. Study Clust. Nanostr. Nanomat. 13, 134 (2021). (In Russian).

AP2-8P/11

The Model of Plasma Etching Using a Spherical Mask

Syrov A.A., Tomilin S.V., Berzhansky V.N.
Institute of Physics and Technology, V.I. Vernadsky Crimean Federal University,
Vernadsky avenue, 4, Simferopol, Russia
anatoly199824@rambler.ru

Modern trends in the development of forensics, defectoscopy, magnetocardiography, and magnetoencephalography set fundamentally new problems that require significant improvements in the parameters and characteristics of highly sensitive magnetic field sensors based on iron-garnet films doped by rare-earth elements [1,2]. The fabrication of film edge smooth profile closed to ellipsoidal by ion etching decreases the influence of edge domains and increases the sensitivity of the film disk sensor.

In this research work the model of non-homogeneous ion-plasma etching using a mask of spherical radius R (Fig. 1,a) is observed. In different areas of the sample argon ions take a different energy Q when they pass a different distances δ accelerating in the field in the gap between a working surface and a spherical mask during a high frequency etching. The rate of sputtering of the target by accelerated argon ions $v(x)$ can be described by Arrhenius equation (probability of activation):

$$v(x) = v_{Q>>W} \exp\left(-\frac{W}{Q}\right), \qquad (1)$$

where W is the output energy, $v_{Q>>W}$ is sputter rate under the condition $Q >> W$.

Fig. 1b demonstrates good agreement between the considered model (dashed line) and the experimentally obtained etch profile. The specific symmetrical protrusions, observed at a distance of about 3 mm from the center of the mask, were formed as a result of redeposition of the sputtered film material and contain an amorphous condensate of garnet-forming oxides.

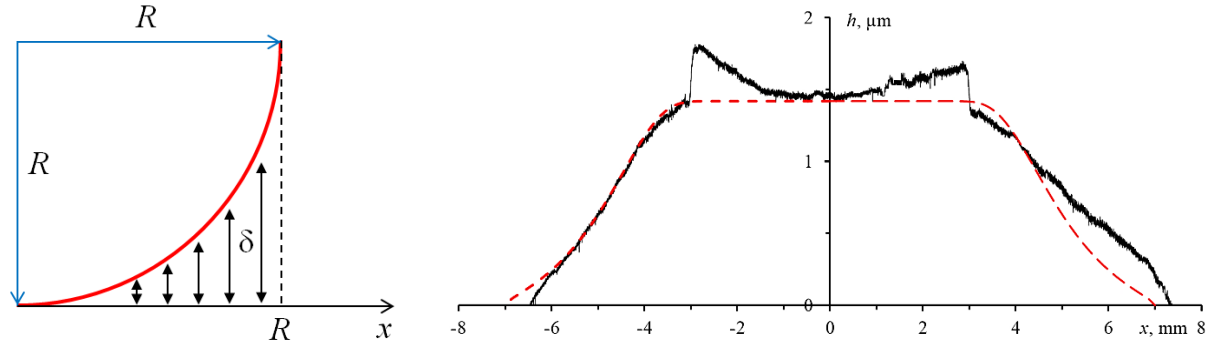

a b

Fig. 1. Ion-plasma etching using a spherical mask:
a – etching scheme, b – profile of the etched surface
(dashed line – calculation model, solid line-experiment).

This work was financially supported by the grant of State Council of Crimean Republic (resolution № p653-2/23 from 30.01.2023).

References

[1] J. Qin, L. Deng, J. Xie, T. Tang, L. Bi. AIP Advances. V. 5. P. 017118 (2015)

AP2-8P/12

Magnetic characteristics of a nanocomposite based on natural polymineral layered aluminosilicates doped with FexOy

Dubas V.V.[1], Aleksashkin I.V.[2], Semuk E.Yu.[3], Polulyakh S.N.[3]

[1] *A.O. Kovalevsky Institute of Biology of the Southern Seas of RAS, Nakhimov avenue, 2, Sevastopol, Russian Federation*
[2] *T.I. Vyazemsky Karadag Scientific Station – Nature Reserve of RAS – Branch of A.O. Kovalevsky Institute of Biology of the Southern Seas of RAS, Nauki st., 24, Kurortnoe, Feodosia, Russian Federation*
[3] *V. I. Vernadsky Crimean Federal University, Vernadsky avenue, 4, Simferopol, Russian Federation*
sergey.polulyakh@cfuv.ru

The development and creation of new functional materials with desired magnetic properties is one of the most relevant and promising areas of modern materials science. Natural aluminosilicates represented by clays are widely distributed throughout the world, which makes their use as functional carrier matrices for magnetic particles of iron oxides promising. At the same time, nanocomposites based on clay matrices modified with iron oxide have a fairly wide range of applications, as presented in many works [1-4].

For the study of magnetic characteristics, samples of natural clay of a polymineral composition, as well as samples of a composite based on it, are presented. The magnetic composite in its classical form was obtained by coprecipitation of Fe^{2+} and Fe^{3+} salts on a clay matrix (with and without HCl pretreatment) in an aqueous ammonia medium.

Figure 1 shows the FMR spectra, which are characterized for samples 2 and 3 by the presence of one spectral line with a width of about 150–180 mT. For sample 1, which is a natural clay, no response to the applied external magnetic flux is observed, which confirms the absence of ferromagnetic properties in the original samples.

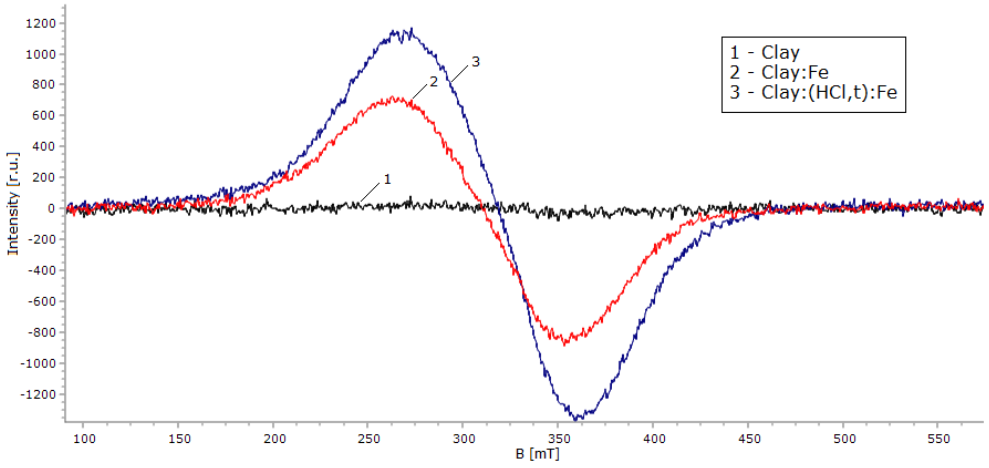

Fig. 1. FMR spectra of samples: 1 – natural polymineral layered aluminosilicate; 2 - natural polymineral layered aluminosilicate alloyed with iron, 3 - natural polymineral layered aluminosilicate, which underwent acid (HCl, 30%) activation and drying at t=100°C, and then alloyed with iron. The magnetic field is oriented parallel to the sample plane.

When natural aluminosilicate is doped with iron, spectral bands appear in the FMR spectrum with maxima at 270 and 360 mT. In this case, the composite that has undergone primary

acid activation exhibits a narrow spectral line of greater intensity in the FMR spectrum, shifted to the region of stronger fields by 5 mT. The use of a non-spherical ferromagnet sample is reflected in the FMR spectrum, which has anisotropy associated, in fact, with the shape of the sample, in the form of asymmetry. Symmetric bands in the FMR spectrum, on the contrary, make it possible to judge the spherical shape of the ferrites in the synthesized composite.

References

[1] A. Awasthi, P. Jadhao, and K. Kumari, Clay nano-adsorbent: structures, applications and mechanism for water treatment. SN Appl. Sci. 1, 1076 (2019).

[2] Y. Jiraskova, J. Bursik, J. Seidlerova, K. Mamulova Kutlakova, I. Safarik, M. Safarikova, K. Pospiskova, O. Zivotsky, Microstructural Analysis and Magnetic Characterization of Native and Magnetically Modified Montmorillonite and Vermiculite, Jour. of Nanomaterials, vol. 2018, 3738106, 14 (2018).

[3] M. Peralta, S. Ocampo, I. Funes, F. Medina, M. Parolo, L. Carlos, Nanomaterials with Tailored Magnetic Properties as Adsorbents of Organic Pollutants from Wastewaters. Inorganics. 8. 24. 10.3390/inorganics8040024 (2020).

[4] L. Chen, C. Zhou, S. Fiore, D. Tong, H. Zhang, C. Li, S. Ji, W. Yu, Functional magnetic nanoparticle/clay mineral nanocomposites: Preparation, magnetism and versatile applications. Applied Clay Science. 127. 10.1016/j.clay.2016.04.009 (2016).

AP2-8P/13

Investigation of the morphology of the surface of films

A.D. Ostaltsova , T.R. Salikhov , R.B. Salikhov
Ufa University of Science and Technology, Ufa, Russia
nastia.ostaltsova@yandex.ru

With the help of a scanning electron microscope (SEM) TESCAN MIRA LMS and the TESCAN Essence software, images of the surface of the studied polymers poly-2-[(2E)-1-methyl-2-butene-1-yl]aniline (1) and poly-2-(cyclohex-2-en-1) were obtained-il)aniline (2) (fig.1). The morphology of surface 2 is ragged, heterogeneous, with large dips in depth, which reduces the surface area available to the molecules of the analyzed gas. The surface 1 has a homogeneous spherical globular structure, which facilitates the access of a large number of gas molecules, compared with 2.

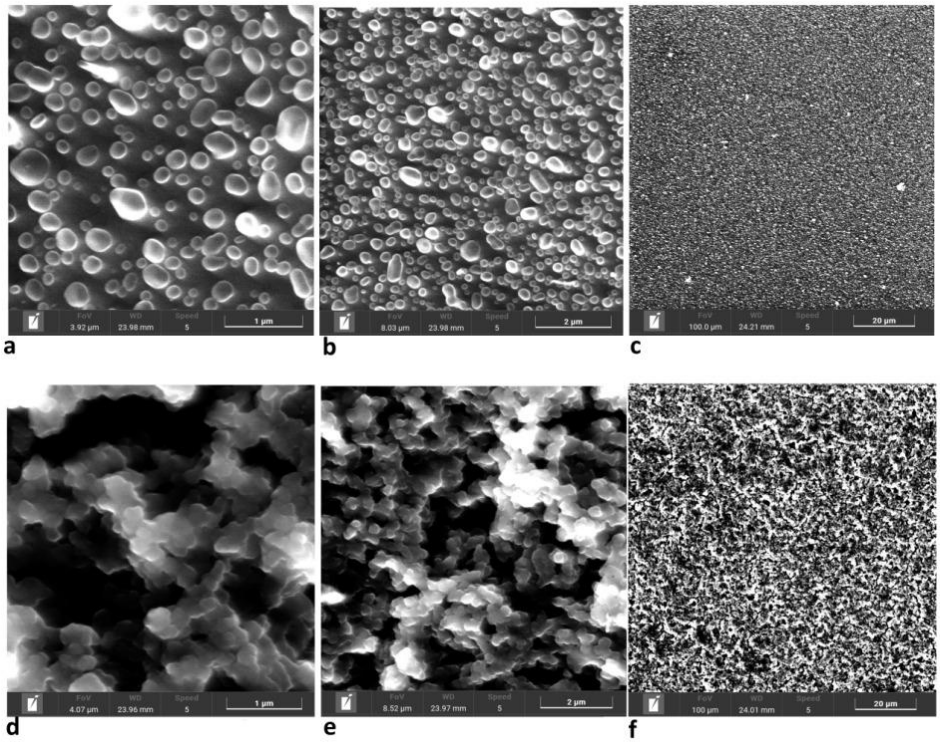

Fig. 1. SEM images of microstructures of film samples. The size of the scanning area of sample P1 (film thickness 500 nm): a – 4 microns, b – 8 microns, c – 100 microns; sample P2 (film thickness 400 nm): g – 4 microns, d – 8 microns, e – 100 microns.

The morphology of surface 2 is ragged, heterogeneous, with large dips in depth, which reduces the surface area available to the molecules of the analyzed gas. The surface 1 has a homogeneous spherical globular structure, which facilitates the access of a large number of gas molecules, compared with 2 [1-3].

The research was funded with the support of a state assignment (scientific code FZWU-2023-0002).

References

[1] R. B. Salikhov, R. A. Zilberg, E. O. Bulysheva, A. D. Ostaltsova, T. R. Salikhov, Yu. B. Teres, Letters on Materials. V. 13 (2), 132-137 (2023)
[2] R. B. Salikhov, I. N. Mullagaliev, T. R. Salikhov. In Functional materals. 309-309 (2021).
[3] A. G. Mustafin, L. R. Latypova, A. N. Andriianova, S. M. Salikhov, A. F. Sattarova, I. N. Mullagaliev, I. B. Abdrakhmanov, Macromolecules. V. 53(18), 8050-8059 (2020)

AP2-8P/14

Design of strip microwave devices for characterization of garnet ferrite films

Pavlyuk E.I.[1], Kuzmichev A.N.[2], Kholin A.A.[1], Fedorenko A.A.[1], Vetoshko P.M.[3]

[1]CFU named after V.I. Vernadsky[2]Affiliation two, Zip, City, Country
[2]International center for Quantum Optics and Quantum Technologies
[3]Kotelnikov Institute of Radioengineering and Electronic RAS, 125009, Moscow, Russia

The relevance of the work lies in the fundamental and applied interest in the conjugation of epitaxial ferrite-garnet structures with strip waveguides when creating such microwave devices as YIG resonators, YIG generators, and YIG filters. The main advantage of such devices is the possible adjustment of their operating frequency in a wide microwave range using an applied magnetic field. The importance of this task is explained by the fact that rare-earth ferrites-garnets are of interest as materials for the elemental support of devices necessary for microelectronics that use the method of information transformation.

To coordinate strip waveguides with film structures, complex three-dimensional modeling of objects of various configurations was carried out and resonators were designed with high accuracy using the CST STUDIO SUITE software package. The modeling was based on the analysis of S-parameters. A modified geometry of the YIG sample is also proposed, the profile of which has the form of a trapezoid, which significantly improves the absorption parameter, in comparison with the rectangular shape of the sample, the new geometry lowers the level of reflection of the signal power S11 by 6 times and, in turn, improves the level of absorption of the signal power S21 by two orders of magnitude.

Three variants of modeling were carried out. All boards are the upper layer with a strip enclosed between the "ground", the dielectric and the lower "ground" layer. In the third case, the model from Figure 2 was used, on top of which there is a metal screen.

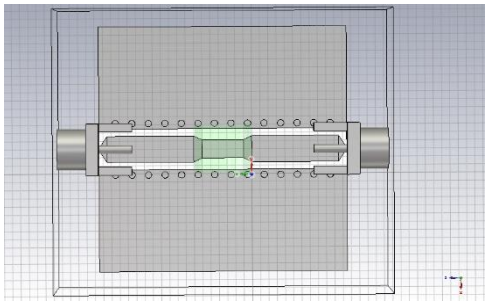

Fig. 1. The model is a straight strip with a narrow part (top view). In the center of the board is a sample (green)

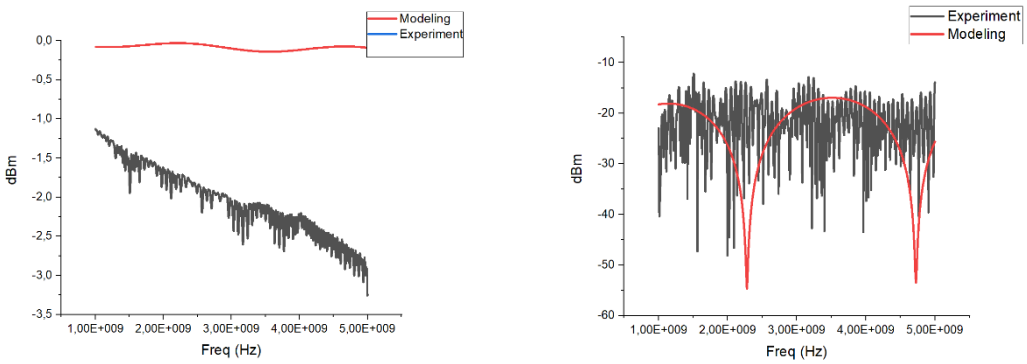

Fig. 2. Comparison of experimental S-parameters and those obtained by simulation. S21 on the right and S11 on the left.

It can be seen from Figure 2 that the graphs obtained experimentally differ slightly from the curves obtained during modeling. In particular, the level of the signal power absorption parameter, also known as S21, fell by 3 times, but the reflection parameter S11 remained at an acceptable level.

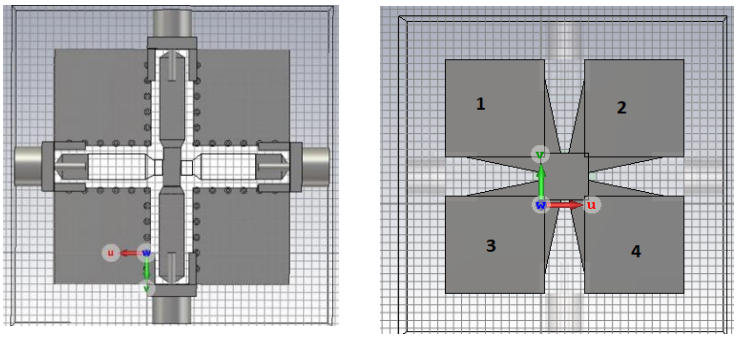

Fig. 3. On the right is a model with crossed stripes, where the horizontal one is recessed 200 microns into the dielectric and connected to the upper platform by transition holes. On the left is a metal screen .

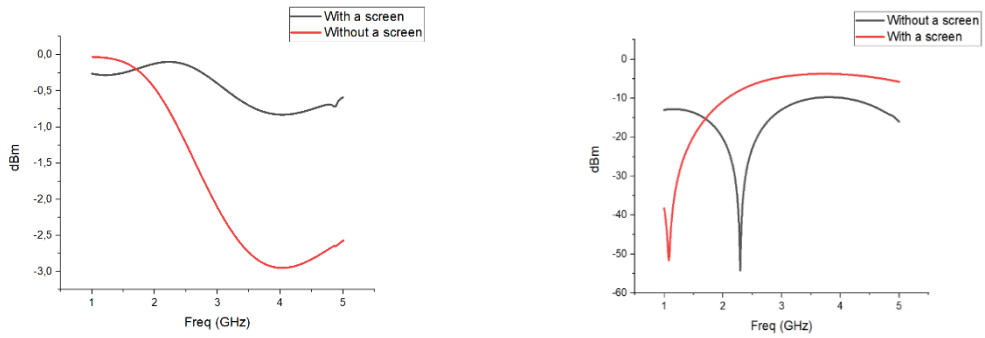

Fig. 4. Comparison of S-parameters for a model with orthogonally arranged strips with and without a metal screen. On the right – S21, on the left – S11.by transition holes. On the left is a metal screen

Figure 4 shows that the overall level of S21 has changed compared to the simulation results without a metal screen and is in the range from -0.015 to -0.5 dB, which is an excellent result for these conditions.

Section
Materials for Medical Applications. Biosensors

BO2-9O/1

Reusable adsorbent based

A.B. Khutieva[1], M.V. Lomova[1], A.V. Sadovnikov[1]

Saratov State University, 410012, Saratov, Russia
abkhutieva@gmail.com

Magnetic materials are divided into magnetically hard (the field strength is tens and hundreds of amperes per square centimeter), as well as soft magnetic materials (the field strength is tenths and hundredths of an ampere per square centimeter). The use of magnetic materials in science and technology is quite widespread, but recently more and more attention has been paid to the issue of the biomedical aspect of the possible use of magnetic media. In addition to diagnostic purposes (magnetite nanoparticles contrast well with MRI, and often simultaneously in two modes), magnetic materials are used for targeted drug delivery systems in the treatment of tumor diseases, tissue repair.

This paper reviewed the use of Brillouin microscopy for the spatial study of biological objects and/or carriers, which is the only non-destructive, non-marking tool for characterizing spatial structures, as well as phonon interaction, which can provide valuable information about the spatial rigidity of biological objects with high resolution, which cannot be obtained by any other method, while the method remains unmarked and non-invasive. It supposed that only the entry of carriers into cells will affect cell survival, and since carriers are magnetic, it is possible to target particles specifically at tumor cells. Consequently, such a system can be extremely useful for reducing the amount of active substance and improving local cancer therapy.

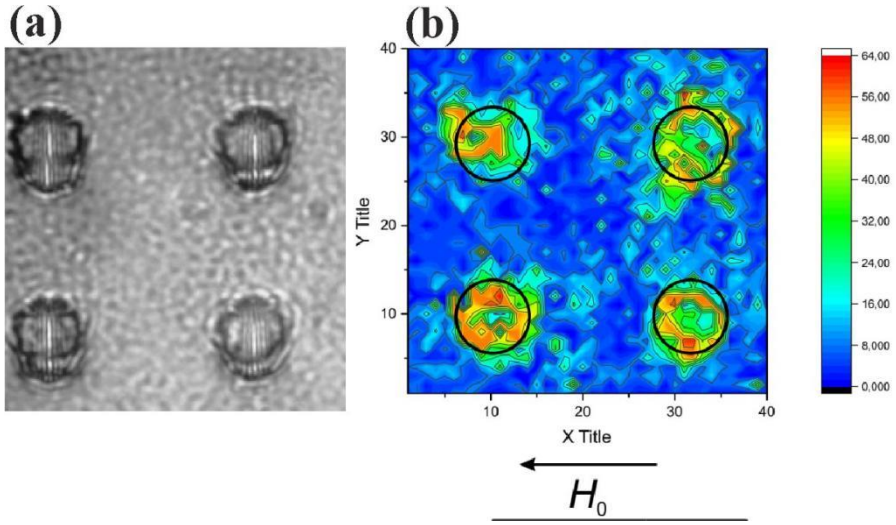

Fig. 1. (a) A snapshot of the experimental sample. (b) Spatial distribution of light intensity.

The Brillouin light scattering method and the determination of the motion of composites in an inhomogeneous magnetic field, as well as the SEM-research of hybrid mineral high-magnetic composites allowed us to characterize the magnetic properties of carriers and determine that 3 cycles of freezing/thawing of magnetic nanoparticles are sufficient to obtain an optimal drug carrier. The effectiveness of magnetic targeting depends on the vehicle's magnetic response, which, in turn, is determined by magnetization (i.e. magnetic moment per unit volume or mass)

the system. The magnetization can be improved by increasing the loading of magnetic nanoparticles into the carrier. In this regard, the recently introduced freeze-induced loading (FIL) method shows excellent results.

The work was supported by the Russian Science Foundation (project №23-13-00373).

References

[1] P. A. Demina, A. A. Abalymov, D. V. Voronin, A. V. Sadovnikov, M. V. Lomova, Mater. Chem. Front. V. 5, 2007-2018 (2021).

[2] R. J. J. Riobóo, M. Desco, M. V. Gómez-Gaviro, Biomed. Opt. Exp. V. 10, 6, 2674-2683 (2019).

[3] S. J. Henley, C. C. Thomas, D. R. Lewis, E. M. Ward, F. Islami, M. Wu, H. K. Weir, S. Scott, R. L. Sherman, J. Ma, B. A. Kohler, K. Cronin, A. Jemal, V. B. Benard, L. C. Richardson, Cancer. V. 126, 10, 2250-2266 (2020).

[4] J. M. Vaughan and J. T. Randall, Nat. V. 284, 489-491 (1980).

BO2-9O/2

Reusable adsorbent based on boron nitride nanoparticles for effective antibiotic water purification

Sorokina L.Yu.[1], Kotyakova K.Yu.[2]

[1] *Laboratory of digital material science, Research center "Inorganic Nanomaterials", National University of Science and Technology MISIS, 119049, Moscow, Russia*
[2] *Research center "Inorganic Nanomaterials", National University of Science and Technology MISIS, 119049, Moscow, Russia*
l.sorokina@misis.ru

Recently, the emergence of antibiotics in water sources, as well as the increasing spread of antibiotic-resistant bacterial genes, has caused serious concern. Wastewater contamination with antibiotics is one of the major social and environmental problems today, as their presence in the aquatic environment poses a risk to aquatic organisms and also negatively affects human health and surrounding flora and fauna. Since the discovery of antibiotics, their use is increasing rapidly every year due to the growth of the world's population and increasing demand. In recent years, due to the COVID-19 epidemic, in the treatment of the effects of which antibacterial drugs are widely used, the consumption of antibiotics in Russia has increased by almost a third in 2020 alone. All this shows the high relevance and scientific significance of this research, aimed at developing effective methods and new ways to detect and remove antibiotics from the aquatic environment.

Nanomaterials with high specific surface area are a promising platform for inexpensive and highly effective sorbents of various contaminating molecules. 2D materials have a large specific surface area and are therefore excellent sorbents for a wide variety of contaminants. Hexagonal boron nitride (h-BN) stands out for its unique properties (non-toxicity, enhanced thermal stability, recyclability, excellent oxidation resistance, high specific surface area and chemical inertness) that make it a good adsorbent.

In this work, we developed an effective platform based on h-BN nanoparticles (BNNPs) with high specific surface area formed by multiple nanoplates. The antibiotic removal efficiency was analyzed at different initial concentrations of antibiotics in the solutions (10, 50, and 100 μg/ml) and at different degrees of acidity of the solutions (pH 4, pH 7, and pH 9) for 28 days. The maximum sorption capacity of the h-BN coatings was 502.78 μg/g for tetracycline, 315.75 μg/g for ciprofloxacin, 400.17 μg/g for amoxicillin, and 269.7 μg/g for amphotericin B, which exceeds the sorption capacity of many currently known materials. The loss of efficacy during reuse of the coatings is no more than 5-15%, which confirms the prospects for reusability.

This work was supported financially by the Russian Science Foundation Project № 21-79-10411.

BO2-9O/3

Novel Zinc complex based on azomethine derivatives of 3-methyl-1-phenyl-pyrazol-5-one exhibiting bright blue fluorescence

Braga E.V.[1], Gusev A.N.[1], Nagaeva A.N[1]

Acad. Vernadsky av.,4, V.I.Vernadsky Crimean federal university, 295007, Simferopol, Russia
braga.yelena@ya.ru

The synthesis and development of new electroactive emitters for high-performance organic light emitting diodes (OLEDs) is one of the key problems of modern materials science. It is well known that a general target for OLED investigations is to develop full-color displays and solid-state lighting (SSL) sources. Despite the significant progress achieved in this field in the last decade, the production of blue monochromatic materials that can be used as active emissive layers in OLEDs remains an important problem that, so far, has hampered the production of a complete white electroluminescence (EL) involving a balanced simultaneous emission of the three primary colors of light. Luminescent metal−organic compounds containing functional emissive ligands represent an emerging class of luminescent materials because they possess the advantages of both organic dyes, and transition-metal-based emitters. To explore the photophysical properties of coordination compounds with bright blue fluorescence, a new azomethin−zinc complex [1] was synthesized and characterized by various techniques (elemental analysis, thermogravimetry, and IR-, ESI-mass-spectroscopy). The crystal structure was determined by X-ray diffraction analysis. Through thermal characterization, this complex was proved to have good thermal stability. Photoluminescence spectra were recorded, both in solution and in the solid state, and the complexes showed noteworthy photoluminescence with a maximum in the blue region [2]. OLED cells based on the resulting complex exhibit blue luminescence and can be recommended for commercial use

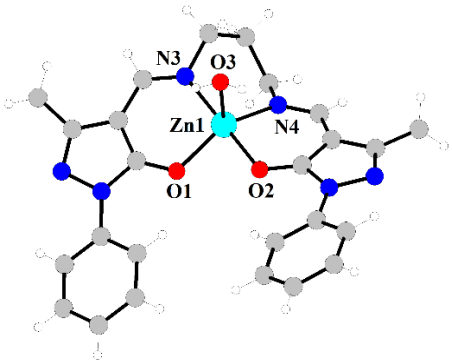

Fig. 1. Structure of complex (thermal ellipsoids are shown with probability 50%).

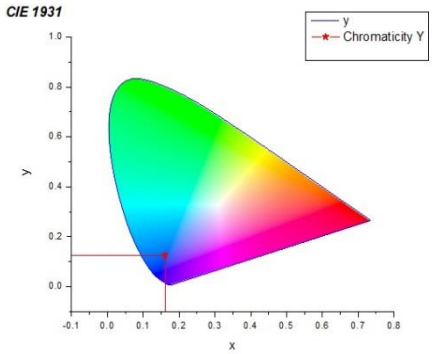

Fig. 2. CIE1931 chromaticity coordinates of photoluminescence

References

[1] Kotova, O. V.; Eliseeva, S. V.; Averjushkin, Russ. Chem, 57, 1880−1889. (2008).
[2] Dumur, F.; Contal, E.; Wantz, Eur. J. Inorg. Chem., 4186− 4198 (2014).

CP3-9P/1

Electronic sensors of ammonia vapor concentration

A.D. Ostaltsova , T.R. Salikhov , R.B. Salikhov

Ufa University of Science and Technology, Ufa, Russia
nastia.ostaltsova@yandex.ru

One of the areas of application of multilayer polymer thin-film materials [1-3] is the development and creation of new sensors for gas detection. The sensory sensitivity of thin-film structures of poly-2-[(2E)-1-methyl-2-butene-1-yl]aniline (1) and poly-2-(cyclohex-2-en-1-yl)aniline (2) to the reaction of ammonia vapors was investigated. Using a scanning electron microscope, the morphology of the surface of thin films obtained from a solution of synthesized polymers by centrifugation on sitall substrates was studied. Studying the nature of morphology is extremely important when creating sensory devices. It is extremely important to detect and measure the exact amount of toxic polluting gases. The response of the sensors to NH_3 was evaluated by the change in the passing current with a change in the concentration of ammonia vapors (Fig. 1).

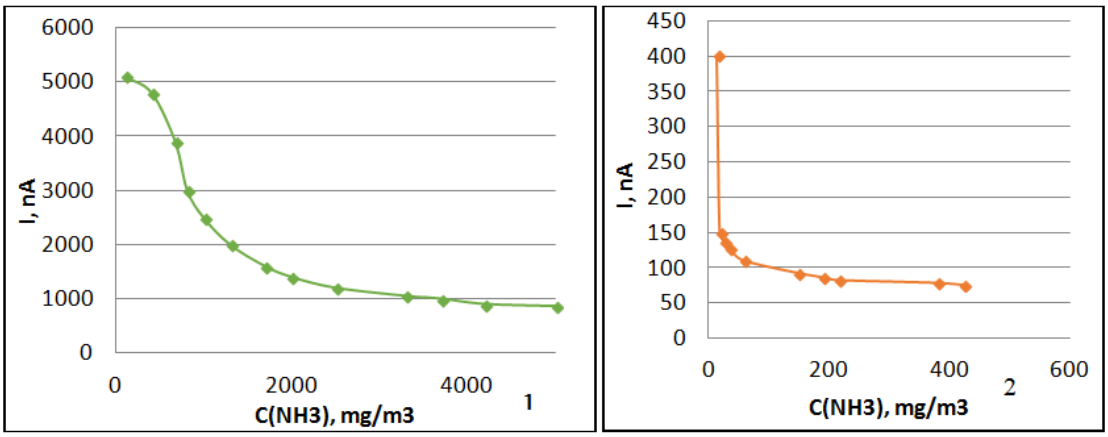

Fig.1. Dependences of the current flowing through films 1 and 2 on the concentration of ammonia vapors.

The use of new derivatives of PANI as a detecting element of the sensor makes it possible to create thin films with a developed surface and well permeable to the analyte. The studied resistive sensors demonstrate very low inertia and good response time. Films 1 react better to the presence of ammonia vapors in the air, their sensitivity is an order of magnitude higher. At the same time, it should be noted that thin films 2 exhibit a much greater change in sensitivity to ammonia vapors compared to films 1, therefore, the possible use of such films in sensors for detecting ultra-low concentrations. The results showed that samples 2 and 1 have high sensitivity, fast response time and recovery. Thus, they are of great practical importance in sensors for detecting ammonia vapors in the air.

The research was funded with the support of a state assignment (scientific code FZWU-2023-0002)

References:

[1] A. G. Mustafin, L. R. Latypova, A. N. Andriianova, S. M. Salikhov, A. F. Sattarova, I. N. Mullagaliev, I. B. Abdrakhmanov, Macromolecules. V. **53(18)**, 8050-8059 (2020)
[2] A. G. Mustafin, L. R. Latypova, A. N. Andriianova, I. N. Mullagaliev, S. M. Salikhov, R. B. Salikhov, G. S. Usmanova, RSC advances. V. **11(34)**, 21006-21016 (2021)
[3] R. B. Salikhov, I. N. Mullagaliev, T. R. Salikhov. In Functional materals. 309-309 (2021).

CP3-9P/2

Phase control of image contrast in magneto-optical eddy current introscopy.

Lugovskoy N.V., Berzhansky V.N.

V. I. Vernadsky Crimean Federal University, 295007, Simferopol, Russia
lugovskoynv@cfuv.ru

In the modern technological world, the issue of technological safety is acute, which is achieved by using new materials and conducting regular non-destructive testing. At the same time, today it is almost impossible to imagine the introduction of new technologies without the possibility of their automation. One of the modern non-destructive testing technologies is the magneto-optical eddy current (MOEC) method, which makes it possible to register surface, subsurface and fatigue defects in products made of both magnetic and non-magnetic metals [1]. The circuit and principle of operation are described in more detail in [1].

When carrying out measurements, single-crystal epitaxial films based on substituted bismuth ferrite garnet (BIFG) with the general formula (R, Bi)3(Fe, M)5012 [2] with the "easy axis" type of magnetic crystallographic anisotropy were used as a magneto-optical sensor.

The experiment examined a model object - a slit with an opening width of 100 microns made in a 1 mm thick sample of aluminum. The installation was designed in such a way that it was possible to change the illumination phase in the range from 0 to 180 degrees. Changing the phase allows you to obtain a MO contrast image of defects by illuminating the MO sensor at the moment of the peak magnetic field in the defect area (phase 2). And it allows you to obtain an image at a moment when the field in the area of the defect is very small, so that the defect practically does not stand out against the background (phase 1). This allows you to obtain almost identical images that take into account all design features and minor nuances that affect the MO image, but are not critical defects.

Several experiments were carried out, during which images of slits in different phases were obtained. In one gap it was clearly visible in the MO image. In the other phase, only the background surrounding the slits was present in the image. Next, a digital processing program was used to subtract one image from another. An example of such an experiment and processing is presented in Figure 1.

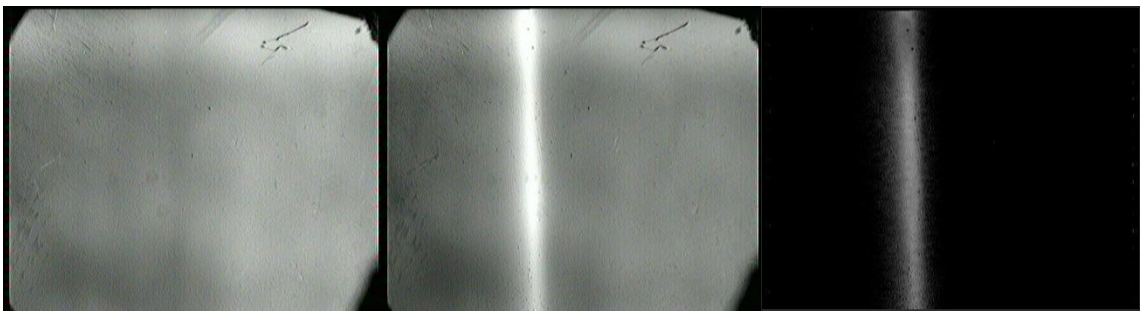

Figure 1. MO Image of the defective area: a) in the position of phase 1, b) in the position of phase 2, c) the result of subtracting two phases.

From Figure 1 it is clear that the image of the defect presented in phase 2 (Fig. 1b) is "easily visible to the eye" of the operator of the MOVT introscope, but is difficult for automatic processing by software methods. The result of phase subtraction is binary in nature, by which the device can very easily "talk" about the presence or absence of a defect.

The entire procedure for obtaining two images in different phases and their subtraction with modern technology is implemented automatically without the use of additional third-party programs on a single computing core. Accordingly, with this technology it is possible to implement a mobile MOVT flaw detector with an automatic defect detection function. The authors received a patent for this invention [3].

Conclusions

The MOVT method of non-destructive testing using illumination in different phases can be automated by simple computational processes of subtracting one phase from another.

References

[1] .Magneto-optical Visualization of Eddy Current Magnetic Fields/ Vladimir N. Berzhansky, Dmitriy M. Filippov, Nazar V. Lugovskoy// Physics Procedia, 2016, Volume 82C, pp. 27-31

[2] V.N. Berzhansky, A.V. Karavainikov, T.V. Mikhailova, V.I. Belotelov, N.V. Lugovskoy // Nano- and Micro-Scale Bi-Substituted Iron Garnets Films for Photonics and Magneto-Optic Eddy Current Defectoscopy/ Journal of Magnetism and Magnetic Materials 440C (2017) pp. 175-178.

[3] Patent for the invention "Device for magneto-optical visualization of defects in electrically conductive materials and their automatic fixation" Lugovskoy N.V., Berzhansky V.N., Lagunov I.M. No. 2753839, 2021.

CP3-9P/3

Influence of heat treatment conditions on the granulometric composition of potassium polytitanate

Saunina S.I.[1], Iagafarov Sh.Sh.[1], Erager. K.R.[1],
Tretyachenko E.V.[2], Maksimova L.A.[2], Vikulova M.A.[2], Makarov A.A.[2], Gorokhovsky A.V.[2]

[1]*Chelyabinsk State University, Chelyabinsk, Russia*
[2]*Yuri Gagarin State Technical University of Saratov,vikulovama@yandex.ru, Saratov, Russia*
shakir@csu.ru

The results of phase, particle size distribution and morphology of potassium polytitanate (PPT) particles obtained by scanning electron microscopy, laser differential analysis, X-ray phase analysis are presented. PPT sample was heat-treated in air and vacuum at 600 and 900°C and under hydrothermal synthesis conditions at 500°C. According to the data obtained with a laser particle size analyzer, the original sample is characterized by a polymodal particle distribution. The study of the morphology of the original sample, using scanning electron microscopy showed that in the sample the aggregates of layered particles of elongated shape are present.

Polymodal distribution of particles is preserved for samples heat-treated in air and vacuum at 600°C and hydrothermal synthesis conditions. Redistribution of particle-aggregates between fractions in intervals 0.01-1, 1-10, and 10-100 microns is observed. The calculated specific surface for samples heat-treated in air and vacuum increases in comparison with initial sample. The increase of specific surface is probably connected with water removal and thermal deformation of aggregate particles. Microphotographs of these samples show loose-layered particles of indefinite shape. According to X-ray diffraction analysis the hexatitanate of potassium is formed in the samples.

The particle size distribution after heat treatment at 900°C in air becomes unimodal with negative asymmetry (Fig.1a). The calculated specific surface area of the sample decreases. The change in the degree of aggregation is due to a change in the small and medium fraction particles. This particle distribution is probably related to the coalescence process [1].

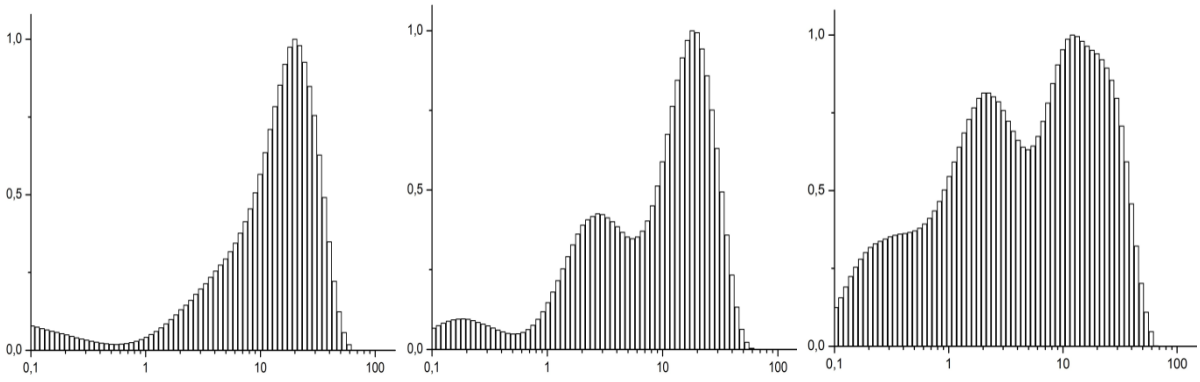

a b c

Fig.1. Histograms of particle size distribution of PPT, heat treatment: 900°C a - air; b - vacuum; c - hydrothermal treatment.

In vacuum, the polymodal distribution is maintained (Fig.1b). The average particle size – D[4,3] increases with increasing temperature of heat treatment in air: ~10.26 (initial); 12.9 (600°C); 17.77 (900°C) μm. In vacuum, it increases slightly: ~11.63 (600°C); 12.4 (900°C) μm.

In a sample heat-treated under hydrothermal synthesis conditions (500°C) the formation of the fourth mode in the region of 10 micrometers or more is observed (Fig.1c). In contrast to samples (air, vacuum) the share of particles of fine fraction increases. This is probably due to the processes of structural rearrangement of the sample particles. The average particle size is ~ 9.3 μm. On microphotographs potassium titanate whiskers are observed [2, 3].

This behaviour of the particle size distribution, the formation of whisker particles, is probably due to the different formation mechanisms of potassium hexatitanate during heat treatment under different conditions (in air, vacuum and hydrothermal conditions).

The particle size distribution up to 600°C is mainly determined by the method of precursor preparation. At 900°C, it is determined by different phase formation mechanisms.

References

[1] P. Ponce-Peña, M. Poisot, A. Rodríguez-Pulido, et al., Materials 12, 24, **(**2019).
[2] Y. Hakuta, H. Hayashi, K. Arai, Journal of materials science 39 (2004).
[3] C.Y. Xu, L. Zhen, Q. Zhang, et al., Material Characterization 59 (2008).

CP3-9P/4

Influence of ultraviolet radiation on a thin fullerene film in a phototransistor

Salikhov R.B., Mullagaliev I.N., Salikhov T.R.,

Ufa University of Science and Technology, 450076, Ufa, Russia
Ilnur9409@mail.ru

Organic materials are promising for use in electronics; thin films of fullerene and spiropyrans are being studied to create phototransistors [1]. Organic photovoltaic devices are being actively studied [2]. The desire of researchers for efficient photoelectric conversion [3]. Certain electrodes and active layers improve carrier injection, charge transfer, and there are designs or padding to ensure photon containment [4].

In this work, thin films of fullerene and spiropyran are studied in a field-effect phototransistor. The structure of the transistor consists of a glass substrate with an indium-tin oxide film, an aluminum oxide dielectric, a spiropyran derivative film, a fullerene film, and contact pads in the form of aluminum films. Films were created by centrifugation and thermal spraying in vacuum. The radiation wavelength is 350 nm. Current-voltage characteristics (Fig. 1) at voltage constant U_{DS}=5V, U_G=5V measured at room temperature in the open air. In the course of the study, it was revealed that the photocurrent decreases in this sample of the phototransistor during prolonged exposure to ultraviolet light.

After three irradiation cycles of three minutes each, the degradation stopped.These materials fullerene and spiropyran are promising for creating phototransistors, because they have good photosensitivity and photocurrent in microamps. However, it is necessary to solve the problem of film degradation using new derivatives of these substances. The time for the phototransistor to reach the operating current is 12 seconds, the recovery time is 3 seconds. These properties are suitable for the use of these phototransistors in an optocoupler.

The research was funded with the support of a state assignment (scientific code FZWU-2023-0002)

References

[1] Tuktarov A. R., Salikhov R. B., Khuzin A. A., Safargalin I. N., Mullagaliev I. N., Venidiktova O. V., Valova T. M.,BarachevskyV. A.,Dzhemilev U. M. MendeleevCommunications. V. 29. № 2. p. 160-162. (2019).

[2] Salikhov R.B., Mustafin A.G., Mullagaliev I.N., Salikhov T.R., Sharafullin I.F., Andriianova A.N., Latypova L.R.Materials. V. 15. № 1. (2022).

[3] Salikhov R.B., Mullagaliev I.N., Salikhov T.R. Mendeleev Communications. T. 31. № 5. C. 641-643. (2021).

[4] R. B. Salikhov, I. N. Mullagaliev and T. R. Salikhov. Mendeleev Commun., 33, 320–322, (2023).

CP3-9P/5

Magnetometer based on the Faraday effect of an iron-garnet film for registration magnetic particles

Evstigneeva S.[1,2], Lutsenko O.[1], Kapralov P.[1,2], Koshev N.[3] , Leontyev A.[1], Zharkov M.[1,4], Pyataev N.[4], Radchenko I.[1], Ostras M.[1,2] and Vetoshko P.[1,2,5]

[1] *QLU, 121205, Moscow, Russia*
[2] *Internationl Center for Quantum Optics and Quantum Technologies, 121205, Moscow, Russia*
[3] *Skolkovo Institute of Science and Technology, 121205, Moscow, Russia*
[4] *National Research Mordovia State University, 430005, Saransk, Russia*
[5] *Kotelnikov Institute of Radioengineering and Electronics of RAS, 125009, Moscow, Russia*
s.evstigneeva@rqc.ru

Nanomedicine is actively developing a new concept known as theranostics, which combines treatment and diagnostic techniques to provide more personalized and precise care for patients. Nanoparticles with magnetic properties (MNPs), such as [1, 2], are of interest in various diagnostic, therapeutic areas and are promising objects for use in theranostic applications.

The magnetic relaxometry (MRX) method is one of the instruments for registering MNPs; it allows to restore the distribution of MNPs in the body, reflect their accumulation in certain organs and tissues, and assess the speed of blood flow. Evaluation of the above can be useful in detecting tumor nodes, as well as in identifying areas of tissue ischemia, which makes the MRX method a powerful instrument in the field of medical diagnostics [3].

As part of these studies, a new type of magnetometer can detect magnetic nanoparticles by recording the MNP relaxation curve.

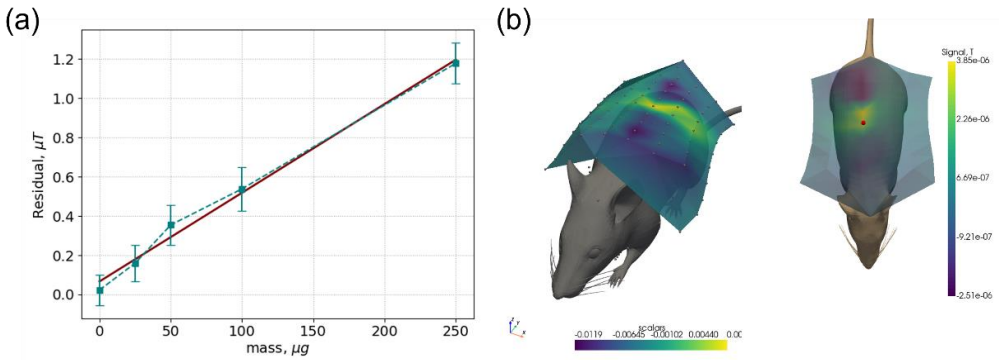

Fig.1. Measured signal of Fe_3O_4@PSS dry remanent magnetization: concentration line of particles (min 25μg)

References

[1] Y.Huang, Langmuir 31, 1172–1179 (2015)
[2] E. Stimphil, Applied Physics Reviews 4(2):021101 (2017)
[3] M. K. Abd-Ellah, A. I. Awad, A. A. Khalaf and H. F. Hamed, Magnetic resonance imaging, 61, 300-318 (2019).

CP3-9P/6

Simple and High Efficiency TADF Organic Light-Emitting Diodes on Copper(I) complexes basis

Gusev A.N.[1], Braga E.V.[1], Zamnius E.A[1]

Acad. Vernadsky av.,4, V.I.Vernadsky Crimean federal university, 295007, Simferopol, Russia
galex0330@gmail.com

Despite considerable advances in recent decades in the synthesis, radiation efficiency and practical use of luminescent d-metal complexes, the development of industrially relevant devices based on them remains an unsolved problem, primarily due to the high cost and low abundance of traditional heavy-atom-based phosphorescent materials, such as platinum, osmium, or iridium. From these reasons luminescent Cu(I) complexes came into focus as a cheaper alternative to the traditional platinum group metal complexes. Herein, we have demonstrated that 4-pyridyl derivatives of 1,2,4-triazole can be also used to design Cu(I) TADF emitters. We report the synthesis and characterization of three mononuclear Cu(I)–halide complexes [$CuX(PPh_3)_2(L)$] (X = Cl-, Br-, or I-; L = 3-phenyl-5-(pyridin-4-yl)-1,2,4-triazole. Obtained complexes demonstrate high intensity efficiency of emission at room temperature due to TADF mechanism of emission

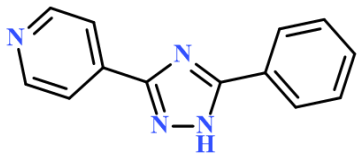

Fig. 1. Chemical structure of 3-phenyl-5-(pyridin-4-yl)-1,2,4-triazole

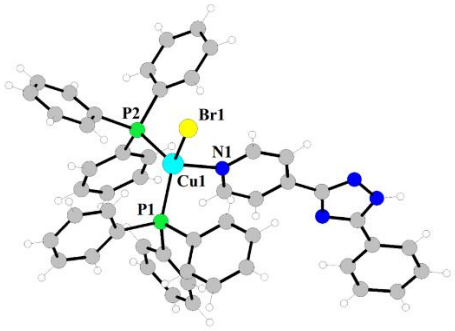

Fig. 2. Molecular structures of complex [CuBr(PPh3)2(L)]

Obtained complexes exhibit blue light emission in solutions and with extremely bright green emission in the crystals with quantum yields up to 100%. The decay analyses and density functional theory calculations revealed that the emission of solid samples at room temperature are mainly delayed fluorescence while those at 77 K are phosphorescence with singlet–triplet energy differences (ΔE = 940-1170 cm^{-1}). Besides this luminescence mechanochromism, corresponding crystalline-to-amorphous transition are also found for this series of complexes. By using the spin coating technique, a series of simple, highly efficient green-emitting OLEDs were demonstrated.

The authors would like to acknowledge the financial support from Russian Science Foundation grant (project no. 22-73-00043).

CP3-9P/7

Influence of phase transitions on the transport of magnetic biocells

Siryuk Yu.A.[1], Bezus A.V.[1], Kapshukov R.A.[1], Kononenko V.V.[2]

[1] *Donetsk State University, 283001, Donetsk, Russia*
[2] *Donetsk Institute for Physics and Engineering named after A.A. Galkin, 283048, Donetsk, Russia*
a.bezus@donnu.ru

In recent years, many works have been published related to the controlled transfer of paramagnetic colloidal particles over the surface of a ferrite-garnet film [1]. The motion of particles both on the surface of stripe domains and on the surface of a lattice of cylindrical magnetic domains (CMD) is being studied. The motion of paramagnetic particles over the surface of the pattern of domain structures (DS) occurs under the influence of external magnetic fields. But these fields also affect the DS, causing phase transitions (PT) in it. This influence must be taken into account in the controlled transport of magnetic particles over the film surface.

The aim of work is to study the peculiarities of behavior of paramagnetic colloidal particles on the surface of a ferrite-garnet film during PT induced by an external magnetic field in domain structures.

Such studies are relevant. As time shows, these results can be demand in different scopes: in microelectronics - recording and storage of information; in medicine - directed transportation of biological particles, i.e. local treatment; in chemistry - sorting particles according to their size. In addition, when creating microdevices, these scopes of applicability can be combined.

The investigations were carried out on a ferrite-garnet film with a developed surface <111> grown by liquid-phase epitaxy method on a gadolinium gallium substrate, a composition of rare-earth sublattice YSmLuCa. Film thickness h=6.8μm. The film at a room temperature has the saturation magnetization 25.8mT and quality factor Q>5.

Yeast cells (Saccharomyces cerevisiae) magneto-marked with iron oxide ions are used as magnetic particles [2]. The test solution is prepared as follows: 10 microliters of the magneto-marked cell suspension is placed in an Eppendorf tube. Then 5 microliters of 10% sodium dodecyl sulfate and 1 milliliter of distilled water are added to it. The contents of the tube are thoroughly mixed. Five microliters of the prepared suspension is applied to the surface of the ferrite-garnet film cleaned with alcohol.

Transportation of magneto-marked cells occurs under the action of a magnetic field with the following parameters: induction B=54mT, frequency ν=2Hz, the shape of the control signal is sawtooth. The formation of external magnetic fields is carried out using the magnetic system. The visual pattern of the DS is observed due to the Faraday Effect. The action of a pulsed magnetic field creates a lattice of CMD in the ferrite-garnet film.

In this work, the localized movement of magneto-marked cells around CMD has been studied. Such movement is created by the control magnetic circular field of induction B=22mT in the frequency range (1-10)Hz. The most pronounced effects of localized cell movement around the CMD are observed in the film saturation magnetization range (0.1–0.22)$4\pi M_S$. It has been noted that the dynamics of localized cell movement depends on the magnitude of the field induction normal to the film surface (displacement field). Cell movement is observed with an

increase in the displacement field within (2.97-5.69)mT. This is explained by the fact that the CMD lattice is preserved in such range of the displacement field. If the displacement field is antiparallel to the magnetization inside the CMD, then at an induction value of B≥5.69mT, a first-order PT occurs in the CMD lattice due to the disappearance of the central domain of hexagonal packing into a new lattice with a smaller CMD diameter and a large period [3].

If the displacement field is coincides in direction with the magnetization inside the CMD, then at an induction value of B≥2.97mT, a second-order PT into a honeycomb structure occurs in the lattice. In this case, the number of domains is conserved and CMDs acquire the shape of a hexagon. The domain structure of a ferrite-garnet film is a thermodynamic system what tends to occupy the most stable state with minimal energy under any external influences. Therefore, magneto-marked cells are inside the hexagonal domains in an equilibrium state.

With a subsequent increase in the induction of the field coinciding with the direction of magnetization inside the CMD, a first-order PT occurs in the honeycomb structure into a cluster structure. The magneto-marked cells visualize the domain boundaries of this structure as well.

As the field induction increases, changes occur in the cluster structure. The sizes of some domains decrease, and the length of domain boundaries also decreases. In this case, the paramagnetic cells move on the surface of domain under the influence of the magnetic field gradient from the pattern of domains.

Conclusion. The action of low value of the induction of external magnetic field (compared to the value of saturation magnetization of the ferrite-garnet film) occur a phase transitions in the domain structure. Domain boundary generates a strong local magnetic field gradient, which affects on peculiarities of the behavior of magneto-marked biological cells. Thus, the cells are localized near the domain boundaries and visualize the magnetic pattern obtained during phase transitions in the ferrite-garnet film.

References

[1] P. Tierno, V. Arthur, Eur. Phys J E Soft Matter. V 39(5), N54, 16054 (2016).

[2] S.V. Bespalova, Yu. A. Legenky, M.G. Holyavka, M.V. Solopov, Proceedings of Voronezh State University. Series: Chemistry. Biology. Pharmacy. № 1, 98 (2017).

[3] Ju.A.Siryuk, A.V.Bezus, E.D.Bondar, V.V.Kononenko, Fiz.Tverd.Tela, 61, №7, 1250 (2019).

CP3-9P/8

Influence of oxygen on the electrically conductive properties of thin films of polyaniline and its derivatives

Badretdinov B.R., Mullagaliev I.N., Salikhov T.R.

Ufa State University of Science and Technology, Ufa, Russia
badretdinovbr@gmail.com

At present, thin films of PANI and its derivatives are promising materials for the creation of organic electronic devices and components. One of the areas of application of multilayer polymeric thin-film materials is the development and creation of resistive sensors for gas sensors, solar panels, etc. [1-4].

The purpose of this work is to establish the mechanism of the effect of adsorbed oxygen on the electrical conductivity of films of polyaniline UG-1 and PANI 1:3 as part of a thin-film resistive sensor. A glove box with a slight overpressure was used to isolate the working samples from oxygen. The deposition of the films, as well as the studies, were carried out in two environments: in a glove box with gaseous nitrogen and in the open air under normal conditions without limiting the access of oxygen to the material.

Based on the results obtained, graphs of the dependence of the current on the influence of the external environment were plotted (Fig. 1). The study showed that the adsorption of oxygen molecules on the surface of PANI noticeably changes their electronic properties and has a strong effect on surface electronic processes that determine many properties of thin-film systems.

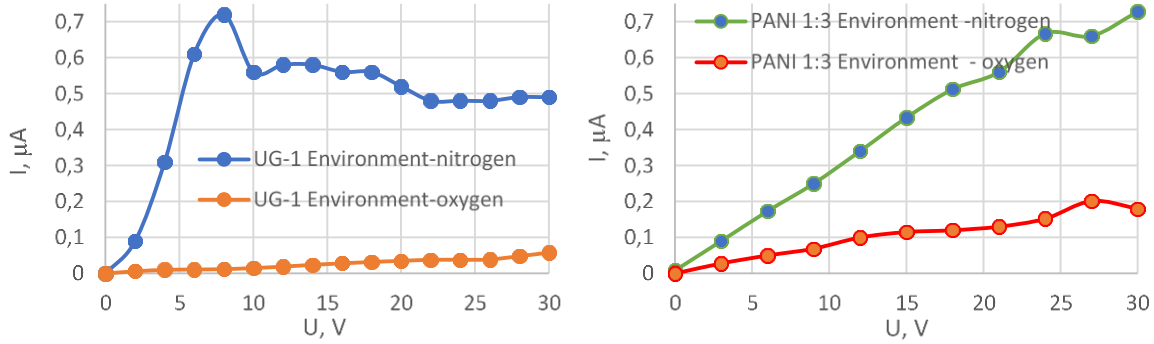

Fig.1. Current-voltage characteristic of derivatives of polyaniline UG-1 and PANI 1:3

The research was funded with the support of a state assignment (scientific code FZWU-2023-0002)

References:

[1] Latypova L.R., Andriianova A.N., Salikhov S.M., Abdrakhmanov I.B., Mustafin A.G., Mullagaliev I.N., Salikhov R.B., Polymer International. V. 69 (9), 804-812 (2020).

[2] Mustafin A.G., Latypova L.R., Andriianova A.N., Salikhov S.M., Sattarova A.F., Abdrakhmanov I.B., Mullagaliev I.N., Salikhov R.B., Macromolecules. V. 53 (18), 8050-8059 (2020).

[3] Mustafin A.G., Latypova L.R., Andriianova A.N., Salikhov S.M., Usmanova G.S., Mullagaliev I.N., Salikhov R.B., RSC Advances. V. 11 (34), 21006-21016 (2021).

[4] Salikhov R.B., Biglova Yu.N., Mullagaliev I.N., Salikhov T.R., Mustafin A.G., Letters on Materials. V. 11 (2), 140-145 (2021).

Author Index

L

M

N

O

P

R

S

T

U

V

Y

Z

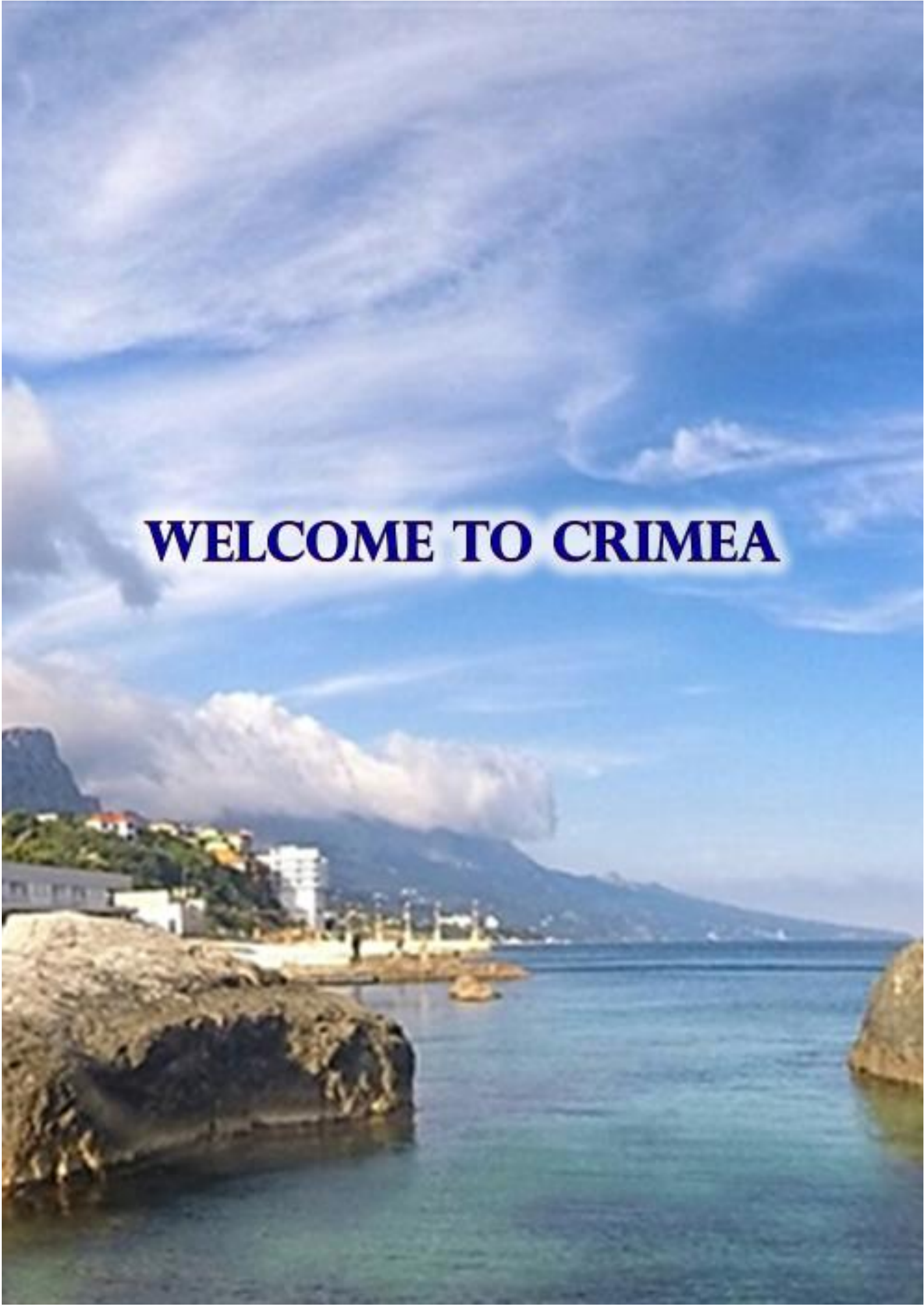
WELCOME TO CRIMEA